UNCLASSIFIED

AD NUMBER

AD486490

NEW LIMITATION CHANGE

TO

Approved for public release, distribution unlimited

FROM

Distribution authorized to U.S. Gov't. agencies and their contractors; Critical Technology; May 1966. Other requests shall be referred to Air Force Materials Lab., Metals and Ceramics Div. [MAM], Wright-Patterson AFB, OH 45433.

AUTHORITY

13 Sep 1972 per USAF ltr

THIS PAGE IS UNCLASSIFIED

H-88

AFML-TR-66-169

MATERIALS CENTRAL TECHNICAL LIBRARY
OFFICIAL FILE COPY

AD 484490

A GRAPHICAL COMPILATION OF DAMPING PROPERTIES OF BOTH METALLIC AND NON-METALLIC MATERIALS

L. T. LEE

UNIVERSITY OF MINNESOTA

TECHNICAL REPORT AFML-TR-66-169

MAY 1966

This document is subject to special export controls and each transmittal to foreign governments or foreign nationals may be made only with prior approval of the Metals and Ceramics Division (MAM), Air Force Materials Laboratory, Wright-Patterson Air Force Base, Ohio.

AIR FORCE MATERIALS LABORATORY
RESEARCH AND TECHNOLOGY DIVISION
AIR FORCE SYSTEMS COMMAND
WRIGHT-PATTERSON AIR FORCE BASE, OHIO

NOTICES

When Government drawings, specifications, or other data are used for any purpose other than in connection with a definitely related Government procurement operation, the United States Government thereby incurs no responsibility nor any obligation whatsoever; and the fact that the Government may have formulated, furnished, or in any way supplied the said drawings, specifications, or other data, is not to be regarded by implication or otherwise as in any manner licensing the holder or any other person or corporation, or conveying any rights or permission to manufacture, use, or sell any patented invention that may in any way be related thereto.

Copies of this report should not be returned to the R[illegible] Technology Division unless return is required by securit[illegible]ations, contractual obligations, or notice on a specific document.

500 - July 1966 - 773-49-1108

AFML-TR-66-169

A GRAPHICAL COMPILATION OF DAMPING PROPERTIES OF BOTH METALLIC AND NON-METALLIC MATERIALS

L. T. LEE

UNIVERSITY OF MINNESOTA

This document is subject to special export controls and each transmittal to foreign governments or foreign nationals may be made only with prior approval of the Metals and Ceramics Division (MAM), Air Force Materials Laboratory, Wright-Patterson Air Force Base, Ohio.

FOREWORD

This report was prepared by the University of Minnesota, Department of Aeronautics and Engineering Mechanics, Minneapolis, Minnesota, 55455, under USAF Contract No. AF 33(615)-1055, Project No. 7351, "Metallic Materials," Task No. 735106, "Behavior of Metals." This work was administered under the direction of the Air Force Materials Laboratory, Research and Technology Division, Wright Patterson Air Force Base, with Mr. J. P. Henderson, MAMD, acting as project engineer.

This report covers work conducted from June 1963 to February 1966.

This compilation is necessarily the combined result of the work of several people and scarcely the sole product of the one under whose name the collection appears. Appreciation is due to Dr. B. J. Lazan for his assistance, contributions, and continued support throughout the endeavor. In addition appreciation is due Mr. R. Wieckowicz for assisting in collecting the data, Mr. A. Pakalns for preparing the figures, and Miss Ginny Stark for typing the complete manuscript.

Manuscript released for publication February 1966 as an RTD Technical Report.

This technical report has been reviewed and is approved.

W. J. TRAPP
Chief, Strength and Dynamics Branch
Metals and Ceramics Division

(187 pp) (59 fig.) ( ) tbls..) (59 ref.)

ABSTRACT

This report is a compilation of data on the damping properties of uniform materials and test specimens that has been collected from a wide range of publications. There are 420 entries on metals and alloys of which 300 are also illustrated with figures. There are 250 entries on polymers, elastomers, wood products, composites and similar synthetic and natural nonmetallic materials of which 85 are illustrated with figures. There are 80 entries on refractories, glass, masonry, minerals, stone, natural crystals, and oxides of which 20 are illustrated with figures. In addition there are 7 entries on particle-type materials, aggregates, soils, and Earth's crust. The earliest data included comes from a 1931 publication while the latest data comes from 1964 publications. If possible the data for metals, alloys, and some nonmetals is given in either unit damping energy D or loss coefficient η, otherwise the data is presented in either total damping energy D_s or loss coefficient η_s of the specimen. The data for the polymers and elastomers is usually given in complex notation (G', G" or E', E"). The primary purpose of this report is to present conveniently and concisely a compilation of published test data in a consistent set of units and to provide a useful reference for engineers and designers.

210 p 159 ref 409 fig

TABLE OF CONTENTS

		PAGE
I.	GENERAL INFORMATION	1
	1.1 Introduction	1
	1.2 Relation to Other Publications	1
	1.3 Damping Units Used in Data Presentation	2
	1.4 Reliability of the Data	2
	1.5 Form and Order of Data Presentation	3
	1.5.1 Data Tabulation	3
	1.5.2 Graphical Presentation	4
	1.6 Coding System Used for References	4
II.	DAMPING DATA ON METALS AND ALLOYS	5
	2.1 Data Tabulation	5
	2.2 Graphs	62
III.	POLYMERS, ELASTOMERS, WOOD PRODUCTS, COMPOSITES, AND SIMILAR SYNTHETIC AND NATURAL NON-METALLIC MATERIALS	108
	3.1 Data Tabulation	108
	3.2 Graphs	140
IV.	REFRACTORIES, GLASS, MASONRY, MINERALS, STONE, NATURAL CRYSTALS, AND OXIDES	153
	4.1 Data Tabulation	153
	4.2 Graphs	163
V.	PARTICLE-TYPE MATERIALS, AGGREGATES, SOILS, SANDS, AND EARTH'S CRUST	166
VI.	REFERENCES	168

ILLUSTRATIONS

FIGURE		PAGE
1.	Aluminum (pure) f = 40 cps.	62
2.	Aluminum (pure).	62
3.	Aluminum (10^5 disloc. per cm^2) f = 1 cps.	62
4.	Aluminum (pure).	62
5.	Aluminum (pure, annealed at 500°C)	62
6.	Aluminum (pure).	62
7.	Aluminum (pure, worked, annealed).	63
8.	Aluminum (pure, 2S, worked).	63
9.	Aluminum (pure 2S)	63
10.	Aluminum (pure 1100, worked)	63
11.	Aluminum	63
12.	Aluminum (iron and copper impurities).	63
13.	Aluminum (worked, annealed).	64
14.	Aluminum Alloys (Russian alloys AM-6, AM5B).	64
15.	Aluminum	64
16.	Aluminum (drawn)	64
17.	Aluminum Alloys (195-T6, 142-T75).	64
18.	Aluminum Alloy (4.7% Cu, annealed)	64
19.	Aluminum Alloy (220-T4, casting)	64
20.	Aluminum Alloys (355-T6, 356-T6)	64
21.	Aluminum Alloy (2014, treated)	64
22.	Aluminum Alloy (2014, treated)	65
23.	Aluminum Alloy (2017, treated)	65
24.	Aluminum Alloy (2017, treated)	65

ILLUSTRATIONS (CONT'D)

FIGURE		PAGE
25.	Aluminum Alloy (2017).	65
26.	Aluminum Alloy (2017).	65
27.	Aluminum Alloy (2017).	65
28.	Aluminum Alloy (2024-T4)	65
29.	Aluminum Alloy (2024-T4)	66
30.	Aluminum Alloy (2024 treated).	66
31.	Aluminum Alloy (2218).	66
32.	Aluminum Alloys (6063-T6, 6061S-T6).	66
33.	Aluminum Alloy (Hinduminium, annealed)	66
34.	Aluminum Alloy (Hinduminium, treated).	66
35.	Aluminum Alloy (Hinduminium, treated).	67
36.	Aluminum Alloys (2.5% Cu, treated)	67
37.	Aluminum Alloys (4% Cu, annealed).	67
38.	Aluminum Alloys (1% Cu, treated)	67
39.	Aluminum Alloys (Cu, treated).	67
40.	Aluminum Alloy (0.08% Cu, treated)	67
41.	Aluminum Alloys (Mg, treated).	68
42.	Aluminum Alloy (11% Mg, extruded).	68
43.	Bismuth.	68
44.	Chromium (pure, annealed).	68
45.	Chromium (pure, annealed).	68
46.	Chromium (pure, annealed).	68
47.	Chromium (pure, annealed).	68
48.	Chromium (annealed).	68

ILLUSTRATIONS (CONT'D)

FIGURE		PAGE
49.	Cobalt Alloy (Stellite 31, cast, polished)	69
50.	Cobalt Alloy (Stellite 31, cast, polished)	69
51.	Cobalt Alloy (Nivco 10, treated)	69
52.	Cobalt Alloy (Stellite 31, cast, aged)	69
53.	Cobalt Alloy (Nivco 10, treated)	69
54.	Cobalt Alloy (Stellite 31, cast, aged)	70
55.	Cobalt Alloy (20% Fe).	70
56.	Cobalt Alloy (28% Ni).	70
57.	Cobalt Alloy (23% Ni, annealed).	70
58.	Cobalt Alloy (35% Ni).	70
59.	Cobalt Alloy (34% Ni, 2% Fe, 2% Ti, annealed). . . .	71
60.	Cobalt Alloy (34% Ni, 2% Fe, 2% Ti, annealed). . . .	71
61.	Cobalt Alloy (S-816, annealed)	71
62.	Cobalt Alloy (S-816, annealed)	71
63.	Cobalt Alloy (S-816, annealed)	72
64.	Cobalt Alloy (S-816, annealed)	72
65.	Cobalt Alloy (30% Fe).	72
66.	Cobalt Alloy (Vitallium, annealed)	72
67.	Copper (pure, annealed) Torsion	72
68.	Copper (crystal) Kilocycle frequency.	73
69.	Copper (crystal, annealed, irradiated) Bending at 10 kps.	73
70.	Copper (pure) Torsion	73
71.	Copper (pure) Bending at 100 cps, shear at 14,500 kps	73

ILLUSTRATIONS (CONT'D)

FIGURE		PAGE
72.	Copper (crystal, annealed) Axial stress	73
73.	Copper (pure, annealed) Bending	73
74.	Copper (pure) Torsion	73
75.	Copper (pure, 44% reduction, annealed) Torsion. . .	73
76.	Copper (pure, drawn) Bending.	73
77.	Copper (Crystal) Axial stress at 30 kps	74
78.	Copper (pure, annealed) Torsion	74
79.	Copper Alloy (2.6% Co, 0.4% Be, treated)	74
80.	Copper (Pure, some silicon) Torsion	74
81.	Copper Alloy (2% Be)	74
82.	Copper Alloy (2.12% Be, Fe, Ni, treated)	74
83.	Copper Alloy (0.81% Cr, 0.02% Si, treated)	74
84.	Copper Alloy (Brass)	74
85.	Copper Alloy (Brass, drawn).	75
86.	Copper Alloy (Brass, drawn).	75
87.	Copper Alloy (a-Brass, crystal).	75
88.	Copper Alloys (Zn)	75
89.	Copper Alloy (Brass)	75
90.	Copper Alloys (Zn)	75
91.	Copper Alloy (Brass)	75
92.	Copper Alloy (a-Brass)	76
93.	Copper Alloy (5.42% Sn).	76
94.	Copper Alloys (Zn)	76
95.	Copper Alloy (Bronze).	76

ILLUSTRATIONS (CONT'D)

FIGURE		PAGE
96.	Copper Alloy (10% Ni)	76
97.	Copper Alloy (Zn)	76
98.	Copper (Red)	76
99.	Gold (pure)	77
100.	Gold (pure)	77
101.	Iron (Electrolytic)	77
102.	Gold (pure)	77
103.	Iron (pure, drawn, heated at 700°C)	77
104.	Iron (pure, drawn, heated at 940°C)	77
105.	Iron (pure, drawn, heated at 940°C)	77
106.	Iron (pure, drawn, heated at 700°C)	77
107.	Iron	78
108.	Iron (pure, drawn, heated at 940°C)	78
109.	Iron (pure, drawn, heated at 800°C)	78
110.	Iron (pure, drawn, heated at 940°C)	78
111.	Iron (pure, drawn, heated at 940°C)	78
112.	Iron (Ca [illegible] free, heat-treated)	78
113.	Iron	78
114.	Iron Alloy	79
115.	Iron (0.02% N)	79
116.	Iron Alloy	79
117.	Iron Alloy (40% Co)	79
118.	Iron Alloy (1.1% Si, annealed)	79
119.	Gray Cast Iron	79

ILLUSTRATIONS (CONT'D)

FIGURE		PAGE
120.	Iron (0.001% C, drawn)	80
121.	Iron (GBC-1, drawn)	80
122.	Iron	80
123.	Iron (GBC-4, drawn)	80
124.	Iron (0.003% C, treated)	80
125.	Iron (0.003% C, treated)	80
126.	Iron (Armco, no carbon)	80
127.	Iron (Armco, 0.020% C, annealed)	80
128.	Iron (Armco, 0.019% C)	81
129.	Iron (Armco)	81
130.	Iron (0.04% C)	81
131.	Iron (Armco, annealed)	81
132.	Iron (Armco, drawn)	81
133.	SAE 1018 Steel (cold rolled)	81
134.	SAE 1020 Steel	81
135.	SAE 1020 Steel (hot rolled)	82
136.	SAE 1020 Steel (hot rolled)	82
137.	SAE 1020 Steel	82
138.	0.21% C Steel (normalized, worked)	82
139.	Mild Steel	82
140.	0.70% C Steel	82
141.	SAE 1020 Steel	82
142.	SAE 1025 Steel	83
143.	0.28% C Steel (annealed)	83

ILLUSTRATIONS (CONT'D)

FIGURE		PAGE
144.	0.38% C Steel	83
145.	0.40% C Steel (drawn, normalized)	83
146.	0.40% C Steel (drawn)	83
147.	Steel	83
148.	0.30% C Steel	83
149.	Steel (normalized)	83
150.	SAE 1045 Steel	8′
151.	SAE 1095 Steel	84
152.	0.42% C Steel	84
153.	0.92% C Steel	84
154.	Russian Steel 8	84
155.	Russian Steel 2	84
156.	Russian Steel U7A (quenched)	84
157.	0.62% C Steel (normalized, worked)	85
158.	Russian Steels	85
159.	0.61% C Steel	85
160.	SAE 1112 Steel	85
161.	Russian Steel U9A	85
162.	0.8% C Steel	85
163.	Russian Steel U12A	85
164.	Russian Steels	85
165.	Sandvik Steel (normalized)	86
166.	Sandvik Steel (quenched, tempered)	86

FIGURE		PAGE
167.	Chromium Alloys.	87
168.	Iron Alloy (13% Cr Alloy).	87
169.	Iron Alloy (13% Cr Alloy).	87
170.	5.0% Cr Steel.	87
171.	Iron Alloy (13% Cr Alloy).	87
172.	Stainless Steel (18% Cr)	87
173.	Stainless Steel (13% Cr)	87
174.	12.5% Cr Steel	87
175.	Stainless Steel.	87
176.	AISI 403 Steel	88
177.	AISI 403 Steel	88
178.	AISI 403 Steel (annealed).	88
179.	AISI 403 Steel (treated)	88
180.	AISI 403 Steel	88
181.	AISI 403 Steel	88
182.	AISI 403 Steel	88
183.	AISI 403 Steel (hot rolled, annealed).	89
184.	AISI 403 Steel (hot rolled, annealed).	89
185.	AISI 403 Steel (hot rolled, annealed).	89
186.	AISI 403 Steel	89
187.	Lapelloy (12.2% Cr).	90
188.	Lapelloy (12.2% Cr).	90
189.	Ni Steel (quenched, tempered).	90
190.	Ni-Cr Steel.	90

ILLUSTRATIONS (CONT'D)

FIGURE		PAGE
191.	Stainless Steel	90
192.	3.5% Ni Steel (quenched)	90
193.	3.5% Ni Steel (quenched)	91
194.	SAE 3140 Steel	91
195.	2.2% Ni Steel (quenched, tempered)	91
196.	2.2% Ni Steel	91
197.	SAE X4130 Steel (normalized)	91
198.	SAE 4130 Steel	91
199.	SAE 4140 Steel (annealed, tempered)	91
200.	SAE 4140 Steel (annealed, tempered)	92
201.	Russian Steels	92
202.	Cr-Mo-V Steel (annealed, quenched)	92
203.	Ni-Cr-Mo Steel (quenched, tempered)	92
204.	SAE 4615 Steel	92
205.	SAE 6145 Steel	92
206.	N-153, Fe-Ni-Cr-Co Alloys	92
207.	N-153, Fe-Ni-Cr-Co Alloys	92
208.	S-495, Fe-Ni-Cr Alloy	92
209.	S-495, Fe-Ni-Cr Alloy	93
210.	Tungsten Carbides (sintered)	93
211.	Cast Iron	93
212.	Cast Iron	93
213.	Cast Iron	93
214.	Cast Iron	93

ILLUSTRATIONS (CONT'D)

FIGURE		PAGE
215.	Cast Iron.	93
216.	Cast Iron.	93
217.	Cast Iron.	93
218.	Gray Cast Iron	93
219.	Cast Iron.	94
220.	Lead (crystal)	94
221.	Lead (pure, polycrystalline)	94
222.	Lead (pure).	94
223.	Lead	94
224.	Lead (polycrystalline)	94
225.	Lead (crystals).	94
226.	Lead	95
227.	Magnesium (castings)	95
228.	Magnesium Alloy (J-1).	95
229.	Magnesium (pure, annealed)	95
230.	Magnesium Alloys	95
231.	Magnesium (pure)	95
232.	Magnesium.	95
233.	Magnesium Alloys	95
234.	Magnesium Alloy.	96
235.	Magnesium Alloy (AZ-81-A).	96
236.	Magnesium Alloys	96
237.	Magnesium Alloys	96
238.	Magnesium Alloy (J-1, extruded).	96

ILLUSTRATIONS (CONT'D)

FIGURE		PAGE
239.	Magnesium Alloy (J).	96
240.	Magnesium Alloy (HK-31-A).	96
241.	Magnesium Alloy (J).	96
242.	Magnesium Alloy (J-1, extruded).	97
243.	Magnesium Alloy (XIXI)	97
244.	Magnesium Alloys (Al).	97
245.	Magnesium Alloy (O).	97
246.	Magnesium Alloys	97
247.	Magnesium Alloys (Al).	97
248.	Manganese Alloys (Cu, worked).	98
249.	Manganese Alloys (Cu, worked).	98
250.	Manganese Alloys (Cu, worked).	98
251.	Manganese Alloys (Cu, worked).	98
252.	Manganese Alloys (Cu, worked).	99
253.	Manganese Alloys (Cu).	99
254.	Manganese Alloy (33% Cu, treated).	99
255.	Magnesium Alloy (0.7% Si).	99
256.	Molybdenum (sintered, annealed).	99
257.	Molybdenum (arc-cast).	99
258.	Nickel (pure, cast).	100
259.	Nickel (A, treated).	100
260.	Nickel (Polycrystalline)	100
261.	Nickel (Polycrystalline)	100
262.	Nickel (Polycrystalline, annealed)	100

ILLUSTRATIONS (CONT'D)

FIGURE		PAGE
263.	Nickel (annealed)	100
264.	0.40% C Steel (quenched, tempered)	100
265.	Nickel Alloy (inconel, annealed)	101
266.	Nickel Alloy (inconel, annealed)	101
267.	Nickel	101
268.	Nickel Alloy (Monel)	101
269.	Nickel Alloy (Refractaloy 26)	101
270.	Nickel Alloy (Refractaloy 26)	101
271.	Silver (pure, annealed)	101
272.	Silver (annealed)	102
273.	Silver (drawn)	102
274.	Silver Alloys (Cd, annealed)	102
275.	Silver Alloys (Cd, annealed)	102
276.	Silver (crystal)	102
277.	Silver Alloys (In, annealed)	102
278.	Rhenium (annealed)	102
279.	Silver Alloys (Sn, annealed)	103
280.	Tin (pure, annealed)	103
281.	Strontium (pure)	103
282.	Tantalum (annealed)	103
283.	Tin	103
284.	Tin Alloy (Solder, 33% Pb)	103
285.	Titanium (pure)	103
286.	Titanium Alloy (A110 AT)	104

ILLUSTRATIONS (CONT'D)

FIGURE		PAGE
287.	Titanium	104
288.	Titanium Alloy (RC 55, annealed)	104
289.	Titanium Alloy (RC 130 B, annealed)	104
290.	Titanium Alloy (RC 130 B, annealed)	105
291.	Titanium Alloy (RC 55, annealed)	105
292.	Titanium Alloy (RC 55, cold drawn)	106
293.	Titanium Alloy (RC 55, cold drawn)	106
294.	Titanium Alloy (RC 55, annealed)	106
295.	Titanium	107
296.	Uranium (pure)	107
297.	Tungsten (annealed)	107
298.	Tungsten (annealed)	107
299.	Zinc (crystal annealed)	107
300.	Zinc (pure crystals)	107
301.	Zinc	107
302.	Cellulose Acetate (FM 6)	140
303.	Cellulose Acetate (butyrate, Tenite II)	140
304.	Plasticized Cellulose Nitrate	140
305.	Polymerized Tung Oil (X-6)	140
306.	Polymerized Tung Oil (X-7)	140
307.	Nylon	140
308.	Polyhexane	141
309.	Perspex	141
310.	Polymethyl Methacrylate	141

ILLUSTRATIONS (CONT'D)

FIGURE		PAGE
311.	Polymethyl Methacrylate.	141
312.	Polymethyl Methacrylate.	141
313.	Polymethyl Methacrylate.	141
314.	Plywood (birch).	141
315.	Polyethyl Methacrylate	142
316.	Methyl Methacrylate (lucite)	142
317.	Polymethyl Methacrylate.	142
318.	Methyl Methacrylate (lucite)	142
319.	Methyl Methacrylate (plexiglass)	142
320.	Methyl Methacrylate (plexiglass)	142
321.	Polystyrene (lustrex).	143
322.	Polystyrene (styrone).	143
323.	Polystyrene.	143
324.	Polystyrene.	143
325.	Polystyrene.	143
326.	Plywood (birch).	143
327.	Polythene.	144
328.	Polyvinyl Acetate (plasticized by tri-m-cresyl).	144
329.	Polyvinyl Butyrate	144
330.	Polyvinyl Chloride (plasticized by tri-m-cresyl)	144
331.	Polyvinyl Chloride	144
332.	Plasticized Polyvinyl Chloride	144
333.	Polyvinyl Chloride Dimethyl-Thien-Threne	144
334.	Plasticized Polyvinyl Chloride (VU-1913)	144

ILLUSTRATIONS (CONT'D)

FIGURE		PAGE
335.	Plasticized Polyvinyl Chloride (VU-1920)	145
336.	Polyvinyl Chloride	145
337.	Poly N Hexyl Methacrylate	145
338.	Plastic (Russian LKF-1)	145
339.	Vinyplasta (Russian plastic)	145
340.	Polyester	145
341.	Polyester	146
342.	Polyester	146
343.	Laminated Plastic (bakelite, grade X)	146
344.	Adhesive (3M transfer tape #466)	146
345.	Rubber (thiokol)	146
346.	Foam (3M double coated polyurethane tape, 4000 series)	146
347.	Laminated Plastic (bakelite, grade X)	147
348.	Laminated Plastic (bakelite, reinforced)	147
349.	Laminated Plastic (bakelite X199, fabric filler)	147
350.	Laminated Plastic (bakelite, grade X, paper base)	147
351.	Laminated Phenolic (bakelite)	147
352.	Laminated Phenolic (bakelite, wood-flour filler)	147
353.	Glass-Resin Composite (1002 crossply "Scotchply")	147
354.	Laminated Plastic (phenolics)	148
355.	Laminated Plastic (phenolic with canvas)	148
356.	Laminated Plastic (phenolic with canvas)	148
357.	Laminated Plastic (phenolic with cotton)	148

ILLUSTRATIONS (CONT'D)

FIGURE		PAGE
358.	Glass-Resin Composite.	148
359.	Glass-Resin Composite.	148
360.	Laminated Plastic (phenolic, Synthane L)	148
361.	Laminated Plastic (phenolic, paper base)	149
362.	Laminated Plastic (phenolic, synthane XX).	149
363.	Laminated Plastic (phenolic, paper and phenol-formaldehyde).	149
364.	Laminated Plastic (phenolic, Rayon-cotton fabric). .	149
365.	Polycaprone and Fiber (reinforced plastic)	149
366.	Rubber (natural gum stock)	149
367.	Rubber (natural, gum stock).	149
368.	Ebonite.	150
369.	Rubber (butyl)	150
370.	Rubber (butyl)	150
371.	Rubber (butyl)	150
372.	Rubber (filled butyl).	150
373.	Rubber (butyl)	150
374.	Rubber (butyl)	151
375.	Rubber (GRS)	151
376.	Rubber (filled butyl).	151
377.	Rubber (GRS + 3% Styrene).	151
378.	Rubber (GRS + 13% Styrene)	151
379.	Rubber (GRS + 23% Styrene)	151
380.	Rubber (GRS + 23.5% Styrene)	151

FIGURE		PAGE
381.	Rubber (nitrile)	151
382.	Rubber (neoprene)	152
383.	Rubber (silicone filled)	152
384.	Rubber (silicone filled)	152
385.	Rubber (thiokol)	152
386.	Wood (birch, along grain)	152
387.	Plywood (birch)	152
388.	Glass (pyrex)	163
389.	Iron Oxide	163
390.	Manganosite (polycrystalline)	163
391.	Quartz (single crystal)	163
392.	Quartz (single crystal)	163
393.	Quartz (single crystal)	163
394.	Sodium Chloride (single crystal, annealed)	163
395.	Aluminum Oxide (single crystals)	164
396.	Aluminum Oxide (single crystals)	164
397.	$Ba_{0.92}\ Ca_{0.08}\ TiO_3$	164
398.	$BaTiO_3$	164
399.	Lithium Fluoride (single crystal)	164
400.	Baruim Titanite	164
401.	$PbZr_{0.52}\ Ti_{0.48}\ O_3$ plus 1% Nb_2O_5	164
402.	$Pb_{0.94}\ Sr_{0.06}\ Zr_{0.53}\ Ti_{0.47}\ O_3$	164
403.	Glass (soft, annealed)	165
404.	Glass	165

ILLUSTRATIONS (CONT'D)

FIGURE		PAGE
405.	Silica (fused)	165
406.	Silica (fused, annealed)	165
407.	Silica (fused, annealed)	165
408.	Silica (fused)	165
409.	Glass.	165

SYMBOLS

D	unit damping energy for a material
D_s	total damping energy for a specimen or part
η	loss coefficient for a material $D/2\ U$
η_s	loss coefficient for a specimen $D_s/2\ U_s$
E'	storage modulus of elasticity under longitudinal stress in pounds per square inch (psi)
E''	loss modulus under longitudinal stress in pounds per square inch (psi)
G'	storage modulus of elasticity under shear stress in pounds per square inch (psi)
G''	loss modulus under shear stress in pounds per square inch (psi)
σ_a	amplitude of cyclic longitudinal stress
ϵ_a	amplitude of cyclic longitudinal strain
τ_a	amplitude of cyclic shear stress
γ_a	amplitude of cyclic shear strain
σ_g	critical stress above which stress history affects damping properties
f	frequency of cyclic stress or strain in cycles per second
N	number of fatigue cycles prior to measurement of damping
T	testing temperature (room temperature unless otherwise indicated)
TR	annealing or other thermal treatment temperature applied before testing
U	unit strain energy of a material
U_s	total strain energy of a specimen

I. GENERAL INFORMATION

1.1 Introduction

In recent years there has been a large increase in the importance of material damping in several areas. In the materials science field "internal friction" measurements are being increasingly utilized to study submicro-, micro-, and macrostructure of crystalline materials. Likewise, rheological and damping tests are being used to determine the molecular structure and deformation mechanisms of polymers and elastomers. In the structural mechanics field damping magnitudes are needed to analyze structural response and are also used to study interface effects. In addition, the alteration of the damping of a structure or member is an important means of controlling and limiting its response to broad excitation spectrums. Damping measurements also provide a sensitive inspection tool, since damping is a very structure-sensitive property. (Preface, 65 L)*

This increased importance has led to a tremendous literature multiplication. The number of publications in the material damping field is already well over 2,700 and appears to be doubling every 9.2 years (Figure 2.7, 65 L). Thus, in order to make damping data more readily available to designers and engineers, there is a need for a reasonably complete and convenient single source of data on the properties of specific uniform materials. A first attempt at this was made in 1962 when Sun Hwan Chi compiled a summary of properties of viscoelastic materials and some miscellaneous nonmetals (62 Chi). The present report, which incorporates most of Chi's data, is an attempt to provide such a single source of data for all uniform materials. Since, however, the amount of literature available with specific data is quite large and increasing very fast, no claim of completeness can be made.

1.2 Relation to Other Publications

The data tabulation sections presented here are very similar to those found in Chapter 8 of Dr. B. J. Lazan's book (65 L). They are presented here to supplement the graphical compilation in two ways. First, they provide information on materials for which the available data was not suitable for graphical presentation. And second, they provide additional information on test conditions for that data that is presented graphically.

Much of the data included here on elastomers, thermoplastics, and polymers is also included in 62 Chi.

---

* See Section 1.6

For a very complete bibliography of the material damping field up to 1964 see 64 Wo, 62 Chi, and 56 D. These three reports list over 2,700 publications and provide abstracts of most of them.

1.3 Damping Units Used in Data Presentation

Many different units were used in the original references from which the data in this report was obtained. These were converted to the standard units η, η_s, D, D_s, E", or G" by the relations given in Figure 2.6 of Dr. B. J. Lazan's book (65 L). Whenever possible the unit values η, D, E", G" of the material are given rather than the test specimen properties η_s, D_s, $\mathcal{A}_s$. Unfortunately, the test data in much of the literature is given in terms of specimen values rather than in unit values for materials; the importance of stress distribution and nonlinear damping was generally not recognized. Since only rarely in reports dealing with nonlinear materials are specimen details and stress distribution data given, it is difficult - if not impossible - to reduce much of the available specimen damping values to unit damping values. In such cases the damping values are generally presented in η_s units. It should be re-emphasized, however, that for highly nonlinear materials, η may be significantly different from η_s. In view of these discrepancies caution should be exercised in utilizing "specimen data" in structural mechanics and in making comparisons between different materials.

For metals, which generally display rate-dependent linear damping at low stress and nonlinear damping at high stress, D (or $D_{\Delta v}$) or η (or η_s) units are used, and the dependence of damping on σ_a, w, N, T, etc. is indicated when known. Nonmetallic materials such as polymers, elastomers, foams, wood, concrete, and viscoelastic materials generally behave linearly at low strain amplitudes, and under these conditions complex notation is used (G', G" or E', E"). At high strain amplitudes these materials also often exhibit nonlinearities, and the damping properties are expressed in terms of unit damping energy D whenever possible.

The elastomer industry has employed a large variety of damping tests, but many of them are primarily for rating materials and are very arbitrary. In these cases the test results often cannot be related to the "standard units" used here.

1.4 Reliability of the Data

Many examples will be observed in the following compilation where the "same" material and the "same" test conditions do not lead to the same results. These discrepancies are due mainly to: (1) variations in the material presumed to be the same, (2) deviations from nominal test conditions, and (3) unsuspected energy losses in the specimen grips and testing machine.

Since damping is very structure-sensitive property, it can be significantly changed by slight differences in composition, thermal treatment, and mechanical processing. But publications often do not include detailed information on important chemical, thermal, and mechanical features, so it is difficult to associate differences in damping with these features. Small differences in temperature and humidity may also have significant effects on damping, particularly in elastomers, polymers, and other nonmetallic materials.

Since for low damping materials the energy absorbed per cycle by the test specimen is very small compared to that generally dissipated by conventional grips, joints, and other connections within the testing apparatus, serious errors in the test results may occur. For low damping metals the lack of proper attention to grip details and machine losses may result in an apparent damping value over ten times higher than the actual damping of the specimen. Some of the very high damping values found in this compilation may be due to such unsuspected energy losses in the specimen grips and testing machine.

Since the dominant mechanisms of energy dissipation change with varying stress level, temperature, frequency, etc., interpolation or extrapolation of data given here may lead to serious errors (Chapter V, 65 L). In addition, the scope of the testing conditions are very often not clearly defined in the literature.

As a result of these factors, published data on damping properties are probably much more unreliable than published data on other properties. No effort is made here to judge the validity of the data given here or to appraise its engineering significance. The primary purpose of this report is to present, in a convenient and concise manner, a graphical compilation of published test data in a consistent set of units and provide a useful reference for engineers and designers.

1.5 Form and Order of Data Presentation

1.5.1 Data Tabulation

In each of the data tabulation sections that follow the materials that fall within that group are listed alphabetically. For each entry the name of the material is followed by additional details on composition, heat treatment, etc. as provided in the original publication. The test conditions (type of stress, stress amplitude, temperature, etc.) are given next, if available, and this data is followed by damping values (D, η, G', E' or D_s, η_s). This is followed by any other significant information on the relation between the test variables and the damping values. For those entries that are also illustrated by a figure, this last information is unnecessary because a better idea of these relations can

be obtained from the figure. The final information given (in parentheses) is a reference to the original publication and, if necessary, a figure number.

Often an asterisk is inserted after the reference, for example (42 Bi*), to indicate that the reference cited is not the original source of the data, but includes it from an earlier publication. In a few cases both the original and the secondary references are included, for example (50 No, 61 U*).

1.5.2 Graphical Presentation

In each of the graphical sections that follow, the materials are arranged approximately in alphabetical order. However, to conserve space a few entries are out of order. Every entry in the graphical presentation is also included in the appropriate tabulation section.

In all of the graphs the damping properties are indicated as ordinate values. In all cases a logarithmic scale is used for the ordinate, with horizontal guide lines to indicate decade lines (10^2, 10, 1, 10^{-1}, 10^{-2}, etc.) and quintuple lines (5×10^2, 5×10, 5, 5×10^{-1}, etc.).

Various variables are plotted along the abscissa depending on what was emphasized in the original reference. Examples of the abscissa variable are stress amplitude, mean stress, temperature, frequency of vibration, prior cold working, and number of fatigue cycles. The reference is included on each graph in parentheses, generally in the lower right-hand corner. Some information is given in the caption and elsewhere in the figure to indicate composition, treatment, type of stress, etc., but this is usually not complete. More complete information is generally included in the data tabulation sections described previously.

1.6 Coding System Used for References

Each reference cited in this compilation is denoted by a code. This code consists of two digits followed by one to four letters, for example 53 B, 41 Ki, 59 Wil, 62 Pisa. The digits are the last two digits of the publication year while the letters are the first letters in the principal author's name. Thus, the code 53 B means a 1953 article by W. J. Barber. This code is consistant with the coding system used in 65 L and 64 Wo.

All references in the bibliography are ordered chronologically by year of publication and alphabetically by principal author within each year. In a few instances a reference is coded and included under the year of the preliminary report, in which case the code and the publication date do not correspond. It must also be noted that the English spelling of Russian names often depends on the translator.

II. DAMPING DATA ON METALS AND ALLOYS
(See the list of symbols on page for units used in following tabulation)

2.1 Data Tabulation

ALUMINUM (Pure). Axial stress. T = 50 to 300°K. $\eta_s = 2 \times 10^{-5}$ to 5×10^{-5} for strained case. $\eta_s = 7 \times 10^{-6}$ to 2×10^{5} for annealed case. (58 Mas, Figure 1)

ALUMINUM (Pure). Axial stress. $\epsilon_a = 2 \times 10^{-7}$ to 5×10^{-5}. T = 25 to 440°C. $\eta_s = 3 \times 10^{-5}$ to 6×10^{-3}. 6x increase with ϵ_a. 35x increase with T. (58 Mas, Figure 2)

ALUMINUM (Single crystal). Axial stress. f = 1. T = 400 to 700°C. $\eta_s = 5 \times 10^{-4}$ to 10^{-2}. (58 Mas, Figure 3)

ALUMINUM (Single crystal). Bending. Medium strain. f = 9. $\eta_s = 6.4 \times 10^{-4}$. (41 Ki*)

ALUMINUM (Pure, annealed, single crystal). f = 7,000. $\epsilon < 10^{-4}$. $\eta = 2.5 \times 10^{-5}$ to 14×10^{-5}. (62 Sm*)

ALUMINUM (Polycrystal and single crystal). Torsion. f = 1. T = 40 to 440°C. $\eta_s = 2 \times 10^{-3}$ to 8×10^{-2} for polycrystal with 40x peak at 240°C. $\eta_s = 10^{-3}$ to 10^{-2} for single crystal. (56 Mas, Figure 11)

ALUMINUM (99.995% pure). Axial stress. σ_a = 10 to 3000 psi. $\eta_s = 7 \times 10^{-4}$ to 3×10^{-2}. (58 Mas, Figure 4)

ALUMINUM (Pure, annealed at 500°C). Bending. Low stress. f = 2,000. T = 50 to 600°C. $\eta_s = 10^{-5}$ to 2×10^{-3}. (38 Fors, Figure 5)

ALUMINUM (99.99% pure). Torsion. $\gamma_a = 10^{-2}$ to 10^{-1}. $\eta_s = 10^{-2}$ to 8×10^{-2} with $\eta_s = 7 \times 10^{-2}$ for all $\gamma_a > 2 \times 10^{-2}$. (57 Kea, Figure 6)

ALUMINUM (99.991% pure, worked to 95% area reduction, annealed at TR = 50 to 450°C). Torsion. Low stress. T = 25 to 450°C. $\eta_s = 3 \times 10^{-3}$ to 2×10^{-1}. 30x peak at 250°C for some TR's. (50 Ke, Figure 7)

ALUMINUM (99.5% pure). f = 10,000. T = 30 to 170°C. $\eta_s = 1.3 \times 10^{-5}$ to 1.7×10^{-4}. 4x increase with T. 8x peak at T = 250°C. (42 Bi*)

ALUMINUM (Pure 2S, worked to 96% area reduction, annealed at TR = 50 to 450°C). Torsion. Low stress. T = 25 to 450°C. $\eta_s = 3 \times 10^{-3}$ to 2×10^{-1}. (50 Ke, Figure 8)

ALUMINUM (Pure 2S). Axial stress. σ_a = 0.04 to 6 ksi. $\eta_s = 6 \times 10^{-4}$ to 9×10^{-1}. (58 Mas, Figure 9)

ALUMINUM (Pure 1100, slightly cold worked). Low stress. Bending mode of vibration = 1, 2, and 5. T = 100 to 1100°F. $\eta_s = 2 \times 10^{-4}$ to 3×10^{-2}. (61 Bo, Figure 10)

ALUMINUM (With iron and copper impurities). Torsion. T = 0 to 450°C. $\eta_s = 10^{-3}$ to 9×10^{-2}. 90x peak at 300°C. (58 Mas, Figure 12)

ALUMINUM (Cold worked heavily and annealed at TR = 150 to 360°C). Torsion. Low frequencies. T = 10 to 350°C. $\eta_s = 3 \times 10^{-3}$

to 2×10^{-1}. 10x change with TR. 50x increase with T. (58 Mas, Figure 13)

ALUMINUM. Torsion. Hollow tubes. Strains of 10^{-4} to 10^{-3}. f = 20. τ_a = 2.4 ksi. $\eta_s = 7.6 \times 10^{-3}$. (41 Ki*)

ALUMINUM (Commercial). At f = 8,000, $\eta_s = 1.8 \times 10^{-5}$ to 8.3×10^{-5}. At f = 0.1 to 10, $\eta_s = 10^{-3}$. At f = 40,000, $\eta_s = 2 \times 10^{-4}$. (42 Bi*)

ALUMINUM. Axial stress. Small strain. f = 10,000. $\eta_s = 2.0 \times 10^{-5}$ to 10^{-4}. (41 Ki*)

ALUMINUM. Torsion. τ_a = 2 to 10 ksi. $\eta_s = 2 \times 10^{-3}$ to 2×10^{-2}. (53 B, Figure 15)

ALUMINUM (Stretched or annealed). Torsion. Small strain. f = 0.25. For stretched case, $\eta_s = 1.4 \times 10^{-5}$. For annealed case, $\eta_s = 7 \times 10^{-7}$. (41 Ki*)

ALUMINUM (Pure, annealed). f = 1,000 to 10,000. $\epsilon_a < 10^{-4}$. $\eta = 1.4 \times 10^{-5}$ to 2.7×10^{-5}. (62 Sm*)

ALUMINUM (Drawn). Bending. f = 0 to 60. $\eta_s = 3 \times 10^{-3}$. (56 Mi, Figure 16)

ALUMINUM. Bending. f = 1 to 5. $\eta_s = 2.6 \times 10^{-4}$. (41 Ki*)

ALUMINUM. Axial stress. Small strain. f = 45,000. $\eta_s = 1.4 \times 10^{-4}$. (41 Ki*)

ALUMINUM (Rolled). Bending. $f = 2$. $\epsilon < 10^{-4}$. $\eta_s = 1.8 \times 10^{-4}$. (41 Ki*)

ALUMINUM (Rolled). Rotating bending. $\epsilon_a \approx 5 \times 10^{-3}$. $\eta_s = 1.1 \times 10^{-3}$. (41 Ki*)

ALUMINUM ALLOY (Russian alloys AM-6 and AM5B, both have equal damping). Bending. $T = 100$ to $400^{\circ}C$. $\eta_s = 2 \times 10^{-3}$ to 4×10^{-2}. (62 Pisa, Figure 14)

ALUMINUM ALLOY (317 STR). Axial stress. Static test. $\sigma_m = 30$ ksi. $\eta_s = 1.2 \times 10^{-3}$. (41 Ki*)

ALUMINUM ALLOY (195-T6 and 142-T75). Bending. $\sigma_a = 2$ to 5 ksi. $\eta_s = 10^{-3}$ to 3×10^{-3} for 195-T6. $\eta_s = 5 \times 10^{-4}$ to 1.5×10^{-3} for 142-T75. (57 Tr, Figure 17)

ALUMINUM ALLOY (4.7% Cu, annealed at $275^{\circ}F$). Torsion. $\tau_a = 1$ to 40 ksi. $\eta_s = 8 \times 10^{-4}$ to 1.5×10^{-3}. (44 B, Figure 18)

ALUMINUM ALLOY (220-T4 casting). Bending. $f = 20$ to 300. $\eta_s = 4 \times 10^{-2}$ to 10^{-2}. (57 Mi, Figure 19)

ALUMINUM ALLOY (355-T6 and 356-T6). Bending. $\sigma_a = 2$ to 5 ksi. $\eta_s = 10^{-3}$ to 3×10^{-3} for 355-T6. $\eta_s = 7 \times 10^{-4}$ to 2×10^{-3} for 356-T6. (57 Tr, Figure 20)

ALUMINUM ALLOYS (British types). Torsion. $\tau_a = 5$ ksi. $\eta_s = 8 \times 10^{-3}$ for Hiduminium 100 (S.A.P.). $\eta_s = 6 \times 10^{-4}$ for Duralumin (HE 14). $\eta_s = 4 \times 10^{-4}$ for R.R. 57 (DTD 5004 WP). $\eta_s = 3 \times 10^{-4}$ for R.R. 58 (DTD 5014 WP). (64 Bi)

ALUMINUM ALLOY (2% Mg.). f = 17,000 to 34,000. $\eta_s = 7 \times 10^{-6}$. (42 Bi*)

ALUMINUM ALLOY (2014 wire, solution-treated, quenched, aged 0.5 to 20 hrs.). T = 24 to 60°C. $\eta_s = 2 \times 10^{-4}$ to 5×10^{-5}. 2x change with aging time. 3x change with T. (59 Wil, Figure 21)

ALUMINUM ALLOY (2014 wire, solution-treated, quenched). Torsion. T = 10 to 130°C. f = 2.2 and 124. $\eta_s = 10^{-4}$ to 6×10^{-4}. 1.5x increase with f. 8x increase with T. (59 Wil, Figure 22)

ALUMINUM ALLOY (2017, solution-treated, quenched). Bending. T = -60 to +40°C. f = 1,250 and 3,400. $\eta_s = 5 \times 10^{-6}$ to 3×10^{-5}. 8x increase with T. 1 to 1.5x change with f. (54 E, Figure 23)

ALUMINUM ALLOY (2017, solution-treated, quenched, aging TR = 20 to 60°C, aging time = 0.1 to 100 hrs.). $\eta_s = 5 \times 10^{-6}$ to 5×10^{-5}. 2 to 8x change with aging. 4x change with TR. (54 E, Figure 24)

ALUMINUM ALLOY (2017). Axial stress. σ_a = 10 to 40 ksi. $\eta = 4 \times 10^{-3}$ to 8×10^{-3}. (43 L, Figure 25)

ALUMINUM ALLOY (2017). Axial stress. σ_a = 10 to 30 ksi. D = 10^{-1} to 2. (54 Y, Figure 26)

ALUMINUM ALLOY (2017). Axial stress. $\sigma_a = 10^{-2}$ to 10 ksi. η_s =

7×10^{-4} to 3×10^{-3}. (56 Mas, Figure 27)

ALUMINUM ALLOY (2024-T4, precipitation hardened). Bending. Vibration modes = 1, 3, and 5. Low stress. T = 100 to 800°F. $\eta_s = 5 \times 10^{-5}$ to 10^{-1}. 1,000x increase with T. (61 Bo, Figure 28)

ALUMINUM ALLOY (2024-T4). σ_a = 0 to 45 ksi. $N = 10^{1.3}$ to 10^4. $D = 10^{-2}$ to 5×10^{1}. $D = 5 \times 10^{-1}$ at $\sigma_a = \sigma_g$ = 25 ksi. 10x decrease with N. (57 A, Figure 29)

ALUMINUM ALLOY (2024, extruded, solution heat-treated at 950°F, aged at 250°F). σ_a = 0 to 15 ksi. σ_m = 0 and 18 ksi. $D = 10^{-3}$ to 10^{-1}. Little change with σ_m. (56 Pe, Figure 30)

ALUMINUM ALLOY (2024-T4). Bending. $\sigma_a < 20$ ksi. At f = 15, $\eta = 2.5 \times 10^{-3}$. At f = 100, $\eta = 7 \times 10^{-4}$. At f = 1,500, $\eta = 5 \times 10^{-5}$. Test values agree well with theory of thermal relaxation or transverse thermo-elastic effects. (65 Gr)

ALUMINUM ALLOY (2024-T4). Decay test. Cantilever beam specimens having a constant rectangular cross-section with an integral enlarged gripped end. Data is based on nominal longitudinal stress distribution and does not consider any stress concentration at the enlarged end, which may produce higher damping. n = 2.01 and $J = 3.82 \times 10^{-11}$ for $\sigma_a < 14$ ksi. (63 Ai)

ALUMINUM ALLOY (2218). Bending. σ_a = 1 to 6 ksi. $\eta_s = 10^{-3}$ to 5×10^{-3}. (57 Tr, Figure 31)

ALUMINUM ALLOY (6063-T6 and 6061S-T6, both have about equal damping). Bending. σ_a = 1 to 6 ksi. η_s = 5 x 10^{-4} to 5 x 10^{-3}. (57 Tr, Figure 32)

ALUMINUM ALLOY (Hinduminium, annealed at 360°C, furnace cooled at 10°C/hr.). Torsion. τ_a = 0 to 2 ksi. η = 5 x 10^{-5} to 2 x 10^{-3}. 20x increase with τ_a. (47 H, Figure 33)

ALUMINUM ALLOY (Hinduminium, solution treated at 530°C, followed by several types of quenching and aging). Torsion. τ_a = 4 to 16 ksi. η = 10^{-5} to 7 x 10^{-3}. 50x increase with τ_a. (47 H, Figure 34)

ALUMINUM ALLOY (Hinduminium, solution treated at 530°C, aged at 170°C). Torsion. Quenched at 100°C, τ_a = 6 to 12 ksi, η = 10^{-5} to 5 x 10^{-4}. Quenched at 20°C, τ_a = 10 to 16 ksi, η = 10^{-5} to 4 x 10^{-4}. (47 H, Figure 35)

ALUMINUM ALLOY (2.5% Cu, 0.1 to 0.9% Mg., solution treated at 460°C, water quenched, aged at 54°C, aged 0.1 to 100 hrs.). Bending. f = 1,900. η_s = 8 x 10^{-6} to 5 x 10^{-5}. Highest damping for 0.59% Mg. 5x increase with aging. 4x change with % Mg. (57 En, Figure 36)

ALUMINUM ALLOY (4% Cu, 0 to 3% Mg., annealed at 500°C, water quenched, aged at 58°C, aged 0.1 to 100 hrs.). Bending. f = 1,900. η_s = 9 x 10^{-6} to 6 x 10^{-5}. 2x change with aging. 5x change with % Mg. (57 En, Figure 37)

ALUMINUM ALLOY (Various types and conditions). f = 10 to 12,000. $\epsilon_a < 10^{-4}$. $\eta = 0.2 \times 10^{-5}$ to 3×10^{-5}. (62 Sm*)

ALUMINUM ALLOYS (1% Cu, cast, extruded, heat treated at 450°C). Torsion. Axial mean strain. $\epsilon_a = 2 \times 10^{-3}$ to 1.8×10^{-2}. T = 32 to 144°C. $\eta_s = 3.5 \times 10^{-2}$ to 10^{-2}. 3x decrease with ϵ_a. 3x change with T. (56 M, Figure 38)

ALUMINUM ALLOYS (0.1 to 4.8% Cu., cast, extruded, heat treated). Torsion. T = 100 to 400°C. $\eta_s = 10^{-3}$ to 10^{-1}. 100x increase with T. 10x change with % Cu. (56 M, Figure 39)

ALUMINUM ALLOY (0.08% Cu, cast, extruded, heat treated at 400°C). Torsion. Axial mean strain. $\epsilon_a = 2 \times 10^{-3}$ to 1.6×10^{-2}. T = 23 to 151°C. $\eta_s = 6 \times 10^{-2}$ to 1.4×10^{-2}. 4x decrease with ϵ_a. 2x decrease with T. (56 M, Figure 40)

ALUMINUM ALLOYS (0.1 to 5.4% Mg., cast, extruded, various heat treatments). Torsion. T = 100 to 500°C. $\eta_s = 10^{-3}$ to 2×10^{-1}. 100x increase with T. 10x decrease with % Mg. (56 M, Figure 41)

ALUMINUM ALLOY (11% Mg., extruded). Torsion. $\epsilon_a = 2 \times 10^{-3}$ to 7×10^{-3}. $N = 2 \times 10^5$ to 10^8. $\eta_s = 6 \times 10^{-6}$ to 10^{-4}. 20x increase with ϵ_a. 10x decrease with N. (46 H, Figure 42)

ALUMINUM ALLOYS (Heat-treated, wrought alloys No. 2014-T6, X2020, 2024-T4, 2219-T62, 2618-T6). Bending. At 300 psi, $\eta_s = 3 \times 10^{-3}$ to 5×10^{-3}. At 1 ksi, $\eta_s = 4 \times 10^{-3}$ to 6×10^{-3}. At 10 ksi, $\eta_s = 5 \times 10^{-3}$ to 8×10^{-3}. (62 K)

ALUMINUM ALLOYS (Cast and heat-treated alloys 319F, 319-T6, and 356-T6). Bending. σ_a = 3 to 10 ksi. $\eta_s = 4 \times 10^{-3}$ to 8×10^{-3}. (62 K)

ALUMINUM ALLOYS (Powder metallurgy type AMP alloys XAP001, XAP004, and M484). At 3 ksi, $\eta_s = 6 \times 10^{-3}$ to 8×10^{-3}. At 10 ksi, $\eta_s = 9 \times 10^{-3}$ to 1.5×10^{-2}. (62 K)

ALUMINUM ALLOYS (Alclad 2024-T3, 5% clad on each side, and alclad 6061-T4, 10% clad on each side). At 1 ksi, $\eta_s = 5 \times 10^{-3}$. At 10 ksi, $\eta_s = 5 \times 10^{-2}$. Damping about 10 times that of bare metal at 10 ksi. (62 K)

ALUMINUM ALLOYS (Alclad 2024-T3, 10% on each side, and alclad 6061-T4, 20% on each side). At 1 ksi, $\eta_s > 8 \times 10^{-2}$. At 10 ksi, $\eta_s = 1.2 \times 10^{-1}$. Damping 20x that of bare metal. (62 K)

ALUMINUM ALLOYS (Electrical conductor alloys, EC-H12, EC-T64, EC-H13). At 300 psi, $\eta_s = 6 \times 10^{-3}$ to 8×10^{-3}. At 5 ksi, $\eta_s = 8 \times 10^{-3}$ to 10^{-2}. At 10 ksi, $\eta_s = 2 \times 10^{-2}$ to 5×10^{-2}. (62 K)

ALUMINUM ALLOY (6061-T6). See Aluminum Alloy 2024-T4, reference 63 Ai. $n = 1.942$ and $J = 4.41 \times 10^{-11}$ for $\sigma < 15.5$ ksi. $n = 2.881$ and $J = 5.13 \times 10^{-15}$ for $\sigma > 15.5$ ksi. (63 Ai)

BERYLLIUM ALLOY (Produced by Brush Beryllium Co.; 18.6 Be, 1.5% Be O, 0.12% Fe, 0.04% Al, 0.03% Mg, 0.01% Ni; $E = 44 \times 10^6$ psi, ultimate tensile strength = 46.7 ksi, 0.2% offset yield

strength = 36.4 ksi, fatigue strength at 2×10^6 cycles = 33.0 ksi). At 2 ksi, D = 0.005. At 5 ksi, D = 0.025. At 10 ksi (cyclic stress sensitivity limit), D = 0.1. At 20 ksi, D = 2.0. At 50 ksi, D = 130. From 2 to 10 ksi η is approximately 0.015, from 10 to 50 ksi η increases from 0.015 to 0.9. (59 Tor)

BISMUTH. Elastic-plastic bending. f = 1. N = 0 to 800. $\eta_s = 3 \times 10^{-3}$ to 1.6×10^{-2}. $\eta_s = 1.6 \times 10^{-2}$ peak at N = 600. (61 Ga, Figure 43)

BISMUTH (Cast). Bending. f = 2,000. $\eta_s = 5.6 \times 10^{-4}$. (38 Fors)

CADMIUM (Cast). Bending. f = 2,000. $\eta_s = 3.5 \times 10^{-4}$. (38 Fors)

CHROMIUM (Pure, annealed at 1150°C, grain size of 2-7 microns). Torsion. T = 0 or 55°C. σ_m = 34 to 232 Kg/cm^2. $\gamma_a = 10^{-5}$ to 10^{-4}. At T = 0°C, $\eta_s = 10^{-4}$ to 5×10^{-4}, 3x increase with γ_a, 2x increase with σ_m. At T = 55°C, $\eta_s \approx 2.5 \times 10^{-5}$, little change with γ_a or σ_m. (61 Mort, Figures 44 and 45)

CHROMIUM (Pure, annealed at 1150°C, grain size of 2-7 microns). Torsion. σ_m = 34 to 232 Kg/cm^2. T = -60 to +50°C. $\eta_s = 7 \times 10^{-4}$ to 3×10^{-5}. 20x decrease with T. 2x increase with σ_m. (61 Mort, Figures 46, 47, and 48)

CHROMIUM IRON (13% Cr). Range of values observed at various temperatures as stress is increased from 5 to 35 ksi. At T = 24°C, $\eta_s = 0.7 \times 10^{-3}$ to 7×10^{-3}. At T = 260°C, $\eta_s = 10^{-3}$

to 7×10^{-3}. At T = 482°C, $\eta_s = 2 \times 10^{-3}$ to 4×10^{-3}. At T = 566°C, $\eta_s = 3 \times 10^{-3}$ to 4.5×10^{-3}. (62 Sm*)

COBALT ALLOY (Stellite 31, cast, polished). Rotating bending. N = 10^2 to 10^4. At T = 1,200°F and σ_a = 10 to 60 ksi, D = 5×10^{-2} to 5×10^2, with D = 8×10^{-1} at $\sigma_a = \sigma_g$ = 25 ksi. At T = 1,500°F and σ_a = 10 to 50 ksi, D = 6×10^{-1} to 1.5×10^2, with D = 5 at $\sigma_a = \sigma_g$ = 34 ksi. In both cases there is a 5x decrease with N. (56 Po, Figures 49 and 50)

COBALT ALLOY (Nivco 10, solution treated, aged). Torsion. T = 70 to 1,200°F. τ_a = 3 to 15 ksi. $\eta_s = 5 \times 10^{-3}$ to 5×10^{-2}. 10x increase with τ_a. 2x increase with T. (59 Co, Figure 51)

COBALT ALLOY (Stellite 31, cast, aged at 1,350°F, furnace cooled to 1,000°F, air cooled). Rotating bending. N = 10^2 to 10^5. At T = 1,200°F and σ_a = 10 to 60 ksi, D = 5×10^{-2} to 8×10^1, with D = 2.5 at $\sigma_a = \sigma_g$ = 38 ksi. At T = 1,500°F and σ_a = 10 to 50 ksi, D = 1.5×10^{-1} to 5×10^1, with D = 4 at $\sigma_a = \sigma_g$ = 30 ksi. In both cases there is a 5 to 10x decrease with N. (56 Po, Figures 52 and 54)

COBALT ALLOY (Nivco 10, heat treated). τ_a = 1 to 20 ksi. $\eta = 5 \times 10^{-3}$ to 8×10^{-2}. (59 Laza, Figure 53)

COBALT ALLOY (20% Fe). Torsion. $\gamma_a = 10^{-4}$ to 6×10^{-4}. $\eta_s = 1.5 \times 10^{-2}$ to 3×10^{-2} with no magnetic field. $\eta_s = 6 \times 10^{-4}$ to 2×10^{-3} with a magnetic field of 500 oersteds. (56 Co, Figure 55)

COBALT ALLOY (28% Ni). Torsion. $\gamma_a = 10^{-4}$ to 6×10^{-4}. $\eta_s = 4 \times 10^{-3}$ to 3×10^{-2} with no magnetic field. $\eta_s = 6 \times 10^{-4}$ to 3×10^{-3} with a magnetic field of 500 oersteds. (56 Co, Figure 56)

COBALT ALLOY (23% Ni, annealed at 1,900°F for 1 hr., air cooled). Bending. T = 75°F. σ_m = 0 to 11 ksi. σ_a = 1 to 30 ksi. $\eta_s = 5 \times 10^{-4}$ to 7×10^{-3}. 7x increase with σ_a. 5x decrease with σ_m. (60 Cl, Figure 57)

COBALT ALLOY (35% Ni). Torsion. $\gamma_a = 10^{-4}$ to 6×10^{-4}. Under magnetic field of 500 oersted, $\eta_s = 10^{-3}$ to 4×10^{-2}. Under no magnetic field, $\eta_s = 8 \times 10^{-3}$ to 6×10^{-2} with $\eta_s = 6 \times 10^{-2}$ peak at $\gamma_a = 2.5 \times 10^{-4}$. (56 Co, Figure 58)

COBALT ALLOY (34% Ni, 2% Fe, 2% Ti, annealed at 1,900°F, air cooled). Bending. σ_a = 1 to 30 ksi. σ_m = 0 and 11 ksi. T = 75,600, and 1,100°F. $\eta_s = 3 \times 10^{-4}$ to 6×10^{-3}. 20x increase with σ_a at T = 75°F. 3x decrease with σ_m at 75°F. 5x increase with σ_a at T = 600°F and σ_m = 11 ksi. 8x increase with σ_a and 2x change with σ_m at T = 1,100°F. (60 Cl, Figures 59 and 60)

COBALT ALLOY (S-816, annealed, ground, annealed at 2,300°F, water quenched, aged at 1,400°F). Rotating bending. $N = 10^{1.3}$ to 10^7. At T = 70°F and σ_a = 20 to 120 ksi, $D = 10^{-1}$ to 2×10^3, with D = 1 at $\sigma_a = \sigma_g$ = 40 ksi. At T = 1,350°F and σ_a = 10 to 80 ksi, $D = 10^{-1}$ to 10^3, with D = 2.6 at $\sigma_a = \sigma_g$

= 40 ksi. At T = 1,650°F and σ_a = 10 to 50 ksi, D = 5 x 10^{-1} to 2 x 10^{2}, with D = 2 at $\sigma_a = \sigma_g$ = 24 ksi. (56 Po, Figures 61, 62, and 64)

COBALT ALLOY (S-816, ground, annealed at 2,300°F, water quenched, aged at 1,400°F). Bending. σ_a = 3 to 50 ksi. σ_m = 0 to 42 ksi. D = 10^{-4} to 5. 10x increase with σ_m. 100x increase with σ_a. (56 Pe, Figure 63)

COBALT ALLOY (30% Fe, air cooled or water quenched). Torsion. With and without magnetic field. τ_a = 1 to 12 ksi. η_s = 2 x 10^{-3} to 3 x 10^{-2}. Air cooled, η_s = 2 x 10^{-3} to 3 x 10^{-3} with magnetic field, η_s = 10^{-2} to 3 x 10^{-2} without magnetic field. Quenched, η_s = 2.5 x 10^{-3} to 8 x 10^{-3} without magnetic field. (53 Co, Figure 65)

COBALT ALLOY (Vitallium, 29% Cr, 5% Mo, 0.5% Mn, cast, annealed at 1,500°F, furnace cooled). Bending. f = 1,000. σ_a = 5 to 35 ksi. T = 75 to 1,200°F. η_s = 5 x 10^{-5} to 10^{-3}. 10x increase with T. 3x increase with σ_a. (44 Sc, Figure 66)

COPPER (Single crystal). f = 40,000. η = 1.1 x 10^{-5} for annealed crystal. η_s = 10^{-3} for unannealed crystal. (42 Bi*)

COPPER (Pure, single crystal). Bending. f = 10,000. Irradiated. Time of radiation = 0 to 360 hr. η_s = 3 x 10^{-3} to 3 x 10^{-4}. (58 Mas, Figure 69)

COPPER (Pure, single crystal). Kilocycle frequency region. ϵ_a =

3×10^{-7} to 35×10^{-7}. $\eta_s = 5 \times 10^{-4}$ to 7×10^{-3}. (50 Koe, Figure 68)

COPPER (Pure, single crystal, annealed). Axial stress. T = 0 and 23°C. $\epsilon_a = 7.5 \times 10^{-7}$ to 1.75×10^{-6}. $\eta = 6 \times 10^{-5}$ to 6×10^{-4}. Little increase with T. (41 R, Figure 72)

COPPER (Pure, annealed). f = 2,000. $\epsilon_a < 10^{-4}$. $\eta = 1.1 \times 10^{-3}$. (62 Sm*)

COPPER (Pure, annealed). Torsion. T = 0 to 400°C. At 4% cold work, $\eta_s = 3 \times 10^{-3}$ to 1.8×10^{-2}. At 55% cold work, $\eta_s = 3 \times 10^{-3}$ to 4×10^{-2}. (54 M, Figure 67)

COPPER (Pure). Torsion. τ_a = 2 to 14 ksi. $\eta_s = 5 \times 10^{-3}$ to 3×10^{-2}. (53 B, Figure 70)

COPPER (Crystal). Axial stress. f = 30,000. T = 10 to 150°K. $\eta_s = 10^{-4}$ to 5×10^{-3}. 50x peak at T = 90°K. (58 Mas, Figure 77)

COPPER (Pure, 44% reduction, annealed). Torsion. T = 20 to 250°C. $\gamma_a = 2 \times 10^{-5}$ to 10^{-4}. $\eta_s = 5 \times 10^{-3}$ to 10^{-1}. 10x increase with γ_a. 5x increase with T. (54 M, Figure 75)

COPPER (Pure, drawn or annealed). Bending. f = 20 to 550. Drawn, $\eta_s = 2.5 \times 10^{-3}$ to 8×10^{-4}. Annealed, $\eta_s = 7 \times 10^{-3}$ to 2×10^{-3}. (56 Mi, Figures 73 and 76)

COPPER (Pure). T = 10 to 300°K. Under bending, f = 100, η_s =

10^{-4} to 3×10^{-3}. Under shear, f = 1.45×10^{7}, $\eta_s = 10^{-4}$ to 10^{-3}. (58 Mas, Figure 71)

COPPER (Pure, annealed). Torsion. T = 10 to 200°K. $\eta_s = 2 \times 10^{-3}$ to 5×10^{-4}. Peak at T = 60°K. Minimum at T = 120°K. (61 Ni, Figure 78)

COPPER (Pure). Torsion. $\gamma_a = 10^{-2}$ to 8×10^{-2}. $\eta_s = 3 \times 10^{-3}$ to 3.2×10^{-2}. (57 Kea, Figure 74)

COPPER (Pure, some silicon). Torsion. T = 100 to 600°C. $\eta_s = 2 \times 10^{-3}$ to 5×10^{-2}. (58 Mas, Figure 80)

COPPER (Annealed 30 min. at 400°C). Bending. f = 2,000. $\eta_s = 1.1 \times 10^{-3}$. (38 Fors)

COPPER. Small strain. Axial stress. f = 10,000. $\eta_s = 1.0 \times 10^{-4}$ to 1.9×10^{-3}. (41 Ki*)

COPPER. Small strains. Bending. f = 1 to 10. $\eta_s = 1.0 \times 10^{-3}$. (41 Ki*)

COPPER. Torsion. $\eta_s = 5.1 \times 10^{-2}$. (41 Ki*)

COPPER (Annealed or rolled). Strain less than 10^{-4}. Bending. f = 2. $\eta_s = 7.6 \times 10^{-4}$ for annealed case. $\eta_s = 4.0 \times 10^{-4}$ for rolled case. (41 Ki*)

COPPER. Small strain. Axial stress. f = 45,000. $\eta_s = 6.4 \times 10^{-4}$. (41 Ki*)

COPPER. Bending. f = 1 to 5. $\eta_s = 2.2 \times 10^{-4}$. (41 Ki*)

COPPER (Annealed). Strains of 10^{-4} to 10^{-3}. Torsion on hollow tubes. f = 20. $\sigma_a = 1.1$ ksi. $\eta_s = 7.6 \times 10^{-3}$. (41 Ki*)

COPPER (Pure, annealed, and cold worked). f = 0.1 to 10,000. $\epsilon < 10^{-4}$. $\eta = 2.2 \times 10^{-4}$ to 6.4×10^{-4}. (62 Sm*)

COPPER (Red). Torsion. T = 50 to 150°C. $\eta_s = 7 \times 10^{-4}$ to 7×10^{-3}. (31 C, Figure 98)

COPPER ALLOY (2.6% Co, 0.4% Be, solution treated at 900°C, quenched, aged at 500°C). Torsion. $\tau_a = 0$ to 10 ksi. $\eta_s = 4 \times 10^{-5}$ to 2×10^{-4}. (38 F1, Figure 79)

COPPER ALLOY (2% Be, four treatments having different quenches and aging). Torsion. $\tau_a = 5$ to 25 ksi. $\eta_s = 10^{-4}$ to 5×10^{-4}. 5x increase with τ_a. 4x changes with treatments. (39 N, Figure 81)

COPPER ALLOY (2.12% Be, 0.30% Fe, 0.30% Ni, solution treated at 800°C, four different age treatments). Torsion. $\tau_a = 5$ to 20 ksi. $\eta_s = 10^{-4}$ to 6×10^{-4}. 5x increase with τ_a. 4x change with treatment. (38 F1, Figure 82)

COPPER ALLOY (0.81% Cr, 0.02% Si, solution treated at 1025°C, aged at 500°C for 20 min. to 2 hr.). Torsion. $\tau_a = 5$ to 15 ksi. $\eta_s = 3 \times 10^{-5}$ to 2×10^{-2}. 10x increase with τ_a. 1,000x change with aging. (38 F1, Figure 83)

COPPER ALLOY (Brass). Bending. f = 50 to 600. $\eta_s = 3 \times 10^{-3}$ to 6×10^{-3}. $\eta_s = 6 \times 10^{-3}$ peak at f = 400. (49 K, Figure 84)

COPPER ALLOY (Brass, drawn). Bending. f = 0 to 3,000. $\eta_s = 3 \times 10^{-4}$ to 2×10^{-5}. (56 Mi, Figure 86)

COPPER ALLOY (Brass). Torsion. σ_m = 2 to 12 ksi. $\eta_s = 2 \times 10^{-4}$ to 2×10^{-3}. (62 Pisa, Figure 89)

COPPER ALLOY (2% Be, aged). f = 1,300. $\epsilon_a < 10^{-4}$. $\eta = 4 \times 10^{-6}$ 1.6×10^{-5}. (62 Sm*)

COPPER ALLOY (Brass). Torsion. τ_a = 5 to 30 ksi. $\eta_s = 2 \times 10^{-3}$ to 4×10^{-2}. (53 B, Figure 91)

COPPER ALLOY (Brass, 70.59% Cu, 29.39% Zn, cold drawn with 65% area reduction, annealed at 400°C, air cooled). Bending. 0 to 25% elongation. $\eta_s = 10^{-6}$ to 2×10^{-4}. (42 Ze, Figure 85)

COPPER ALLOY (α-Brass, single crystal). f = 620. T = 320 to 560°C. $\eta_s = 5 \times 10^{-4}$ to 10^{-2}. $\eta_s = 10^{-2}$ peak at T = 420°C. (58 Mas, Figure 87)

COPPER ALLOY (α-Brass, not of high purity). Torsion. T = 350 to 600°C. $\eta_s = 7 \times 10^{-4}$ to 7×10^{-2}. $\eta_s = 7 \times 10^{-2}$ peak at T = 500°C. (58 Mas, Figure 92)

COPPER ALLOY (0 to 9.7% Zn). Bending. f = 2,000. $\epsilon_a = 10^{-7}$ to

10^{-3}. $\eta_s = 10^{-4}$ to 10^{-2}. 10x increase with ϵ_a. 20x increase with % Zn. (58 Mas, Figure 88)

COPPER ALLOY (31.5%, 19.7%, or 11.1% Zn). Torsion. T = 50 to 200°C. $\eta_s = 2 \times 10^{-4}$ to 2×10^{-3}. 10x increase with T. 1.5 change with % Zn. (31 C, Figure 90)

COPPER ALLOY (38 to 47% Zn, 0 to 1% Fe, 0 to 1% Sn, 0 to 1% Mn). Torsion. $\tau_a = 1$ to 7 ksi. $\eta_s = 2 \times 10^{-4}$ to 10^{-3}. 2x increase with τ_a. 1.5x change with % Zn. (44 B, Figure 94)

COPPER ALLOY (5.42% Sn). Torsion. $\tau_a = 2$ to 7 ksi. $\eta_s = 5 \times 10^{-4}$ to 7×10^{-4}. (44 B, Figure 93)

COPPER ALLOY (9%, 6%, or 3% Sn, also 3% Sn plus 0.05% Be, annealed). Low stress. Torsion. T = 0 to 500°C. $\eta_s = 3 \times 10^{-4}$ to 7×10^{-2}. 200x increase with T. 5x change with composition. (54 M, Figure 97)

COPPER ALLOY (5 to 15% Sn, annealed) f = 13,000. $\epsilon_a < 10^{-4}$. $\eta = 1.3 \times 10^{-4}$ to 1.8×10^{-4}. (62 Sm*)

COPPER ALLOY (α-Brass, 30% Zn, annealed and cold worked up to 30%). f = 10 to 36,000. $\epsilon_a < 10^{-4}$. $\eta = 3 \times 10^{-6}$ to 10^{-4}. (62 Sm*)

COPPER ALLOY (British types). Torsion. $\tau_a = 5$ ksi. Hidurel 6 (as cast), $\eta_s = 19 \times 10^{-4}$. Gun metal (88% Cu., 10% Zn, 2% Sn), $\eta_s = 16 \times 10^{-4}$. Brass (B.S. 265 as extruded), $\eta_s = 7 \times 10^{-4}$. Hidurel 5 (as cast), $\eta_s = 7 \times 10^{-4}$. Hidurel 7

(as cast), $\eta_s = 5 \times 10^{-4}$. High tensile brass (E. Ih. C. 2C100, as cast), $\eta_s = 5 \times 10^{-4}$. Novaston, $\eta_s = 5 \times 10^{-5}$. (64 Bi)

COPPER ALLOY (Bronze). Torsion. σ_m = 2 to 12 ksi. $\eta_s = 1.5 \times 10^{-4}$ to 10^{-2}. (62 Pisa, Figure 95)

COPPER ALLOY (Phosphorous bronze). Torsion in hollow tubes. f = 20. $\gamma_a = 10^{-4}$ to 10^{-3}. $\eta_s = 1.8 \times 10^{-3}$. (41 Ki*)

COPPER ALLOY (Phosphorous bronze). Rotating bending. $\epsilon_a = 5 \times 10^{-3}$. $\eta_s = 1.2 \times 10^{-4}$. (41 Ki*)

COPPER ALLOY (Phosphorous bronze). Static tests. At σ_m = 60 ksi, $\eta_s = 5.8 \times 10^{-4}$. At σ_m = 100 ksi, $\eta_s = 2.1 \times 10^{-3}$. (41 Ki*)

COPPER ALLOY (10% Ni). Torsion. T = 50 to 300°C. $\eta_s = 3 \times 10^{-4}$ to 10^{-2}. (31 C, Figure 96)

GOLD (99.998% pure. Various annealing temperatures and cold working). Torsion. f = 1. T = 200 to 1,200°F. Low stress. $\eta_s = 2 \times 10^{-3}$ to 5×10^{-2}. 30x increase with T. (58 Mas, Figures 99, 100, and 102)

IRON (Pure, cold drawn, heated in wet H_2 at temperature, various treatments and aging). Torsion. $\gamma_a = 0$ to 8×10^{-5}. f = 0.83. In various magnetic fields. T = -150 to 70°C. $\eta_s = 2 \times 10^{-3}$ to 2×10^{-2}. (61 Fa, Figures 103, 104, 105, 106, 108, 109, 110, and 111)

IRON (Electrolytic). Torsion. f = 1. T = 100 to 150°K. η_s = 1.2×10^{-2}. Negligible change with T. (53 Ch, Figure 101)

IRON (0.003% C, heat treated, quenched). Torsion. f = 1. T = -15°C. $\gamma_a = 10^{-5}$ to 8×10^{-5}. $\eta_s = 2 \times 10^{-3}$ to 10^{-2}. 5x increase with γ_a. 5x change with time after deformation. (61 Fa, Figures 124 and 125)

IRON (Note of high purity). Torsion. T = 300 to 550°C. η_s = 2×10^{-3} to 7×10^{-2}. $\eta_s = 6 \times 10^{-2}$ peak at T = 500°C. (58 Mas, Figure 107)

IRON (Carbon free, heat-treated). Torsion. T = -15°C. γ_a = 10^{-5} to 7×10^{-5}. A magnetic field of 200 oersteds. η_s = 2.5×10^{-3} to 2×10^{-2}. 4x increase with γ_a. 5x increase with time after deformation. (61 Fa, Figure 112)

IRON (Various amounts of N). Torsion. T = -80 to +40°C. η_s = 3×10^{-3} to 3×10^{-2}. 10x peak at T = -20°C. 10x change with composition and treatment. (58 Mas, Figure 113)

IRON (0.0028% C, 0.0014% N, various treatments). Torsion. γ_a = 10^{-4} to 6×10^{-4}. $\eta_s = 10^{-3}$ to 3×10^{-2}. 20x peak at γ_a = 1.5×10^{-4}. 4x change with treatment. (58 Su, Figure 122)

IRON (0.04% C, three treatments). Torsion. T = 0 to 60°C. η_s = 10^{-3} to 2×10^{-2}. 20x peak at 40°C. 5x change with treatment. (51 F, Figure 130)

IRON (0.02% N, two treatments). Torsion. T = -20 to 60°C. η_s =

10^{-3} to 2×10^{-2}. 20x peak at T = 25°C. 4x change with treatment. (51 F, Figure 115)

IRON (0.001% C, cold drawn, heated in H_2 with 0.001% CH_4, quenched from 600°C). Torsion. f = 1. $\gamma_a = 2 \times 10^{-5}$ to 6×10^{-5}. $\eta_s = 2 \times 10^{-3}$ to 10^{-2}. 5x increase with γ_a. 5x change with deformaging and aging. (61 Fa, Figure 120)

IRON (Annealed 30 min. at 930°C, air cooled). Bending. f = 2,000. $\eta_s = 1.8 \times 10^{-4}$. (38 Fors)

IRON (GBC-1, annealed, drawn, recrystallized at 750°C). Torsion. f = 2.5. T = 420 to 620°C. $\eta_s = 4 \times 10^{-2}$ to 8×10^{-2}. $\eta_s = 8 \times 10^{-2}$ peaks at T = 500 and 620°C. (61 Lea, Figure 121)

IRON (Pure, annealed). f = 2,000. $\epsilon_a < 10^{-4}$. $\eta = 1.8 \times 10^{-4}$. (62 Sm*)

IRON (GBC-4, annealed, drawn, recrystallized at 750°C). Torsion. f = 1.79. T = 440 to 600°C. $\eta_s = 3 \times 10^{-2}$ to 10^{-1}. $\eta_s = 10^{-1}$ peak at T = 530°C. (61 Lea, Figure 123)

IRON (Armco, no carbon). Torsion. $\gamma_a = 10^{-2}$ to 8×10^{-2}. $\eta_s = 3 \times 10^{-3}$ to 4×10^{-2}. $\eta_s \approx 3.5 \times 10^{-2}$ for $\gamma_a > 2 \times 10^{-2}$. (57 Kea, Figure 126)

IRON (Armco, 0.020% C, annealed in vacuum at 720°C, cooled slowly). Torsion. f = 2. $\gamma_a = 10^{-2}$ to 8×10^{-2}. $\eta_s = 8 \times 10^{-3}$ to 3×10^{-2}. (57 Kea, Figure 127)

IRON (Armco). $\eta = 5 \times 10^{-5}$. (62 P1)

IRON (Armco, annealed in vacuum at 720°C, cooled slowly). Torsion. f = 2. $\gamma_a = 10^{-2}$ to 8×10^{-2}. T = 280°C. $\eta_s = 4 \times 10^{-3}$ to 1.4×10^{-2}. (57 Kea, Figure 131)

IRON (Armco, 0.019% C, 75% and 25% drawn). f = 1. T = 0 to 400°C. $\eta_s = 10^{-3}$ to 5×10^{-3}. 4x change with T. (60 Pigu, Figure 128)

IRON (Armco). Torsion. τ_a = 2 to 14 ksi. $\eta_s = 2.5 \times 10^{-3}$ to 7×10^{-3}. Minimum at τ_a = 10 ksi. (62 Pisa, Figure 129)

IRON (Armco, 25% and 80% cold drawn, aged). T = 20°C. $\eta_s = 10^{-3}$ to 2×10^{-4}. 5x decrease with time after deformation. (58 Mas, Figure 132)

IRON (Armco). $\gamma_a = 10^{-4}$ to 10^{-3}. Torsion on hollow tubes. f = 20. σ_a = 11.6 ksi. $\eta_s = 6.4 \times 10^{-3}$. (41 Ki*)

IRON (Armco, annealed). Static test. σ_a = 8 ksi. $\eta_s = 3.7 \times 10^{-3}$. (41 Ki*)

IRON ALLOY (1.1% Si, 0.005% Mn, 0.005% S, 0.0035% N, 0.0034% C, annealed, quenched from 1,050°C). Torsion. f = 0.93. T = 0 to 80°C. $\eta_s = 3 \times 10^{-3}$ to 3×10^{-4}. $\eta_s = 3 \times 10^{-3}$ peak at T = 20°C. (61 R, Figure 118)

IRON ALLOY (0.5% Mn, 0.04% C, three treatments). Torsion. T = 0 to 60°C. $\eta_s = 10^{-3}$ to 10^{-2}. 10x peak at T = 40°C. 5x change with treatments. (51 F, Figure 114)

IRON ALLOY (0.5% Mn, 0.02% N, two treatments). Torsion. T = -20 to 60°C. $\eta_s = 10^{-3}$ to 10^{-2}. 10x peak at T = 30°C. (51 F, Figure 116)

IRON ALLOY (40% Co, forged, ground, heat treated at 900°C in H_2). Torsion. τ_a = 5 to 40 ksi. σ_m = 0.3 to 10 ksi. $\eta_s = 3 \times 10^{-3}$ o 7×10^{-2}. 5x increase with τ_a. 10x decrease with σ_m. (53 Coc, Figure 117)

IRON ALLOY (Steel). Bending. Strain < 10^{-4}. f = 2. σ_m = 3 ksi. $\eta_s = 4.8 \times 10^{-4}$. (41 Ki*)

IRON ALLOY (Steel). Torsion on hollow tubes. At σ_m = 6 ksi, $\eta_s = 1.4 \times 10^{-4}$. At σ_m = 10 ksi, $\eta_s = 2.4 \times 10^{-4}$. (41 Ki*)

IRON ALLOY (Steel, annealed at 800°C). Static test. σ_m = 6 ksi. $\eta_s = 1.4 \times 10^{-3}$. (41 Ki*)

IRON ALLOY (Steel, hard drawn). Small strain. Torsion. f = 0.25. $\eta_s = 6 \times 10^{-7}$. (41 Ki*)

IRON ALLOY (Steel). Medium strain. Bending. f = 9. $\eta_s = 1.3 \times 10^{-3}$. (41 Ki*)

IRON ALLOY (Steel, cold rolled). Torsion on hollow tubes. γ_a = 10^{-4} to 10^{-3}. f = 20. σ_a = 9.9 ksi. $\eta_s = 5.9 \times 10^{-3}$. (41 Ki*)

IRON ALLOY (Steel, annealed at 800°C). Torsion. f = 67. σ_m = 6 ksi. $\eta_s = 7.6 \times 10^{-4}$. (41 Ki*)

IRON ALLOY (Bearing steel). Torsion. $\eta_s = 1.3 \times 10^{-4}$. (41 Ki*)

IRON ALLOY (Steel). Small strain. Axial stress. f = 10,000. $\eta_s = 2.4 \times 10^{-5}$ to 2.4×10^{-4}. (41 Ki*)

IRON ALLOY (Steel). Torsion. $\eta_s = 2.9 \times 10^{-2}$. (41 Ki*)

IRON ALLOY (Ball bearing steel). Torsion. $\sigma_m = 30$ ksi. $\eta_s = 6.7 \times 10^{-4}$. (41 Ki*)

IRON ALLOY (SAE 1018 Steel, soft cold rolled, strip). Uniaxial stress for beams. Biaxial stress for plate. $\sigma_a = 0.1$ to 8 ksi. $\eta_s = 10^{-4}$ to 2×10^{-3}. 10x increase with σ_a. 2x change with rolling direction. (61 W, Figure 133)

IRON ALLOY (SAE 1020 Steel). $\sigma_a = 2$ to 40 ksi. $N = 10^{1.3}$ to 10^6. $D = 10^{-2}$ to 5×10^1. 4,000x increase with σ_a. 10x increase with N. (57 A, Figure 134)

IRON ALLOY (SAE 1020 Steel, hot rolled). Bending. f = 1,000. $\sigma_a = 5$ to 35 ksi. T = 75 to 500°F. $\eta_s = 5 \times 10^{-4}$ to 3×10^{-3}. 9x increase with σ_a. 3x change with T. (44 Sc, Figure 135)

IRON ALLOY (SAE 1020 Steel, hot rolled). Bending. $\sigma_a = 5$ to 35 ksi. $\sigma_m = 0$ to 21 ksi. $D = 10^{-3}$ to 10^{-1}. 20x increase with σ_a. 10x increase with σ_m. (56 Pe, Figure 136)

IRON ALLOY (SAE 1020 Steel). Torsion. $\tau_a = 10$ to 35 ksi. $\eta_s = 10^{-3}$ to 4×10^{-2}. (53 B, Figure 137)

IRON ALLOY (1020 Steel, annealed). See Aluminum Alloy 2024-T4, reference 63 Ai. $n = 2.286$ and $J = 2.626 \times 10^{-13}$ for $\sigma_a <$ 15 ksi. (63 Ai)

IRON ALLOY (0.21% C Steel, 0.37% Mn, normalized, then cold worked by 90° permanent set, aged 10 min. to 1 yr.). Torsion. $\tau_a =$ 5 to 25 ksi. $\eta_s = 2 \times 10^{-3}$ to 5×10^{-2}. 10x increase with aging. 10x increase with τ_a. (38 C, Figure 138)

IRON ALLOY (Mild steel). Bending. $\sigma_a = 2.5$ to 5.5 ksi. $\eta_s = 9 \times 10^{-4}$ to 1.4×10^{-3}. (57 Tr, Figure 139)

IRON ALLOY (Mild steel, cold rolled). Strains of about 5×10^{-3}. Rotating bending. $\eta_s = 1.6 \times 10^{-3}$. (41 Ki*)

IRON ALLOY (0.70% C Steel, annealed, or pickled, or both). $f = 1$. $T = 100$ to 150°K. $\eta_s = 10^{-3}$ to 2×10^{-3}. Little change with T. 2x increase with treatment. (53 Ch, Figure 140)

IRON ALLOY (SAE 1020 Steel). Under axial stress, $\sigma_a = 4$ to 18 ksi, $D = 3 \times 10^{-2}$ to 3. Under shear, $\tau_a = 8$ to 40 ksi, $D = 3 \times 10^{-2}$ to 10. (57 Y, Figure 141)

IRON ALLOY (SAE 1025 Steel, seam-welded tubing). Axial stress. $\sigma_a = 5$ to 40 ksi. $D = 10^{-2}$ to 3×10^{-1}. (46 Ro, Figure 142)

IRON ALLOY (0.28% C Steel, 0.79% Mn, 0.20% Si, 0.44% other, annealed in vacuum at 625°C). Magnetic field of 0 and 200 oersteds. Torsion. $f = 20$. $\gamma_a = 2 \times 10^{-4}$ to 16×10^{-4}. $\eta_s = 10^{-4}$ to 5×10^{-3}. 100x increase with magnetization. (58 Su, Figure 143)

IRON ALLOY (0.38% C Steel, 0.85% Mn, normalized, then cold worked by 90° permanent set, aged 10 min. to 60 days). Torsion. τ_a = 5 to 10 ksi. $\eta_s = 2.5 \times 10^{-3}$ to 2×10^{-2}. 5x increase with τ_a. 10x increase with aging. (38 C, Figure 144)

IRON ALLOY (0.40% C Steel, normalized from 850°C, drawn at 650°C). Torsion. τ_a = 1 to 15 ksi. $\eta_s = 8 \times 10^{-4}$ to 4×10^{-3}. (38 F1, Figure 145)

IRON ALLOY (0.40% C Steel, air cooled from 1,560°F, drawn at 1,200°F). Torsion. With and without magnetic field. τ_a = 4 to 18 ksi. $\eta_s = 5.5 \times 10^{-4}$ to 4×10^{-3}. 2x increase with τ_a. 5x increase with magnetization. (40 P, Figure 146)

IRON ALLOY (0.17% C mild steel, normalized, En 3). Torsion. τ_a = 5 ksi. $\eta_s = 2.4 \times 10^{-3}$. (64 Bi)

IRON ALLOY (Three silvers steels, B.S. 140?). Torsion. τ_a = 5 ksi. Speriodized, $\eta_s = 1.2 \times 10^{-3}$. Water quenched at 800°C, $\eta_s = 8 \times 10^{-4}$. Water quenched at 800°C and aged 1.5 hrs. at 100°C, $\eta_s = 3 \times 10^{-4}$. (64 Bi)

IRON ALLOY (Steel B.S. S62, 12% Cr, 0.2% C, quenched and tempered to 225 B.H.N.). Torsion. τ_a = 5 ksi. $\eta_s = 6 \times 10^{-3}$. (64 Bi)

IRON ALLOY (Cr-Ni steels, solution treated 1,050°C and water quenched). Torsion. τ_a = 5 ksi. For En 58B (18% Cr, 8% Ni, 0.6% Ti, 0.1% C), $\eta_s = 3 \times 10^{-3}$. For NMC (0.62% C, 3.86% Cr,

8.6% Ni, 7.3% Mn), $\eta_s = 1.3 \times 10^{-3}$. For En 58A (18% Cr, 8% Ni, 0.1% C), $\eta_s = 6 \times 10^{-4}$. (64 Bi)

IRON ALLOY (0.40% C Steel, water quenched, tempered at 650°C). Torsion. τ_a = 5 to 20 ksi. $\eta_s = 2 \times 10^{-3}$ to 5×10^{-3}. (51 Fer, Figure 264)

IRON ALLOY (Steel). Bending. f = 20 to 200. $\eta_s = 2.5 \times 10^{-3}$ to 6×10^{-3}. $\eta_s = 6 \times 10^{-3}$ peaks at f = 40 and 160. (49 K, Figure 147)

IRON ALLOY (0.30% C Steel, carbide-forming 25-20 type austenitic). Low stress. Torsion. T = 0 to 800°C. $\eta_s = 10^{-4}$ to 2×10^{-3}. Peaks at 300 and 650°C. (53 Ro, Figure 148)

IRON ALLOY (Steel, normalized at 1,650°F, various compositions) Torsion. τ_a = 4 to 12 ksi. $\eta_s = 1.5 \times 10^{-3}$ to 7×10^{-3}. 3x increase with stress. 3x change with composition. (44 B, Figure 149)

IRON ALLOY (SAE 1045 Steel). Torsion. τ_a = 5 to 40 ksi. $\eta_s = 2 \times 10^{-3}$ to 4×10^{-2}. (53 B, Figure 150)

IRON ALLOY (SAE 1095 Steel). Torsion. τ_a = 5 to 40 ksi. $\eta_s = 2 \times 10^{-3}$ to 3×10^{-2}. (53 B, Figure 151)

IRON ALLOY (0.42% C Steel, 0.99% Mn, 0.32% Si). f = 20. A magnetic field of 0 and 200 oersteds. $\eta_s = 6 \times 10^{-5}$ to 2×10^{-3}. 10x increase with magnetic field. 10x increase with f. (58 Su, Figure 152)

IRON ALLOY (0.92% C Steel, 0.24% Mn, 0.26% Si, annealed at 1100°C, quenched from TR = 660 to 730°C). Low stress. Torsion. f = 1. T = 0 to 300°C. $\eta_s = 10^{-3}$ to 10^{-2}. 10x change with T. 10x change with TR. Peaks at T = 40 and 200°C. (61 Shu, Figure 153)

IRON ALLOY (Russian steel 8). Torsion. τ_a = 2 to 10 ksi. η_s = 9×10^{-3} to 2×10^{-2}. (62 Pisa, Figure 154)

IRON ALLOY (Russian Steel 2). Torsion. Wire specimens of 10 to 20 mm diameter. τ_a = 2 to 10 ksi. $\eta_s = 3 \times 10^{-4}$ to 2×10^{-2}. 20x increase with τ_a. 10x increase with diameter. (62 Pisa, Figure 155)

IRON ALLOY (Russian Steel U7A, 0.47% Mn, 0.34% Si, quenched in vacuum from 900°C, two treatments). f = 1.1. T = 20 to 400°C. $\eta_s = 2 \times 10^{-3}$ to 1.4×10^{-2}. $\eta_s = 1.4 \times 10^{-2}$ peak at 220°C. (60 Pigu, Figure 156)

IRON ALLOY (0.62% C Steel, 1.14% Mn, normalized, then cold worked by 90° permanent set, aged 10 min. to 1 yr.). Torsion. τ_a = 5 to 30 ksi. $\eta_s = 2 \times 10^{-3}$ to 2×10^{-2}. 3x increase with τ_a. 5x increase with aging. (38 C, Figure 157)

IRON ALLOY (Russian Steels SCHX-9, EU-612, 40X, and carbon steel). Torsion. τ_a = 2 to 18 ksi. $\eta_s = 3 \times 10^{-4}$ to 6×10^{-3}. (62 Pisa, Figure 158)

IRON ALLOY (0.61% C Steel, 1.12% Mn, normalized, then cold worked by 90° permanent set, aged 10 min. to 14 days, or normalized).

Torsion. τ_a = 5 to 30 ksi. $\eta_s = 2 \times 10^{-3}$ to 2×10^{-2}. 5x increase with τ_a. 6x increase with aging. (38 C, Figure 159)

IRON ALLOY (SAE 1112 Steel, deformed, aged at room temperature or annealed). Torsion. τ_a = 10 to 160 ksi. $\eta_s = 2 \times 10^{-3}$ to 1.5×10^{-2}. 6x increase with τ_a. 6x change with treatment. (39 N, Figure 160)

IRON ALLOY (Russian Steel U9A, 0.02% C, 0.26% Si, 0.24% Mn, quenched from 670 or 720°C). f = 0.85. T = 20 to 300°C. $\eta_s = 8 \times 10^{-4}$ to 4×10^{-3}. Peak at 50 and 200°C. Little change with treatment. (60 Pigu, Figure 161)

IRON ALLOY (0.8% C Steel, drawn). Bending. f = 0 to 300. $\eta_s = 3 \times 10^{-3}$ to 3×10^{-4}. Most of decrease in η_s is for f < 20. (56 Mi, Figure 162)

IRON ALLOY (Russian Steel U12A, 1.16% C, quenched from 900°C, two treatments). f = 1.1. T = 0 to 400°C. $\eta_s = 2 \times 10^{-3}$ to 1.6×10^{-2}. $\eta_s = 1.6 \times 10^{-2}$ peak at T = 250°C. Little change with treatment. (60 Pigu, Figure 163)

IRON ALLOY (Russian Steel 45). Axial or bending stress. σ_a = 4 to 30 ksi. $\eta_s = 10^{-3}$ to 5×10^{-3}. 3x increase with σ_a. 2x increase with axial stress. (62 Pisa, Figure 164)

IRON ALLOY (Sandvik Steel, normalized). σ_a = 5 to 75 ksi. N = $10^{1.3}$ to 10^4. D = 7×10^{-3} to 3×10. D = 1 at $\sigma_a = \sigma_g$ = 55 ksi. 4x increase with N. (57 A, Figure 165)

IRON ALLOY (Sandvik Steel, quenched, tempered). σ_a = 30 to 120 ksi. N = $10^{1.3}$ to 10^4. D = 2 x 10^{-1} to 4 x 10^2. D = 3 at $\sigma_a = \sigma_g$ = 100 ksi. 40x increase with N. (57 A, Figure 166)

IRON ALLOY (Chromium alloys, 4 to 30% Cr). σ_a = 4 to 10 ksi. η_s = 2 x 10^{-3} to 1.3 x 10^{-2}. Peaks at 12% Cr. 4x increase with σ_a. (58 Co, Figure 167)

IRON ALLOY (13% Cr alloy, 0.06 to 0.13% C, 0.25 to 0.80% Mn, oil quenched from 950°C, air cooled from 600°C). Bending. f = 1,000. σ_a = 5 to 35 ksi. T = 75 to 1,050°F. η_s = 6 x 10^{-4} to 7 x 10^{-3}. 10x increase with σ_a. 2x change with T. (44 Sc, Figures 168 and 169)

IRON ALLOY (5.0% Cr Steel, 0.20% C, 0.50% Mn, annealed). Torsion. Steady and alternating magnetic fields. τ_a = 2 to 16 ksi. η_s = 10^{-3} to 1.5 x 10^{-2}. 10x change with magnetic fields. 5x increase with τ_a. (40 P, Figure 170)

IRON ALLOY (13% Cr alloy, forged, swaged). Torsion. τ_a = 5 to 30 ksi. σ_m = 0.37 to 7.7 ksi. With and without magnetic field. η_s = 6 x 10^{-3} to 6 x 10^{-2}. 1.5x change with τ_a. 2x decrease with σ_m. (53 Coc, Figure 171)

IRON ALLOY (Stainless steel, about 0.12% C, 18% Cr, 8% Ni). Torsion. τ_a = 10 to 70 ksi. η_s = 2 x 10^{-3} to 1.5 x 10^{-2}. (53 B, Figure 172)

IRON ALLOY (Stainless steel, 13% Cr, 0.12% C, about 1% other, oil

quenched, two treatments). Torsion. τ_a = 4 to 12 ksi. η_s = 1.5 x 10^{-3} to 1.5 x 10^{-2}. 3x increase with τ_a. 10x change with treatment. (44 B, Figure 173)

IRON ALLOY (12.5% Cr Steel, 0.5% Ni, 0.1% C, forged at 1,950°F, annealed at 1,750°C). Torsion. With and without magnetic field. τ_a = 1 to 12 ksi. η_s = 1.3 x 10^{-3} to 1.5 x 10^{-2}. 10x change with magnetic field. 4x change with τ_a. (53 Co, Figure 174)

IRON ALLOY (Stainless steel). Bending. σ_a = 3 to 6 ksi. η_s = 4 x 10^{-4} to 8 x 10^{-4}. (57 Tr, Figure 175)

IRON ALLOY (Stainless steel, 13 to 26% Cr, quenched or air cooled). Torsion. τ_a = 3 to 12 ksi. η_s = 5 x 10^{-4} to 10^{-2}. 2x increase with τ_a. 10x change with composition. (44 B, Figure 191)

IRON ALLOY (17-7 PH Stainless Steel, annealed). See Aluminum Alloy 2024-T4, reference 63 Ai. n = 2.359 and J = 1.688 x 10^{-13} for σ_a < 14 ksi. n = 3.534 and J = 2.34 x 10^{-18} for σ_a > 14 ksi. (63 Ai)

IRON ALLOY (17-4 PH Stainless Steel, annealed). See Aluminum Alloy 2024-T4, reference 63 Ai. n = 2.124 and J = 1.088 x 10^{-13} for σ_a < 45 ksi. (63 Ai)

IRON ALLOY (410 Stainless Steel, R"C"24). See Aluminum Alloy 2024-T4, reference 63 Ai. n = 2.441 and J = 2.317 x 10^{-13}

for $\sigma_a < 15.92$ ksi. $n = 2.128$ and $J = 4.725 \times 10^{-12}$ for $15.92 \text{ ksi} < \sigma_a < 27.95$ ksi. $n = 1.702$ and $J = 3.758 \times 10^{-10}$ for $\sigma_a > 27.95$ ksi. (63 Af)

IRON ALLOY (AISI 403 steel). Bending. $\sigma_a = 1$ to 35 ksi. $\sigma_m =$ 0 to 19 ksi. $\eta_s = 2 \times 10^{-4}$ to 9×10^{-3}. 10x increase with σ_a. 9x decrease with σ_m. (57 H, Figure 176)

IRON ALLOY (AISI 403 steel, annealed at 1,850°F, air cooled, annealed at 1,300°F, air cooled). Bending. $\sigma_m = 0$ or 19 ksi. $\sigma_a = 1$ to 30 ksi. T = 75 or 1,000°F. $\eta_s = 2 \times 10^{-4}$ to 7×10^{-3}. 10x change with σ_m. 10x change with σ_a. (60 Cl, Figures 177 and 178)

IRON ALLOY (AISI 403 steel, heat-treated). $\tau_a = 2$ to 20 ksi. $\eta =$ 7×10^{-3} to 1.5×10^{-2}. $\eta = 1.5 \times 10^{-2}$ peak at $\tau_a = 10$ ksi. (59 Laza, Figure 179)

IRON ALLOY (AISI 403 steel). Torsion. $\sigma_m = 0.9$ or 51 ksi. T = 70 to 1,300°F. $\gamma_a = 0.5 \times 10^{-3}$ to 2.4×10^{-3}. $\eta_s = 2 \times 10^{-3}$ to 7×10^{-2}. 4x increase with γ_a. 20x change with T. (55 Co, Figures 180 and 181)

IRON ALLOY (AISI 403 steel). Brinell hardness from 220 to 380. Bending. $\sigma_m = 0$ and 19 ksi. $\eta_s = 4 \times 10^{-4}$ to 10^{-2}. 9x change with σ_m. 20x decrease with hardness. (57 H, Figure 182)

IRON ALLOY (AISI 403 steel, hot rolled, annealed at 1,750°F, oil

quenched, tempered at 1,050°F, air cooled). Rotating bending. σ_a = 5 to 80 ksi. N = $10^{1.3}$ to 10^4. At T = 70°F, D = 5 x 10^{-2} to 10^3, with D = 1.4 at $\sigma_a = \sigma_g$ = 60 ksi, and a 10x increase with N. At T = 700°F, D = 5 x 10^{-2} to 3 x 10^2, with D = 1.6 at $\sigma_a = \sigma_g$ = 50 ksi, and a 10x increase with N. At T = 900°F, D = 5 x 10^{-2} to 10^2, with D = 5 at $\sigma_a = \sigma_g$ = 40 ksi, and a 5x increase with N. (56 Po, Figures 183 and 184)

IRON ALLOY (AISI 403 steel, hot-rolled, annealed at 1,750°F, oil quenched, tempered at 1,050°F, air cooled). Bending. σ_a = 5 to 50 ksi. σ_m = 0 to 40 ksi. D = 2 x 10^{-3} to 5 x 10^{-1}. 250x increase with σ_a. 20x decrease with σ_m. (56 Pe, Figure 185)

IRON ALLOY (AISI 403 steel, tempered at 1,200 to 1,350°F or not tempered). Torsion. τ_a = 1 to 28 ksi. η_s = 2 x 10^{-3} to 2 x 10^{-2}. 15x increase with tempering. 8x change with τ_a. Peak at τ_a = 8 ksi. (58 Co, Figure 186)

IRON ALLOY (Lapealloy, 12.2% Cr, forged at 2,035 to 1,750°F, annealed at 1,275°F, air cooled, salt bath, quenched, reheated, air cooled). Rotating bending. σ_a = 5 to 80 ksi. N = $10^{1.3}$ to 10^5. At T = 70°F, D = 4 x 10^{-2} to 10^2, with D = 1.6 at $\sigma_a = \sigma_g$ = 65 ksi, and a 10x increase with N. At T = 900°F, D = 5 x 10^{-1} to 10^2, with D = 5 at $\sigma_a = \sigma_g$ = 40 ksi, and a 10x increase with N. (56 Po, Figures 187 and 188)

IRON ALLOY (Ni steel). Small strains. Bending. f = 1 to 10. η_s = 5.4 x 10^{-4}. (41 Ki*)

IRON ALLOY (Ni steel, swaged). Strains of about 5×10^{-3}. Rotating bending. $\eta_s = 7.3 \times 10^{-4}$. (41 Ki*)

IRON ALLOY (Ni steel, oil quenched, tempered, two treatments). Torsion. τ_a = 4 to 12 ksi. $\eta_s = 7 \times 10^{-4}$ to 1.6×10^{-3}. (44 B, Figure 189)

IRON ALLOY (Ni-Cr steel, air cooled or oil quenched, tempered, two treatments). Torsion. τ_a = 4 to 12 ksi. $\eta_s = 6 \times 10^{-4}$ to 10^{-3}. (44 B, Figure 190)

IRON ALLOY (3.5% Ni steel, 0.38 to 0.43% C, 0.8% Mn, oil quenched from 900°D, air cooled from 625°C). Bending. f = 1,000. σ_a = 5 to 40 ksi. T = 75 to 1,200°F. $\eta_s = 2 \times 10^{-4}$ to 3×10^{-3}. 10x increase with T. 9x increase with σ_a. (44 Sc, Figures 192 and 193)

IRON ALLOY (SAE 3140 steel). Torsion. τ_a = 10 to 40 ksi. $\eta_s = 2 \times 10^{-3}$ to 2×10^{-2}. (53 B, Figure 194)

IRON ALLOY (2.2% Ni steel, 0.38% C, 0.6% Cr, quenched in oil, tempered at 650°C). Torsion. τ_a = 5 to 30 ksi. $\eta_s = 5 \times 10^{-4}$ to 4×10^{-3}. (51 Fer, Figure 195)

IRON ALLOY (2.2% Ni steel, 0.38% C, 0.6% Cr, two treatments). Torsion. τ_a = 5 to 20 ksi. $\eta_s = 2 \times 10^{-4}$ to 2.5×10^{-3}. 3x increase with τ_a. 6x change with treatment. (51 Fer, Figure 196)

IRON ALLOY (SAE X4130 steel, seam-tubing, normalized). Axial

stress. σ_a = 5 to 50 ksi. D = 5 x 10^{-2} to 5. (46 Ro, Figure 197)

IRON ALLOY (SAE 4130 steel). Axial stress or shear. σ_a = 5 to 40 ksi. D = 4 x 10^{-2} to 5. 20x increase with shear. 100x increase with σ_a. (54 Y, Figure 198)

IRON ALLOY (SAE 4140 steel, annealed at 950°C, air cooled, tempered at 600°C, air cooled). Bending. f = 1,000. σ_a = 10 to 40 ksi. T = 75 to 1,200°F. η_s = 3 x 10^{-4} to 2 x 10^{-3}. 4x increase with σ_a. 3x increase with T. (44 Sc, Figures 199 and 200)

IRON ALLOY (High temperature Russian Steels, 3N-415, 3N-4376, 3N-766A, 3N-617, 3N-612). T = 100 to 700°C. η_s = 10^{-3} to 4 x 10^{-2}. (62 Pisa, Figure 201)

IRON ALLOY (4340 Steel, R"C"40). See Aluminum Alloy 2024-T4, reference 63 Ai. n = 3.343 and J = 2.153 x 10^{-17} for σ_a < 38 ksi. n = 5.360 and J = 1.224 x 10^{-26} for σ_a > 38 ksi. (63 Ai)

IRON ALLOY (4340 Steel, R"C"52). See Aluminum Alloy 2024-T4, reference 63 Ai. n = 2.166 and J = 4.750 x 10^{-13} for σ_a < 55 ksi. n = 2.579 and J = 5.290 x 10^{-15} for σ_a > 55 ksi. (63 Ai)

IRON ALLOY (4340 Steel, annealed). See Aluminum Alloy 2024-T4, reference 63 Ai. n = 2.765 and J = 5.37 x 10^{-15} for σ_a < 14.5 ksi. n = 3.502 and J = 3.548 x 10^{-16} for σ_a > 14.5 ksi. (63 Ai)

IRON ALLOY (Cr-V steel). Torsion. σ_m = 30 ksi. η_s = 2.7 x 10^{-3}. (41 Ki*)

IRON ALLOY (Cr-Mo-V steel, C < 0.5%, 0.4 to 0.7% Mn, 0.8 to 1.1% Cr, 0.45 to 0.65% Mo, 0.25 to 0.35% V, annealed at 900°C, oil quenched, tempered at 675°C, air cooled). Bending. f = 1,000. σ_a = 5 to 40 ksi. T = 75 to 1,050°F. η_s = 1.4 x 10^{-4} to 1.2 x 10^{-3}. 4x increase with σ_a. 5x increase with T. (44 Sc, Figure 202)

IRON ALLOY (Cr-Ni-W-Mo steel). Torsion. σ_m = 30 ksi. η_s = 3.2 x 10^{-3}. (41 Ki*)

IRON ALLOY (Ni-Cr-Mo steel, oil quenched, tempered). Torsion. τ_a = 5 to 20 ksi. η_s = 3.5 x 10^{-4} to 9 x 10^{-4}. (44 B, Figure 203)

IRON ALLOY (Cr-Ni-Mo steel). Torsion. σ_m = 30 ksi. η_s = 1.1 x 10^{-2}. (41 Ki*)

IRON ALLOY (SAE 4615 steel). Torsion. τ_a = 10 to 30 ksi. η_s = 1.5 x 10^{-3} to 10^{-2}. (53 B, Figure 204)

IRON ALLOY (SAE 6145 steel). Torsion. τ_a = 10 to 60 ksi. η_s = 7 x 10^{-4} to 1.5 x 10^{-2}. (53 B, Figure 205)

IRON ALLOY (N-153, Fe-Ni-Cr-Co Alloy, annealed at 2,175°F, for 15 min., water quenched, cold worked at 1,400°F, annealed at 1,500°F for 2 hrs., air cooled). Bending. f = 1,000. σ_a =

10 to 30 ksi. T = 75 to 1,300°F. η_s = 2 x 10^{-4} to 10^{-3}. 3x increase with σ_a. 2x change with T. (44 Sc, Figures 206 and 207)

IRON ALLOY (Steel, martensite with a little austenite). η = 6 x 10^{-5} to 10^{-4}. (62 Pl)

IRON ALLOY (Three different steels: troostite with a little martensite, sorbite with a little ferrite, perlite in fine globules). η = 3 x 10^{-5}. (62 Pl)

IRON ALLOY (0.2% C steel). At T = 24°C and at stress of 5 to 35 ksi, η_s = 0.3 x 10^{-3} to 1.8 x 10^{-3}. At T = 260°C and at stress of 5 to 25 ksi, η_s = 0.6 x 10^{-3} to 3 x 10^{-3}. At T = 371°C and stress of 5 to 15 ksi, η_s = 1.6 x 10^{-3} to 2.4 x 10^{-3}. (62 Sm*)

IRON ALLOY (3.5% nickel). Range of values as stress is increased from 5 to 35 ksi. At T = 24°C, η_s = 0.2 x 10^{-3} to 1.6 x 10^{-3}. At T = 260°C, η_s = 0.2 x 10^{-3} to 2 x 10^{-3}. At T = 482°C, η_s = 0.3 x 10^{-3} to 3 x 10^{-3}. At T = 649°C, η_s = 2 x 10^{-3} to 3.3 x 10^{-3}. (62 Sm*)

IRON ALLOY (19.7% Ni, 14.2% Cr, plus W, Mo, and Nb). At T = 24°C and at stress of 5 to 35 ksi, η_s = 10^{-4} to 10^{-3}. At T = 260°C and at stress of 15 to 35 ksi, η_s = 0.7 x 10^{-3} to 2.9 x 10^{-3}. At T = 482°C and at stress of 5 to 35 ksi, η_s = 0.2 x 10^{-3} to 0.4 x 10^{-3}. At T = 649°C and at stress of 15 to 25 ksi, η_s = 0.3 x 10^{-3}. At T = 760°C and at stress of 15 to 25 ksi, η_s = 0.4 x 10^{-3}. (62 Sm*)

IRON ALLOY (15% Ni, 15% Cr, 12% Co, plus W, Mo, and Nb). At T = 24°C and at stress of 15 to 35 ksi, $\eta_s = 0.3 \times 10^{-3}$ to 1.2×10^{-3}. At T = 260°C and at stress of 15 to 25 ksi, $\eta_s = 0.3 \times 10^{-3}$. At T = 566°C and at stress of 15 to 25 ksi, $\eta_s = 0.2 \times 10^{-3}$. At T = 704°C and at stress of 5 to 25 ksi, $\eta_s = 0.2 \times 10^{-3}$ to 0.4×10^{-3}. (62 Sm*)

IRON ALLOY (S-495, Fe-Ni-Cr Alloy, annealed at 2,175°F for 15 min., water quenched, cold worked at 1,400°F, annealed at 1,500°F for 2 hrs., air cooled). Bending. f = 1,000. σ_a = 5 to 40 ksi. T = 75 to 1,400°F. $\eta_s = 10^{-4}$ to 2×10^{-3}. 5x change with T. 5x increase with σ_a. (44 Sc, Figures 208 and 209)

IRON ALLOY (0.95% Cr, 0.2% Mo). Range of values as stress is increased from 15 to 35 ksi. At T = 24°C, $\eta_s = 5 \times 10^{-4}$ to 12×10^{-4}. At T = 260°C, $\eta_s = 8 \times 10^{-4}$ to 17×10^{-4}. At T = 480°C, $\eta_s = 1.3 \times 10^{-3}$ to 2×10^{-3}. At T = 650°C, $\eta_s = 1.7 \times 10^{-3}$ to 2×10^{-3}. (62 Sm*)

IRON ALLOY (0.95% Cr, 0.55% Mo, 0.3% V). Range of values as stress is increased from 5 to 25 ksi. At T = 24°C, $\eta_s = 10^{-4}$ to 2×10^{-4}. At T = 260°C, $\eta_s = 2 \times 10^{-4}$ to 4×10^{-4}. At T = 480°C, $\eta_s = 2 \times 10^{-4}$ to 12×10^{-4}. At T = 566°C, $\eta_s = 3 \times 10^{-4}$ to 10^{-3}. (62 Sm*)

IRON ALLOY (Cast iron, Lamellar). For various cast irons having graphite content from 1.8 to 3.3%. (ASTM classification A1 to A8), $\eta = 1.9 \times 10^{-3}$ to 16×10^{-3}. (62 P1)

IRON ALLOY (Cast Iron with spheroidal graphite). For various cast irons having graphite content from 2.5 to 3.3%. η = 1.4×10^{-4} to 6.3×10^{-4}. (62 P1)

IRON ALLOY (Cast Iron, Malleable). $\eta = 4 \times 10^{-4}$. (62 P1)

IRON ALLOY (Cast Iron, varying engineering types). f = 10. $\epsilon < 10^{-4}$. $\eta = 6.3 \times 10^{-3}$ to 10^{-2}. (62 Sm*)

IRON ALLOY (Cast iron, Meehanite GA). Shear. τ_a = 6 to 20 ksi. D = 3×10^{-1} to 10^{1}. (54 Y, Figure 211)

IRON ALLOY (Cast iron, 3.26 to 3.71% C). τ_a = 2 to 8 ksi. η_s = 10^{-2} to 7×10^{-2}. 2x change with composition. 3x change with τ_a. (44 B, Figure 212)

IRON ALLOY (Cast iron). Bending. σ_a = 1 to 4 ksi. $\eta_s = 7 \times 10^{-3}$ to 2.5×10^{-2}. (57 Tr, Figure 213)

IRON ALLOY (Cast iron, cut from a cast block, then annealed or tested as is). Bending. f = 100 to 2,000. $\eta_s = 1.2 \times 10^{-3}$ to 3×10^{-3}. (56 Mi, Figure 214)

IRON ALLOY (Cast iron, machined from cast bars, various compositions). Torsion. τ_a = 4 to 24 ksi. $\eta_s = 10^{-2}$ to 4×10^{-2}. Little change with composition. (40 Lor, Figure 215)

IRON ALLOY (Cast iron, 2.9 to 3.2% C, 1.6% Si, 0 to 3.0% Cu, 0.6% Mn). Bending. σ_a = 0.1 to 1 ksi. $\eta_s = 1.2 \times 10^{-2}$ to 3.8×10^{-2}. (57 Tr, Figure 216)

IRON ALLOY (Cast iron, about 3.3% C, 1.1% Si, 0 to 3.0% Cu, 0.5% Mn). Torsion. τ_a = 4 to 20 ksi. $\eta_s = 1.2 \times 10^{-2}$ to 5×10^{-2}. (40 Lor, Figure 217)

IRON ALLOY (High carbon, inoculated flake iron, 2.5% T.C., 1.9% Si, 1% Mn, 20.7% Ni, 1% Cr, 0.13% P). Torsion. τ_a = 5 ksi. $\eta_s = 2.8 \times 10^{-2}$. (64 Bi)

IRON ALLOY (Spun cast iron, 3.5% T.C., 3.4% G.C., 1.9% Si, 0.4% Mn, 0.4% , 0.38% P). Torsion. τ_a = 5 ksi. $\eta_s = 1.9 \times 10^{-2}$. (64 Bi)

IRON ALLOY (3.3% T.C., 2.2% Si, 0.5% Mn, 0.14% P, 0.03% S). Torsion. τ_a = 5 ksi. For inoculated flake iron, $\eta_s = 6.4 \times 10^{-3}$. For non-inoculated flake iron $\eta_s = 10^{-2}$. (64 Bi)

IRON ALLOY (Austenitic flake iron, 2.5% T.C., 1.9% Si, 1% Mn, 20.7% Ni, 1.9% Cr, 0.03% P, 0.03% S). Torsion. τ_a = 5 ksi. $\eta_s = 1.1 \times 10^{-2}$. (64 Bi)

IRON ALLOY (Alloyed flake graphite, 3.14% T.C., 2% Si, 0.6% Mn, 0.7% Ni, 0.4% Mo, 0.14% P, 0.03% S). $\eta_s = 9.5 \times 10^{-3}$. (64 Bi)

IRON ALLOY (Nickel-copper austenitic flake, 2.55% T.C., 1.9% Si, 1.25% Mn, 15.2% Ni, 7.3% Cu, 2% Cr, 0.03% P, 0.04% S). $\eta_s = 6 \times 10^{-3}$. (64 Bi)

IRON ALLOY (Undercooled flake graphite, titanium/CO_2 treated, 3.27% T.C., 2.2% Si, 0.6% Mn, 0.35% Ti, 1.4% P, 0.03% S). $\eta_s = 6 \times 10^{-3}$. (64 Bi)

IRON ALLOY (Annealed ferritic nodular, 3.7% T.C., 1.8% Si, 0.4% Mn, 0.76% Ni, 0.06% Mg, 0.03% P, 0.01% S, < 0.003% Ce). $\eta_s = 4 \times 10^{-3}$. (64 Bi)

IRON ALLOY (Pearlitic malleable). $\eta_s = 3 \times 10^{-3}$. (64 Bi)

IRON ALLOY (Blackheart malleable). $\eta_s = 3 \times 10^{-3}$. (64 Bi)

IRON ALLOY (Cast pearlitic nodular). $\eta_s = 3 \times 10^{-3}$. (64 Bi)

IRON ALLOY (Cast iron, magnesium treated, nodular, heated 15 hrs. at 1,400°F, cooled to 1,000°F in 3 hrs., then air cooled). Under static bending, σ_a = 30 to 60 ksi, $\eta_s = 1.6 \times 10^{-2}$ to 7×10^{-2}. Under torsion, τ_a = 10 to 30 ksi, $\eta_s = 10^{-3}$ to 2.5×10^{-2}. Under static axial stress, σ_a = 20 to 50 ksi, $\eta_s = 1.5 \times 10^{-2}$ to 9×10^{-2}. (52 M, Figure 219)

IRON ALLOY (Gray cast iron). Torsion. τ_a = 2 to 18 ksi. $\eta_s = 3 \times 10^{-2}$ to 9×10^{-2}. (53 B, Figure 218)

IRON ALLOY (Gray cast iron). σ_a = 1 to 20 ksi. $N = 10^{1.3}$ to 10^4. $D = 5 \times 10^{-2}$ to 5. At $\sigma_a = \sigma_g$ = 12 ksi, $D = 5 \times 10^{-1}$. 3x decrease with N. (57 A, Figure 119)

LEAD (Single crystal, annealed). f = 40,000. $\eta_s = 9 \times 10^{-5}$. (42 Bi*)

LEAD (99.999% pure single crystal). Axial stress. T = -80 to 220°C. ϵ_a = 0 to 1.2×10^{-5}. $\eta_s = 2 \times 10^{-3}$ to 7×10^{-2}. 9x increase with ϵ_a. 30x increase with T. (58 Mas, Figure 220)

LEAD (99.995% pure or 99% pure, polycrystalline). Axial stress. σ_a = 0.01 to 1 ksi. $\eta_s = 2 \times 10^{-3}$ to 2×10^{-1}. Little change with purity. (58 Mas, Figure 221)

LEAD (99.99% pure). $\epsilon_a = 10^{-6}$ to 10^{-3}. $\eta_s = 5 \times 10^{-4}$ to 3×10^{-2}. (58 Mas, Figure 222)

LEAD. Axial stress. f = 10,000 or 26,500,000. T = 10 to 300°K. $\eta_s = 10^{-5}$ to 10^{-3}. 40x increase with T. 6x change with f. (58 Mas, Figure 223)

LEAD (Polycrystalline). Elastic-plastic bending. T = 20 to 250°C. N = 820 to 1,920. $\eta_s = 4 \times 10^{-3}$ to 1.4×10^{-2}. 1.5 increase with T. 2.5 increase with N. (61 Ga, Figure 224)

LEAD (Polycrystalline). At f = 10,000, $\eta_s = 5 \times 10^{-3}$ to 2.7×10^{-2}. At f = 1,000, $\eta_s = 1.5 \times 10^{-3}$. (42 Bi*)

LEAD (Commercially and chemically pure grades, single crystals). Small strains. Axial stress. f = 10,300. T = 10 to 140°K. $\eta_s = 2 \times 10^{-5}$ to 9×10^{-5}. Little change with purity. (58 Mas, Figure 225)

LEAD. Bending. f = 20 to 160. $\eta_s = 8 \times 10^{-3}$ to 1.4×10^{-2}. (49 K, Figure 226)

LEAD (Pure, cast). $\epsilon < 10^{-4}$. f = 2,000 to 10,000. $\eta = 10^{-4}$ to 1.9×10^{-2}. (62 Sm*)

LEAD (Cast). Bending. f = 2,000. $\eta_s = 1.4 \times 10^{-3}$. (38 Fors)

MAGNESIUM (99% pure, casting). Bending. f = 60 to 400. η_s = 6 x 10^{-2} to 1.4 x 10^{-2}. (57 Mi)

MAGNESIUM (K1X1 alloy, casting). Bending. f = 60 to 400. η_s = 1.5 x 10^{-1} to 5 x 10^{-2}. (57 Mi, Figure 227)

MAGNESIUM (99.99% pure, annealed at 550°C). Bending. Low stress. f = 2,000. T = 50 to 500°C. η_s = 6 x 10^{-5} to 10^{-2}. (38 Fors, Figure 229)

MAGNESIUM (99% pure, sheet). Bending. f = 40 to 200. η_s = 2 x 10^{-1} to 4 x 10^{-2}. (57 Mi, Figure 231)

MAGNESIUM (Not of high purity). Torsion. T = 100 to 400°C. η_s = 3 x 10^{-3} to 6 x 10^{-2}. η_s = 6 x 10^{-2} peak at T = 220°C. (58 Mas, Figure 232)

MAGNESIUM (Pure, annealed). f = 2,000 to 10,000. $\epsilon < 10^{-4}$. η = 4 x 10^{-5} to 6.7 x 10^{-4}. (62 Sm*)

MAGNESIUM ALLOY (J-1). Under axial stress, σ_a = 4 to 11 ksi, D = 3 x 10^{-2} to 6 x 10^{-1}. Under shear, τ_a = 2 to 6 ksi, D = 3 x 10^{-2} to 9 x 10^{-1}. (54 Y, Figure 228)

MAGNESIUM ALLOY (J-1, extruded). Bending. σ_a = 1 to 5 ksi. σ_m = 0 and 6 ksi. D = 3 x 10^{-4} to 5 x 10^{-3}. 2x decrease with σ_m. (56 Pe, Figure 238)

MAGNESIUM ALLOY (British types). Torsion. τ_a = 3 ksi. Mg-Zn-Zr-Th alloy DTD 5005, $\eta_s > 1.2 \times 10^{-2}$. Mg-Zn-Mn alloy BS1278,

$\eta_s = 2.5 \times 10^{-3}$. Mn-Zn-Zr alloy DTD 721A, $\eta_s = 1.3 \times 10^{-3}$. Elektron MSR alloy (Mg-Ag-Zr), $\eta_s = 8 \times 10^{-4}$. (64 Bi)

MAGNESIUM ALLOY (J). Torsion. τ_a = 3 to 8 ksi. $\eta_s = 6 \times 10^{-3}$ to 7×10^{-2}. N = 0 to 3×10^5. 5x increase with τ_a. 2x change with N and stress history. (43 Ku, Figure 239)

MAGNESIUM ALLOY (J). σ_a = 1 to 30 ksi. N = 10^2 to 10^5. D = 10^{-2} to 10^1. D = 10^{-1} at $\sigma_a = \sigma_g$ = 5 ksi. 5x decrease with N. (57 A, Figure 241)

MAGNESIUM ALLOY (J-1, extruded tubing). Axial stress. σ_a = 4 to 10 ksi. D = 4×10^{-2} to 8×10^{-1}. (46 Ro, Figure 242)

MAGNESIUM ALLOY (EM-52-T6, extrusion, and M-1-A, forging). Bending. σ_a = 1 to 5 ksi. $\eta_s = 5 \times 10^{-4}$ to 10^{-2}. (57 Tr, Figure 230)

MAGNESIUM ALLOY (AZ-63-A and AM-80-A). Bending. σ_a = 1 to 4 ksi. $\eta_s = 5 \times 10^{-4}$ to 10^{-2}. (57 Tr, Figure 233)

MAGNESIUM ALLOY (Extruded or sand cast). Torsion. τ_a = 0.75 to 2.25 ksi. $\eta_s = 5 \times 10^{-4}$ to 5×10^{-3}. 5x increase with τ_a. 2x increase with sand cast. (44 B, Figure 234)

MAGNESIUM ALLOY (AZ-81-A, sand cast). Bending. $\epsilon_a = 10^{-4}$ to 10^{-3}. $\eta = 2 \times 10^{-3}$ to 3×10^{-2}. (58 Wei, Figure 235)

MAGNESIUM ALLOY (A-15 and die cast AZ-91-C). Bending. σ_a = 1 to 6 ksi. $\eta_s = 6 \times 10^{-4}$ to 8×10^{-3}. (57 Tr, Figure 236)

MAGNESIUM ALLOY (AZ-92-A and AZ-92A-T6). Bending. σ_a = 1 to 5 ksi. $\eta_s = 5 \times 10^{-4}$ to 10^{-2}. (57 Tr, Figure 237)

MAGNESIUM ALLOY (AZ-31-B-H24, T6). See Aluminum Alloy 2024-T4, reference 63 Ai. n = 1.986 and $J = 5.56 \times 10^{-11}$ for $\sigma_a < 2.35$ ksi. n = 2.297 and $J = 4.915 \times 10^{-12}$ for $\sigma_a > 2.35$ ksi. (63 Ai)

MAGNESIUM ALLOY (HK-31-A, 3% Th, 1% Zr). Bending. f = 50 to 400. $\eta_s = 8 \times 10^{-2}$ to 2×10^{-2}. (57 Mi, Figure 240)

MAGNESIUM ALLOY (K1X1, die cast or sand cast). Bending. $\epsilon_a = 10^{-4}$ to 12 to 10^{-4}. $\eta = 10^{-2}$ to 2×10^{-1}. 5x increase with ϵ_a. 3x increase with sand cast. (58 Wei, Figure 243)

MAGNESIUM ALLOY (7.5% Al, 1.1% Zn, forged and annealed). f = 500 to 12,000. $\epsilon < 10^{-4}$. $\eta = 3 \times 10^{-6}$ to 10^{-4}. (62 Sm*)

MAGNESIUM ALLOY (1 to 15% Al). Bending. σ_a = 1 to 6 ksi. $\eta_s = 10^{-3}$ to 10^{-2}. 10x increase with σ_a. 2x change with % Al. (57 Tr, Figure 244)

MAGNESIUM ALLOY (0). Torsion. N = 0 to 4.5×10^5. τ_a = 2 to 8 ksi. $\eta_s = 5 \times 10^{-3}$ to 8×10^{-2}. 10x increase with τ_a. 3x change with N. (43 Ku, Figure 245)

MAGNESIUM ALLOY (M1A-0, M1A-H24, and AZ-61A-H24). Bending. σ_a = 1 to 6 ksi. $\eta_s = 10^{-4}$ to 10^{-2}. (57 Tr, Figure 246)

MAGNESIUM ALLOY (1.07 and 1.2% Al). Bending. σ_a = 1 to 3 ksi. $\eta_s = 7 \times 10^{-4}$ to 10^{-2}. (57 Tr, Figure 247)

MAGNESIUM ALLOY (0.7% Si). Rotating bending. $N = 10^{1.3}$ to 10^{5}. σ_a = 1 to 10 ksi. $D = 5 \times 10^{-2}$ to 1.6. $D = 3 \times 10^{-1}$ at $\sigma_a = \sigma_g$ = 3 ksi. 1.6x decrease with N. (57 A, Figure 255)

MANGANESE ALLOY (12 to 64% Cu, cold worked, quenched, reheated to TR = 350 to 700°C). Low axial stress. $\eta = 10^{-2}$ to 1. 5 to 40x peaks at TR $\approx$ 450°C. (41 D, Figures 248 and 249)

MANGANESE ALLOY (4 to 50% Cu, cold worked, quenched, reheated to TR = 500 to 700°C). Low axial stress. $\eta = 2 \times 10^{-2}$ to 3×10^{-1}. 20x decrease with TR. Little change with % Cu. (41 D, Figures 250 and 251)

MANGANESE ALLOY (10-50% Cu, solution treated, quenched, and stabilized). $\epsilon < 10^{-4}$. $\eta = 4.8 \times 10^{-3}$ to 6.4×10^{-3}. (62 Sm*)

MAGNESIUM ALLOY (Cast Alloys, K1A-F and SD10A-F). At σ_a = 0.1 ksi, $\eta_s = 2 \times 10^{-2}$ to 3×10^{-2}. At σ_a = 1 ksi, $\eta_s = 3 \times 10^{-2}$ to 6×10^{-2}. At σ_a = 10 ksi, $\eta_s = 9 \times 10^{-2}$ to 17×10^{-2}. (62 K)

MAGNESIUM ALLOY (Cast Alloys; ZK51A-T5, AZ-92A-T4, AM100A-T4, and EZ-334-T5). At σ_a = 2 ksi, $\eta_s = 3 \times 10^{-3}$ to 6×10^{-3}. At σ_a = 10 ksi, $\eta_s = 8 \times 10^{-3}$ to 50×10^{-3}. (62 K)

MAGNESIUM ALLOY (50-90% Mn, 50 to 10% Cu). Torsion. τ_a = 5 ksi. At 90% Mn, $\eta_s = 3.4 \times 10^{-2}$. At 85% Mn, $\eta_s = 4.4 \times 10^{-2}$. At 80% Mn, $\eta_s = 3.5 \times 10^{-2}$. At 70% Mn, $\eta_s = 7.0 \times 10^{-2}$. At 60% Mn, $\eta_s = 7.0 \times 10^{-2}$. At 50% Mn, $\eta_s = 5.3 \times 10^{-2}$. (64 Bi)

MANGANESE ALLOY (70% Mn, 30% Cu, solution treated for 2 hrs. at 750°C, water quenched and aged at 450°C, water quenched). Torsion. τ_a = 5 ksi. At -60 to 0°C, $\eta_s = 5.6 \times 10^{-2}$. At 50°C, $\eta_s = 1.7 \times 10^{-2}$. At 100°C, $\eta_s = 1.1 \times 10^{-3}$. (64 Bi)

MANGANESE ALLOY (Chicago Devel. Corp., Riverdale, Maryland, Alloy 780; 80% manganese and 20% copper; ultimate strength = 68 ksi, yield strength = 24 ksi, proportional limit = 13 ksi, fatigue strength at 10^8 cycles as reported by Chicago Devel. Corp. = 17 ksi, fatigue strength at 10^5 cycles as measured at Univ. of Minn. = 40 ksi). At σ_a = 6 ksi, D = 1. At σ_a = 10 ksi, D = 3. At σ_a = 20 ksi, D = 18. At σ_a = 50 ksi, D = 100. (59 Tor)

MANGANESE ALLOY (30% Cu, 5% Ni, solution treated, quenched and stabilized). $\epsilon < 10^{-4}$. $\eta = 2.7 \times 10^{-3}$. (62 Sm*)

MANGANESE ALLOY (6 to 8% Cu, cold worked, quenched, reheated to TR = 350 to 550°C). Low axial stress. $\eta = 10^{-1}$ to 7×10^{-1}. 3x change with % Cu. Peaks at TR $\approx$ 450°C. (41 D, Figure 252).

MANGANESE ALLOY (20 to 90% Cu, solution treated or aged). σ_a = 5 ksi. Solution treated, $\eta_s = 10^{-3}$ to 2×10^{-2}. Aged, $\eta_s = 5 \times 10^{-2}$ to 3×10^{-2}. (55 Ro, Figure 253)

MANGANESE ALLOY (33% Cu, heat-treated, swaged or heat-treated, quenched, aged at 450°C for 2 hrs.). Rotating bending. $N = 10^{1.3}$ to 10^{4}. σ_a = 1 to 50 ksi. $D = 2 \times 10^{-2}$ to 10^{2}. D = 12 at $\sigma_a = \sigma_g$ = 20 ksi. (57 A, Figure 254)

MOLYBDENUM (Sintered, annealed at 900°C). Low stress. Bending. f = 2,000. T = 50 to 600°C. $\eta_s = 1.6 \times 10^{-4}$ to 7×10^{-4}. (38 Fors, Figure 256)

MOLYBDENUM (Arc-cast). Torsion. f = 1. T = 225 to 300°K. $\eta_s = 5.5 \times 10^{-3}$. (53 Ch, Figure 257)

MOLYBDENUM (Swaged). Rotating bending. Strains of about 5×10^{-3}. $\eta_s = 2.1 \times 10^{-3}$. (41 Ki*)

MOLYBDENUM (Sintered). f = 2,000. $\epsilon_a < 10^{-4}$. $\eta = 1.6 \times 10^{-4}$. (62 Sm*)

NICKEL (99.5% pure, cast). Torsion. τ_a = 1.5 to 7 ksi. $\eta_s = 1.5 \times 10^{-4}$ to 4×10^{-3}. (51 Fer, Figure 258)

NICKEL (A, 99.47% Ni, heat-treated at 1,400°F, air cooled). Bending. σ_m = 0 to 11 ksi. σ_a = 1 to 40 ksi. $\eta_s = 2 \times 10^{-4}$ to 10^{-2}. 20x increase with σ_a. 2x decrease with σ_m. (57 H, Figure 259)

NICKEL (Polycrystalline). Torsion. f = 10 to 180. $\eta_s = 10^{-2}$ to 3.5×10^{-2}. (58 Mas, Figure 260)

NICKEL (Pure, annealed). $\epsilon < 10^{-4}$. f = 2,000. $\eta = 2.3 \times 10^{-3}$. (62 Sm*)

NICKEL (Polycrystalline, well annealed). Axial stress. A magnetic field of 0 to 200 oersteds. $\eta_s = 2.5 \times 10^{-2}$ to 6×10^{-4}. (51 Bozo, Figure 261)

NICKEL (Polycrystalline, annealed at 1,100°C). Axial stress. f = 20 to 160. $\eta_s = 4.5 \times 10^{-3}$. Negligible change with f. (51 Bozo, Figure 262)

NICKEL (Annealed at TR = 1,300 to 2,400°F). T = 100 to 680°F. $\eta_s = 4 \times 10^{-2}$ to 10^{-4}. η_s approaches 0 as T approaches 680°F. 25x decrease with TR. (58 Co, Figure 263)

NICKEL (Cold worked or annealed). A magnetic field of 0 to 300 oersteds. $\eta_s = 10^{-5}$ to 10^{-3}. 40x decrease with magnetic field. 10x decrease with anneal. (58 Co, Figure 267)

NICKEL (Rolled). Strain less than 10^{-4}. Bending. f = 2. $\eta_s = 5.4 \times 10^{-4}$. (41 Ki*)

NICKEL (Unstretched or stretched). Medium strain. Bending. f = 9. Unstretched, $\eta_s = 5.7 \times 10^{-3}$. Stretched, $\eta_s = 1.3 \times 10^{-3}$. (41 Ki*)

NICKEL (Rolled). Rotating bending. Strains of about 5×10^{-3}. $\eta_s = 1.0 \times 10^{-3}$. (41 Ki*)

NICKEL (Annealed 30 min. at 700°C). Bending. f = 2,000. $\eta_s = 2.3 \times 10^{-3}$. (38 Fors)

NICKEL. f = 10,000. $\eta_s = 10^{-4}$ to 5×10^{-4}. (42 Bi*)

NICKEL ALLOY (Inconel, 74% Ni, 15 Cr, 6.7 Fe, 2.4% Ti). Range of values as stress is increased from 5 to 35 ksi. At T = 24°C, $\eta_s = 10^{-4}$. At T = 260°C, $\eta_s = 1.5 \times 10^{-4}$. At T = 480°C, $\eta_s = 2.5 \times 10^{-4}$. At T = 650°C, $\eta_s = 2 \times 10^{-4}$. (62 Sm*)

NICKEL ALLOY (Inconel, annealed at 1,975°F, water quenched, reheated to 1,300°F for 15 hrs., air cooled). Bending. f = 1,000. σ_a = 5 to 40 ksi. T = 75 to 1,200°F. $\eta_s = 10^{-4}$ to 4×10^{-4}. 4x change with T. Little change with σ_a. (44 Sc, Figures 265 and 266)

NICKEL ALLOY (Inconel X). See Aluminum Alloy 2024-T4, reference 63 Ai. n = 2.224 and $J = 4.586 \times 10^{-13}$ for $\sigma_a < 33$ ksi. n = 2.531 and $J = 1.565 \times 10^{-14}$ for $\sigma_a > 33$ ksi. (63 Ai)

NICKEL ALLOY (Monel, 67% Ni, 30% Cu, 1.4% Fe, 1.0% Mn). Under axial stress, σ_a = 8 to 27 ksi, $D = 4 \times 10^{-2}$ to 1. Under shear, τ_a = 5 to 22 ksi, $D = 4 \times 10^{-2}$ to 5. (54 Y, Figure 268)

NICKEL ALLOY (Monel). Strains of 10^{-4} to 10^{-3}. Torsion on hollow tubes. f = 20. σ_a = 1.6 ksi. $\eta_s = 6.4 \times 10^{-3}$. (41 Ki*)

NICKEL ALLOY (Monel). Rotating bending. Strains of about 5×10^{-3}. $\eta_s = 4.4 \times 10^{-4}$. (41 Ki*)

NICKEL ALLOY (Nitinol, 55% Ni, 45% Ti). Torsion. τ_a = 10 ksi. $\eta_s = 4.2 \times 10^{-2}$. (64 Bi)

NICKEL ALLOY (2% Thoria). Torsion. τ_a = 10 ksi. $\eta_s = 2 \times 10^{-2}$. (64 Bi)

NICKEL ALLOY (Refractaloy 26, aged or unaged). Torsion. γ_a = 0.5 x 10^{-3} to 3.2 x 10^{-3}. At σ_m = 0.91 ksi, aged, η_s = 3 x 10^{-4} to 7 x 10^{-4}. At σ_m = 0.91 ksi, unaged, η_s = 2 x 10^{-3} to 5 x 10^{-3}. At σ_m = 51 ksi, aged, η_s = 10^{-3} to 2 x 10^{-3}. At σ_m = 51 ksi, unaged, η_s = 2 x 10^{-3} to 5 x 10^{-3}. At T = 750 to 1,300°F, σ_m = 0.91 or 51 ksi, η_s = 10^{-3} to 2 x 10^{-2}, 5x increase with γ_a, 6x increase with T. (55 Co, Figures 269 and 270)

PLATINUM (Pure). $\epsilon < 10^{-4}$. η = 8 x 10^{-5}. (62 Sm*)

RHENIUM (Annealed at 1,500°C for 1 hr. followed by 1 hr. at 1,800°C). Torsion. T = 900 to 1,600°C. η_s = 2 x 10^{-2} to 10^{-1}. (59 Sc, Figure 278)

SILVER (Single crystal, annealed or unannealed). Low axial stress. T = 25 to 250°K. Unannealed, η_s = 3 x 10^{-5} to 10^{-4}. Annealed, η_s = 5 x 10^{-6} to 9 x 10^{-6}. (58 Mas, Figure 276)

SILVER (Spectroscopically pure, annealed at 700°C). Torsion. f = 0.5 to 1.5. T = 10 to 600°C. η_s = 3 x 10^{-4} to 3 x 10^{-2}. 1.5x change with f. 10x increase with T. 8x change with grain size. (53 Pe, Figure 271)

SILVER (Pure). f = 10,000. ϵ = 10^{-4}. η = 1.5 x 10^{-4} to 2.3 x 10^{-4}. (62 Sm*)

SILVER (Annealed at 500°C). Bending. f = 0 to 900. η_s = 3 x 10^{-3} to 6 x 10^{-4}. (56 Mi, Figure 272)

SILVER. f = 10,000. $\eta_s = 2 \times 10^{-4}$. (42 Bi*)

SILVER (Drawn). Bending. f = 0 to 900. $\eta_s = 5 \times 10^{-3}$ to 3×10^{-3}. (56 Mi, Figure 273)

SILVER ALLOY (0.9 to 32.4 atomic % Cd, annealed at 600°C). Torsion. f = 1.5. T = 0 to 550°C. $\eta_s = 4 \times 10^{-4}$ to 7×10^{-2}. 100x increase with T. 3x change with % Cd. (53 Pe, Figures 274 and 275)

SILVER ALLOY (3.1 or 8.1 atomic % In, annealed at 600°C). Torsion. f = 1.5. T = 0 to 550°C. $\eta_s = 3 \times 10^{-4}$ to 6×10^{-2}. 100x increase with T. Little change with % In. (53 Pe, Figure 277)

SILVER ALLOY (0.9 or 3.1 atomic % Sn, annealed at 600°C). Torsion. f = 1.5. T = 0 to 550°C. $\eta_s = 3 \times 10^{-4}$ to 8×10^{-2}. 200x increase with T. Little change with % Sn. (53 Pe, Figure 279)

STRONTIUM (99.93% pure). Torsion. T = 100 to 700°C. $\eta_s = 1.5 \times 10^{-3}$ to 1.6×10^{-2}. (61 Dash, Figure 281)

TANTALUM (Annealed at 1,850°C). Torsion. T = 1,000 to 1,500°C. Annealed, $\eta_s = 3 \times 10^{-2}$ to 6×10^{-2}. Large grains, $\eta_s = 4 \times 10^{-3}$ to 2×10^{-2}. (59 Sc, Figure 282)

TIN (Single crystal, annealed). f = 40,000. $\eta_s = 2.2 \times 10^{-5}$. (42 Bi*)

TIN (99.992% pure, polycrystalline or single crystal, annealed). Bending. T = 20 to 160°C. Polycrystalline, $\eta_s = 2 \times 10^{-3}$ to 6×10^{-3}. Single crystal, $\eta_s = 4 \times 10^{-4}$ to 10^{-3}. (51 Rot, Figure 280)

TIN. f = 1,000. $\eta_s = 2 \times 10^{-3}$. (Bi*)

TIN. Bending. f = 100 to 600. $\eta_s = 8 \times 10^{-6}$ to 10^{-5}. (46 K, Figure 283)

TIN. Bending. f = 1 to 5. $\eta_s = 4.1 \times 10^{-3}$. (41 Ki*)

TIN (Cast). Bending. f = 2,000. $\eta_s = 1.7 \times 10^{-3}$. (38 Fors)

TIN. Small strain. Torsion. f = 0.25. $\eta_s = 2 \times 10^{-5}$. (41 Ki*)

TIN (Pure, cast). f = 2,000 to 10,000. $\epsilon < 10^{-3}$. $\eta = 1.6$ to 2.4×10^{-6}. (62 Sm*)

TIN ALLOY (Solder, 33% Pb). Torsion. $\tau_a = 0.2$ to 0.7 ksi. $\eta_s = 4 \times 10^{-2}$ to 6×10^{-2}. (44 B, Figure 284)

TITANIUM (99.8% pure). Torsion. f = 0.5. For 0.019 mm grain size, T = 400 to 650°C, $\eta_s = 10^{-3}$ to 7×10^{-2}. For large grains, T = 500 to 800°C, $\eta_s = 10^{-3}$ to 7×10^{-2}. (54 Pr, Figure 285)

TITANIUM. Bending. Tuning fork specimen. T = 200 to 1,000°F. $\eta_s = 8 \times 10^{-5}$ to 3×10^{-3}. 3x change with specimen size. 20x increase with T. (56 Hun, Figure 287)

TITANIUM (1.5 to 4.5 atomic % oxygen, heated to obtain oxide coat, annealed). Torsion. f = 0.5 or 4.5. T = 350 to 800°C. $\eta_s = 10^{-4}$ to 5×10^{-2}. 500x increase with T. Little change with % oxygen. (54 Pr, Figure 295)

TITANIUM (Arc melted). Stress = 5 to 25 ksi. At T = 24°C, $\eta_s = 8 \times 10^{-5}$ to 10^{-4}. At T = 316°C, $\eta_s = 10^{-4}$ to 4×10^{-4}. At T = 482°C, $\eta_s = 2 \times 10^{-4}$ to 4×10^{-4}. At T = 566°C, $\eta_s = 5 \times 10^{-4}$ to 6×10^{-4}. (62 Sm*)

TITANIUM ALLOY (A110 AT, 4.5% Al, 2.16% Sn, hot-rolled, twice annealed at 500°F, furnace cooled). Bending. σ_a = 1 to 30 ksi. T = 75 to 525°F. $\eta_s = 8 \times 10^{-5}$ to 10^{-3}. 4x change with σ_a. 10x change with T. (60 Cl, Figure 286)

TITANIUM ALLOY (90-6Al-4V, annealed). See Aluminum Alloy 2024-T4, reference 63 Ai. n = 1.969 and $J = 3.382 \times 10^{-12}$ for $\sigma_a <$ 16 ksi. n = 2.091 and $J = 1.035 \times 10^{-12}$ for $\sigma_a >$ 16 ksi. (63 Ai)

TITANIUM ALLOY (90-6Al-4V, sintered). See Aluminum Alloy 2024-T4, reference 63 Ai. n = 2.032 and $J = 3.493 \times 10^{-12}$ for $\sigma_a <$ 26.5 ksi. n = 2.488 and $J = 3.360 \times 10^{-14}$ for $\sigma_a >$ 26.5 ksi. (63 Ai)

TITANIUM ALLOY (RC 130 B, annealed at 1,300°F, furnace cooled). Rotating bending. $N = 10^{1.3}$ to 10^4. At T = 70°F, σ_a = 50 to 150 ksi, $D = 3 \times 10^{-1}$ to 10^3, with D = 2.5 at $\sigma_a = \sigma_g$ = 100 ksi, and a 20x increase with N. At T = 600°F, σ_a = 15

to 100 ksi, D = 10^{-1} to 10^{3}, with D = 1.4 at $\sigma_a = \sigma_g$ = 50 ksi, and a 20x increase with N. (56 Po, Figures 289 and 290)

TITANIUM ALLOY (RC 55, forged at 1,700 to 1,800°F, hot-rolled, annealed at 1,300°F). Rotating bending. σ_a = 1 to 30 ksi. σ_m = 5 to 20 ksi. D = 2 x 10^{-4} to 2 x 10^{-2}. 5x increase with σ_m. 10x increase with σ_a. (56 Pe, Figure 288)

TITANIUM ALLOY (RC 55, forged at 1,750°F, hot-rolled at 1,450°F, annealed at 1,300°F). Rotating bending. N = $10^{1.3}$ to 10^{4}. At T = 70°F, σ_a = 10 to 50 ksi, D = 3 x 10^{-2} to 3 x 10^{2}, with D = 1.2 x 10^{-1} at $\sigma_a = \sigma_g$ = 24 ksi, and a 20x increase with N. At T = 600°F, σ_a = 5 to 30 ksi, D = 2 x 10^{-2} to 2 x 10^{2}, with D = 6 x 10^{-2} at $\sigma_a = \sigma_g$ = 10 ksi, and a 20x increase with N. (56 Po, Figures 291 and 294)

TITANIUM ALLOY (RC 55, forged, hot-rolled, annealed at 1,350°F, air cooled, cold drawn, heated to 1,300°F, air cooled). Rotating bending. N = $10^{1.3}$ to 10^{5}. At T = 70°F, σ_a = 10 to 70 ksi, D = 3 x 10^{-2} to 3 x 10^{2}, with D = 4 x 10^{-2} at $\sigma_a = \sigma_g$ = 15 ksi, and a 10x change with N. At T = 600°F, σ_a = 5 to 30 ksi, D = 3 x 10^{-2} to 2 x 10^{2}, with D = 5 x 10^{-1} at $\sigma_a = \sigma_g$ = 20 ksi, and a 10x change with N. (56 Po, Figures 292 and 293)

TUNGSTEN (Annealed at TR = 1,580 or 2,000°C). Torsion. T = 800 to 1,800°F. η_s = 10^{-2} to 10^{-1}. 2x change with TR. 10x increase with T. (59 Sc, Figure 297)

TUNGSTEN (Pure). f = 0.1. $\epsilon < 10^{-3}$. $\eta = 2.2 \times 10^{-4}$. (62 Sm*)

TUNGSTEN (Annealed at 1,410, 1,750, or 2,300°C, also large grains). Torsion. T = 800 to 1,800°F. $\eta_s = 2 \times 10^{-3}$ to 1.5×10^{-1}. 20x increase with T. 10x change with anneal or grain size. (59 Sc, Figure 298)

TUNGSTEN (Swaged). Strains of about 5×10^{-3}. Rotating bending. $\eta_s = 5.2 \times 10^{-3}$. (41 Ki*)

TUNGSTEN CARBIDES (Sintered tungsten with 13 or 6% Co). Torsion. τ_a = 8 to 16 ksi. $\eta_s = 10^{-3}$ to 3×10^{-3}. Little change with % Co. (44 B, Figure 210)

URANIUM (99.95% pure). Axial stress. Tension only, N = 50 to 200, σ_a = 48 ksi, D $\approx 1.5 \times 10^1$. Compression only, N = 10 to 100, σ_a = 70 ksi, D = 2.5×10^1 to 1.7×10^1. Compression only, N = 50 to 300, σ_a = 56 ksi, D $\approx$ 4.5. (53 Jo, Figure 296)

ZINC (Single crystal, annealed). f = 40,000. $\eta_s = 7 \times 10^{-6}$ to 3×10^{-6}. (42 Bi*)

ZINC (99.999% pure single crystals, annealed). Axial stress. f = 39,000. $\epsilon_a = 10^{-6}$ to 10^{-5}. $\eta = 5 \times 10^{-6}$ to 2×10^{-4}. 10x orientation effect. 10x increase with ϵ_a. (41 R, Figure 299)

ZINC (99.999% pure single crystals, not annealed). Axial stress. f = 39,000. $\eta = 5 \times 10^{-3}$ to 10^{-3} as crystal ages for 130 hrs. (41 R, Figure 300)

ZINC (99.99% pure, extruded, annealed at 200°C). Bending. f = 2,000. $\eta_s = 2.4 \times 10^{-4}$. (38 Fors)

ZINC. Bending. f = 50 to 400. $\eta_s = 4 \times 10^{-3}$ to 9×10^{-3}. 2x peak at f = 150. (49 K, Figure 301)

ZINC (Pure, annealed). $\epsilon < 10^{-4}$. f = 200 to 12,000. $\eta = 0.7 \times 10^{-4}$ to 2.5×10^{-4}. (62 Sm*)

ZINC (Annealed or rolled). Strain less than 10^{-4}. Bending. f = 2. Annealed, $\eta_s = 5.4 \times 10^{-4}$. Rolled, $\eta_s = 1.6 \times 10^{-3}$. (41 Ki*)

ZINC. Bending. f = 1 to 5. $\eta_s = 1.9 \times 10^{-3}$. (41 Ki*)

ZINC (0.07 mm grain size). f = 180. At T = 20°C, $\eta_s = 5 \times 10^{-4}$. At T = 100°C, $\eta_s = 4 \times 10^{-3}$. (42 Bi*)

ZINC (0.04 mm grain size). f = 180. At T = 20°C, $\eta_s = 1.2 \times 10^{-3}$. At T = 100°C, $\eta_s = 8 \times 10^{-3}$. (42 Bi*)

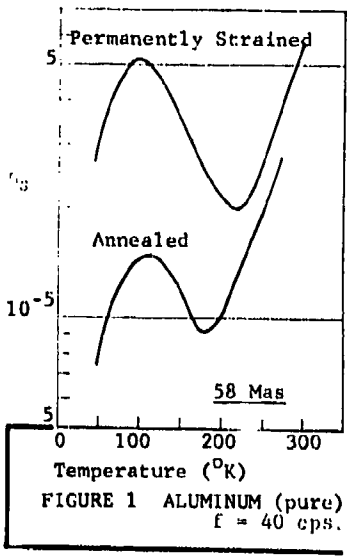

FIGURE 1 ALUMINUM (pure) f = 40 cps.

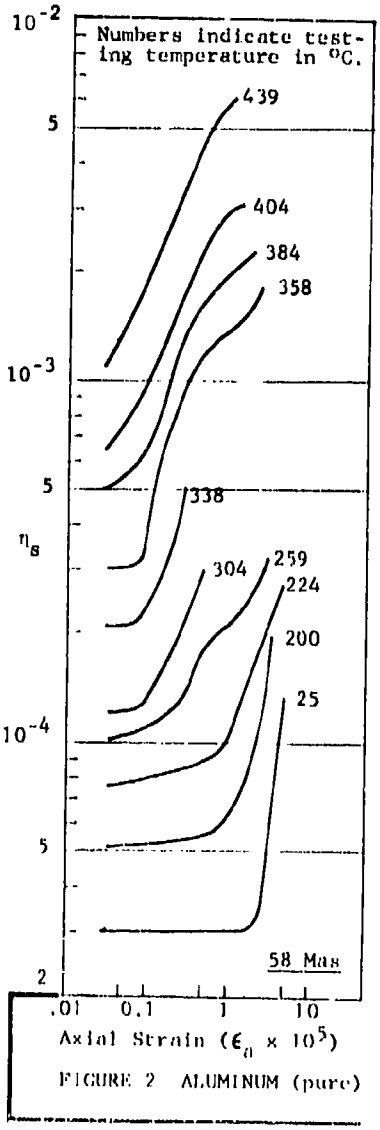

FIGURE 2 ALUMINUM (pure)

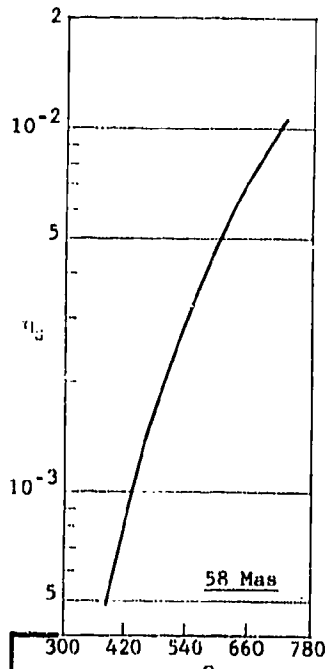

FIGURE 3 ALUMINUM (10^5 disloc. per cm^2) f=1 cps.

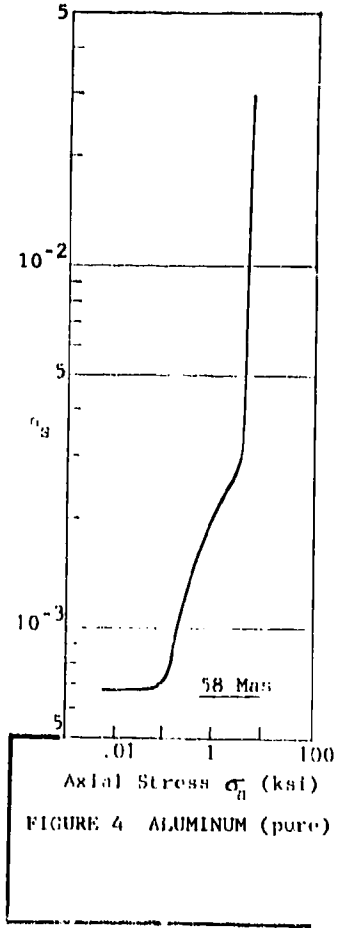

FIGURE 4 ALUMINUM (pure)

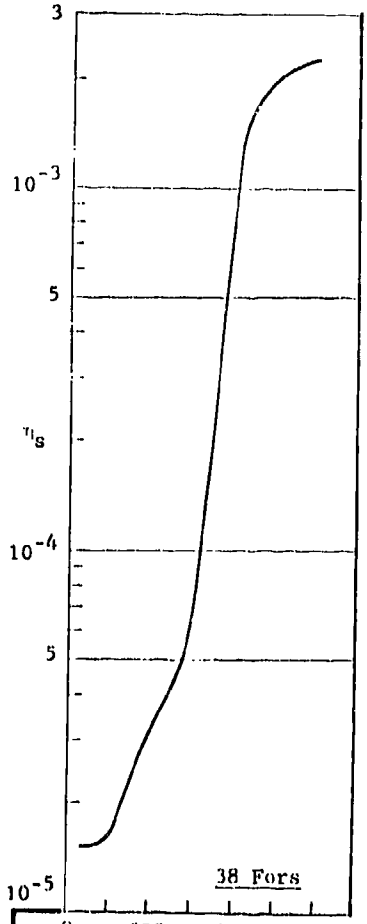

FIGURE 5 ALUMINUM (pure, annealed at 500°C)

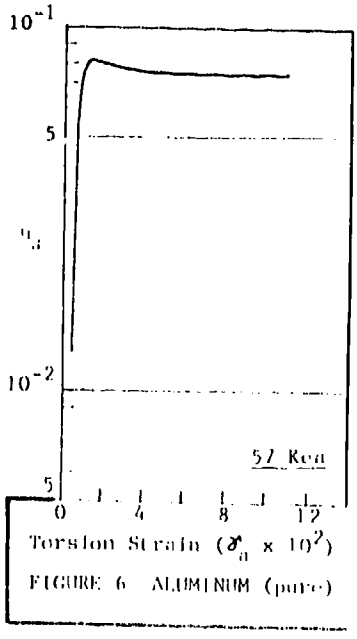

FIGURE 6 ALUMINUM (pure)

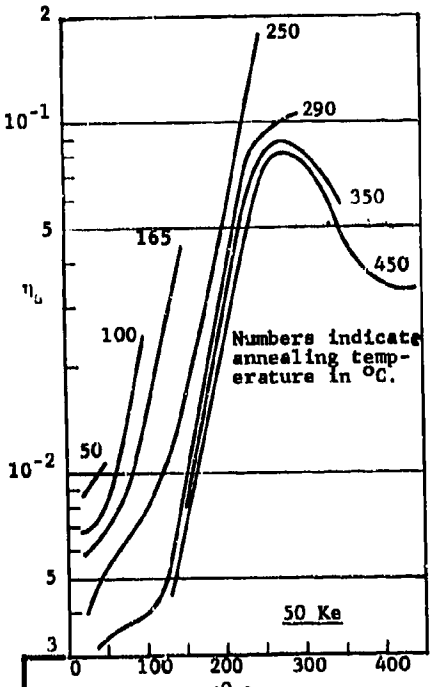

FIGURE 7 ALUMINUM (pure, worked, annealed)

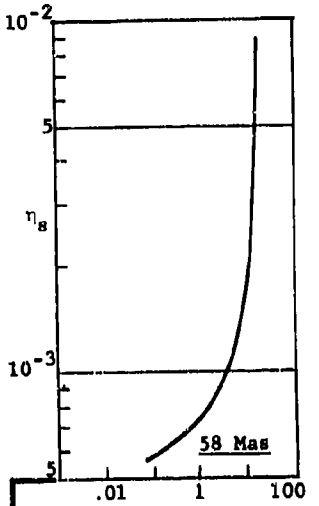

FIGURE 9 ALUMINUM (pure 2S)

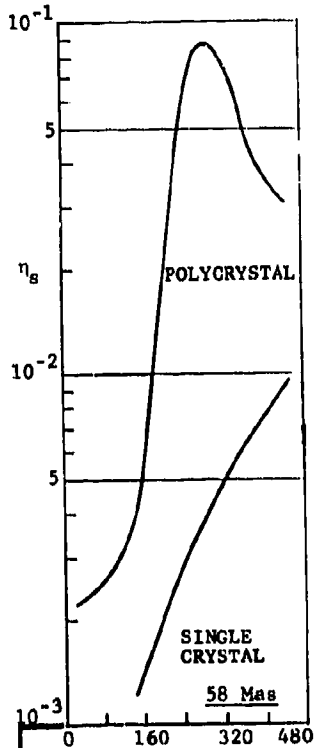

FIGURE 11 ALUMINUM

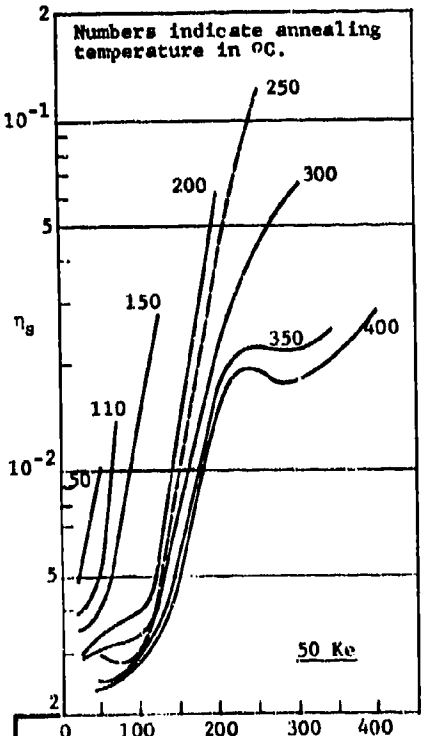

FIGURE 8 ALUMINUM (pure, 2S, worked)

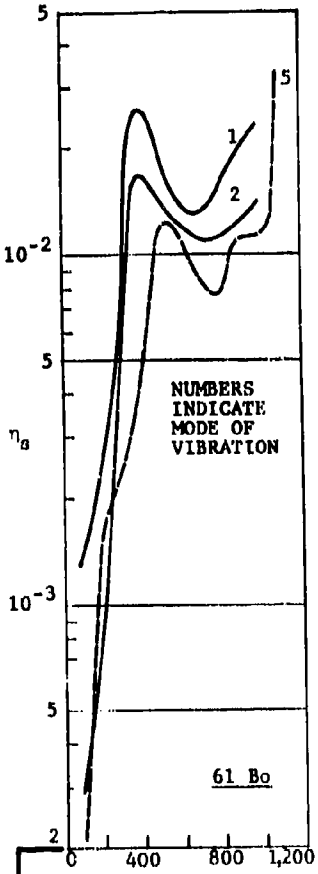

FIGURE 10 ALUMINUM (pure 1100, worked)

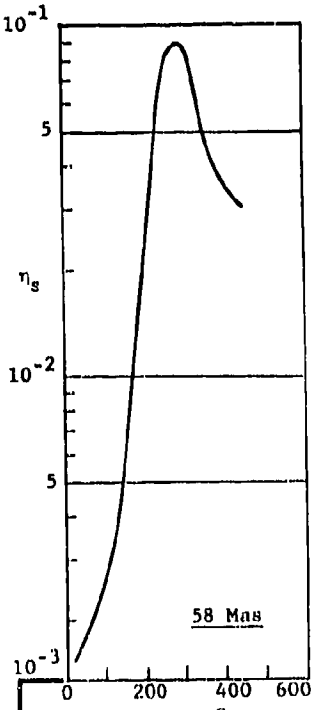

FIGURE 12 ALUMINUM (iron and copper impurities)

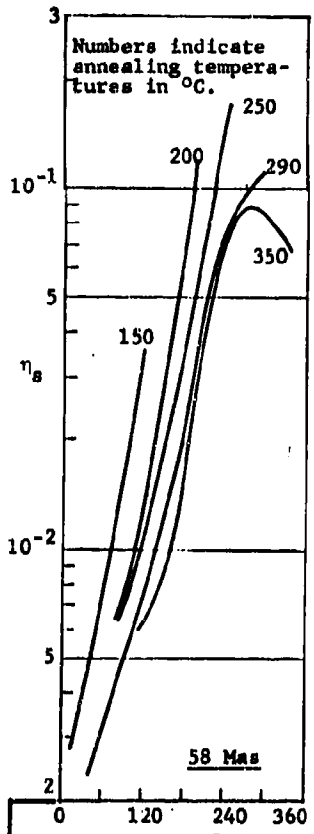

FIGURE 13 ALUMINUM (worked, annealed)

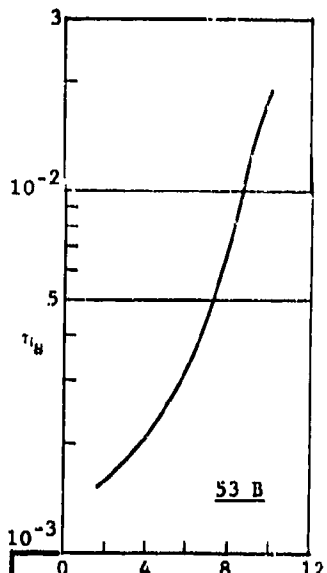

FIGURE 15 ALUMINUM

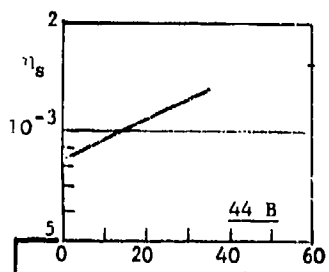

FIGURE 18 ALUMINUM ALLOY (4.7% Cu, annealed)

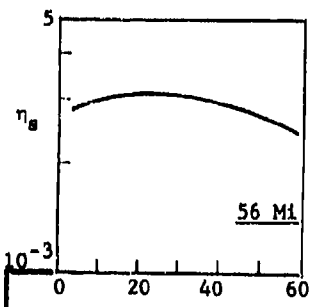

FIGURE 16 ALUMINUM (drawn)

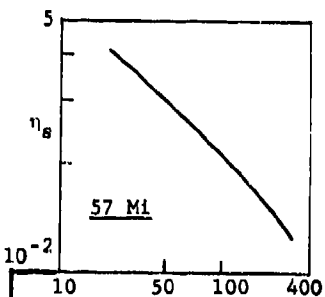

FIGURE 19 ALUMINUM ALLOY (220-T4, casting)

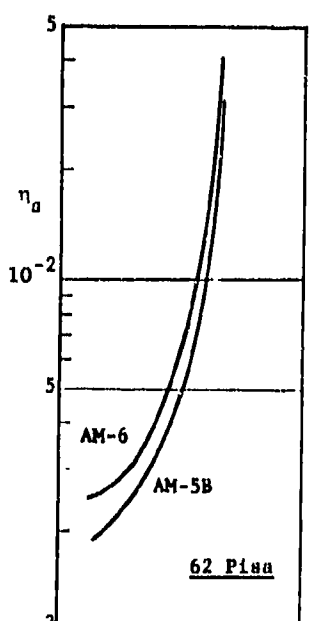

FIGURE 14 ALUMINUM ALLOYS (Russian alloys AM-6, AM5B)

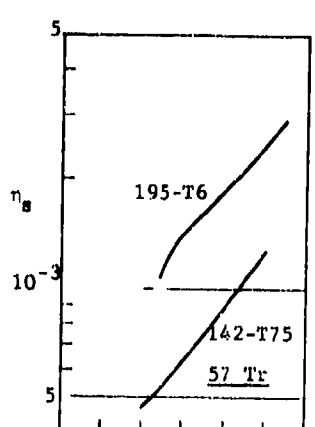

FIGURE 17 ALUMINUM ALLOYS (195-T6, 142-T75)

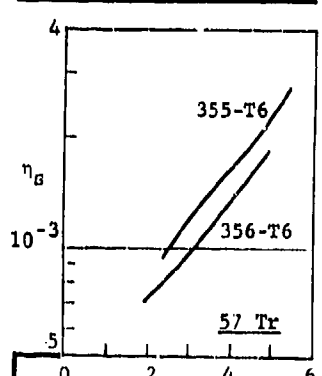

FIGURE 20 ALUMINUM ALLOYS (355-T6, 356-T6)

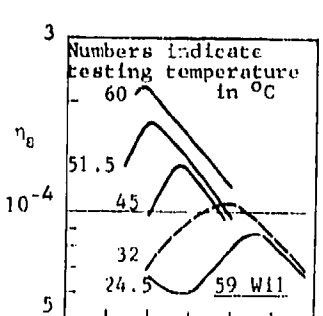

FIGURE 21 ALUMINUM ALLOY (2014, treated)

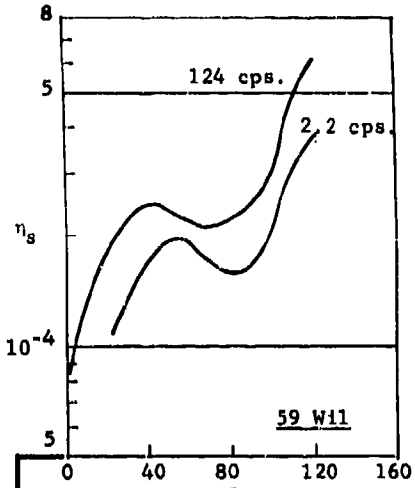

FIGURE 22 ALUMINUM ALLOY (2014, treated)

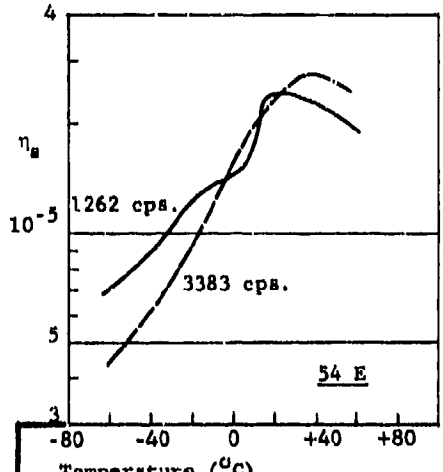

FIGURE 23 ALUMINUM ALLOY (2017, treated)

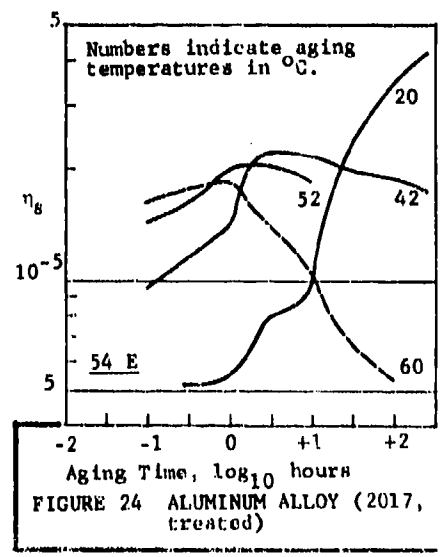

FIGURE 24 ALUMINUM ALLOY (2017, treated)

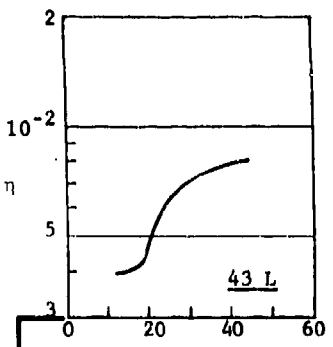

FIGURE 25 ALUMINUM ALLOY (2017)

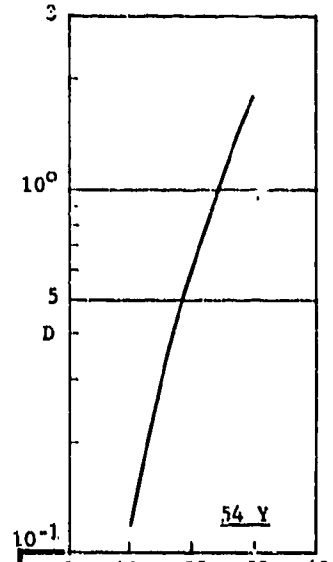

FIGURE 26 ALUMINUM ALLOY (2017)

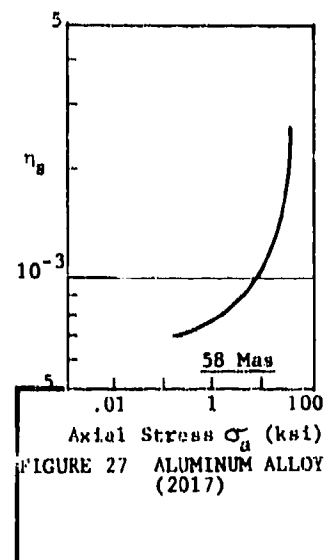

FIGURE 27 ALUMINUM ALLOY (2017)

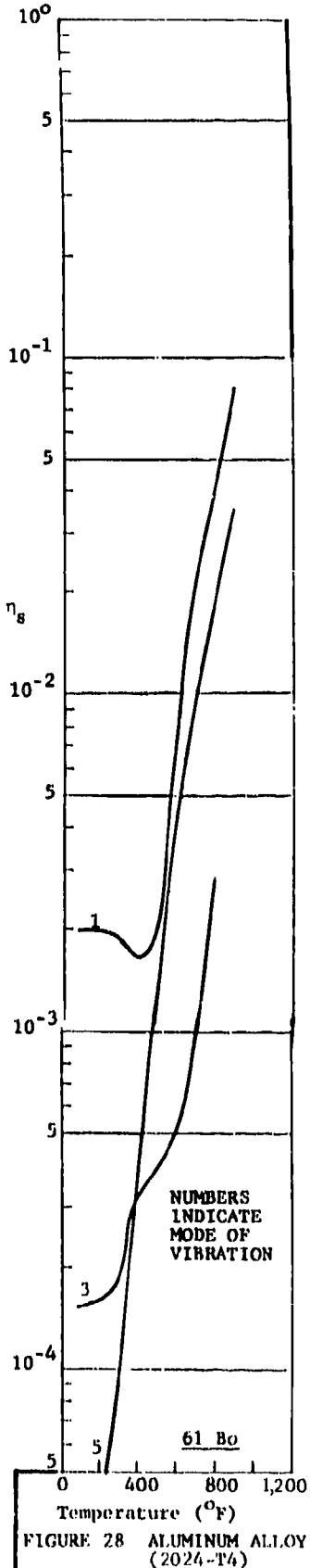

FIGURE 28 ALUMINUM ALLOY (2024-T4)

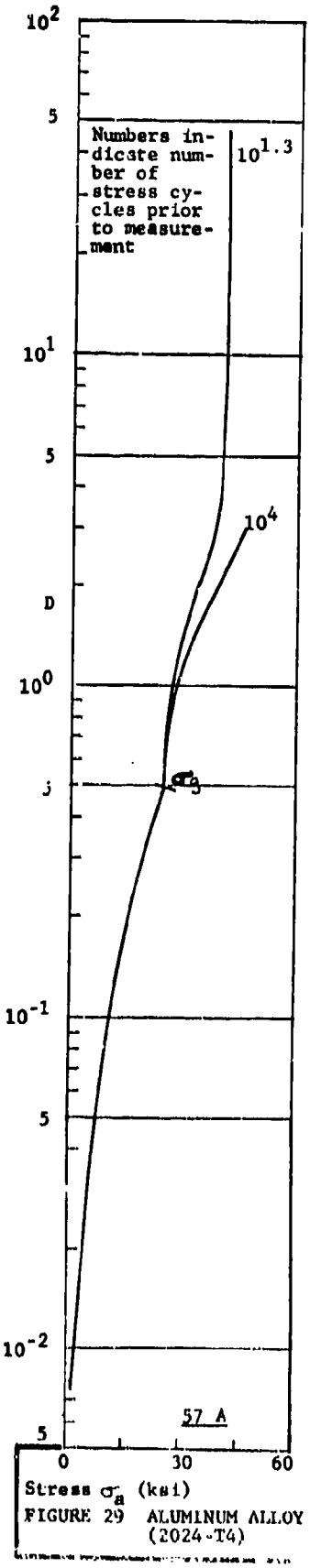

FIGURE 29 ALUMINUM ALLOY (2024-T4)

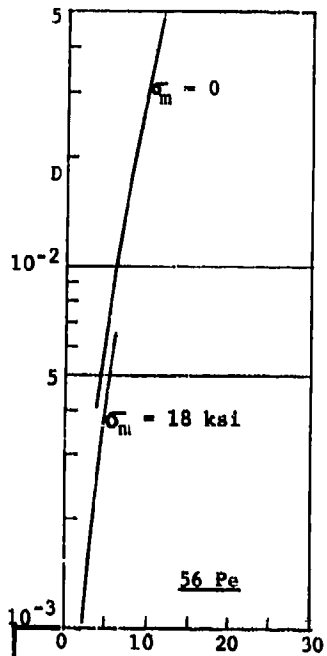

FIGURE 30 ALUMINUM ALLOY (2024 treated)

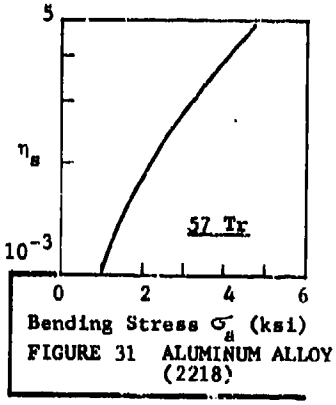

FIGURE 31 ALUMINUM ALLOY (2218)

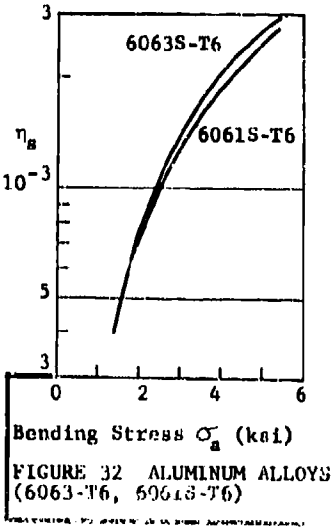

FIGURE 32 ALUMINUM ALLOYS (6063-T6, 6061S-T6)

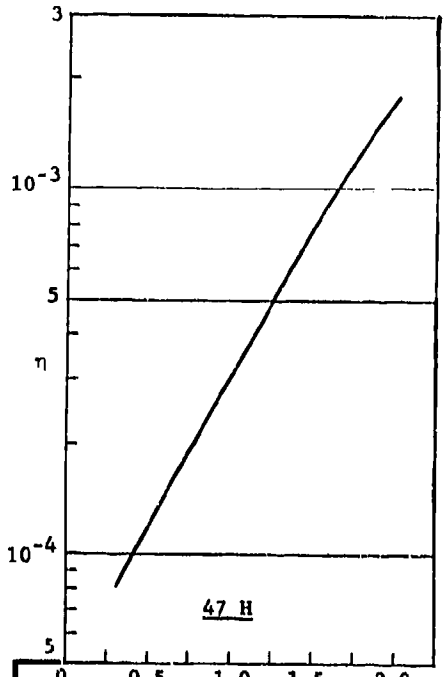

FIGURE 33 ALUMINUM ALLOY (Hinduminium, annealed)

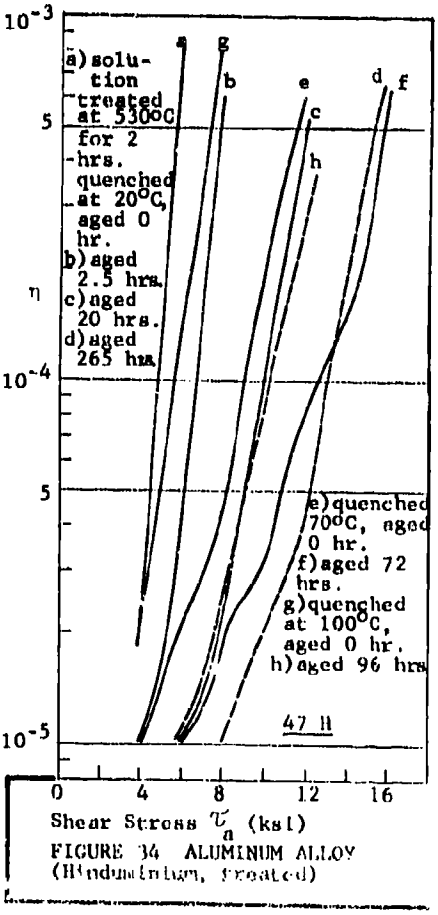

FIGURE 34 ALUMINUM ALLOY (Hinduminium, treated)

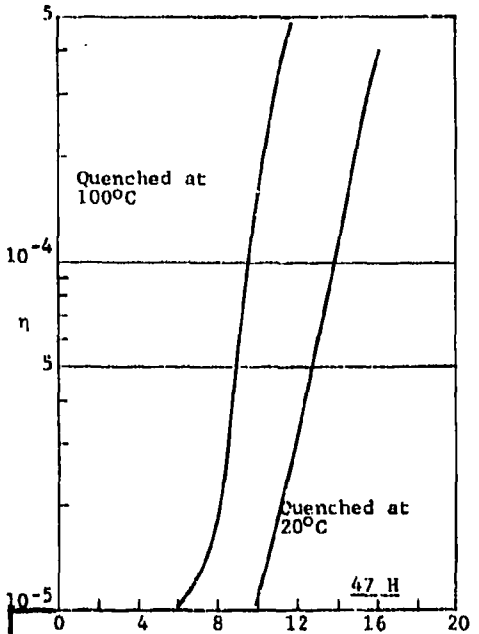

FIGURE 35 ALUMINUM ALLOY (Hinduminium, treated)

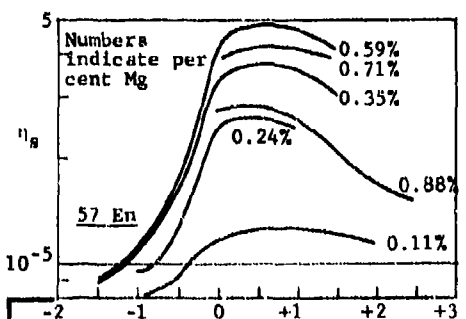

FIGURE 36 ALUMINUM ALLOYS (2.5% Cu, treated)

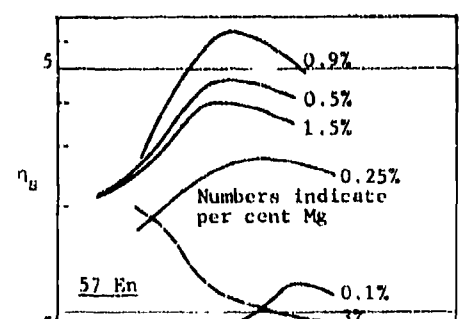

FIGURE 37 ALUMINUM ALLOYS (4% Cu, annealed)

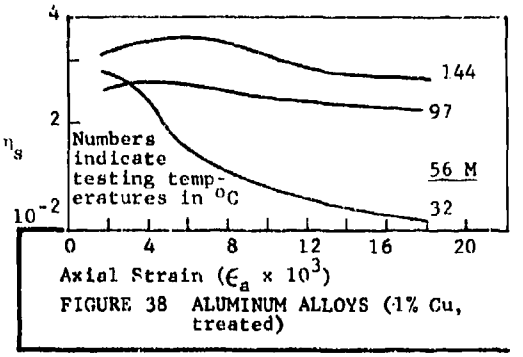

FIGURE 38 ALUMINUM ALLOYS (1% Cu, treated)

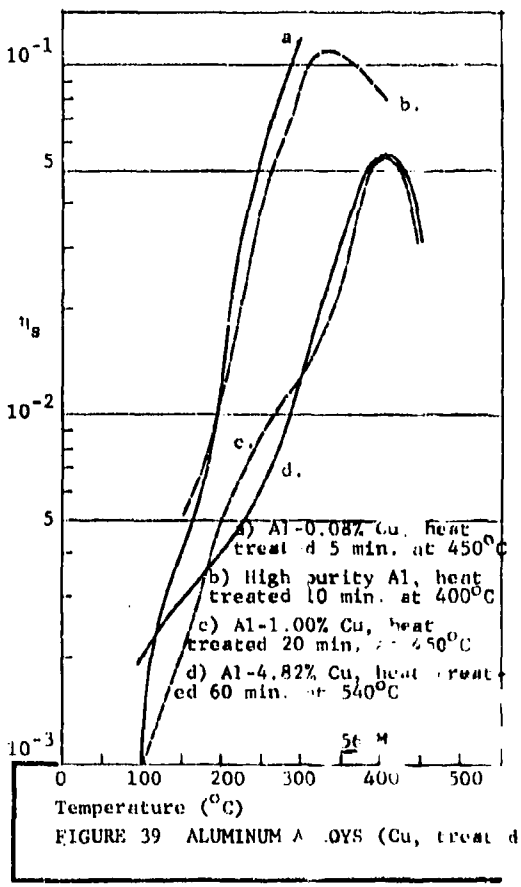

FIGURE 39 ALUMINUM ALLOYS (Cu, treated)

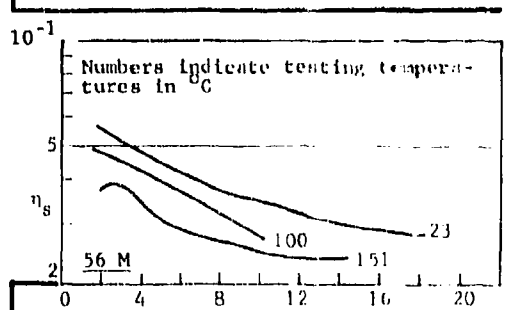

FIGURE 40 ALUMINUM ALLOY (0.08% Cu, treated)

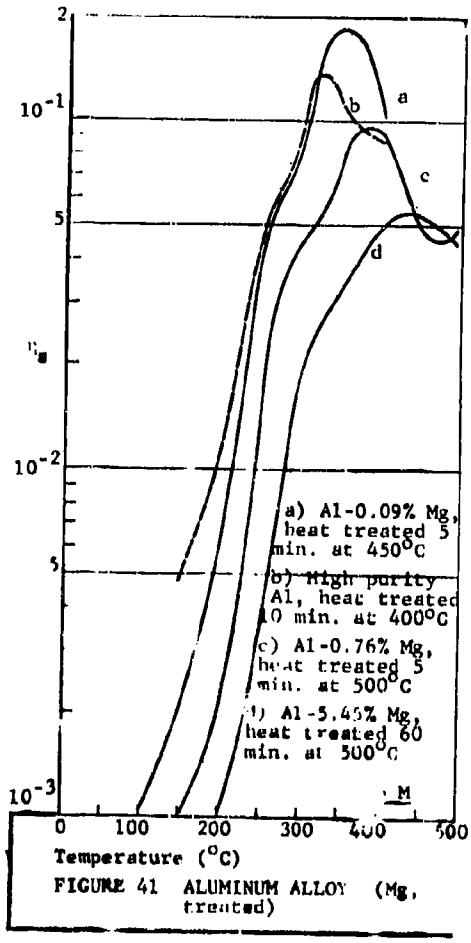

FIGURE 41 ALUMINUM ALLOY (Mg, treated)

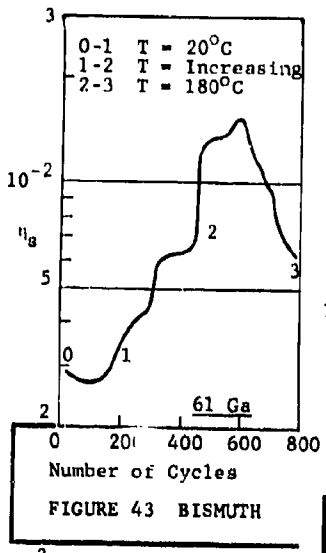

FIGURE 43 BISMUTH

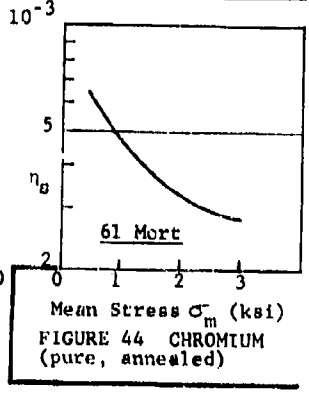

FIGURE 44 CHROMIUM (pure, annealed)

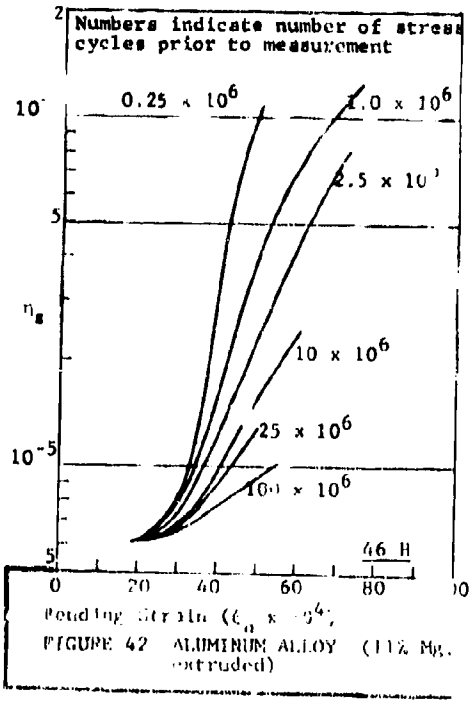

FIGURE 42 ALUMINUM ALLOY (11% Mg, extruded)

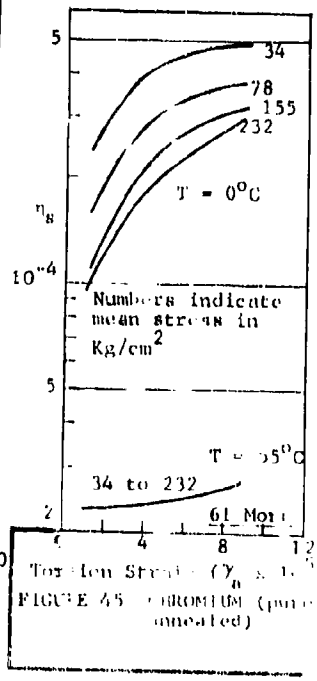

FIGURE 45 CHROMIUM (pure, annealed)

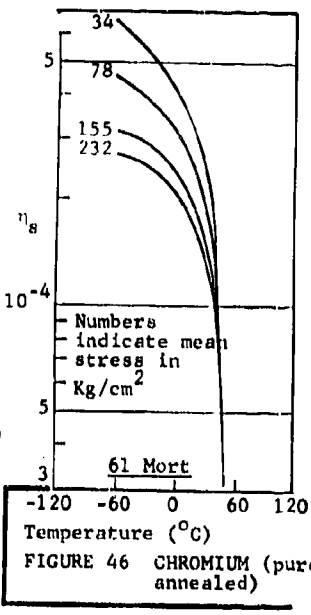

FIGURE 46 CHROMIUM (pure, annealed)

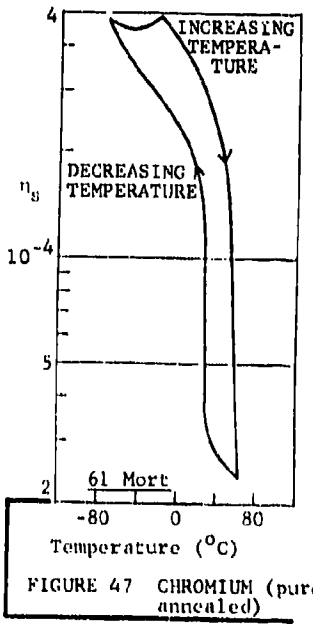

FIGURE 47 CHROMIUM (pure annealed)

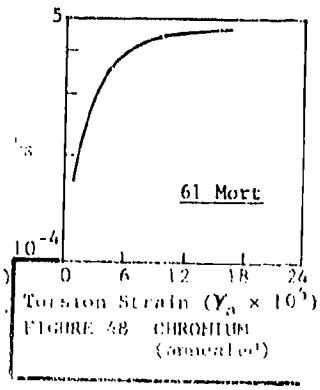

FIGURE 48 CHROMIUM (annealed)

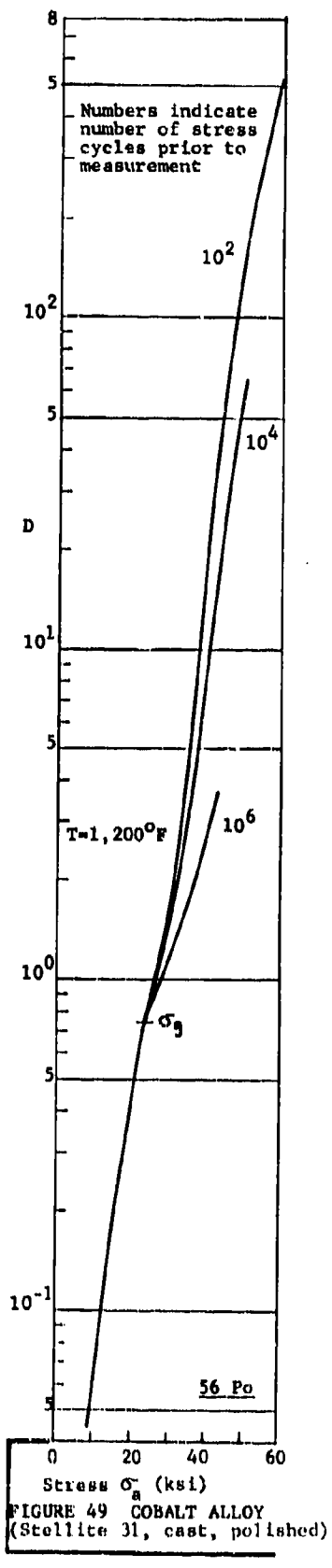

FIGURE 49 COBALT ALLOY
(Stellite 31, cast, polished)

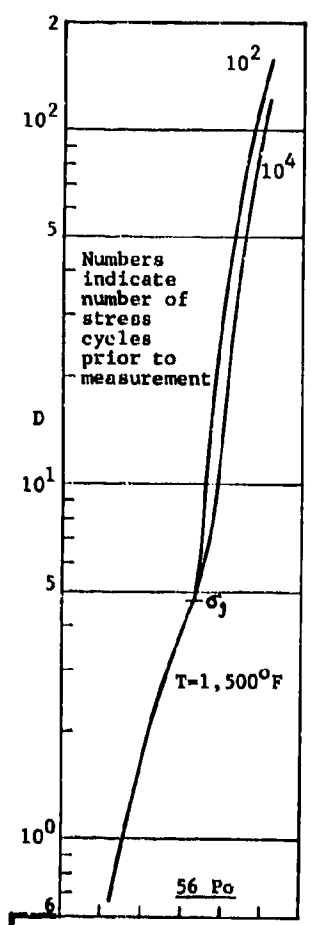

FIGURE 50 COBALT ALLOY
(Stellite 31, cast, polished)

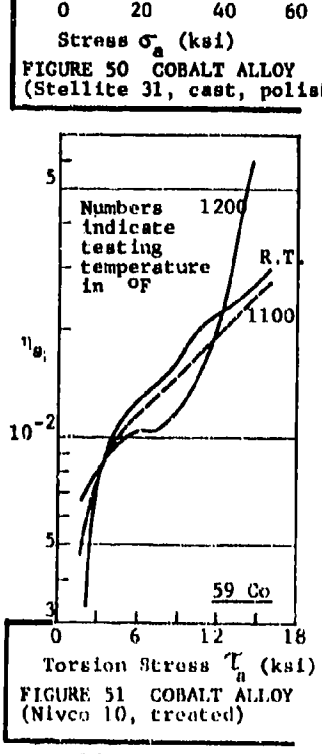

FIGURE 51 COBALT ALLOY
(Nivco 10, treated)

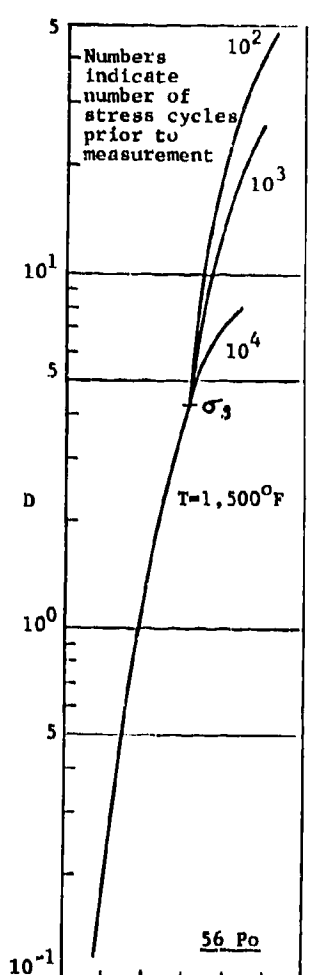

FIGURE 52 COBALT ALLOY
(Stellite 31, cast, aged)

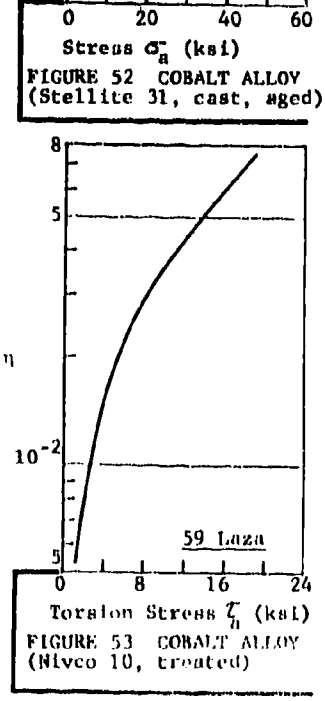

FIGURE 53 COBALT ALLOY
(Nivco 10, treated)

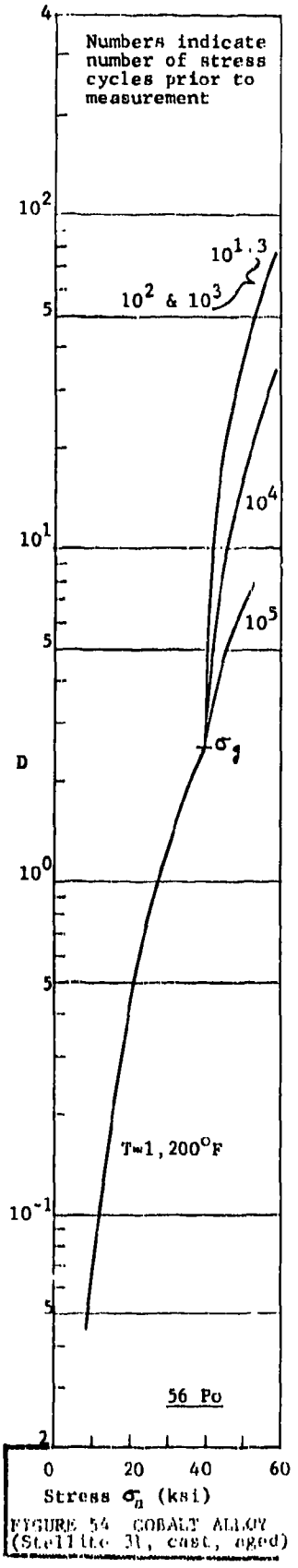

FIGURE 54 COBALT ALLOY (Stellite 31, cast, aged)

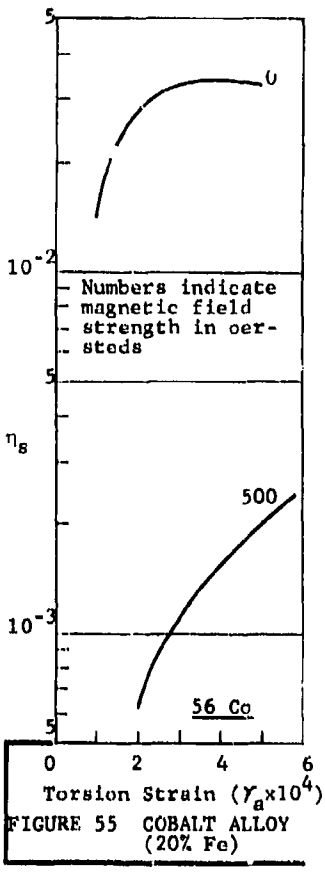

FIGURE 55 COBALT ALLOY (20% Fe)

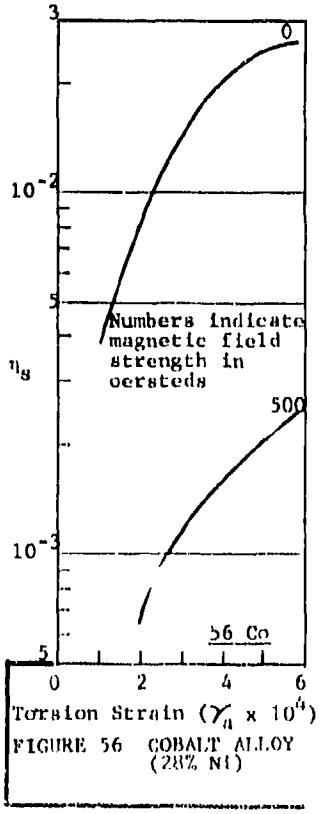

FIGURE 56 COBALT ALLOY (28% Ni)

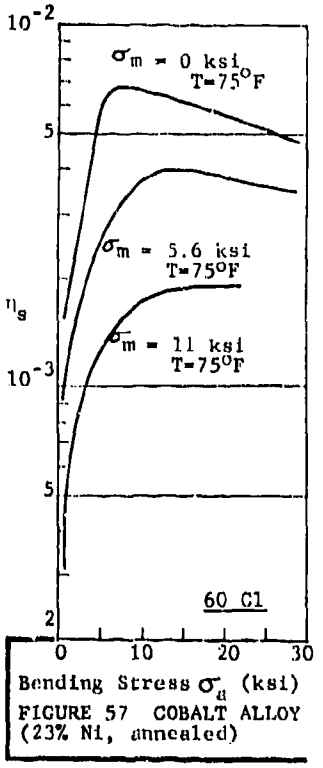

FIGURE 57 COBALT ALLOY (23% Ni, annealed)

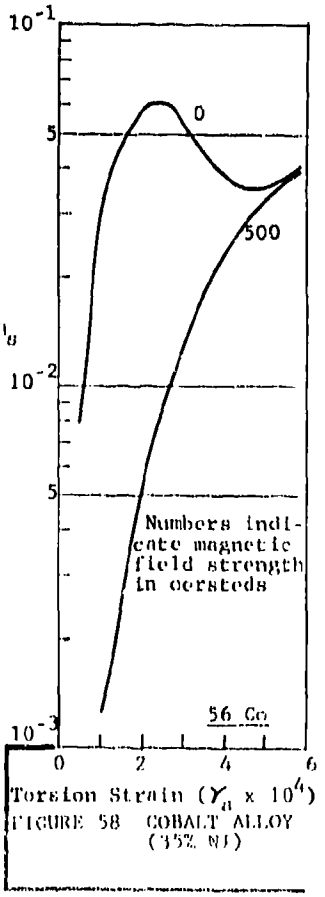

FIGURE 58 COBALT ALLOY (35% Ni)

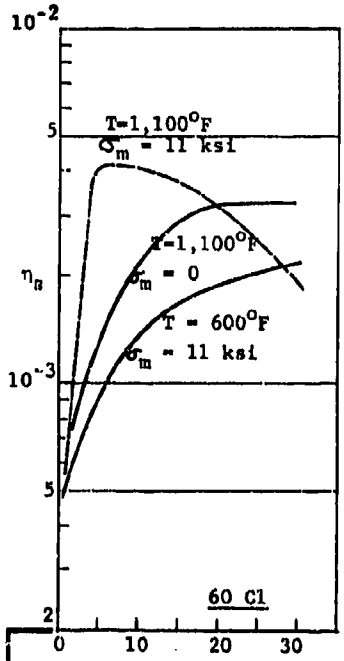

FIGURE 59 COBALT ALLOY (34% Ni, 2% Fe, 2% Ti, annealed)

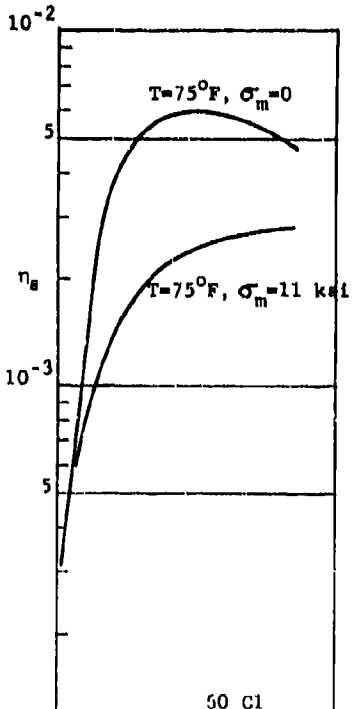

FIGURE 60 COBALT ALLOY (34% Ni, 2% Fe, 2% Ti, annealed)

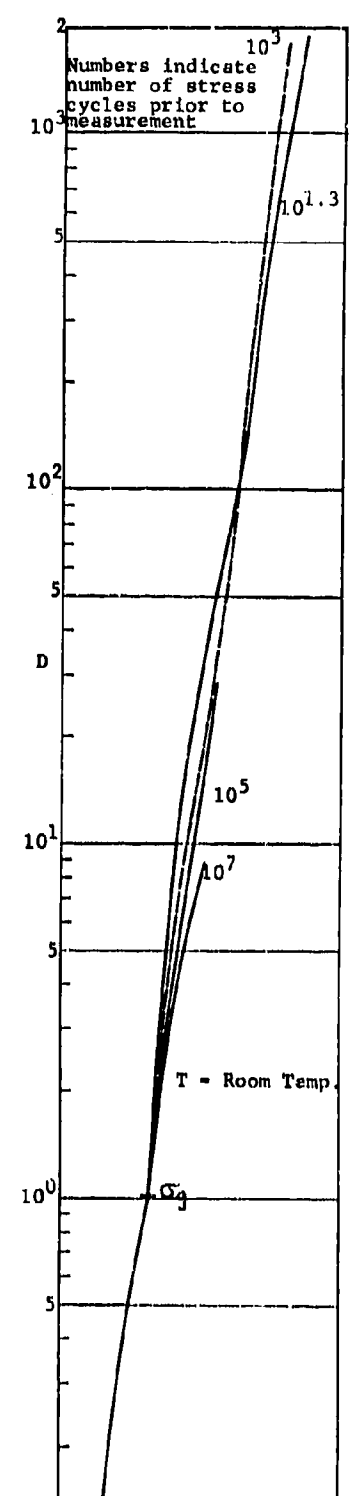

FIGURE 61 COBALT ALLOY (S-816, annealed)

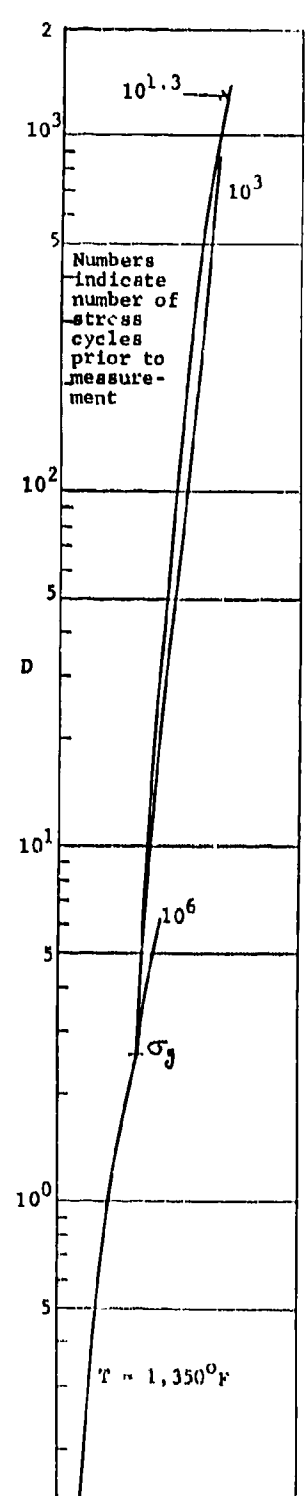

FIGURE 62 COBALT ALLOY (S-816, annealed)

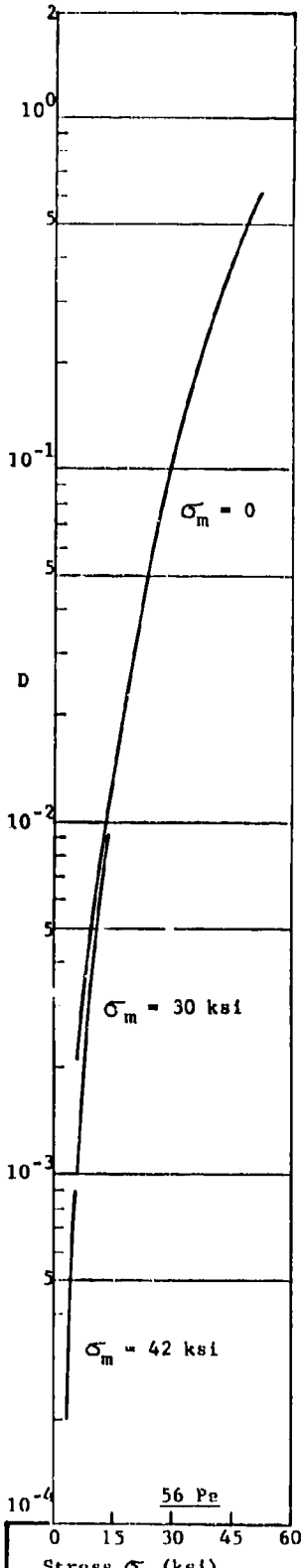

FIGURE 63 COBALT ALLOY (S-816, annealed)

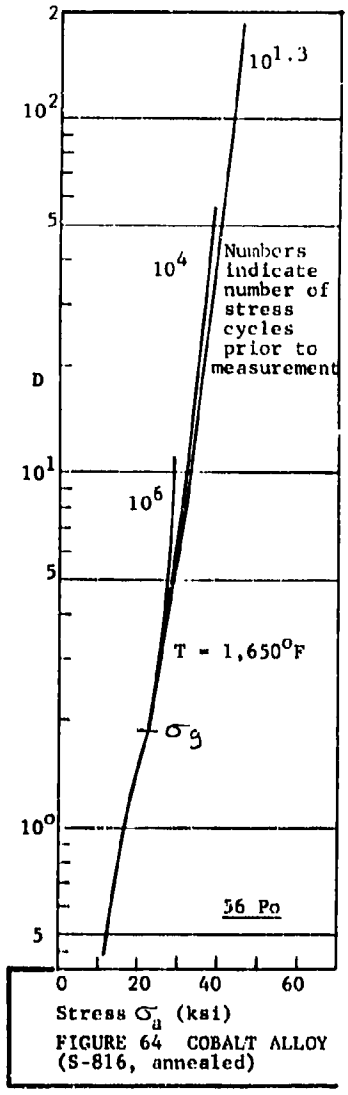

FIGURE 64 COBALT ALLOY (S-816, annealed)

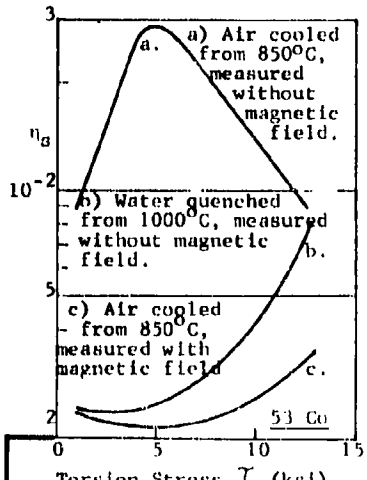

FIGURE 65 COBALT ALLOY (30% Fe)

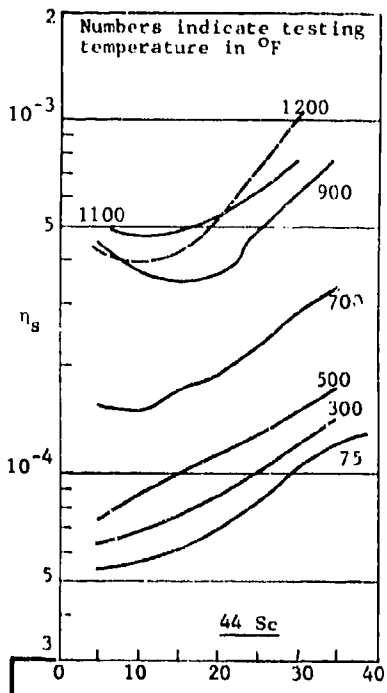

FIGURE 66 COBALT ALLOY (Vitallium, annealed)

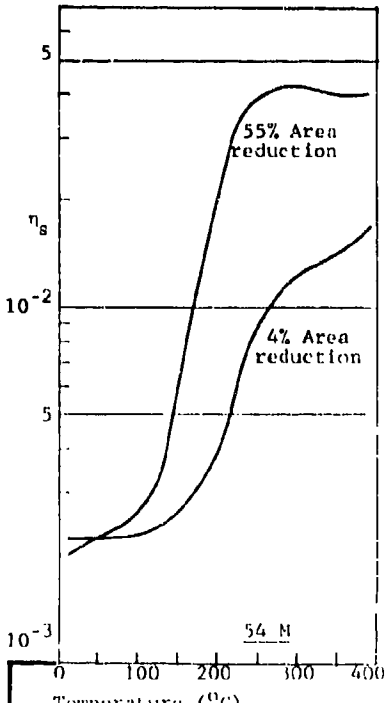

FIGURE 67 COPPER (pure, annealed) Torsion.

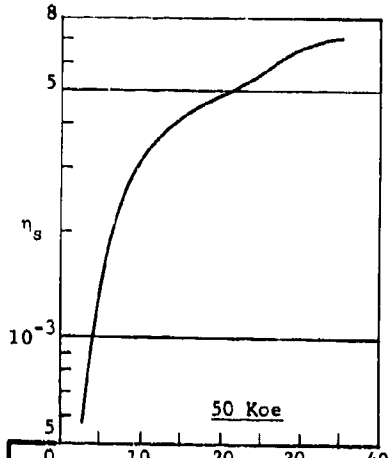

FIGURE 68 COPPER (crystal) Kilocycle frequency.

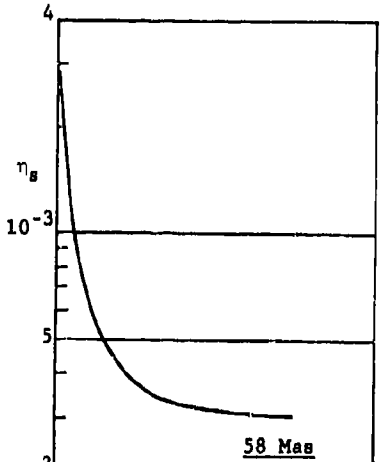

FIGURE 69 COPPER (crystal, annealed, irradiated) Bending at 10 kps.

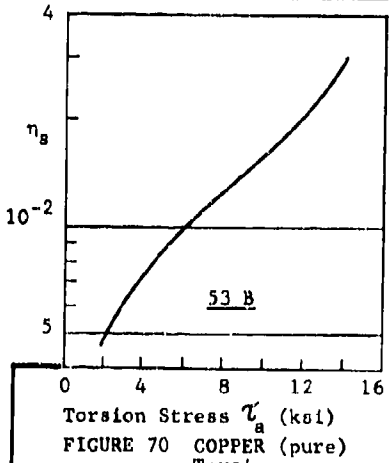

FIGURE 70 COPPER (pure) Torsion.

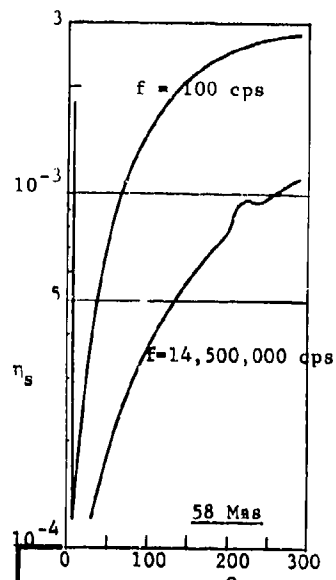

FIGURE 71 COPPER (pure) Bending at 100 cps, shear at 14,500 kps.

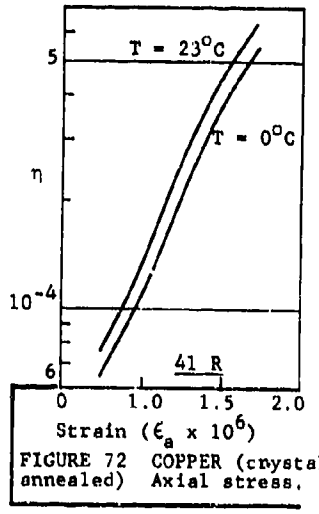

FIGURE 72 COPPER (crystal, annealed) Axial stress.

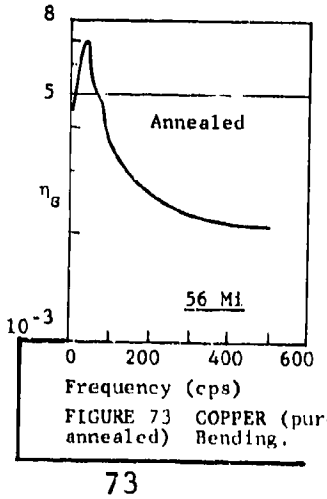

FIGURE 73 COPPER (pure, annealed) Bending.

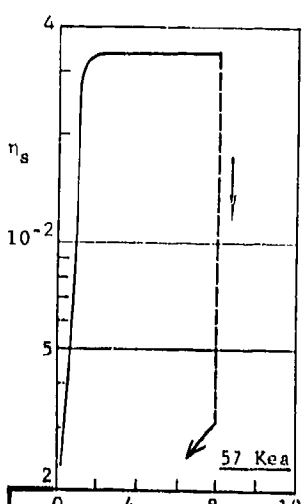

FIGURE 74 COPPER (pure) Torsion.

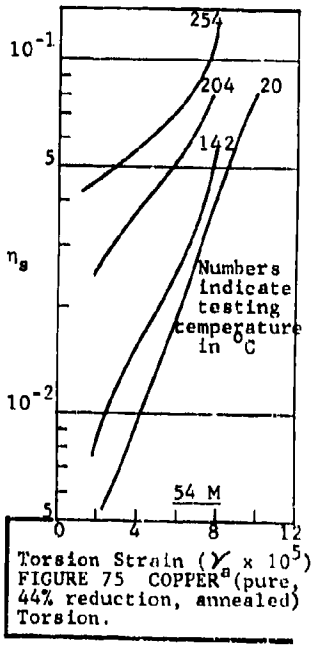

FIGURE 75 COPPER[a] (pure, 44% reduction, annealed) Torsion.

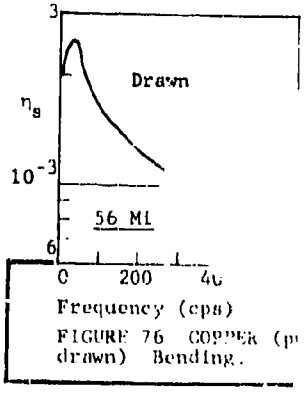

FIGURE 76 COPPER (pure, drawn) Bending.

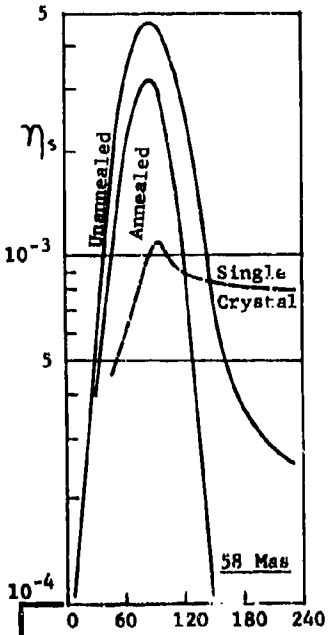

FIGURE 77 COPPER (Crystal) Axial stress at 30 kps.

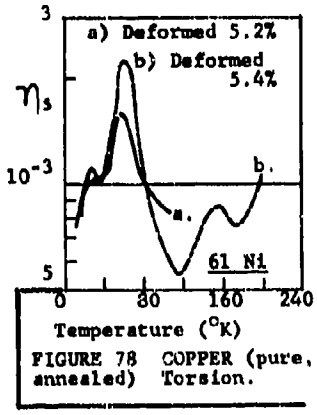

FIGURE 78 COPPER (pure, annealed) Torsion.

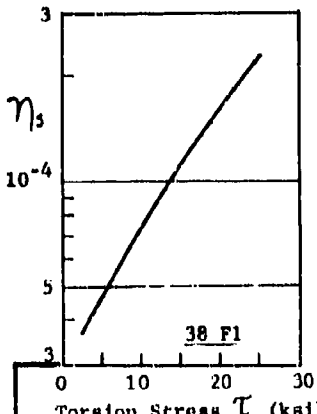

FIGURE 79 COPPER ALLOY (2.6% Co, 0.4% Be, treated)

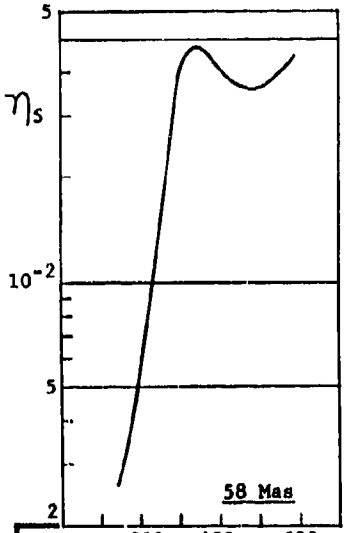

FIGURE 80 COPPER (Pure, some silicon) Torsion.

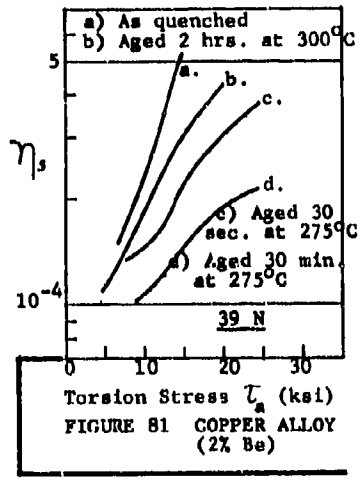

FIGURE 81 COPPER ALLOY (2% Be)

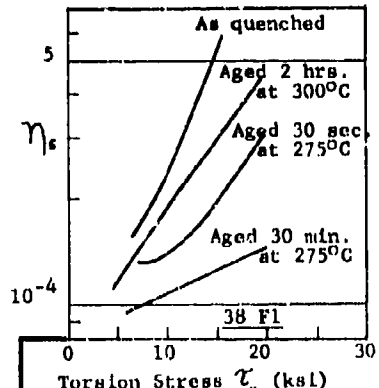

FIGURE 82 COPPER ALLOY (2.12% Be, Fe, Ni, treated)

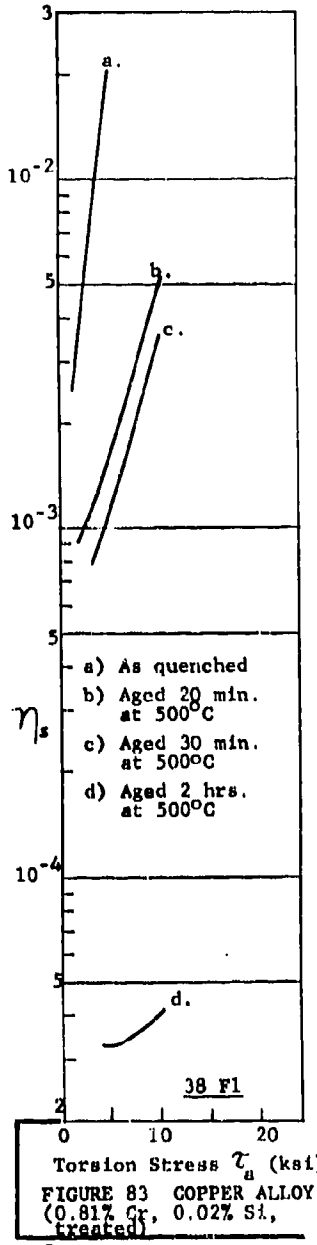

FIGURE 83 COPPER ALLOY (0.81% Cr, 0.02% Si, treated)

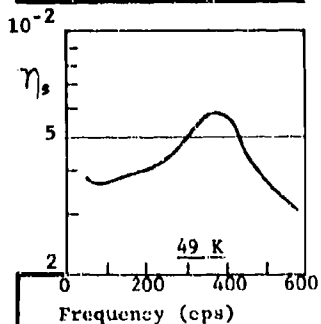

FIGURE 84 COPPER ALLOY (Brass)

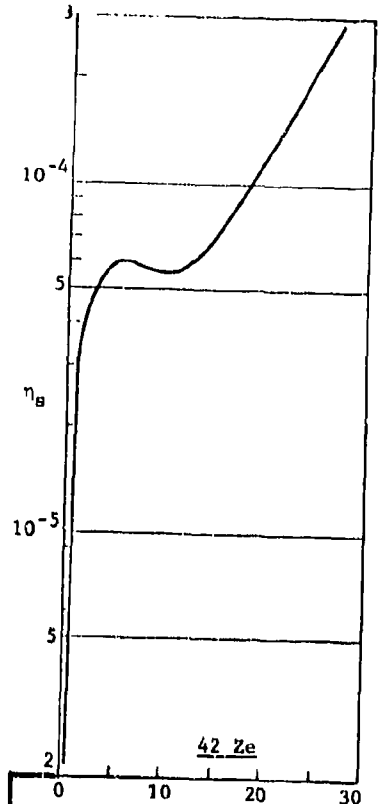

FIGURE 85 COPPER ALLOY (Brass, drawn)

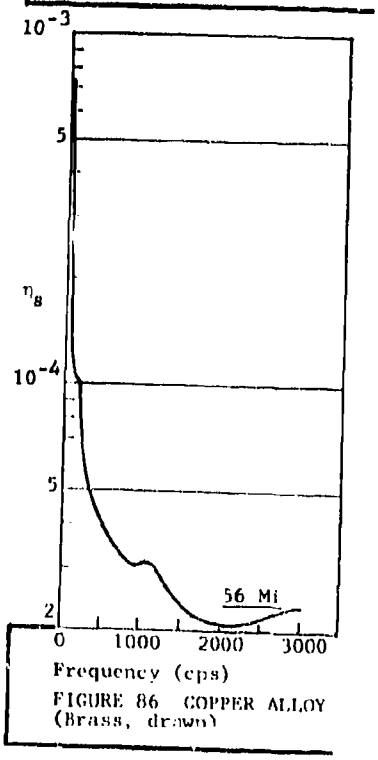

FIGURE 86 COPPER ALLOY (Brass, drawn)

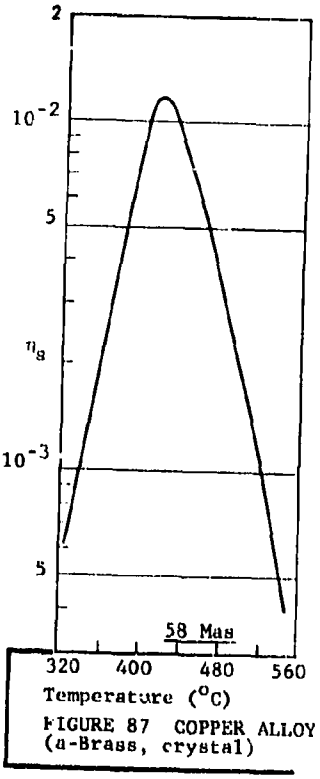

FIGURE 87 COPPER ALLOY (a-Brass, crystal)

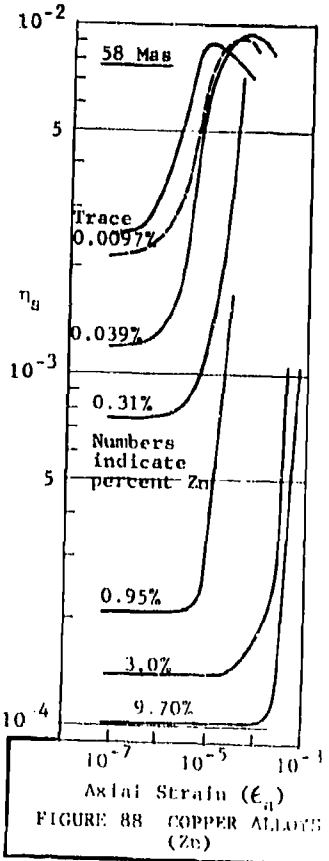

FIGURE 88 COPPER ALLOYS (Zn)

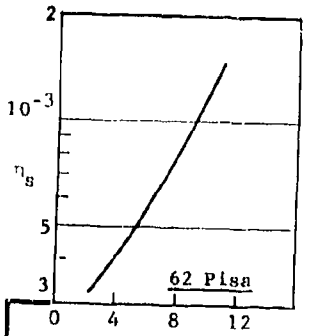

FIGURE 89 COPPER ALLOY (Brass)

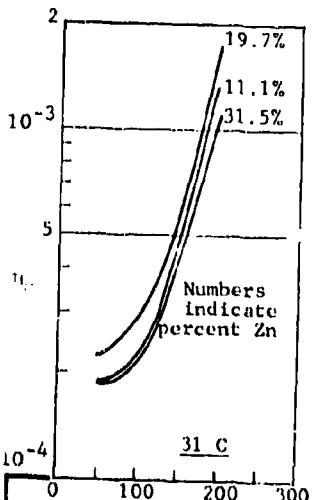

FIGURE 90 COPPER ALLOYS (Zn)

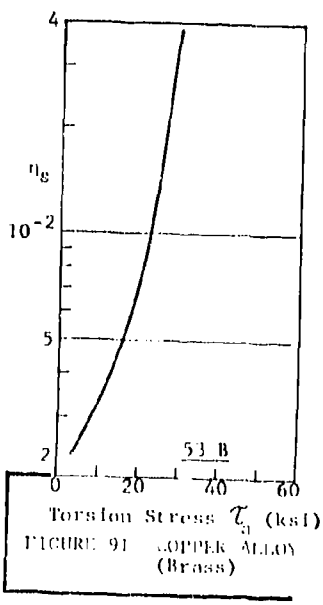

FIGURE 91 COPPER ALLOY (Brass)

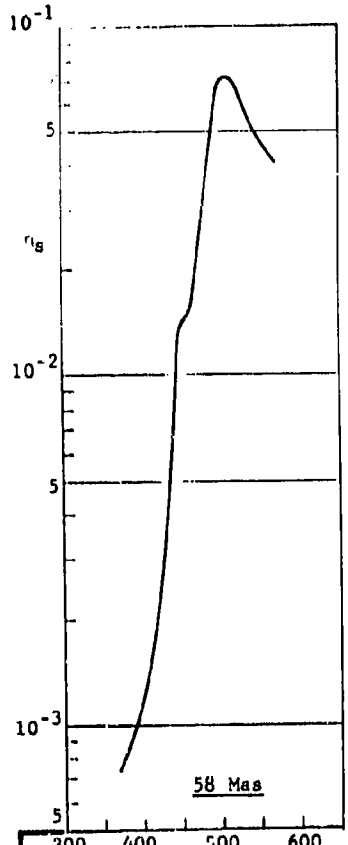

FIGURE 92 COPPER ALLOY (α-Brass)

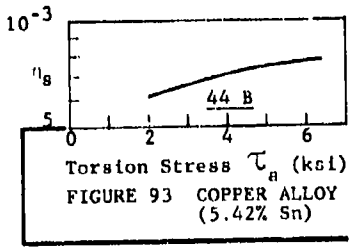

FIGURE 93 COPPER ALLOY (5.42% Sn)

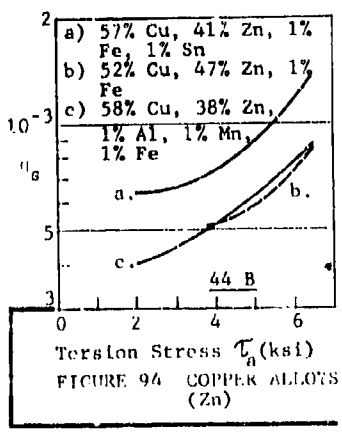

FIGURE 94 COPPER ALLOYS (Zn)

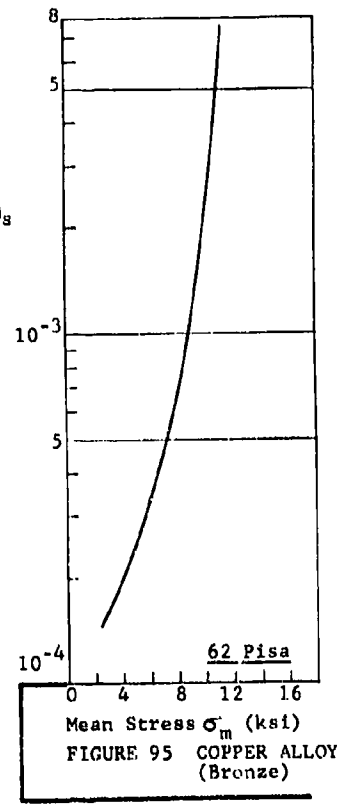

FIGURE 95 COPPER ALLOY (Bronze)

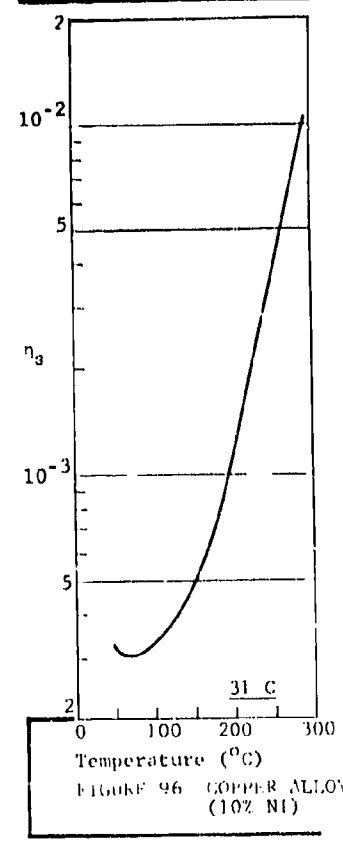

FIGURE 96 COPPER ALLOY (10% Ni)

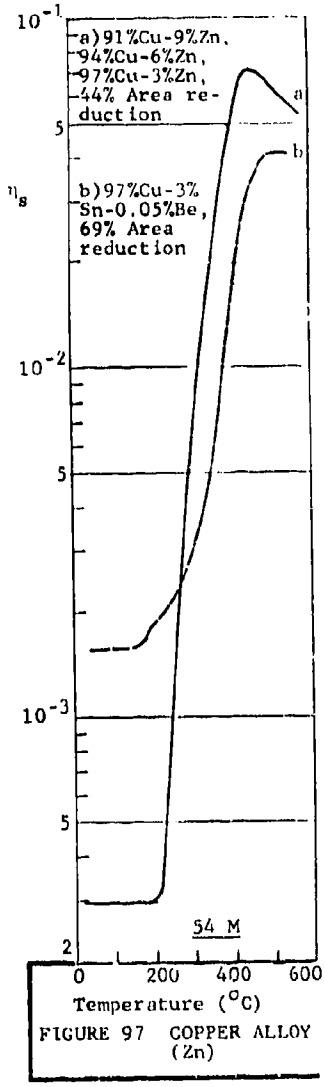

FIGURE 97 COPPER ALLOY (Zn)

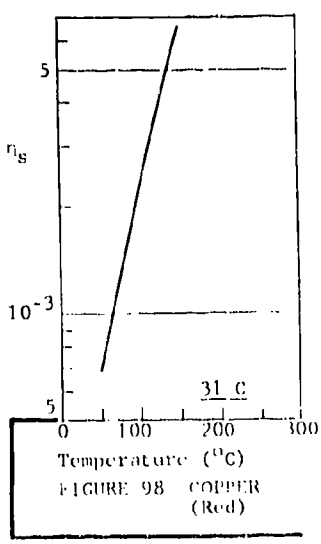

FIGURE 98 COPPER (Red)

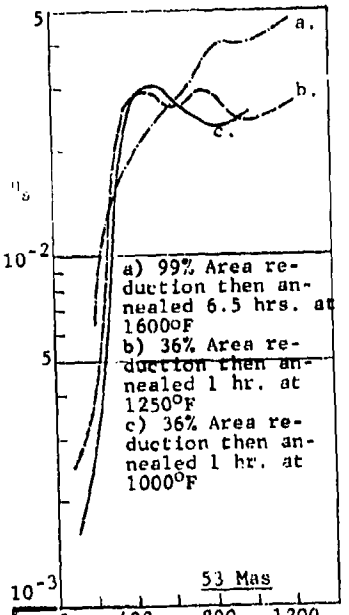

FIGURE 99 GOLD (pure)

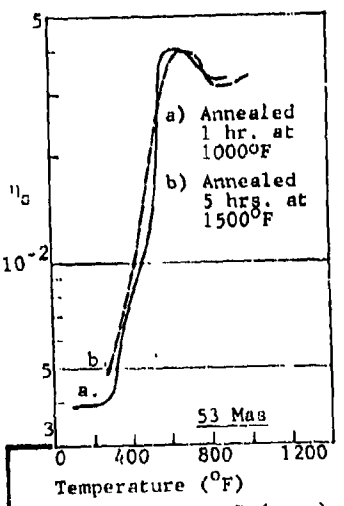

FIGURE 100 GOLD (pure)

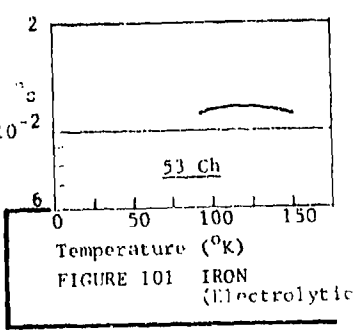

FIGURE 101 IRON (Electrolytic)

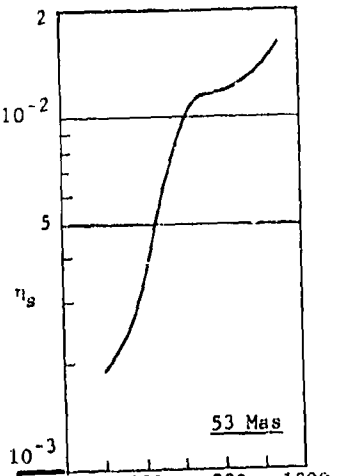

FIGURE 102 GOLD (pure)

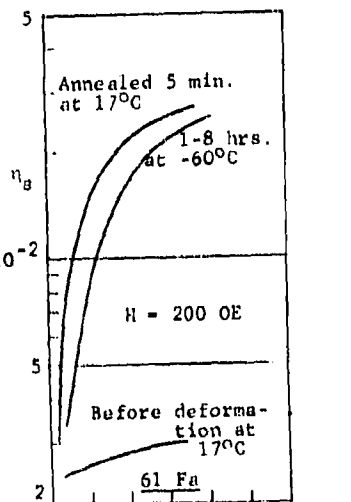

FIGURE 103 IRON (pure, drawn, heated at 700°C)

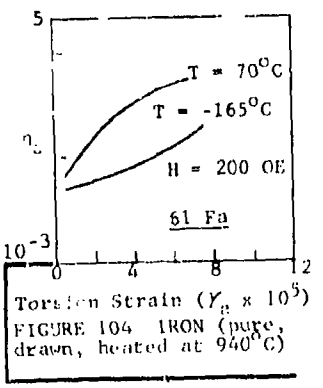

FIGURE 104 IRON (pure, drawn, heated at 940°C)

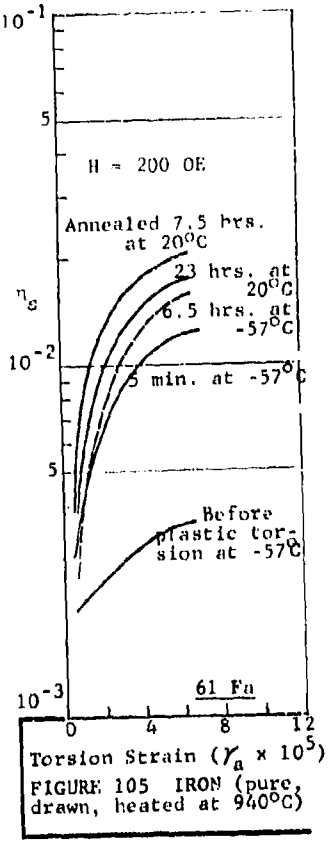

FIGURE 105 IRON (pure, drawn, heated at 940°C)

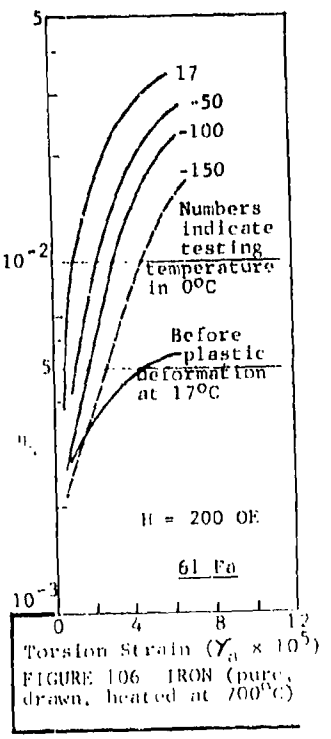

FIGURE 106 IRON (pure, drawn, heated at 700°C)

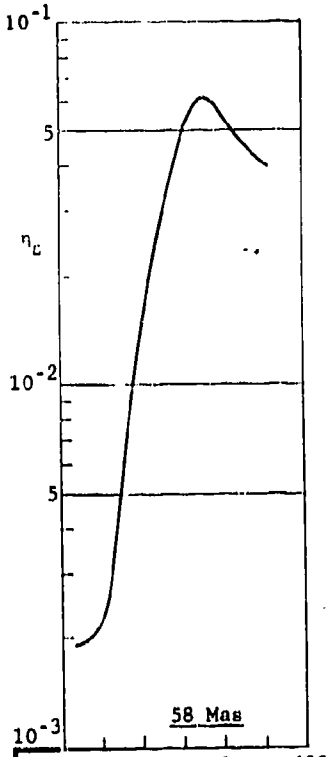

FIGURE 107 IRON

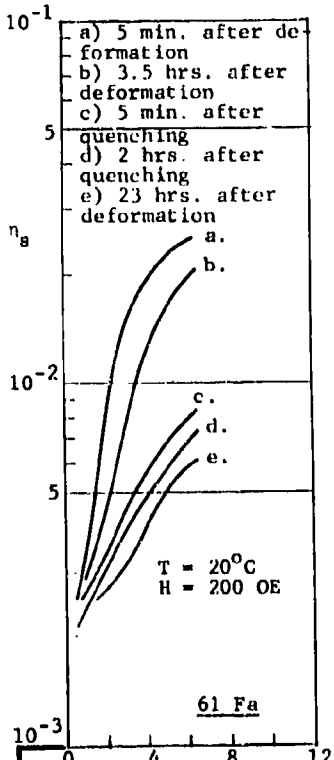

FIGURE 109 IRON (pure, drawn, heated at 800°C)

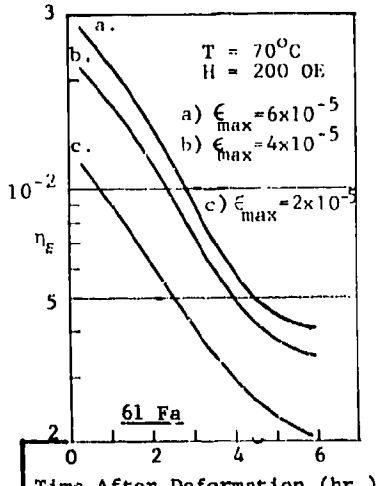

FIGURE 111 IRON (pure, drawn, heated at 940°C)

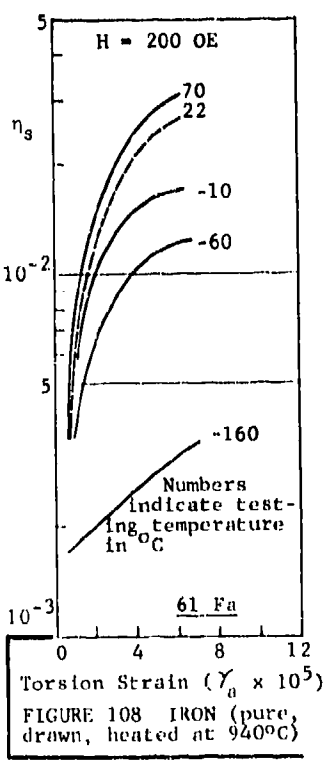

FIGURE 108 IRON (pure, drawn, heated at 940°C)

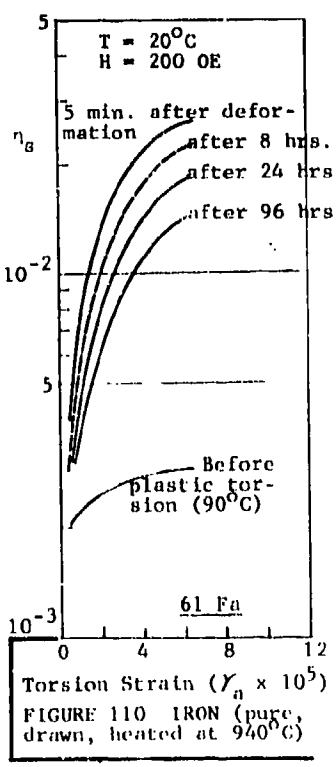

FIGURE 110 IRON (pure, drawn, heated at 940°C)

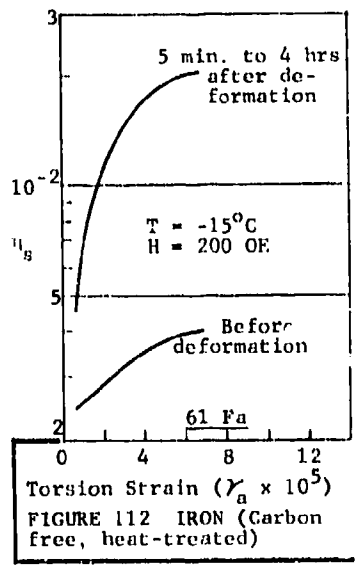

FIGURE 112 IRON (Carbon free, heat-treated)

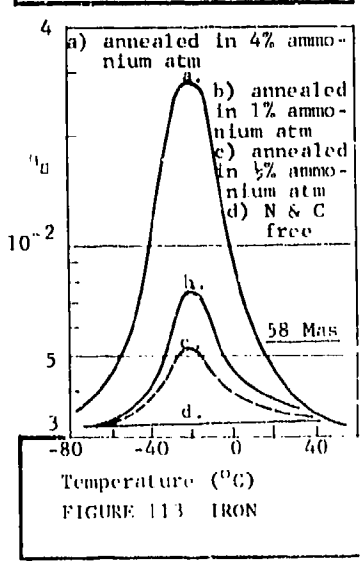

FIGURE 113 IRON

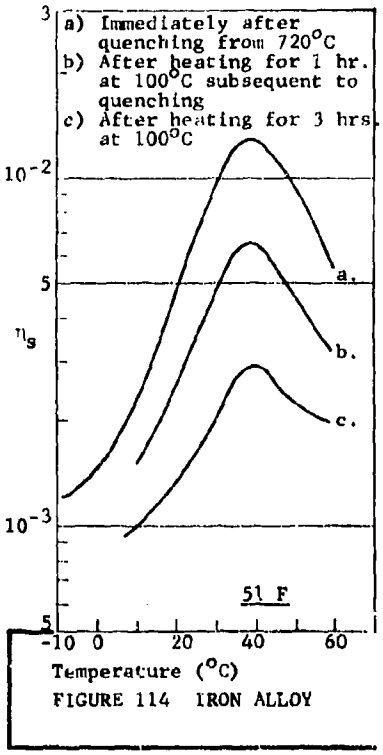

FIGURE 114 IRON ALLOY

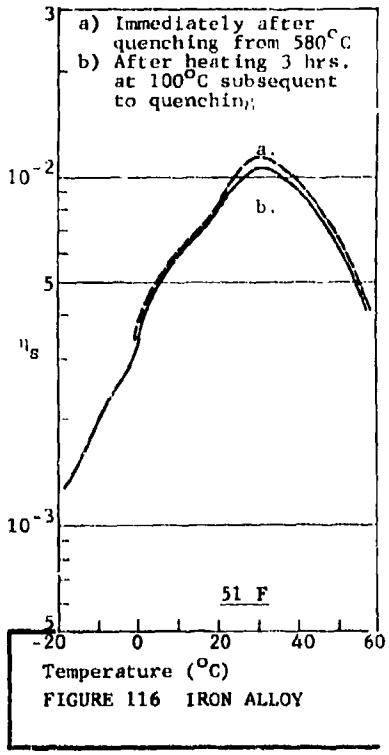

FIGURE 116 IRON ALLOY

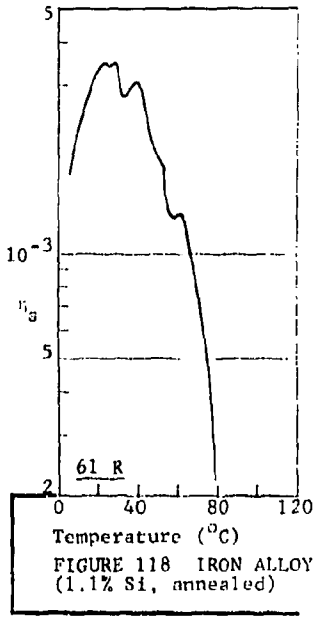

FIGURE 118 IRON ALLOY (1.1% Si, annealed)

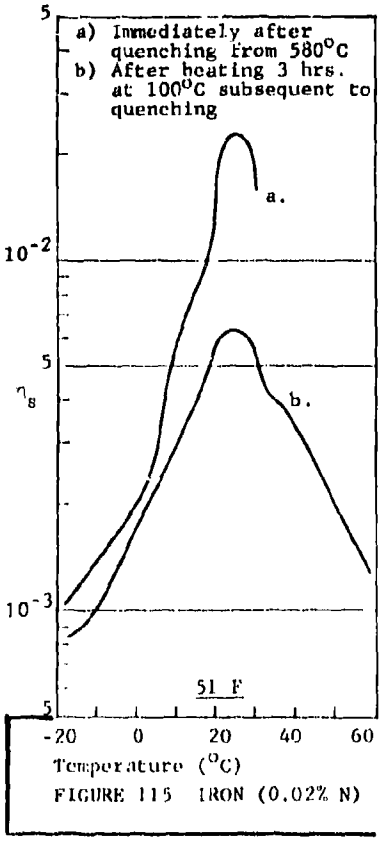

FIGURE 115 IRON (0.02% N)

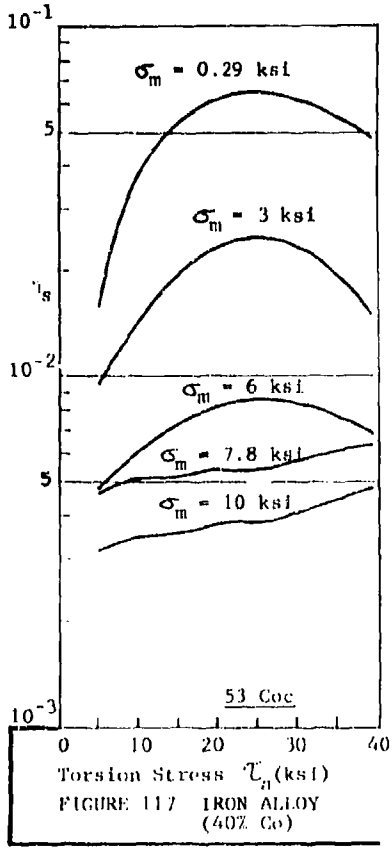

FIGURE 117 IRON ALLOY (40% Co)

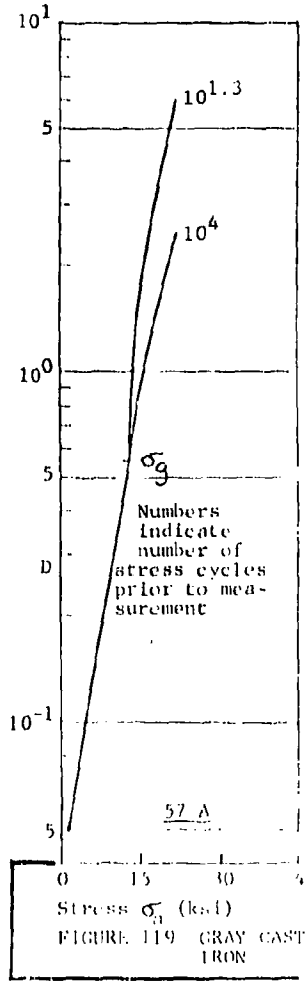

FIGURE 119 GRAY CAST IRON

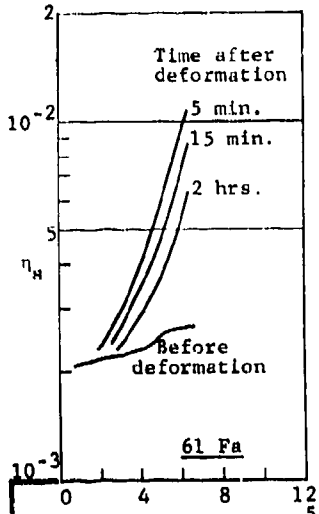

FIGURE 120 IRON (0.001% C, drawn)

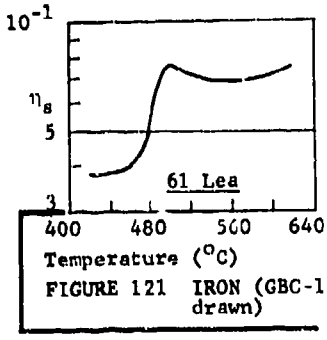

FIGURE 121 IRON (GBC-1, drawn)

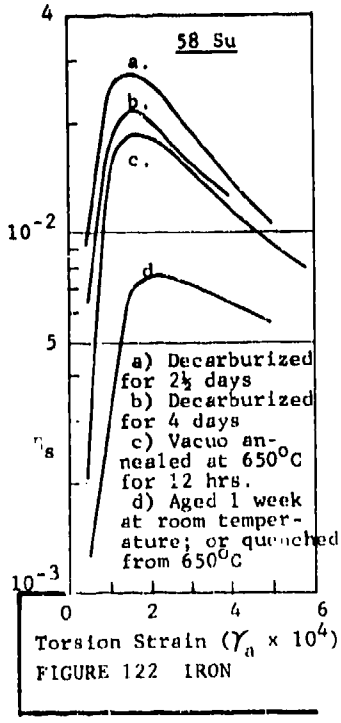

FIGURE 122 IRON

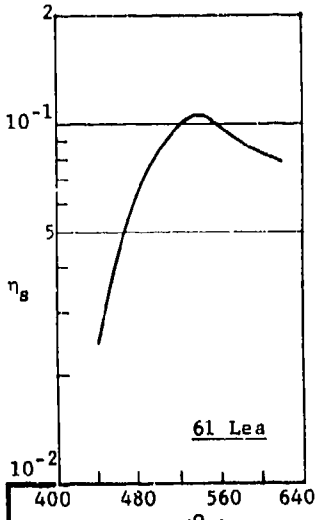

FIGURE 123 IRON (GBC-4, drawn)

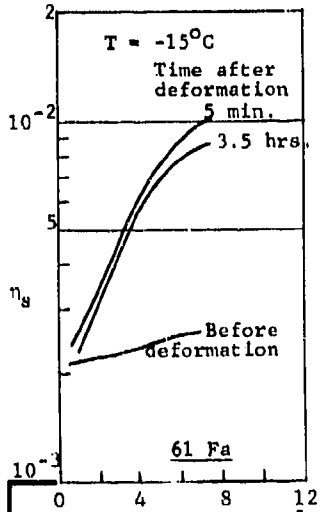

FIGURE 124 IRON (0.003% C, treated)

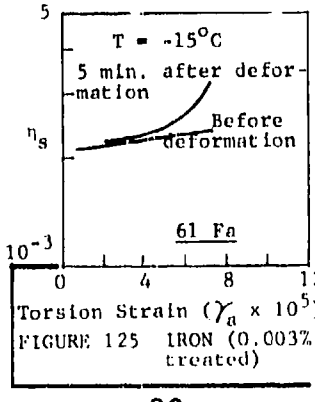

FIGURE 125 IRON (0.003% C, treated)

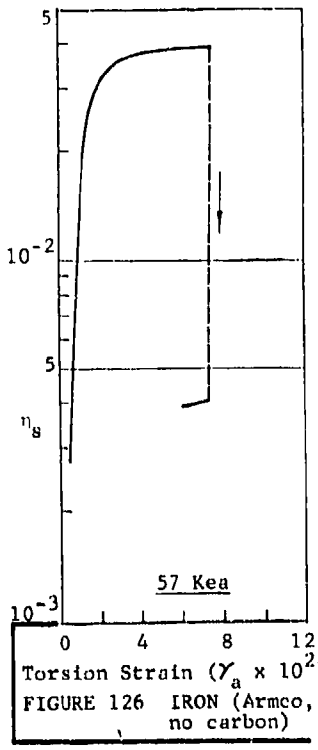

FIGURE 126 IRON (Armco, no carbon)

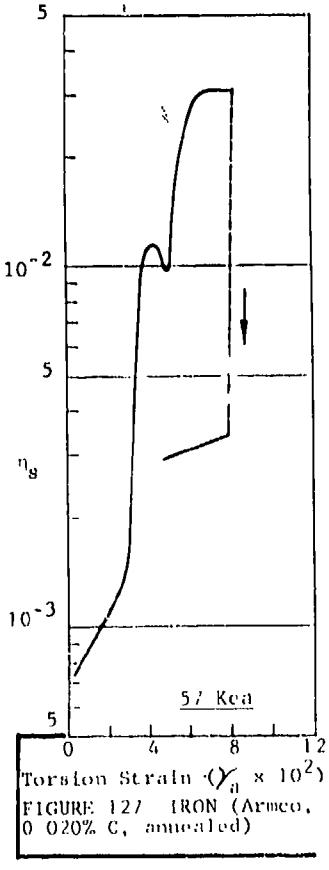

FIGURE 127 IRON (Armco, 0.020% C, annealed)

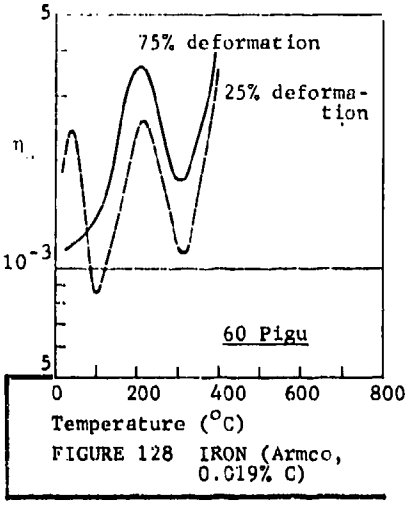

FIGURE 128 IRON (Armco, 0.019% C)

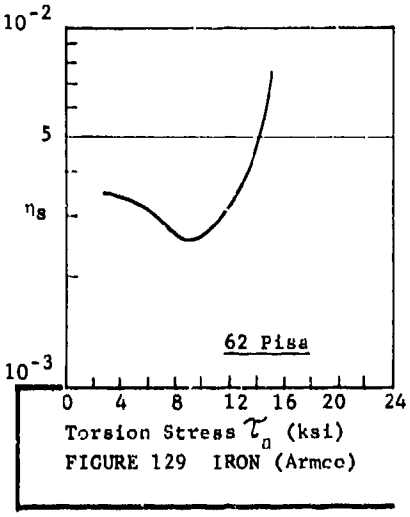

FIGURE 129 IRON (Armco)

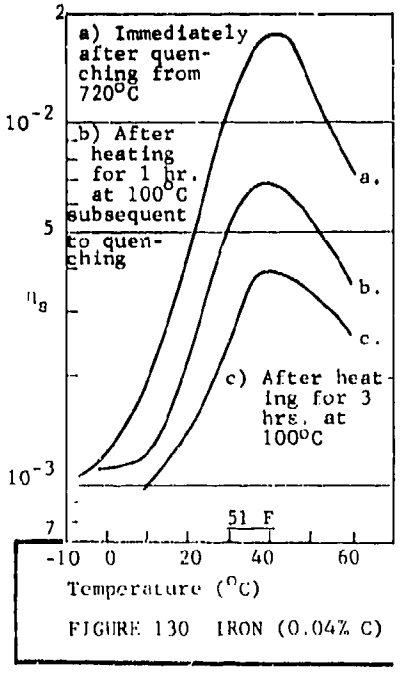

FIGURE 130 IRON (0.04% C)

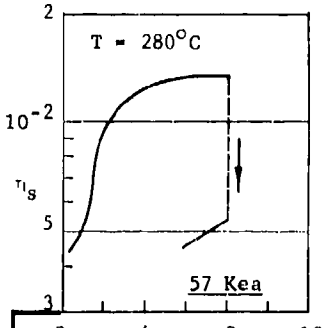

FIGURE 131 IRON (Armco, annealed)

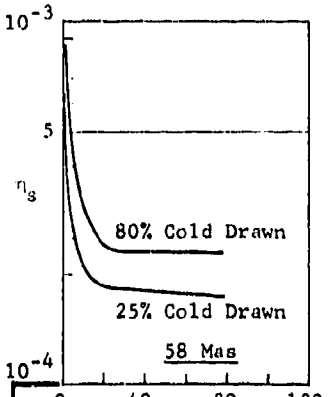

FIGURE 132 IRON (Armco, drawn)

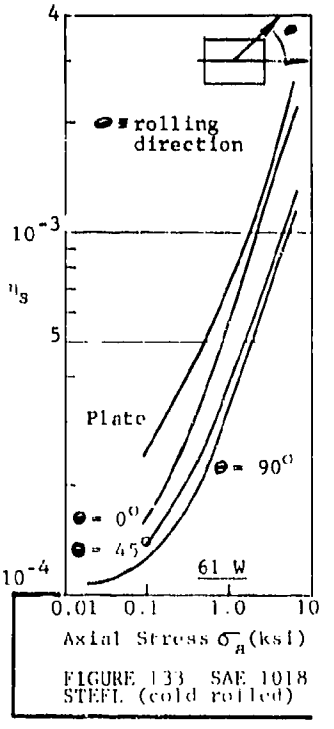

FIGURE 133 SAE 1018 STEEL (cold rolled)

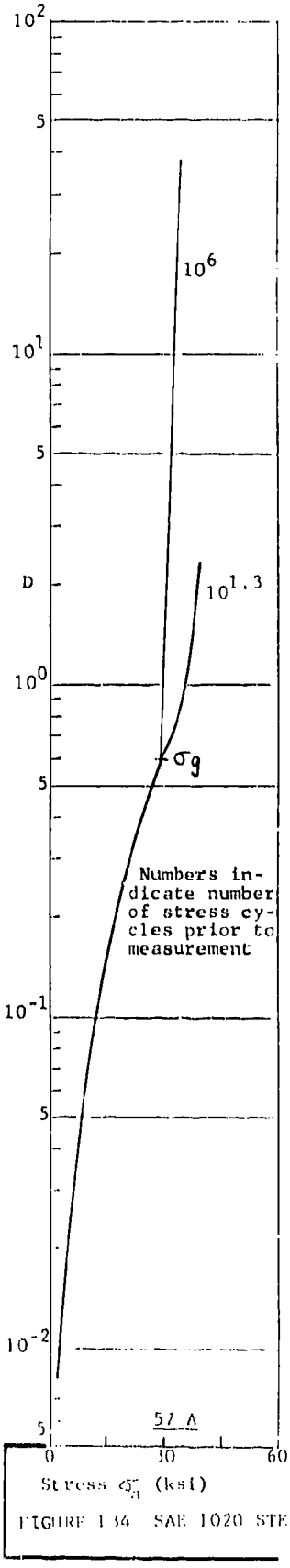

FIGURE 134 SAE 1020 STEEL

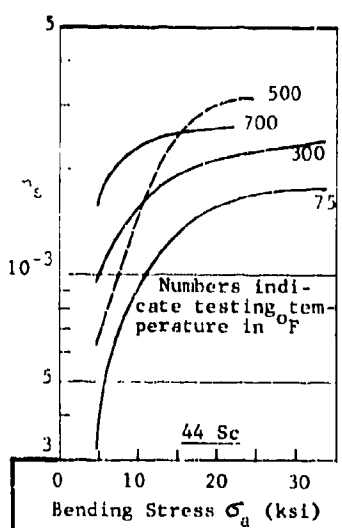

FIGURE 135 SAE 1020 STEEL (hot rolled)

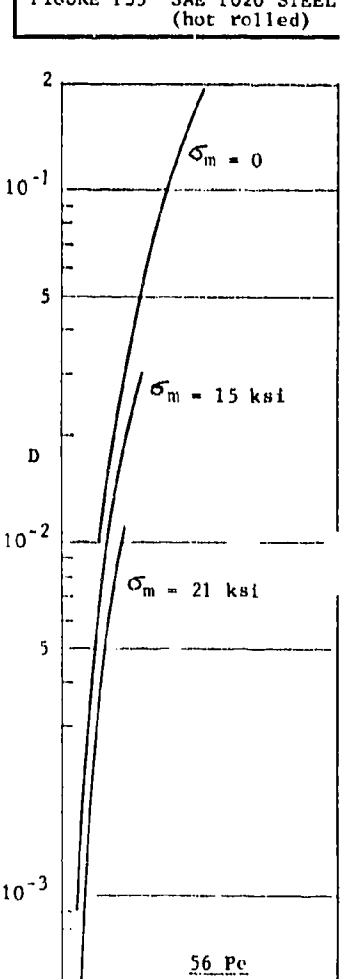

FIGURE 136 SAE 1020 STEEL (hot rolled)

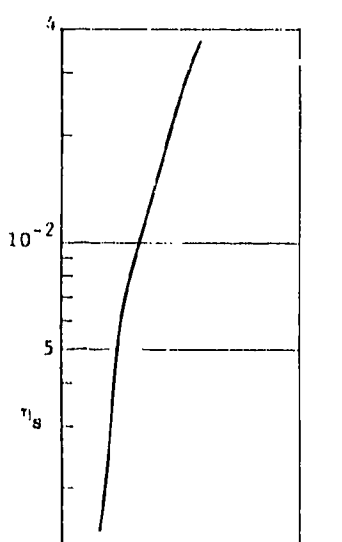

FIGURE 137 SAE 1020 STEEL

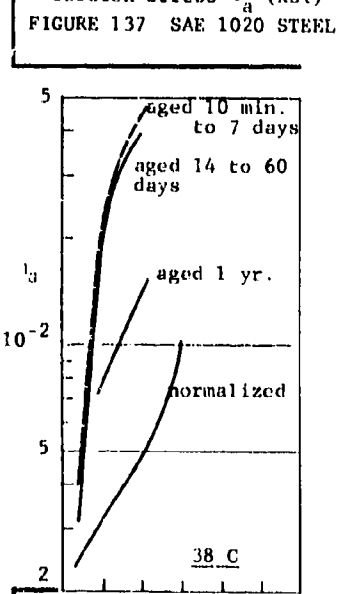

FIGURE 138 0.21% C STEEL (normalized, worked)

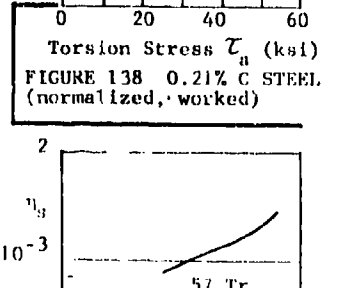

FIGURE 139 MILD STEEL

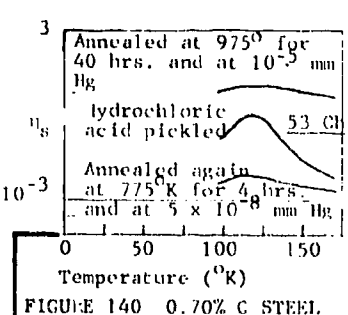

FIGURE 140 0.70% C STEEL

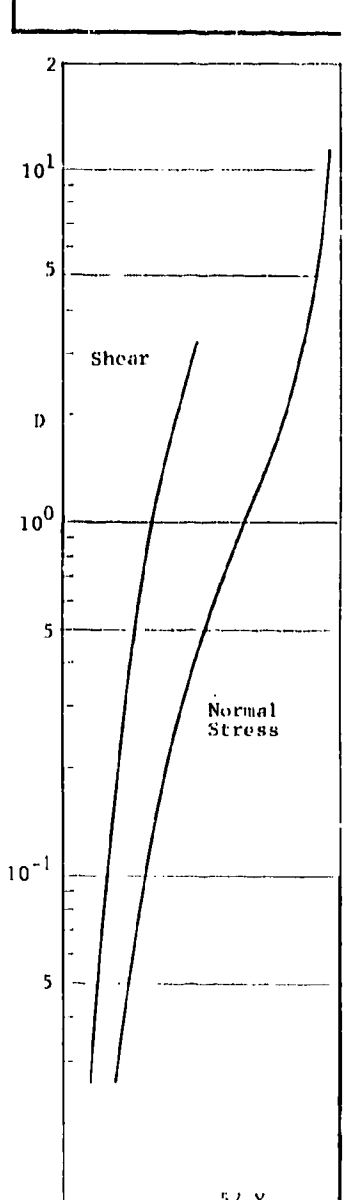

FIGURE 141 SAE 1020 STEEL

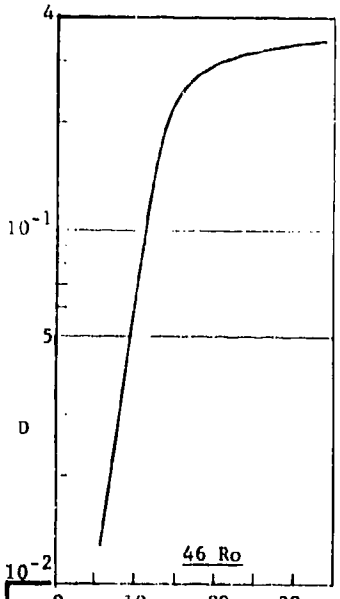

FIGURE 142 SAE 1025 STEEL

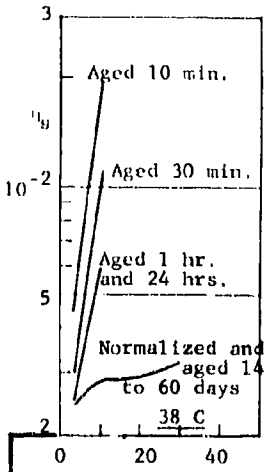

FIGURE 144 0.38% C STEEL (worked)

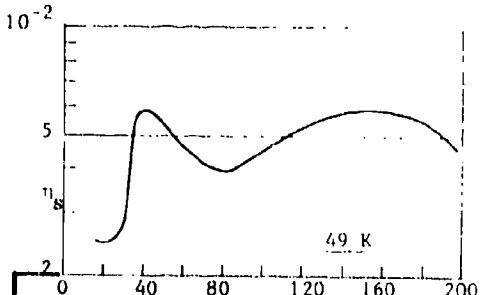

FIGURE 147 STEEL

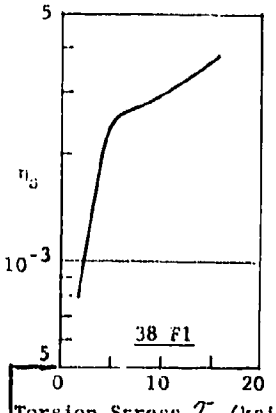

FIGURE 145 0.40% C STEEL (drawn, normalized)

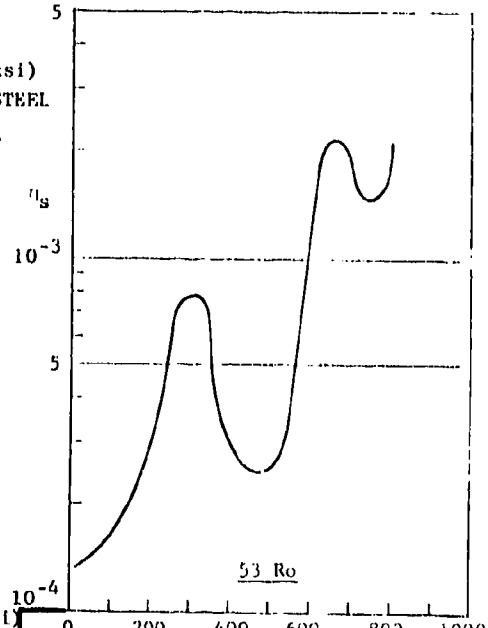

FIGURE 148 0.30% C STEEL

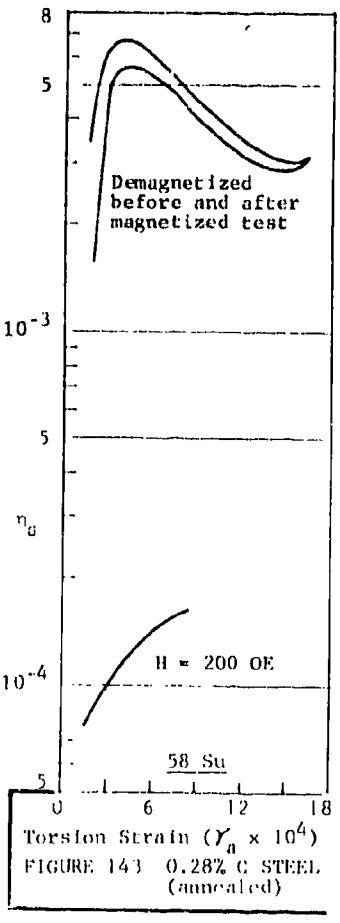

FIGURE 143 0.28% C STEEL (annealed)

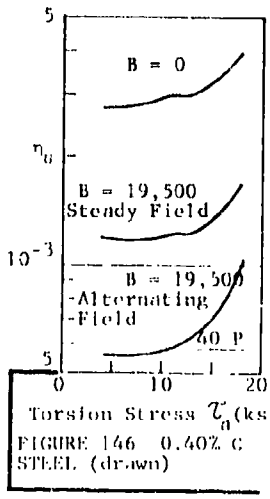

FIGURE 146 0.40% C STEEL (drawn)

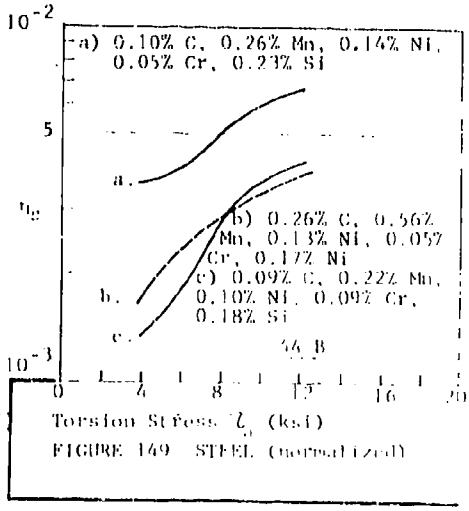

FIGURE 149 STEEL (normalized)

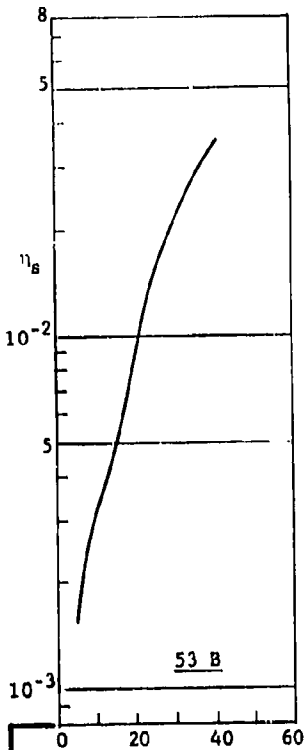

FIGURE 150 SAE 1045 STEEL

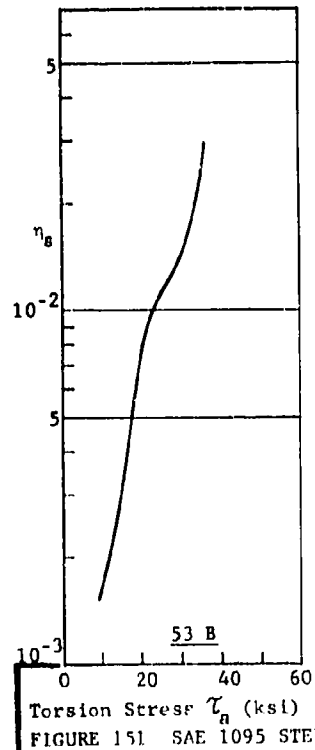

FIGURE 151 SAE 1095 STEEL

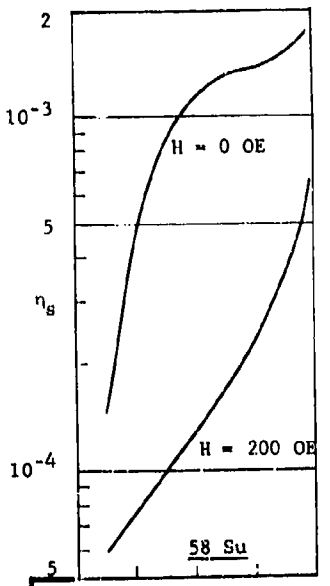

FIGURE 152 0.42% C STEEL

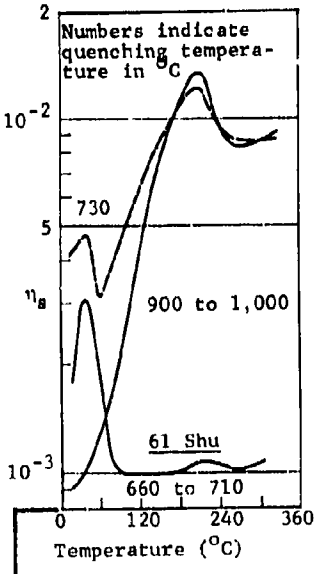

FIGURE 153 0.92% C STEEL

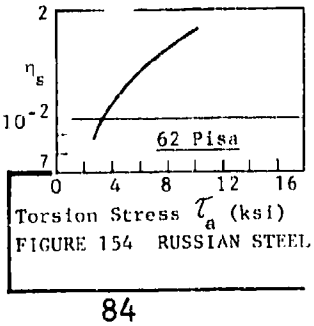

FIGURE 154 RUSSIAN STEEL 8

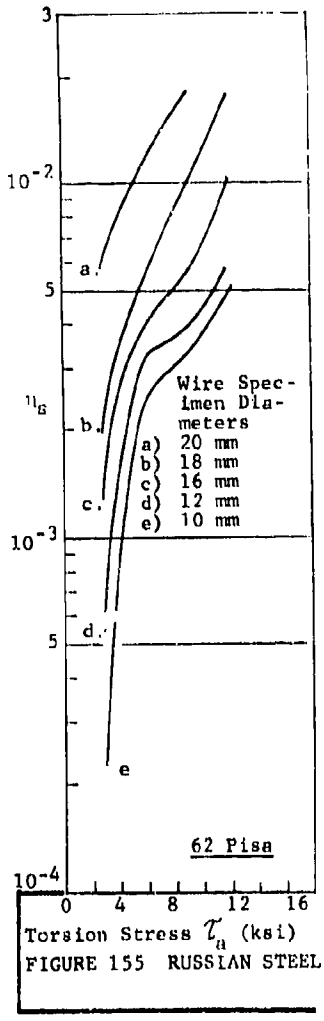

FIGURE 155 RUSSIAN STEEL 2

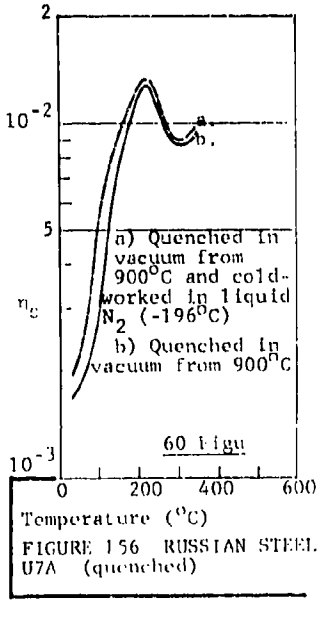

FIGURE 156 RUSSIAN STEEL U7A (quenched)

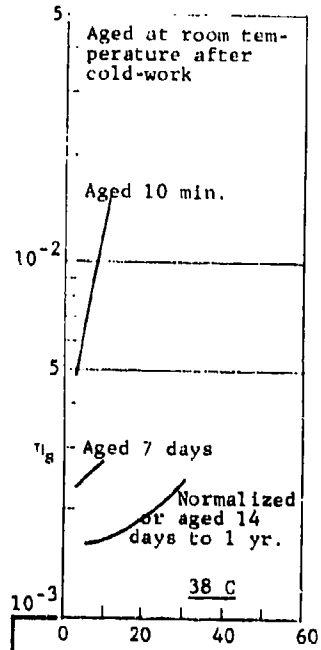

FIGURE 157 0.62% C STEEL (normalized, worked)

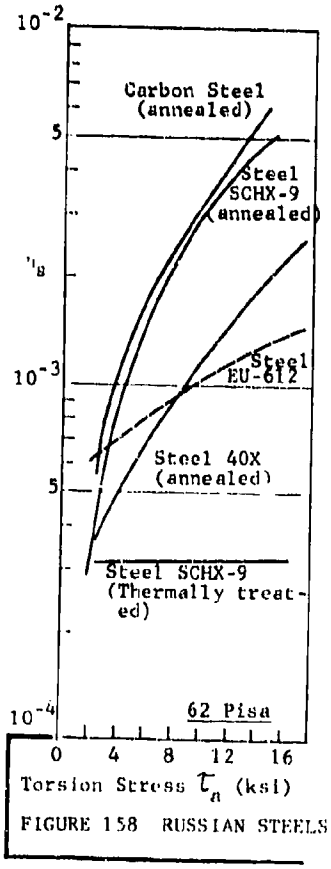

FIGURE 158 RUSSIAN STEELS

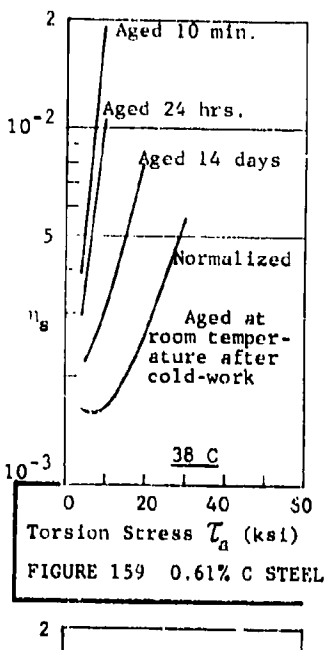

FIGURE 159 0.61% C STEEL

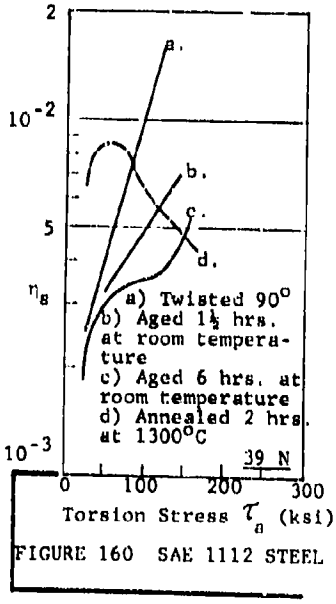

FIGURE 160 SAE 1112 STEEL

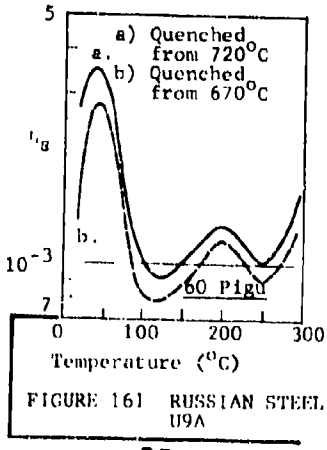

FIGURE 161 RUSSIAN STEEL U9A

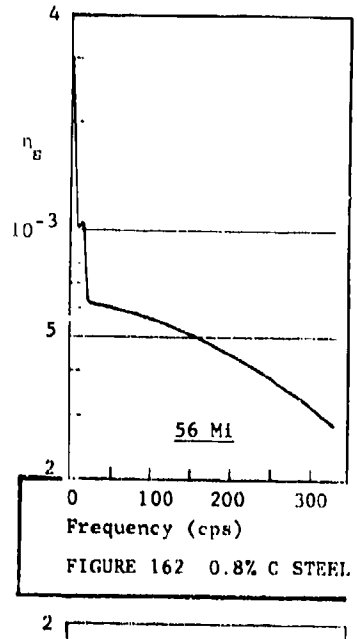

FIGURE 162 0.8% C STEEL

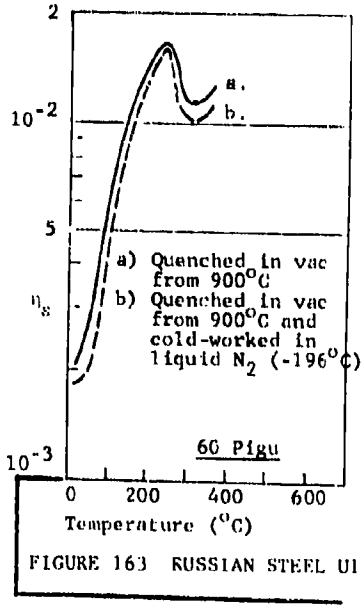

FIGURE 163 RUSSIAN STEEL U1A

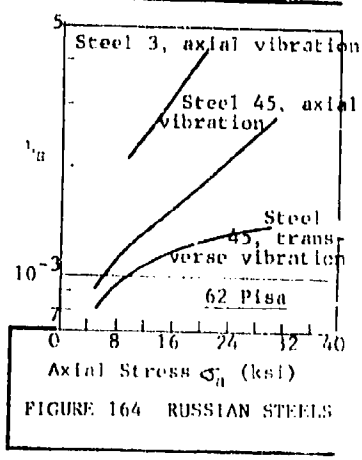

FIGURE 164 RUSSIAN STEELS

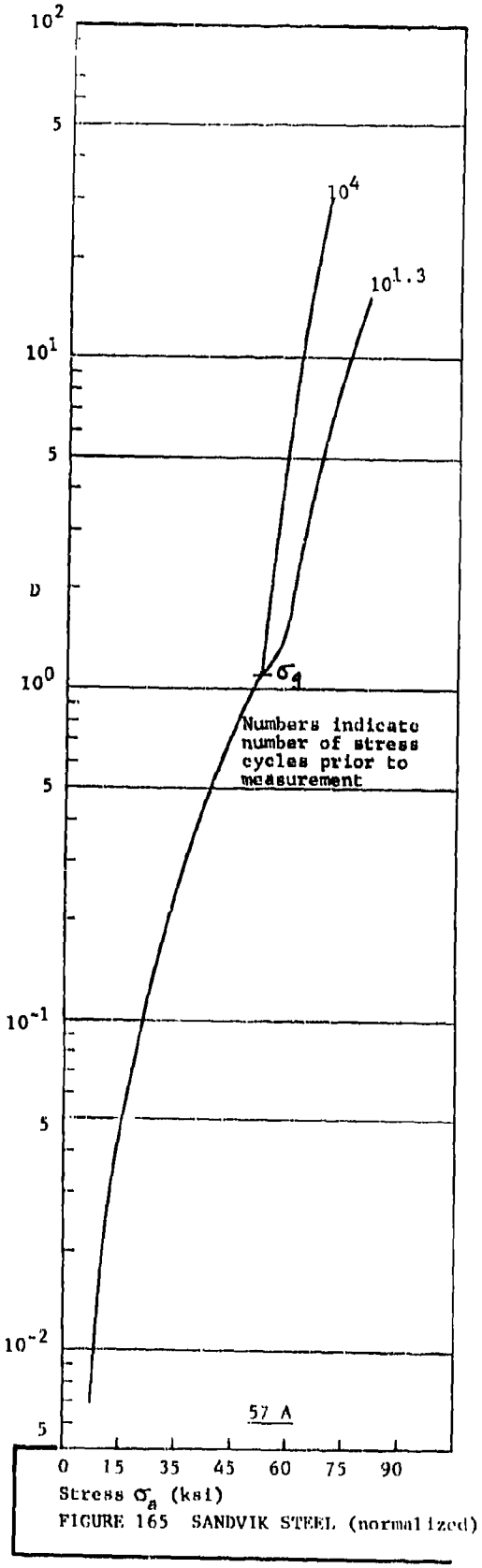

FIGURE 165 SANDVIK STEEL (normalized)

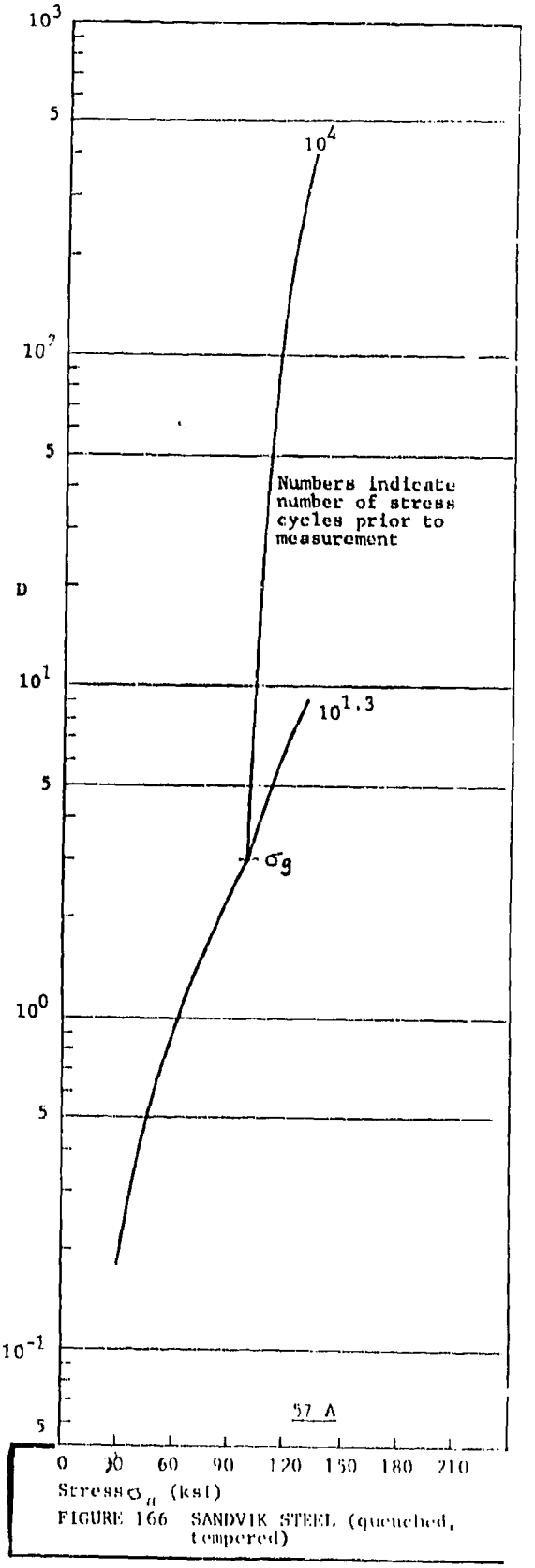

FIGURE 166 SANDVIK STEEL (quenched, tempered)

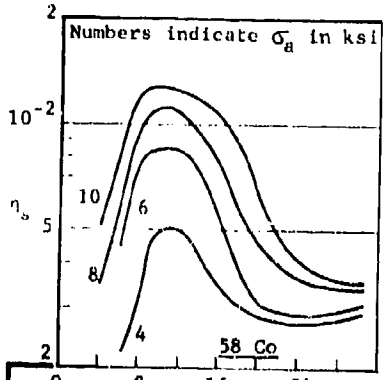

FIGURE 167 CHROMIUM ALLOYS

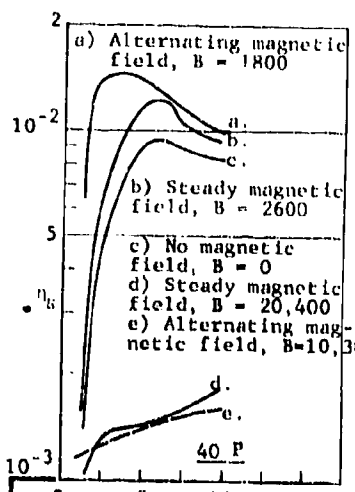

FIGURE 170 5.0% CR STEEL

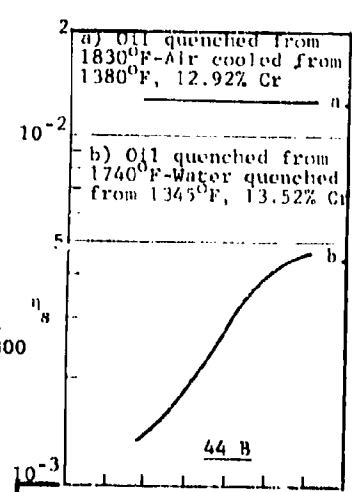

FIGURE 173 STAINLESS STEEL (13% Cr)

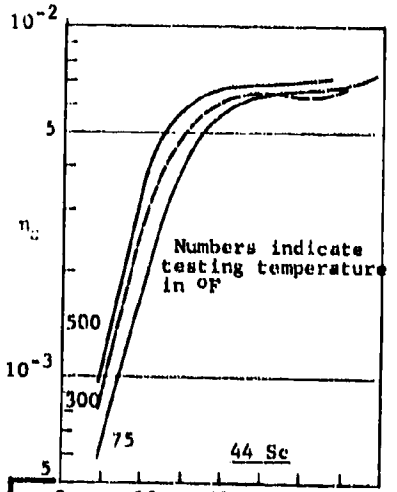

FIGURE 168 IRON ALLOY (13% Cr Alloy)

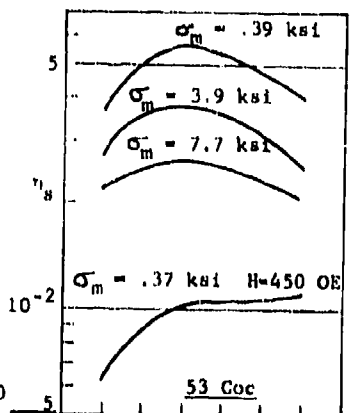

FIGURE 171 IRON ALLOY (13% Cr Alloy)

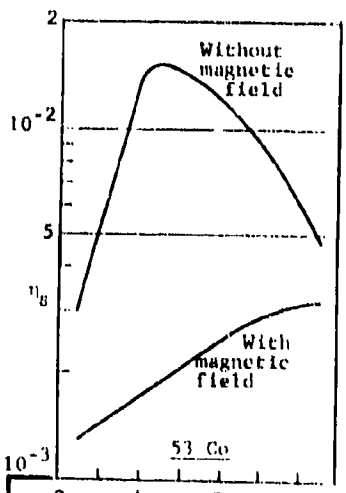

FIGURE 174 12.5% CR STEEL

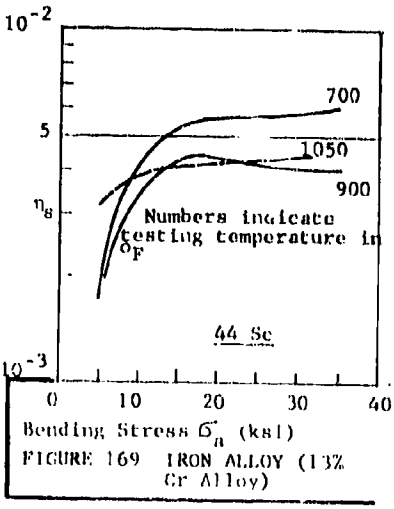

FIGURE 169 IRON ALLOY (13% Cr Alloy)

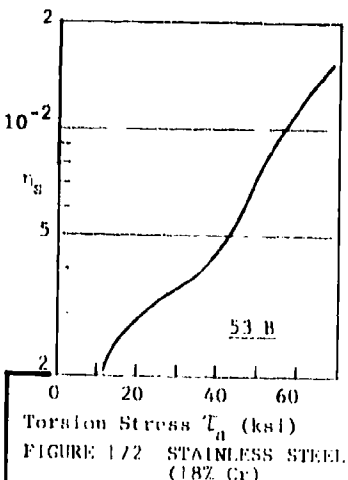

FIGURE 172 STAINLESS STEEL (18% Cr)

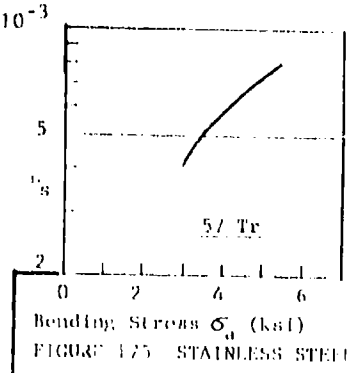

FIGURE 175 STAINLESS STEEL

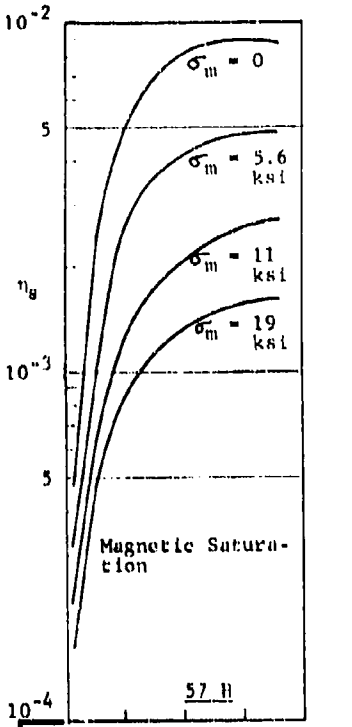

Bending Stress σ_a (ksi)

FIGURE 176 AISI 403 STEEL

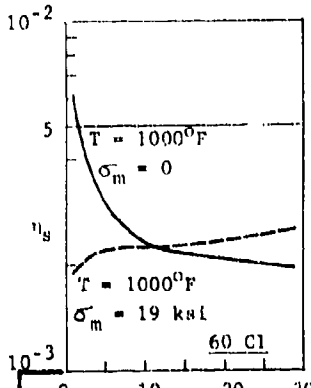

Bending Stress σ_a (ksi)

FIGURE 178 AISI 403 STEEL (annealed)

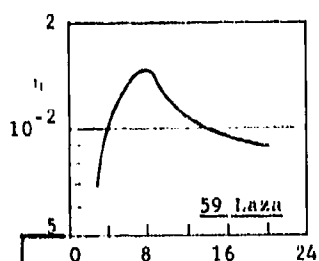

Torsion Stress τ_a (ksi)

FIGURE 179 AISI 403 STEEL (treated)

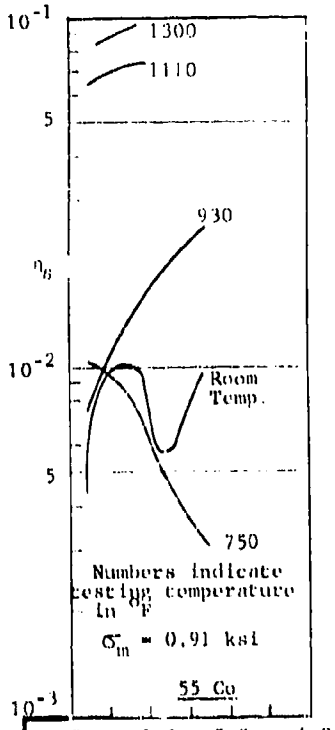

Torsion Strain ($\gamma_a \times 10^3$)

FIGURE 181 AISI 403 STEEL

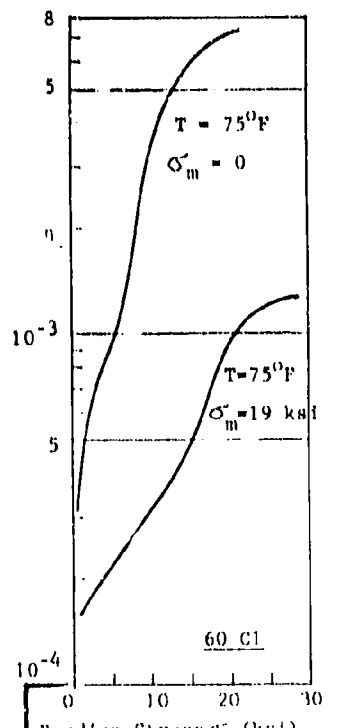

Bending Stress σ_a (ksi)

FIGURE 177 AISI 403 STEEL (annealed)

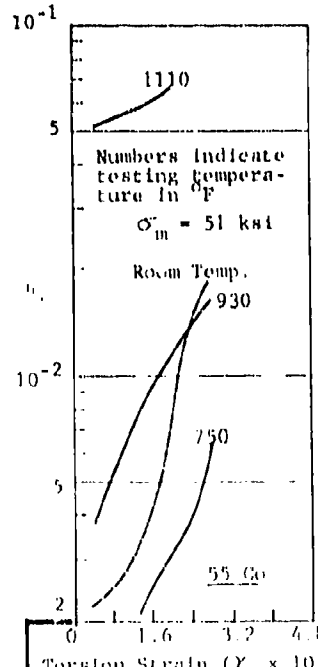

Torsion Strain ($\gamma_a \times 10^3$)

FIGURE 180 AISI 403 STEEL

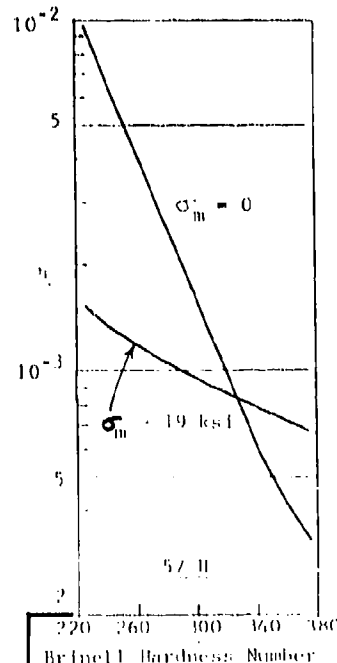

Brinell Hardness Number

FIGURE 182 AISI 403 STEEL

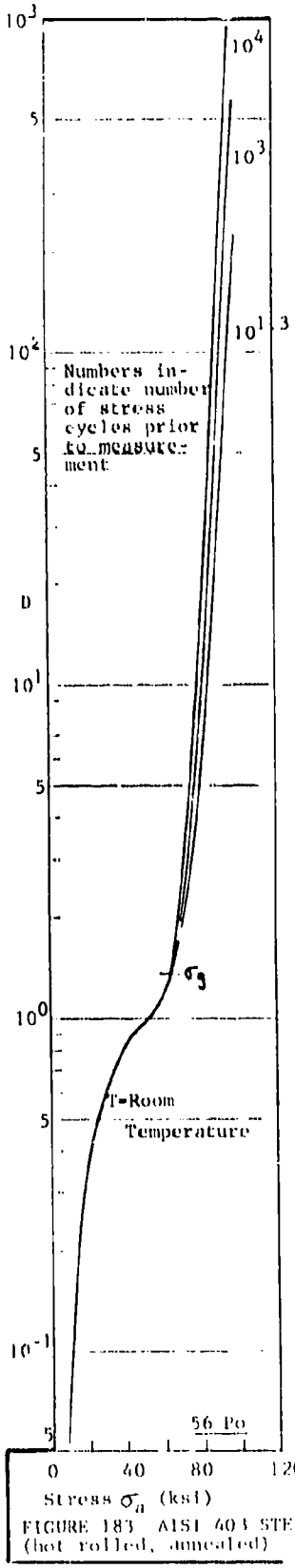

FIGURE 183 AISI 403 STEEL (hot rolled, annealed)

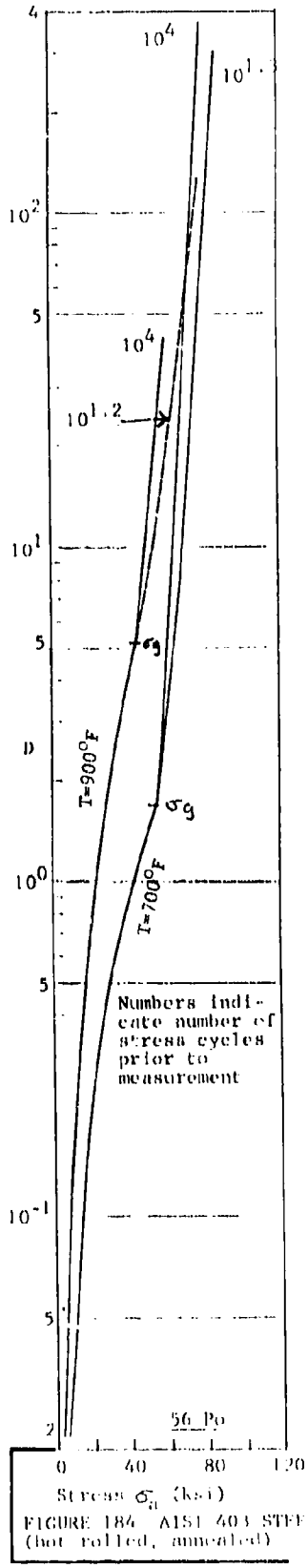

FIGURE 184 AISI 403 STEEL (hot rolled, annealed)

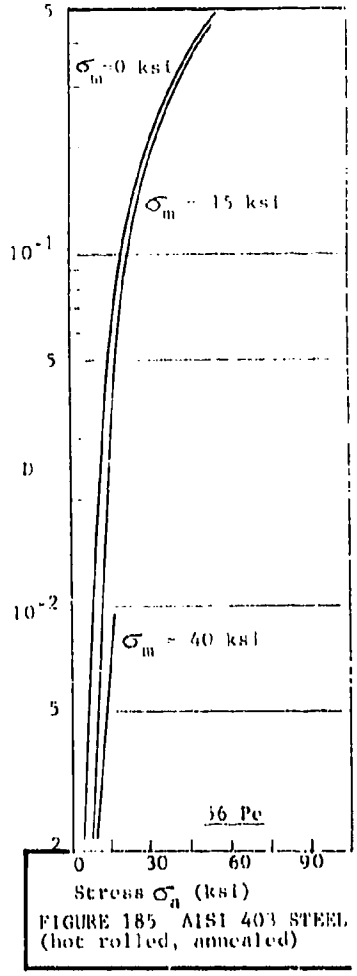

FIGURE 185 AISI 403 STEEL (hot rolled, annealed)

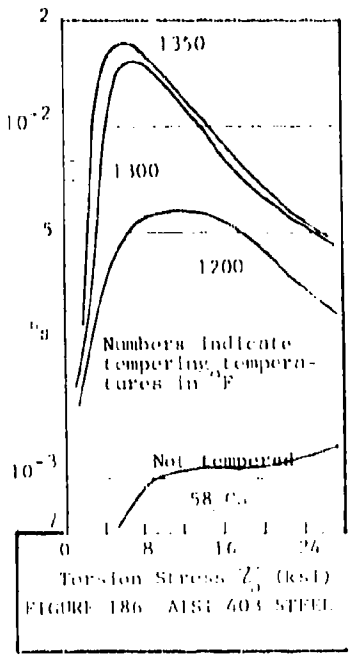

FIGURE 186 AISI 403 STEEL

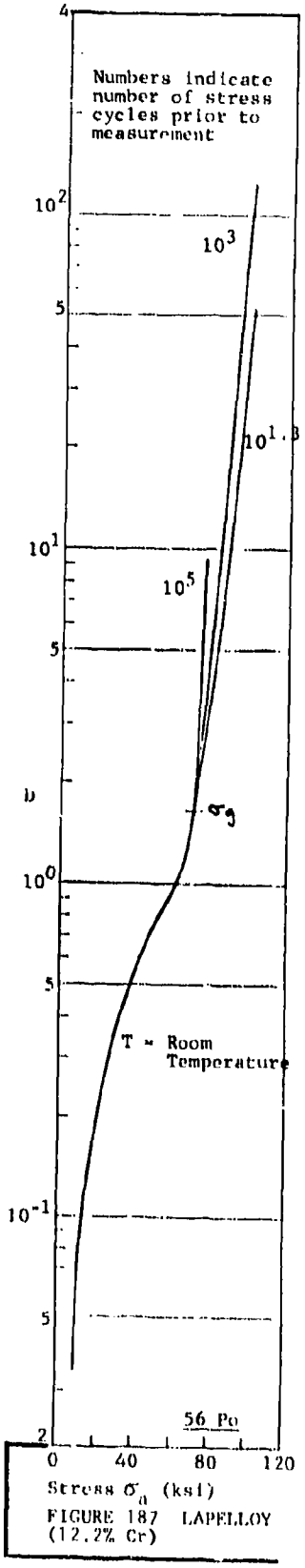

FIGURE 187 LAPELLOY (12.2% Cr)

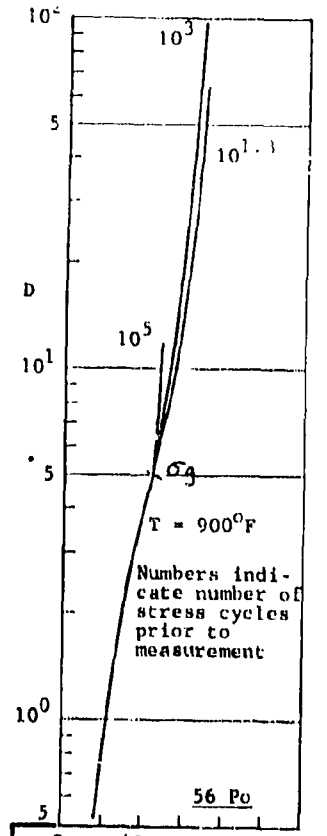

FIGURE 188 LAPELLOY (12.2% Cr)

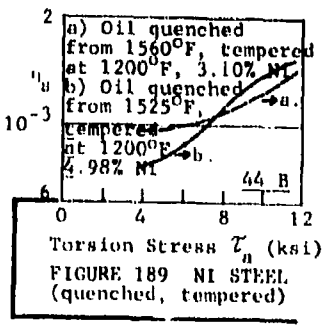

FIGURE 189 NI STEEL (quenched, tempered)

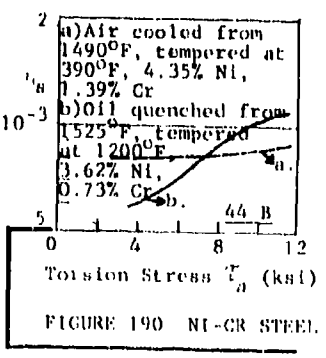

FIGURE 190 NI-CR STEEL

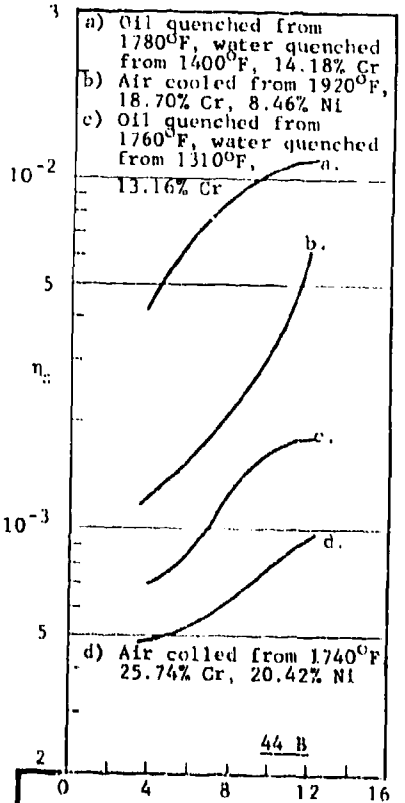

FIGURE 191 STAINLESS STEEL

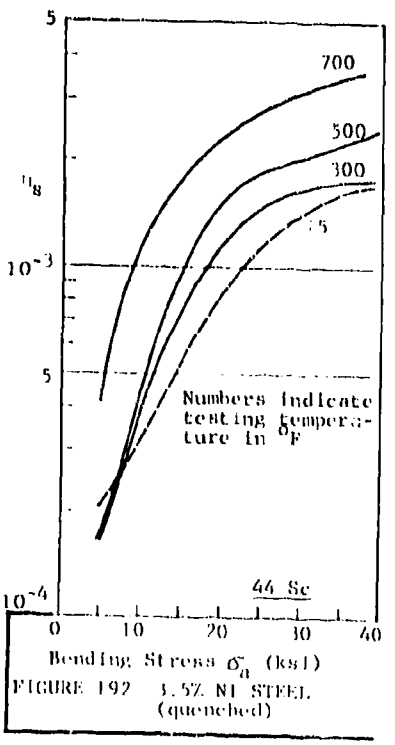

FIGURE 192 3.5% NI STEEL (quenched)

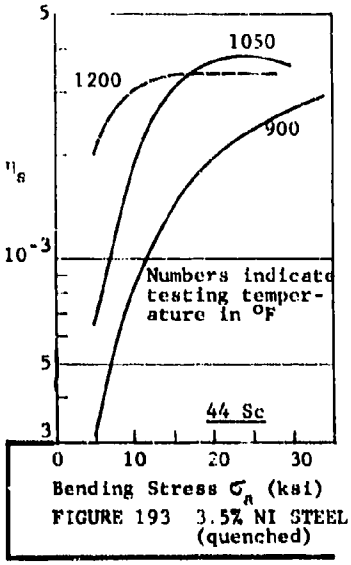

FIGURE 193 3.5% NI STEEL (quenched)

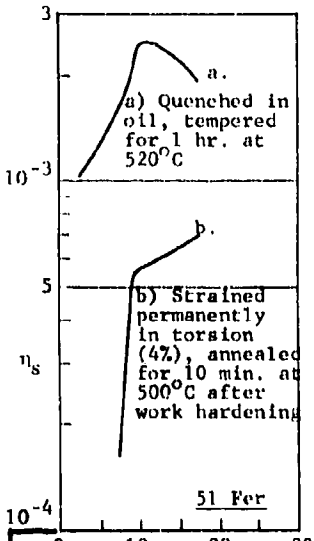

FIGURE 196 2.2% NI STEEL

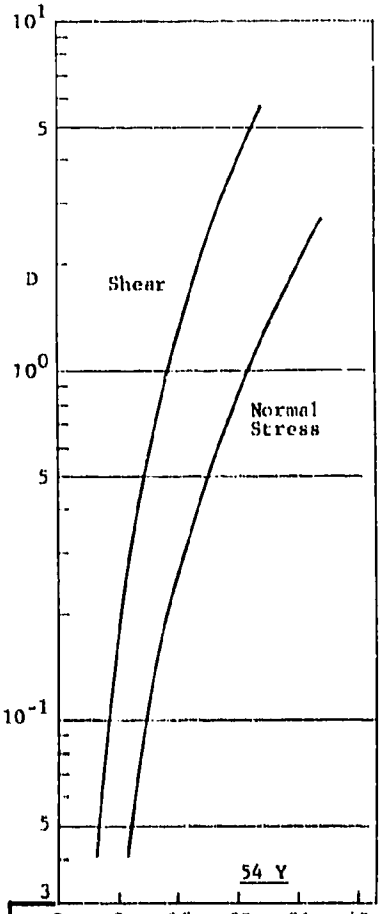

FIGURE 198 SAE 4130 STEEL

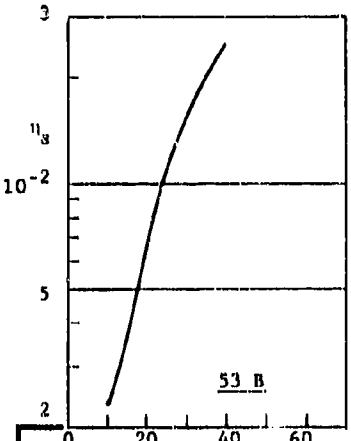

FIGURE 194 SAE 3140 STEEL

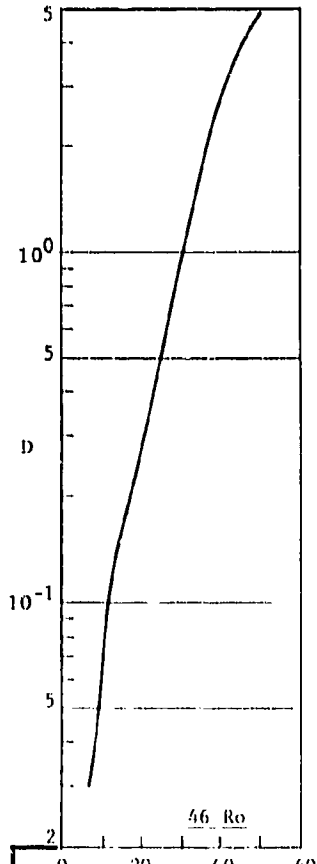

FIGURE 197 SAE X4130 STEEL (normalized)

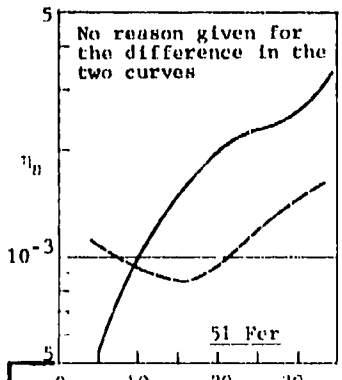

FIGURE 195 2.2% NI STEEL (quenched, tempered)

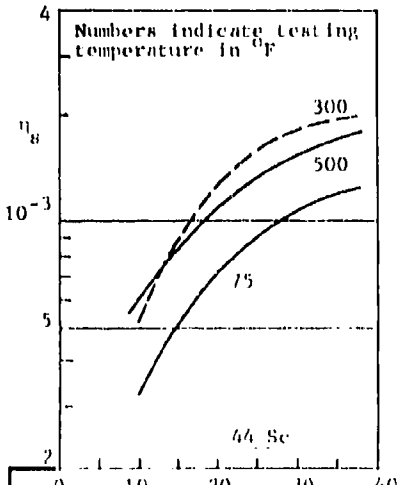

FIGURE 199 SAE 4140 STEEL (annealed, tempered)

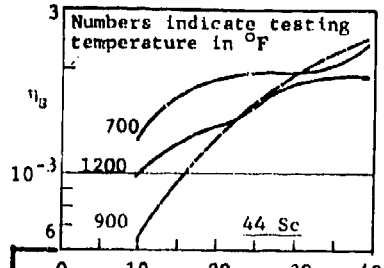

FIGURE 200 SAE 4140 STEEL (annealed, tempered)

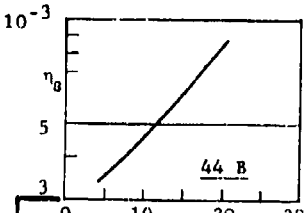

FIGURE 203 NI-CR-MO STEEL (quenched, tempered)

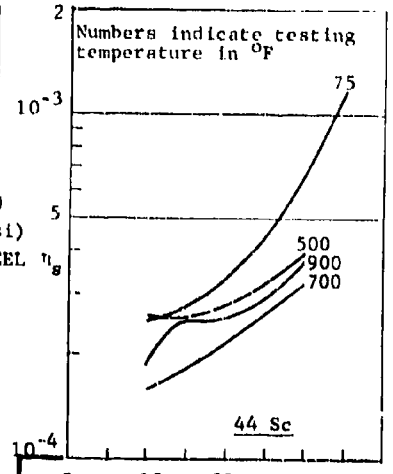

FIGURE 206 N-153, FE-NI-CR-CO ALLOY

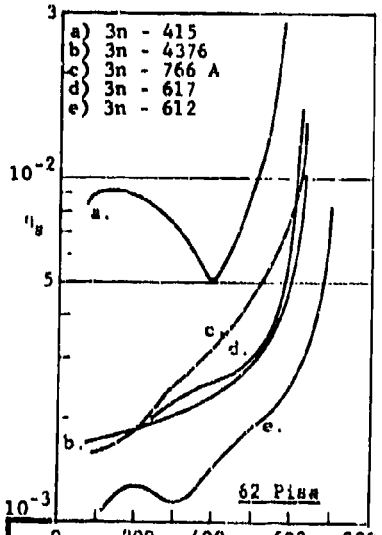

FIGURE 201 RUSSIAN STEELS

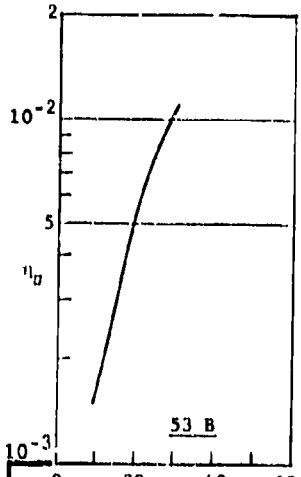

FIGURE 204 SAE 4615 STEEL

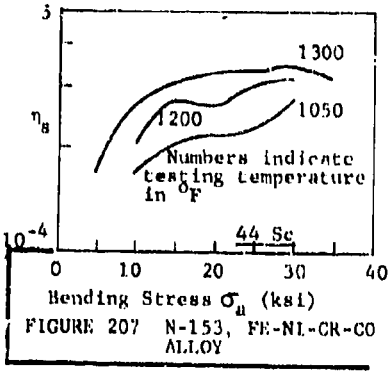

FIGURE 207 N-153, FE-NI-CR-CO ALLOY

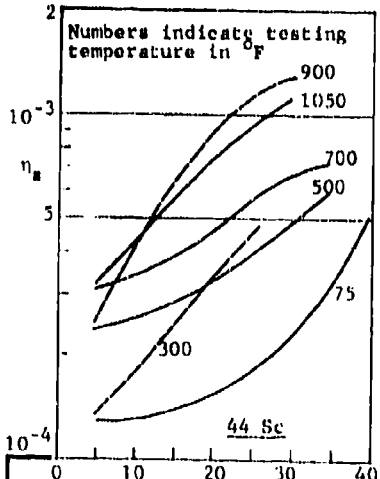

FIGURE 202 CR-MO-V STEEL (annealed, quenched)

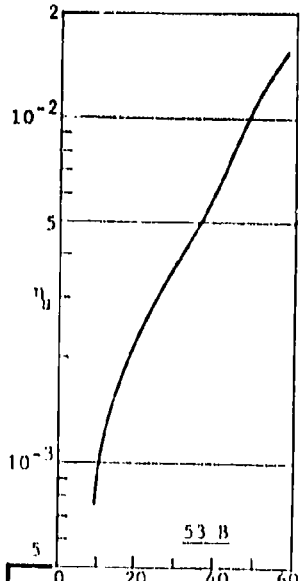

FIGURE 205 SAE 6145 STEEL

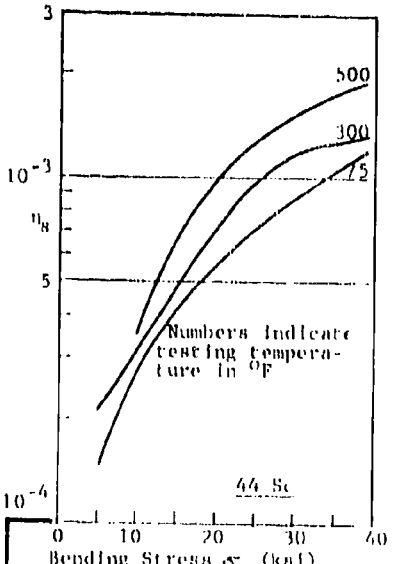

FIGURE 208 S-495, FE-NI-CR ALLOY

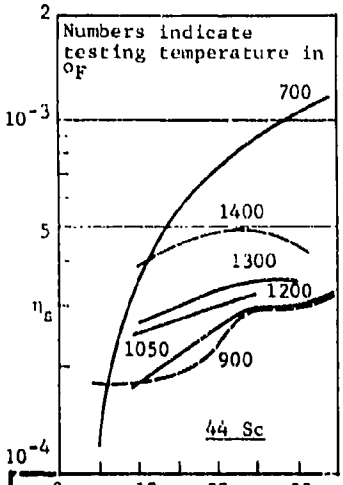

FIGURE 209 S-495, FE-NI-CR ALLOY

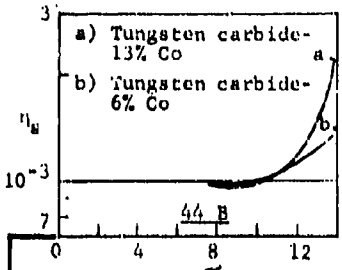

FIGURE 210 TUNGSTEN CARBIDES (sintered)

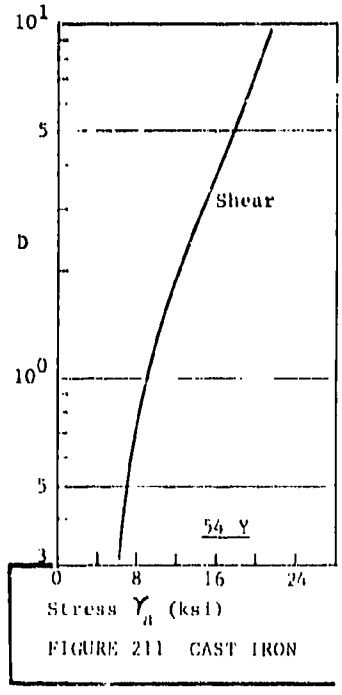

FIGURE 211 CAST IRON

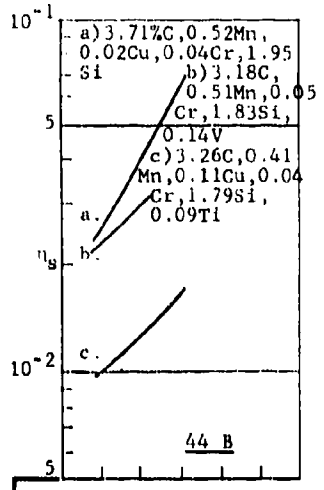

FIGURE 212 CAST IRON

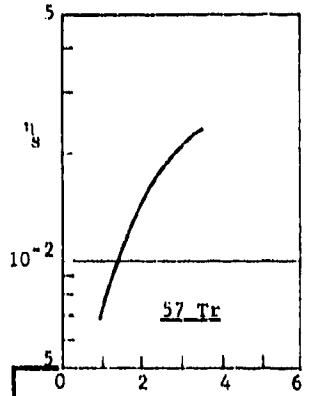

FIGURE 213 CAST IRON

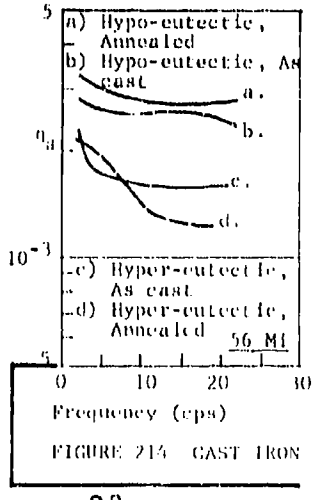

FIGURE 214 CAST IRON

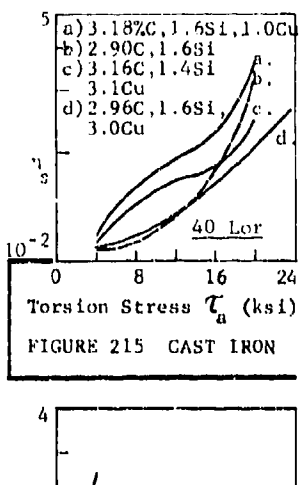

FIGURE 215 CAST IRON

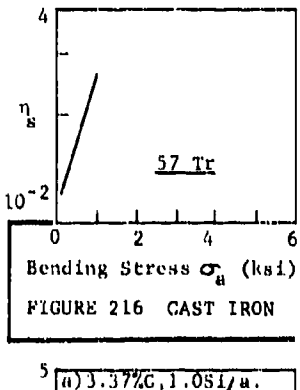

FIGURE 216 CAST IRON

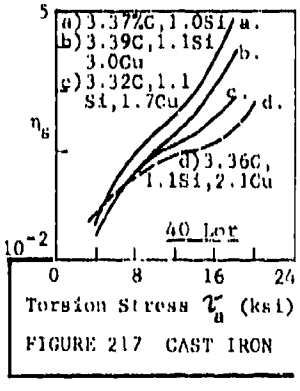

FIGURE 217 CAST IRON

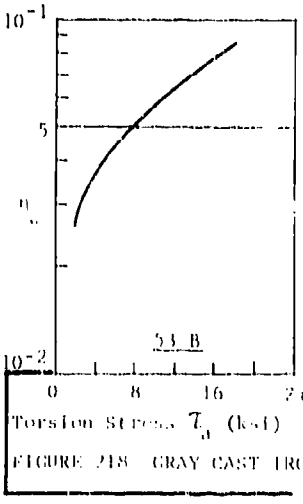

FIGURE 218 GRAY CAST IRON

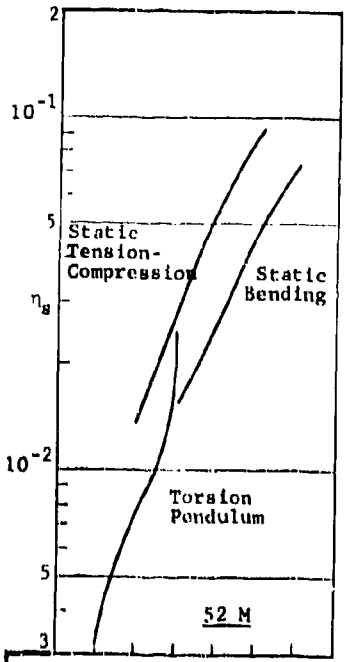

FIGURE 219 CAST IRON

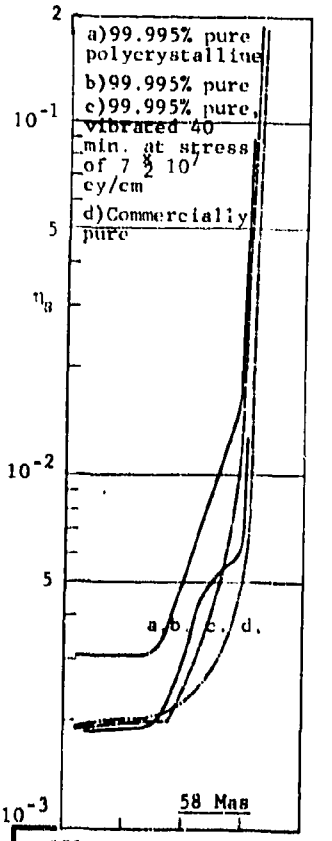

FIGURE 221 LEAD (pure, polycrystalline)

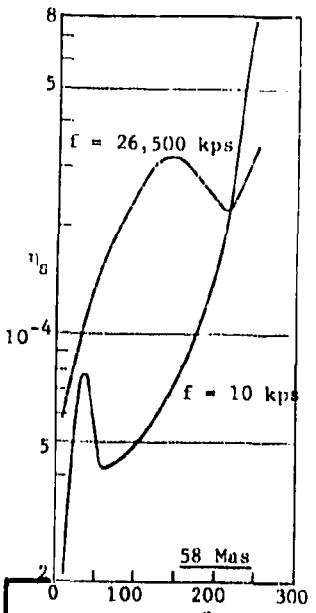

FIGURE 223 LEAD

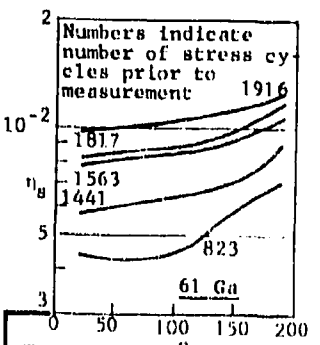

FIGURE 224 LEAD (polycrystalline)

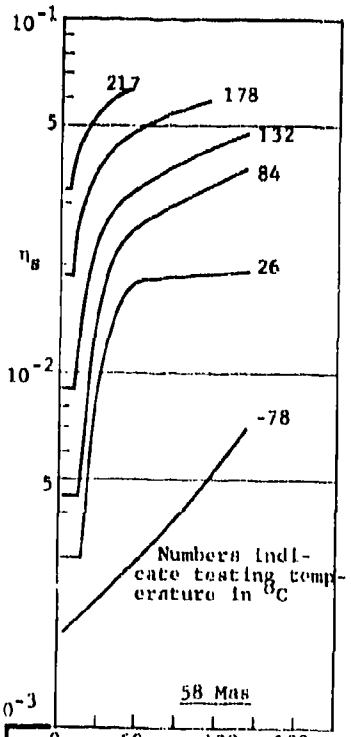

FIGURE 220 LEAD (crystal)

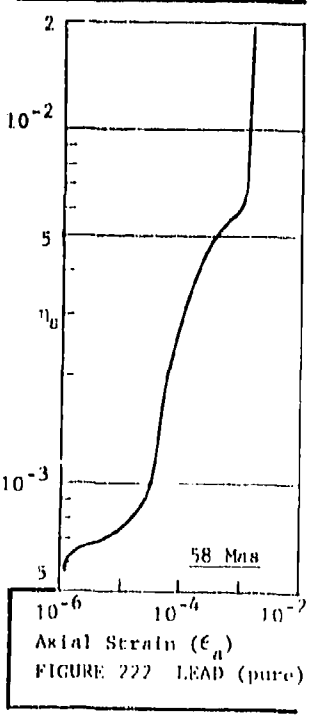

FIGURE 222 LEAD (pure)

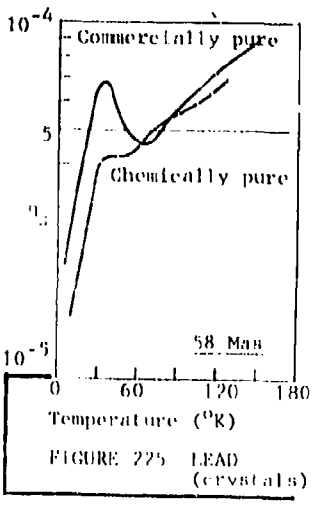

FIGURE 225 LEAD (crystals)

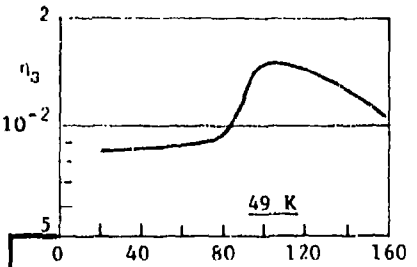

FIGURE 226 LEAD

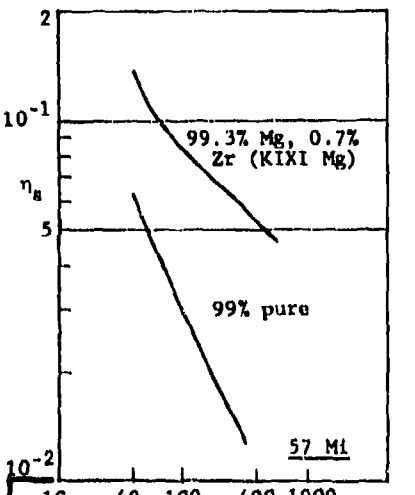

FIGURE 227 MAGNESIUM (castings)

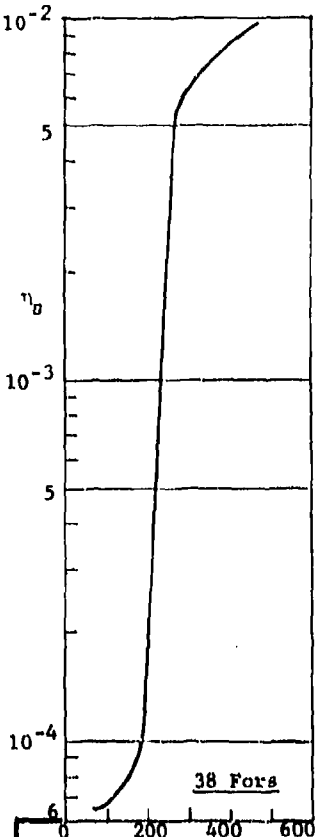

FIGURE 229 MAGNESIUM (pure, annealed)

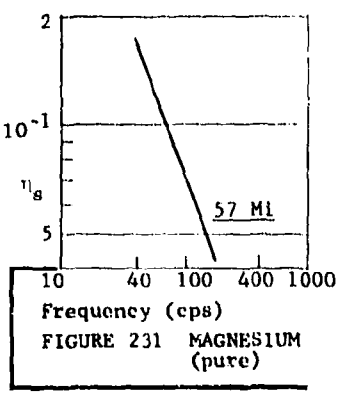

FIGURE 231 MAGNESIUM (pure)

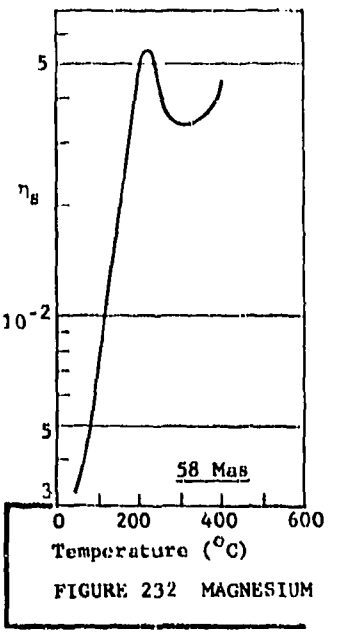

FIGURE 232 MAGNESIUM

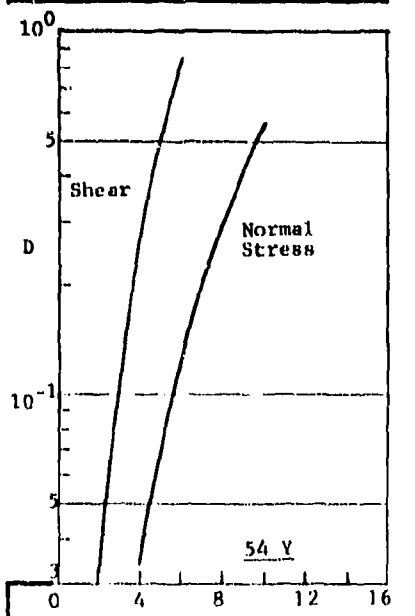

FIGURE 228 MAGNESIUM ALLOY (J-1)

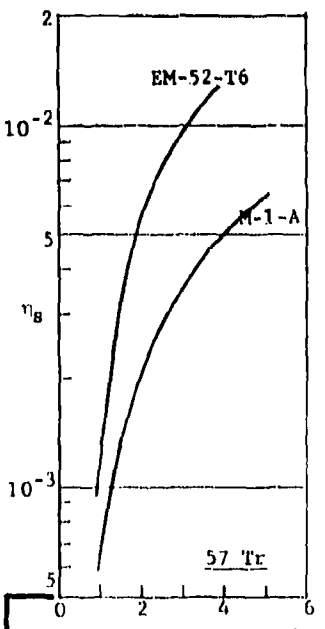

FIGURE 230 MAGNESIUM ALLOYS

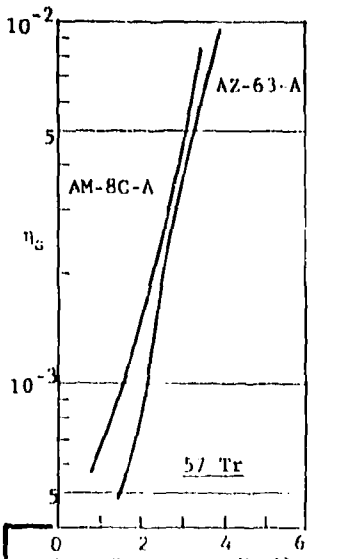

FIGURE 233 MAGNESIUM ALLOYS

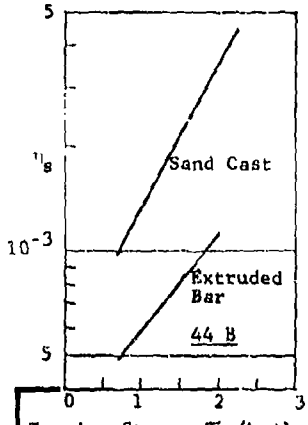

FIGURE 234 MAGNESIUM ALLOY

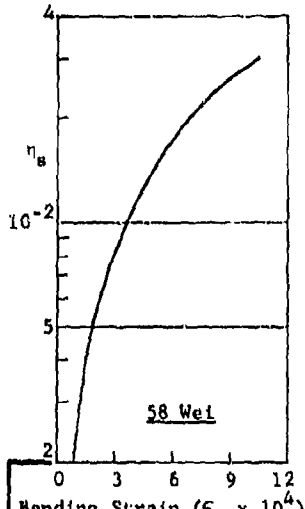

FIGURE 235 MAGNESIUM ALLOY (AZ-81-A)

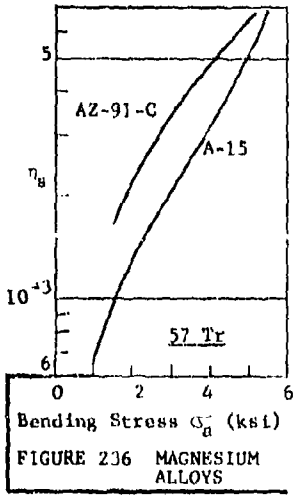

FIGURE 236 MAGNESIUM ALLOYS

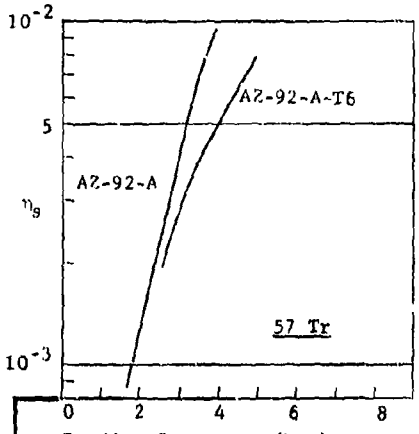

FIGURE 237 MAGNESIUM ALLOYS

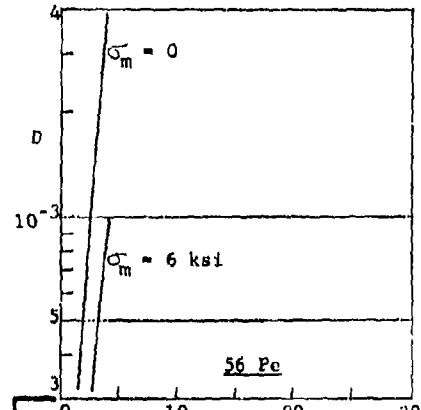

FIGURE 238 MAGNESIUM ALLOY (J-1, extruded)

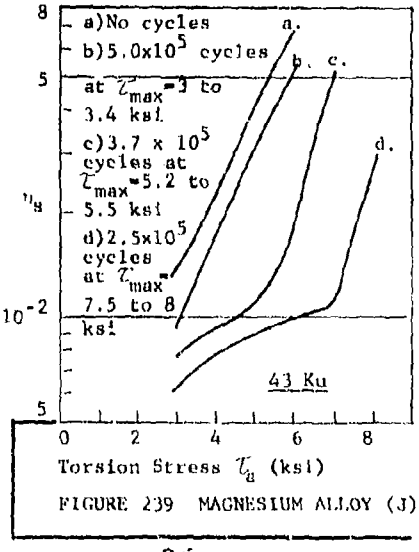

FIGURE 239 MAGNESIUM ALLOY (J)

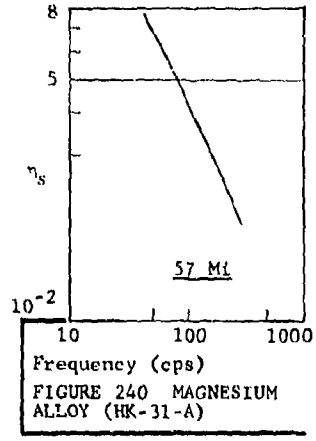

FIGURE 240 MAGNESIUM ALLOY (HK-31-A)

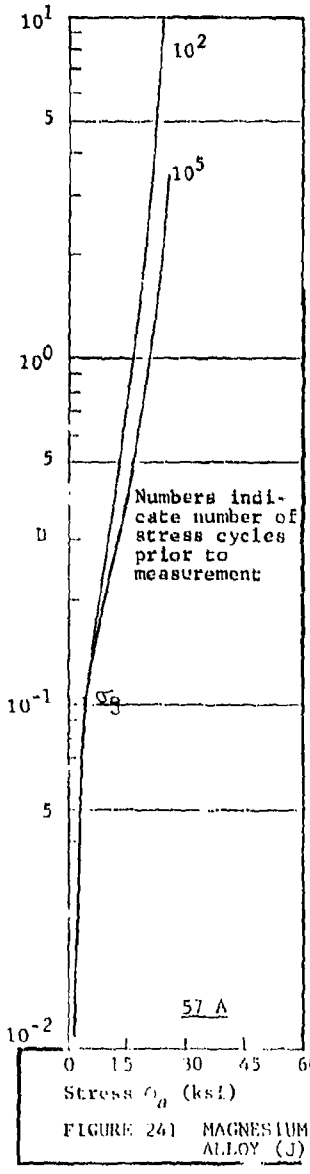

FIGURE 241 MAGNESIUM ALLOY (J)

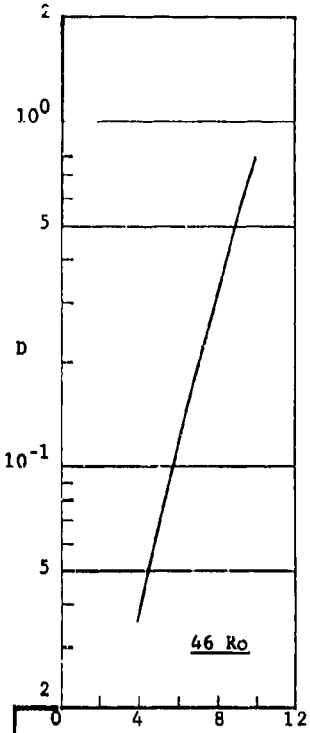

FIGURE 242 MAGNESIUM ALLOY (J-1, extruded)

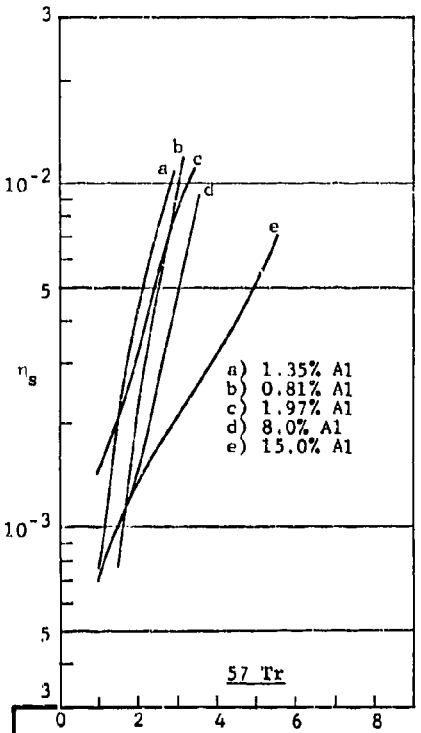

FIGURE 244 MAGNESIUM ALLOYS (A1)

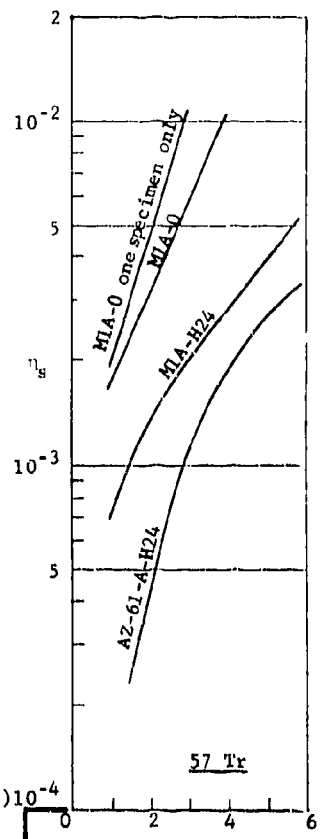

FIGURE 246 MAGNESIUM ALLOYS

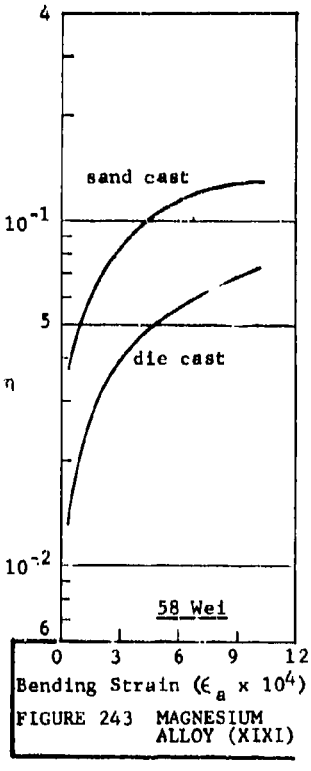

FIGURE 243 MAGNESIUM ALLOY (XIXI)

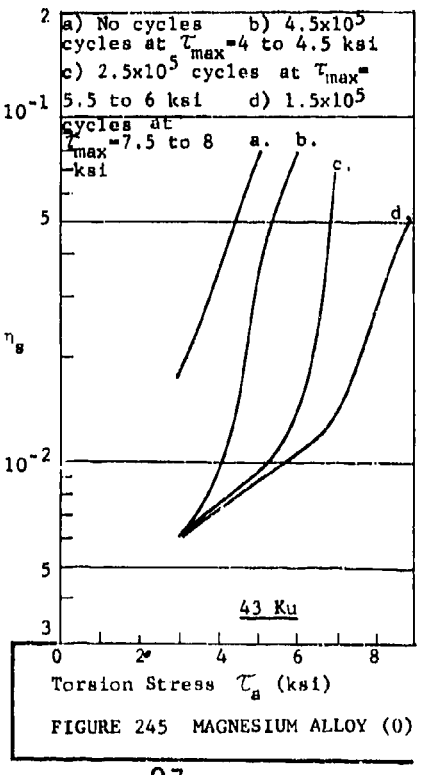

FIGURE 245 MAGNESIUM ALLOY (0)

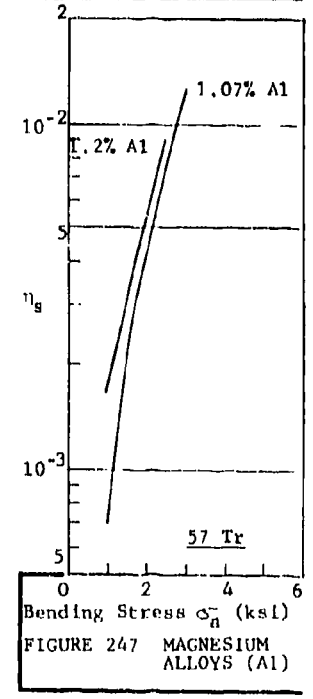

FIGURE 247 MAGNESIUM ALLOYS (A1)

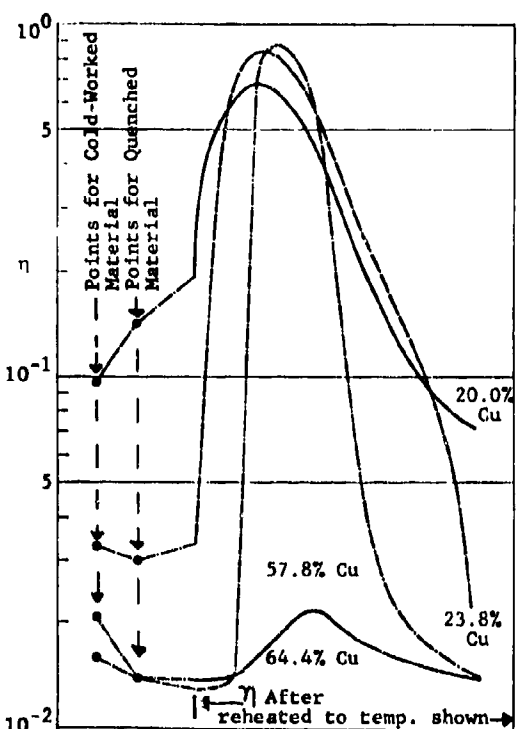

FIGURE 248 MANGANESE ALLOYS (Cu, worked)

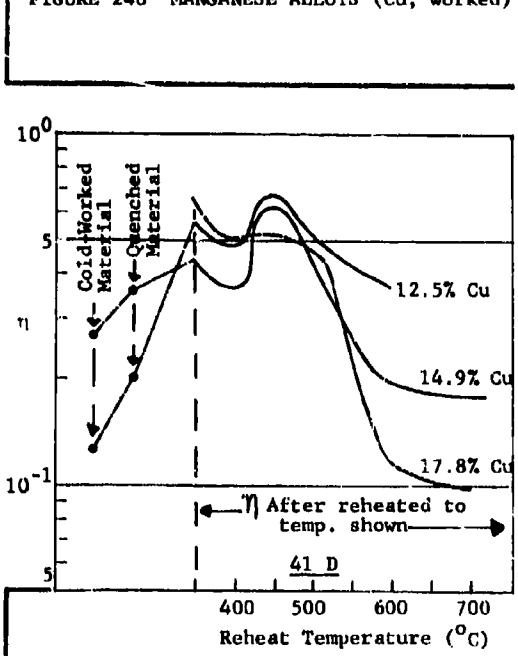

FIGURE 249 MANGANESE ALLOYS (Cu, worked)

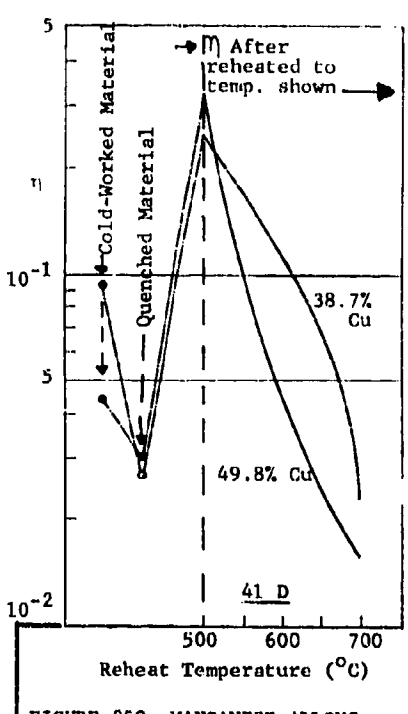

FIGURE 250 MANGANESE ALLOYS (Cu, worked)

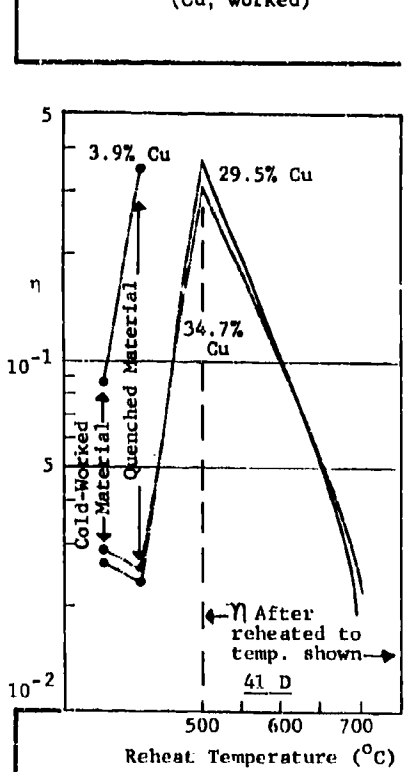

FIGURE 251 MANGANESE ALLOYS (Cu, worked)

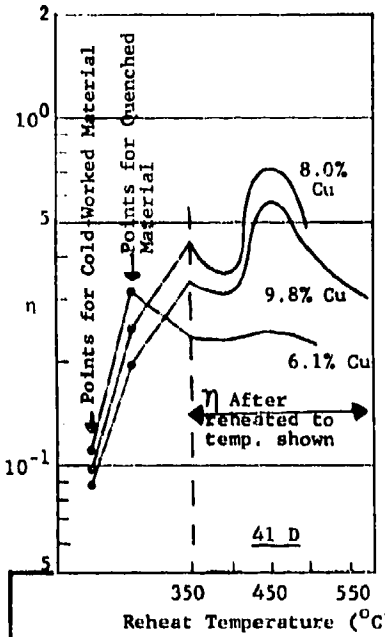

FIGURE 252 MANGANESE ALLOYS (Cu, worked)

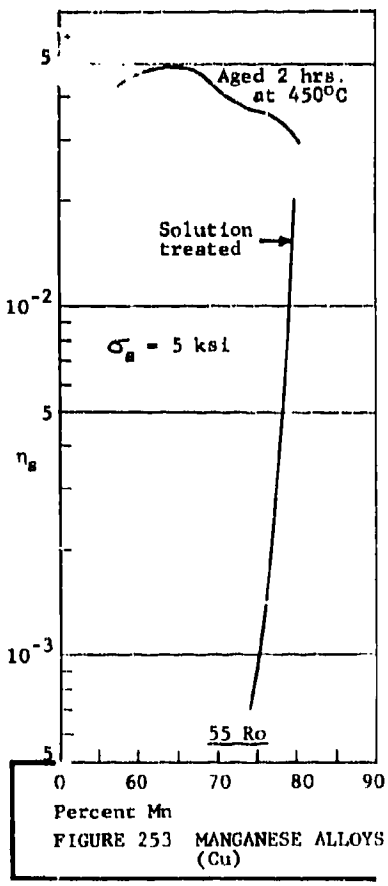

FIGURE 253 MANGANESE ALLOYS (Cu)

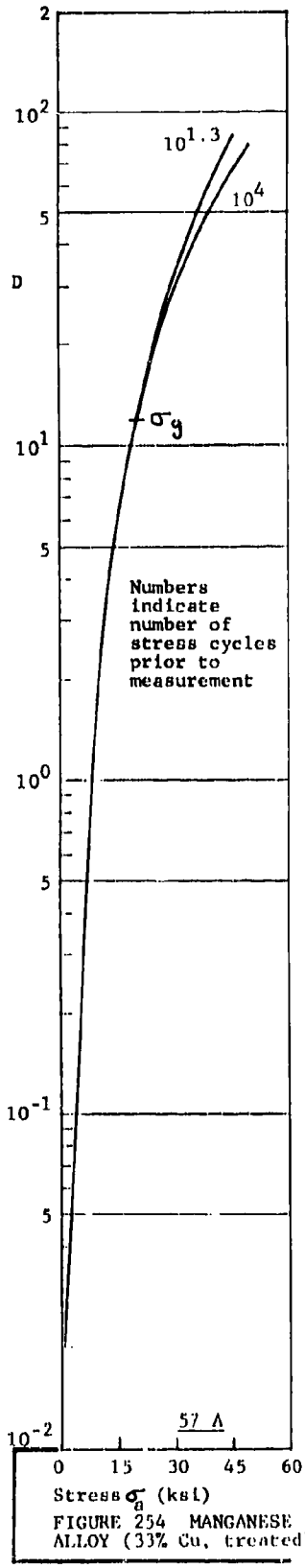

FIGURE 254 MANGANESE ALLOY (33% Cu, treated)

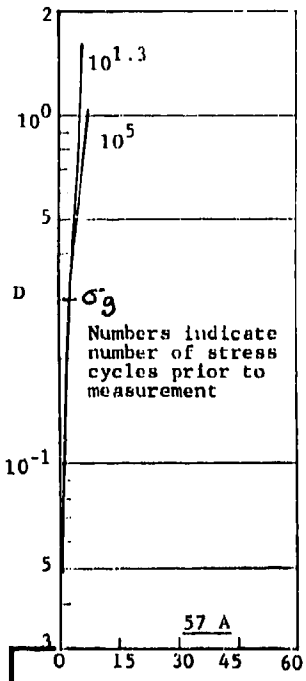

FIGURE 255 MAGNESIUM ALLOY (0.7% Si)

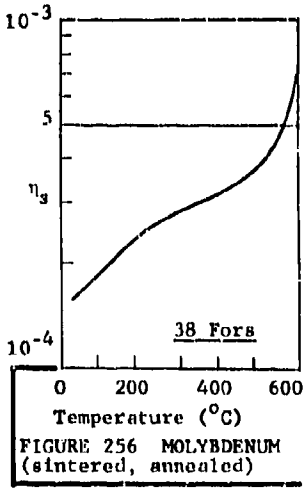

FIGURE 256 MOLYBDENUM (sintered, annealed)

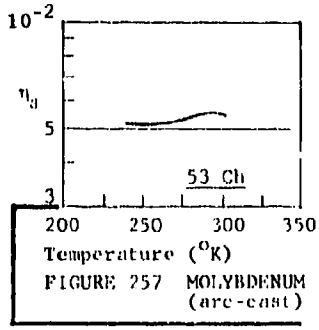

FIGURE 257 MOLYBDENUM (arc-cast)

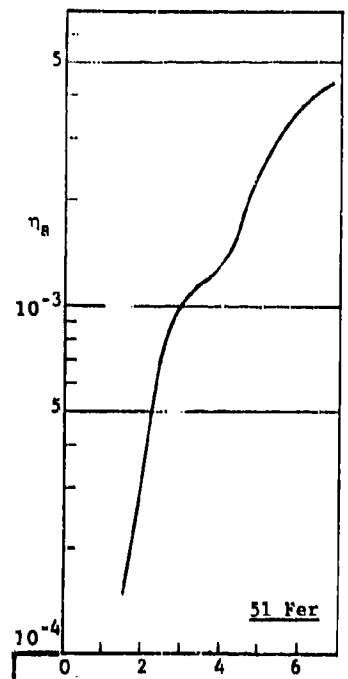

FIGURE 258 NICKEL (pure, cast)

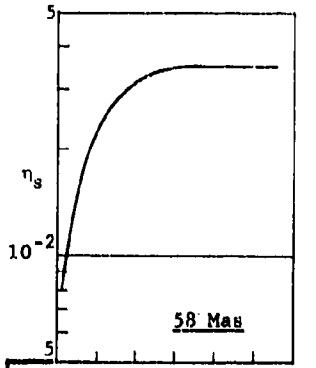

FIGURE 260 NICKEL (Polycrystalline)

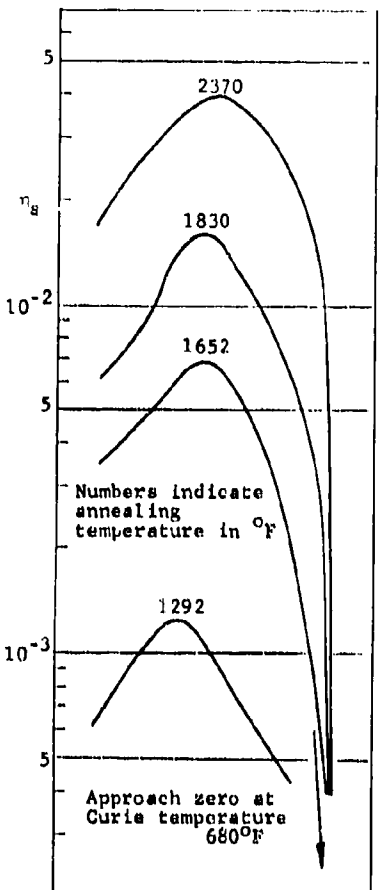

FIGURE 263 NICKEL (annealed)

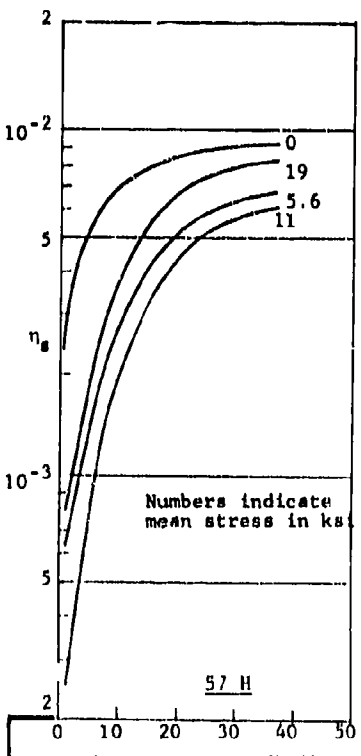

FIGURE 259 NICKEL (A, treated)

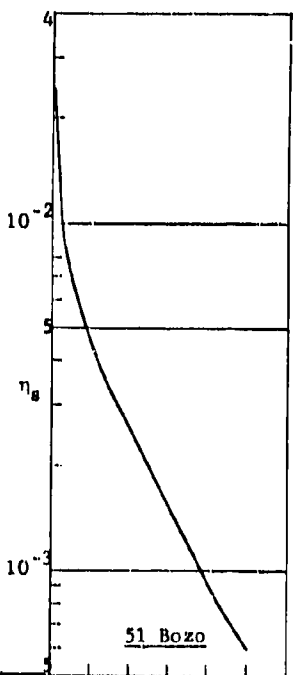

FIGURE 261 NICKEL (Polycrystalline)

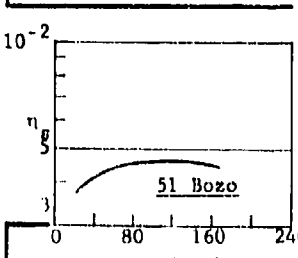

FIGURE 262 NICKEL (Polycrystalline, annealed)

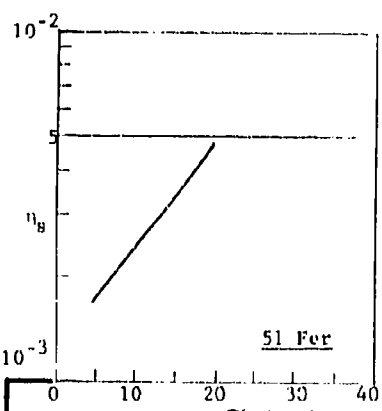

FIGURE 264 0.40% C STEEL (quenched, tempered)

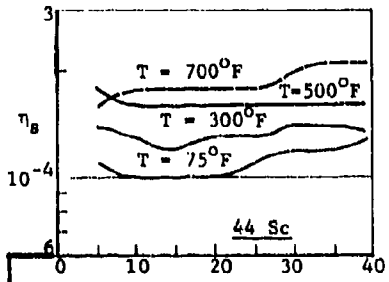

FIGURE 265 NICKEL ALLOY (Inconel, annealed)

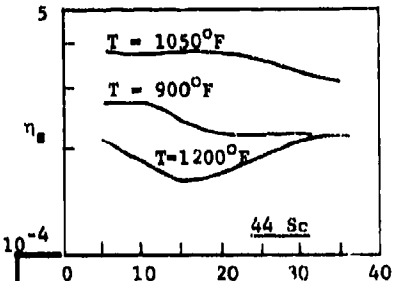

FIGURE 266 NICKEL ALLOY (Inconel, annealed)

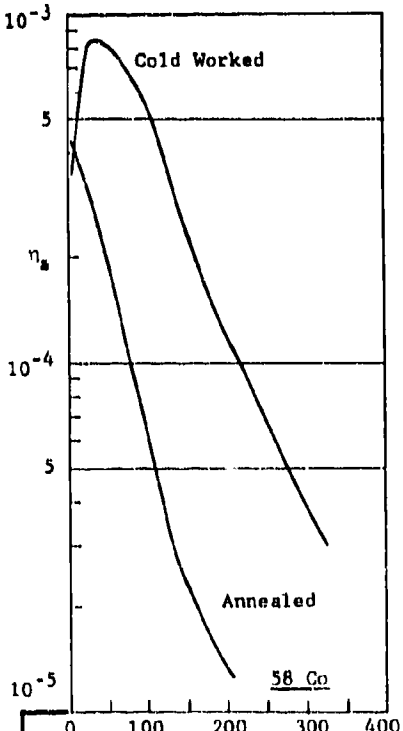

FIGURE 267 NICKEL

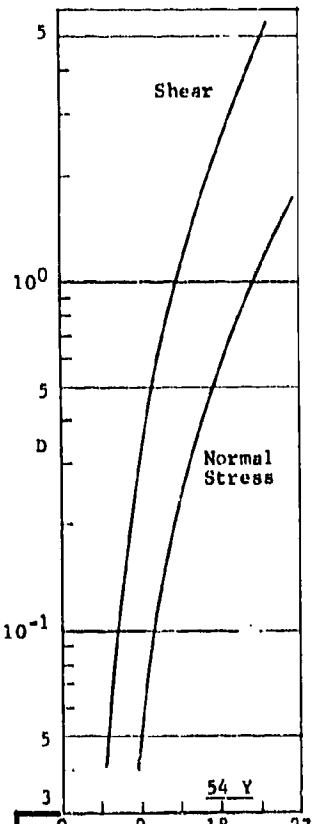

FIGURE 268 NICKEL ALLOY (Monel)

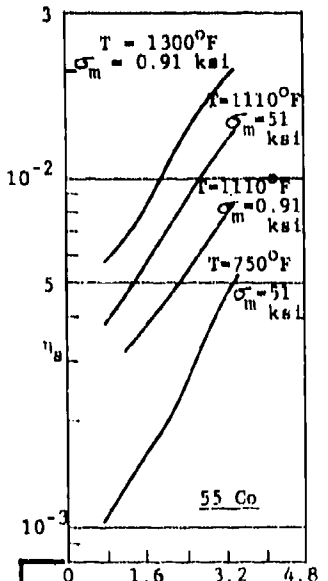

FIGURE 269 NICKEL ALLOY (Refractaloy 26)

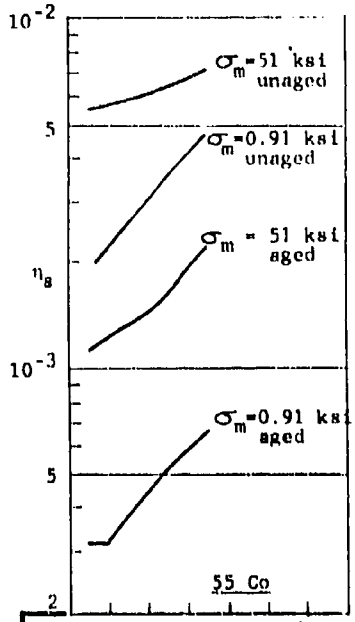

FIGURE 270 NICKEL ALLOY (Refractaloy 26)

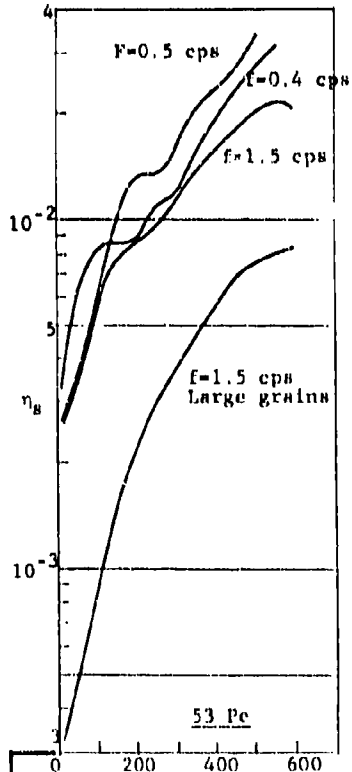

FIGURE 271 SILVER (pure, annealed)

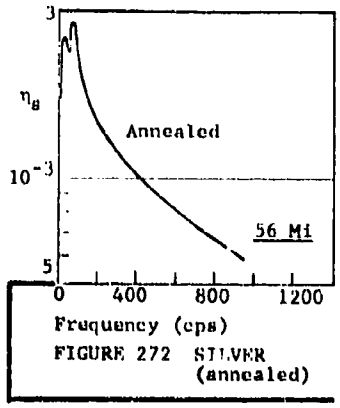

FIGURE 272 SILVER (annealed)

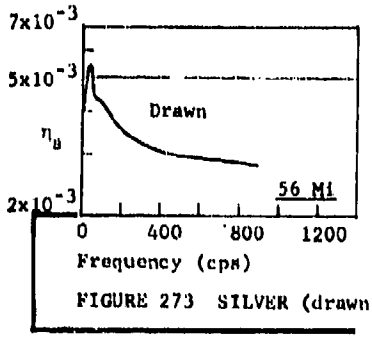

FIGURE 273 SILVER (drawn)

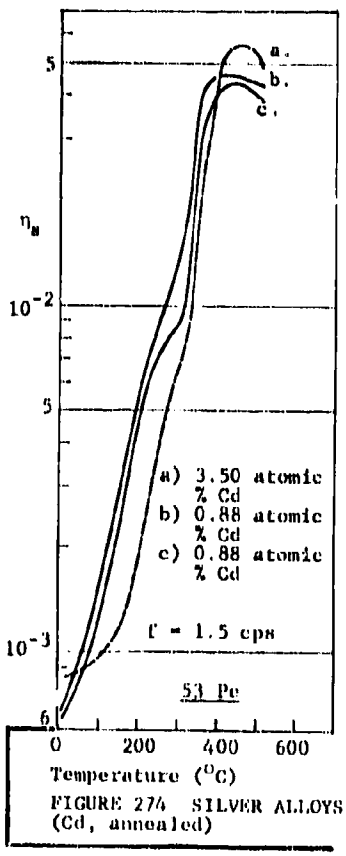

FIGURE 274 SILVER ALLOYS (Cd, annealed)

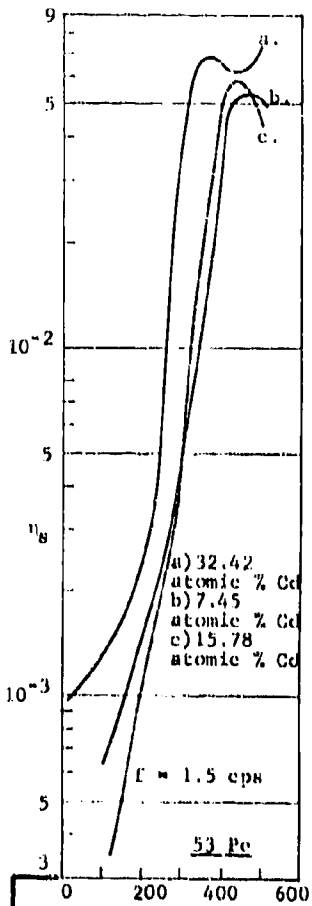

FIGURE 275 SILVER ALLOYS (Cd, annealed)

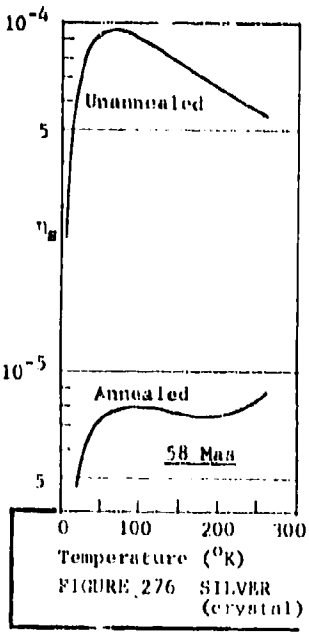

FIGURE 276 SILVER (crystal)

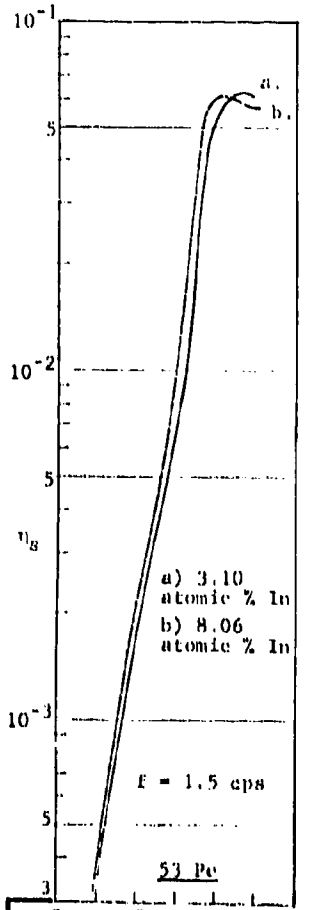

FIGURE 277 SILVER ALLOYS (In, annealed)

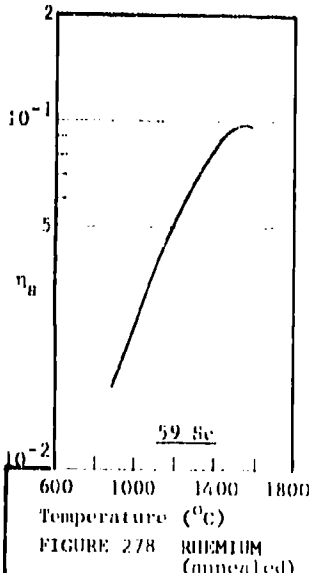

FIGURE 278 RHENIUM (annealed)

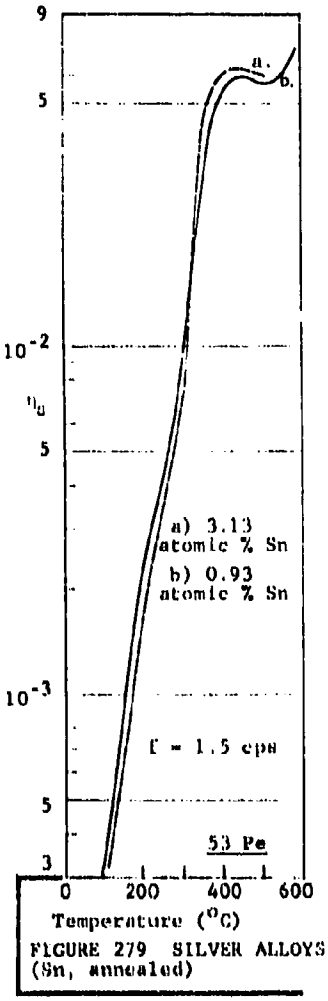

FIGURE 279 SILVER ALLOYS (Sn, annealed)

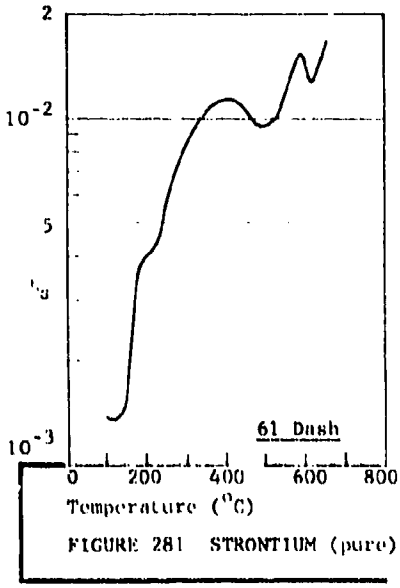

FIGURE 281 STRONTIUM (pure)

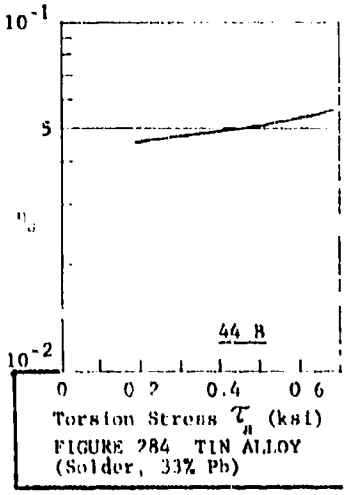

FIGURE 284 TIN ALLOY (Solder, 33% Pb)

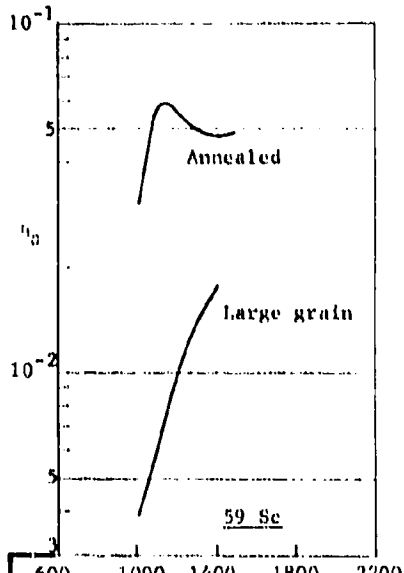

FIGURE 282 TANTALUM (annealed)

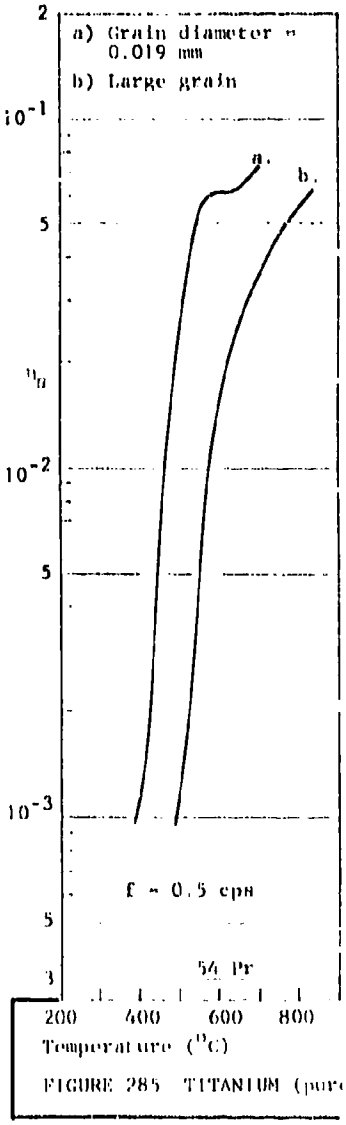

FIGURE 285 TITANIUM (pure)

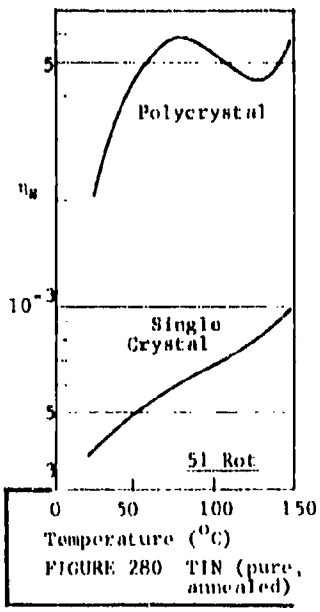

FIGURE 280 TIN (pure, annealed)

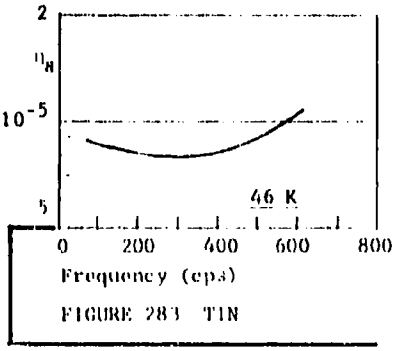

FIGURE 283 TIN

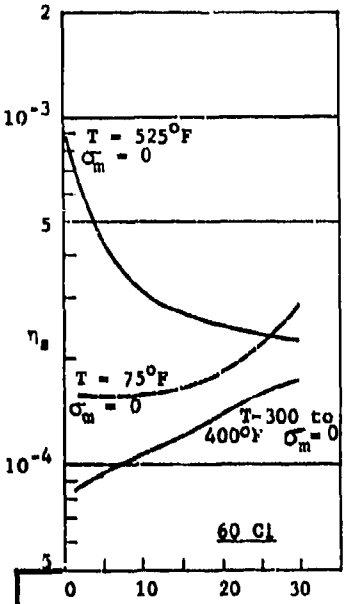

FIGURE 286 TITANIUM ALLOY (A110 AT)

FIGURE 288 TITANIUM ALLOY (RC 55, annealed)

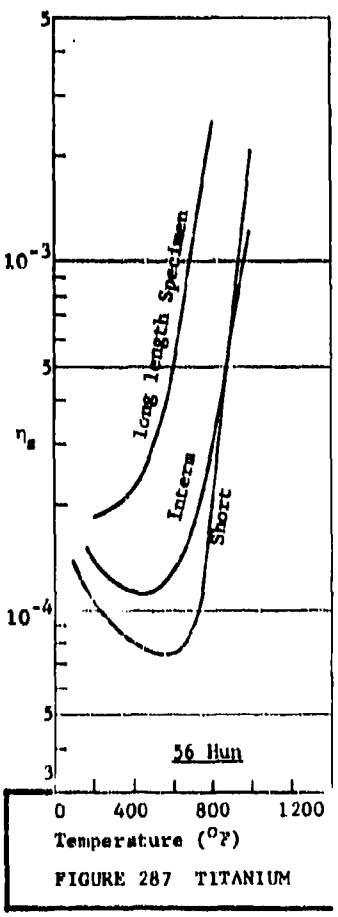

FIGURE 287 TITANIUM

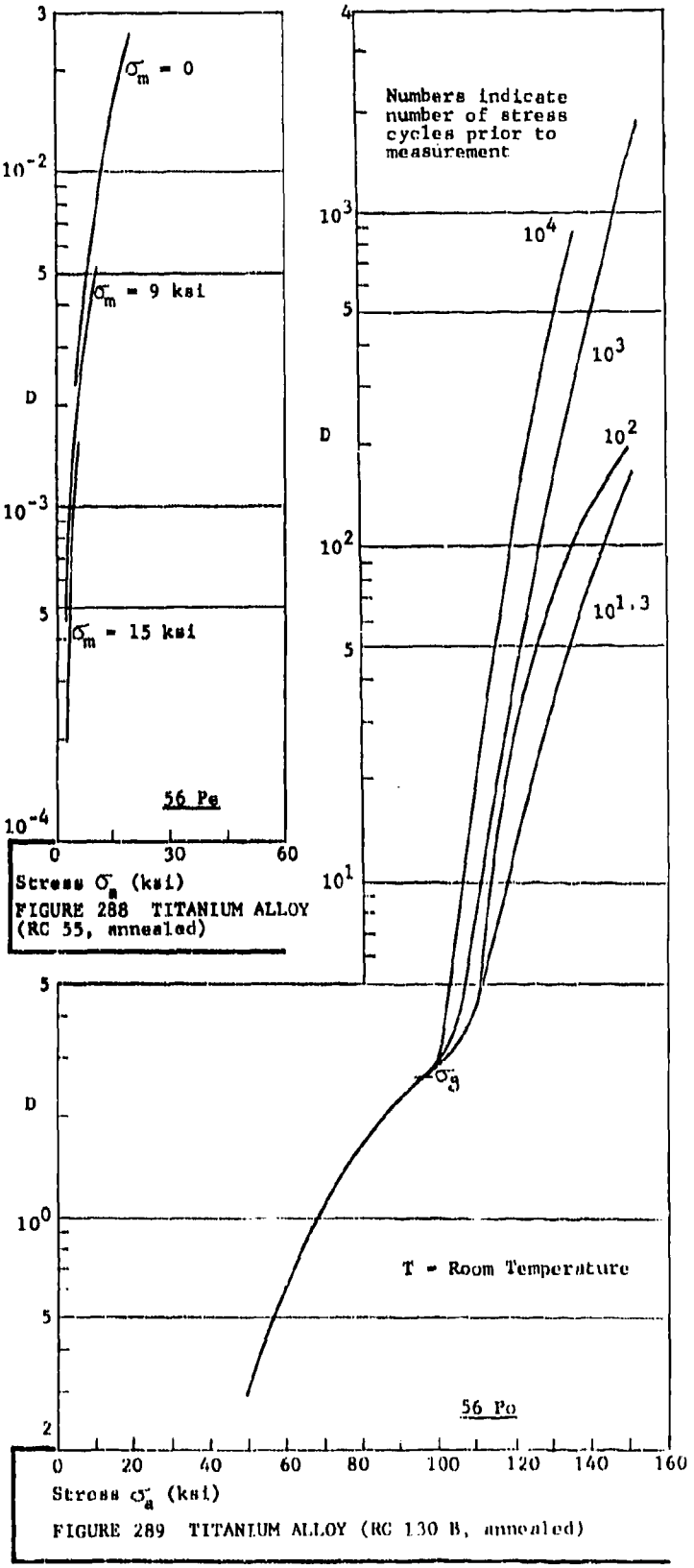

FIGURE 289 TITANIUM ALLOY (RC 130 B, annealed)

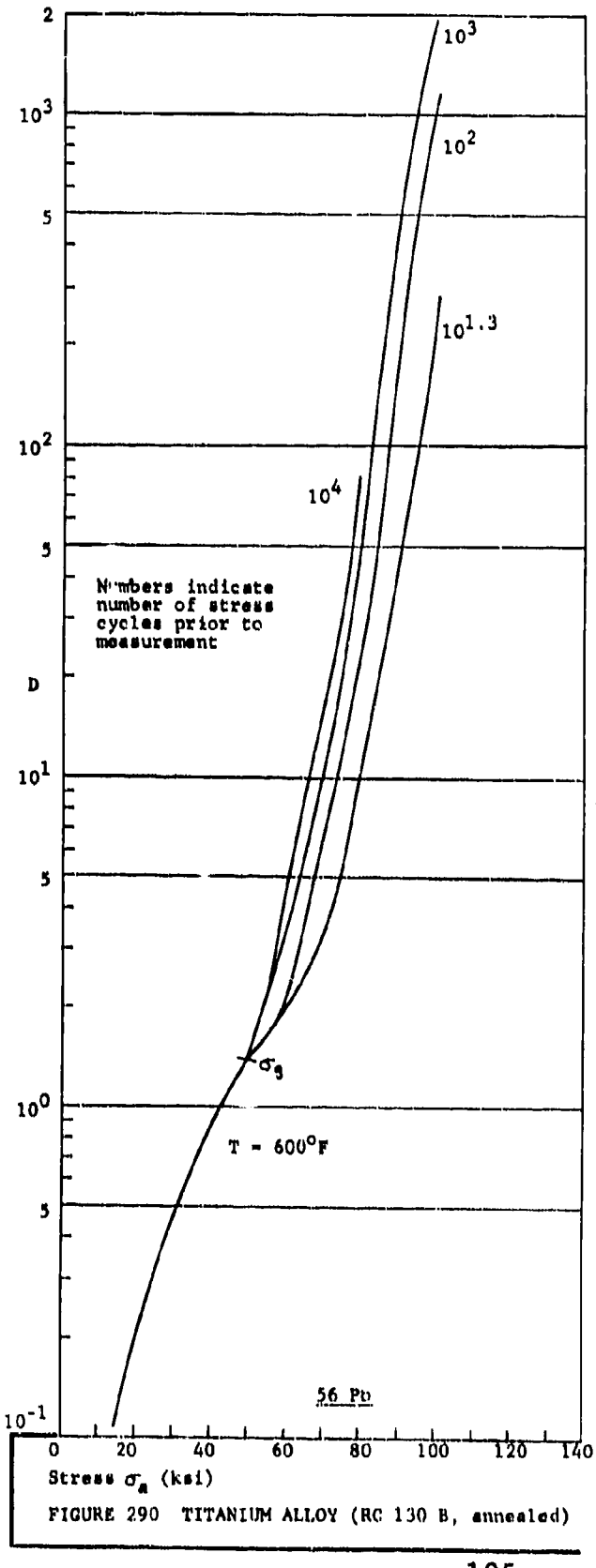

FIGURE 290 TITANIUM ALLOY (RC 130 B, annealed)

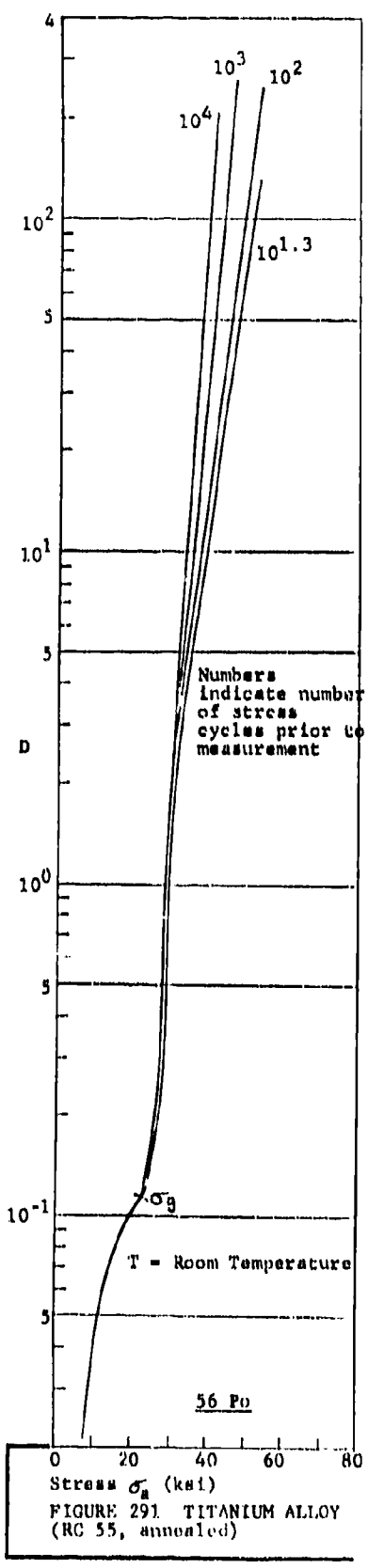

FIGURE 291 TITANIUM ALLOY (RC 55, annealed)

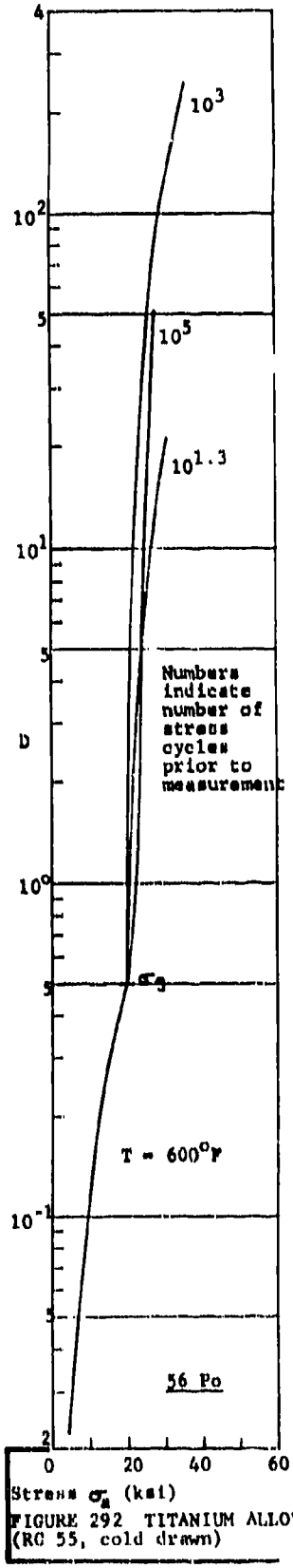

FIGURE 292 TITANIUM ALLOY (RC 55, cold drawn)

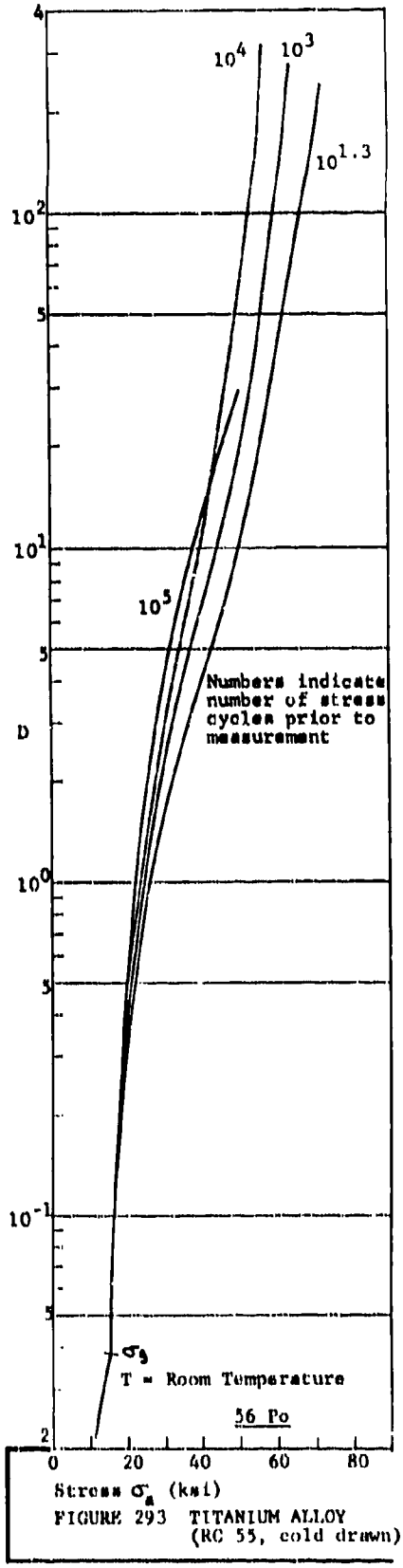

FIGURE 293 TITANIUM ALLOY (RC 55, cold drawn)

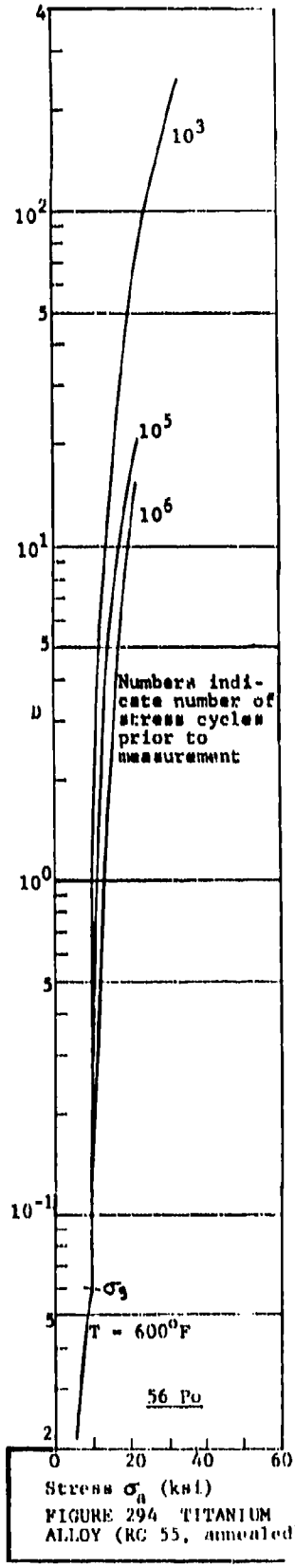

FIGURE 294 TITANIUM ALLOY (RC 55, annealed)

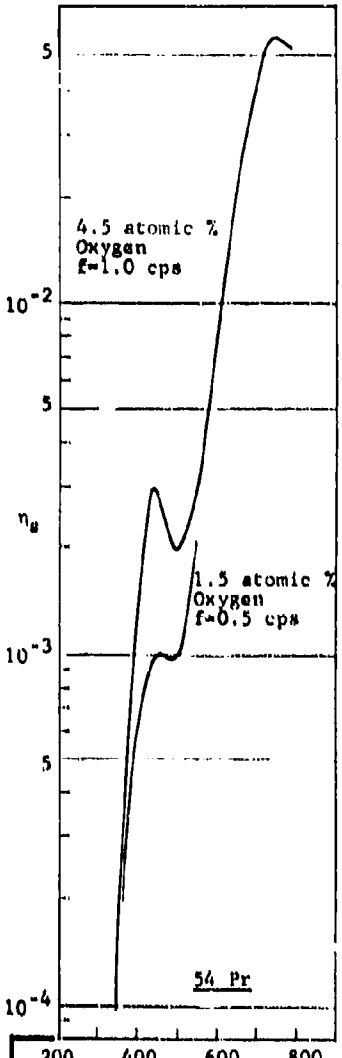

FIGURE 295 TITANIUM

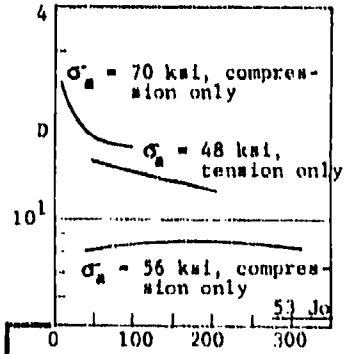

FIGURE 296 URANIUM (pure)

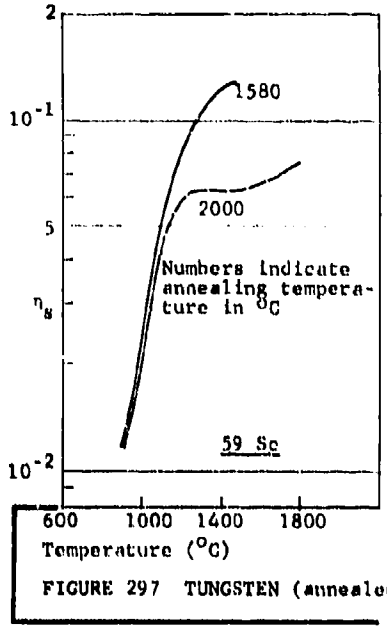

FIGURE 297 TUNGSTEN (annealed)

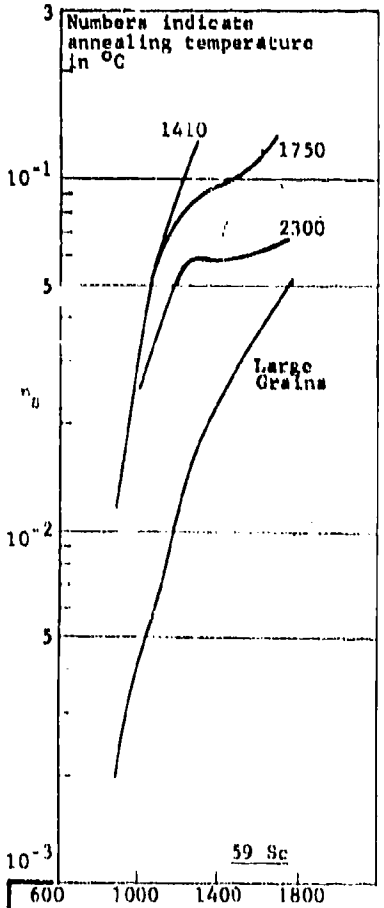

FIGURE 298 TUNGSTEN (annealed)

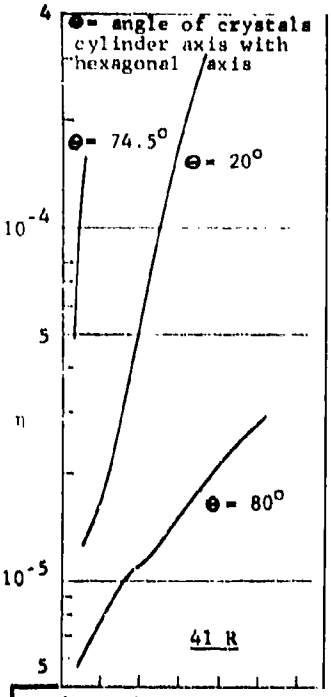

FIGURE 299 ZINC (crystal annealed)

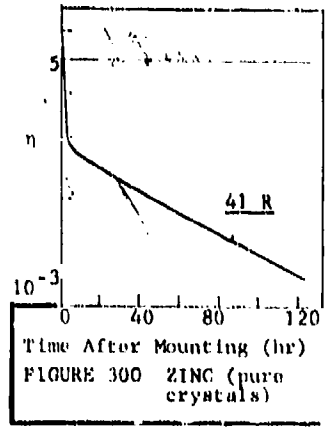

FIGURE 300 ZINC (pure crystals)

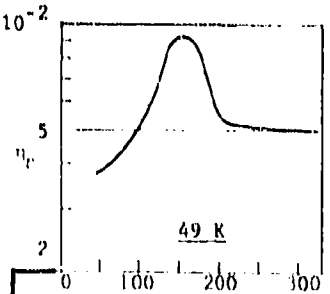

FIGURE 301 ZINC

III. POLYMERS, ELASTOMERS, WOOD PRODUCTS, COMPOSITES, AND SIMILAR SYNTHETIC AND NATURAL NON-METALLIC MATERIALS

3.1 Data Tabulation

Since the differences between a soft viscoelastic polymer and a liquid becomes indistinct, it is arbitrarily assumed in this compilation that if G* is roughly greater than 1 psi the material may be identified as a viscoelastic material. The units of G', G", E', E" are pounds per square inch.

ADHESIVE (3M Tape #466). T = 25°C. At f = 2, G' = 45 and G" = 18. At f = 10, G' = 49 and G" = 41. At f = 40, G' = 60 and G" = 52. (57 D)

ADHESIVE (3M Transfer tape #466). T = 25°C. f = 10^{-1} to 10^{5}. G' = 8 to 5,000 and G" = 4 to 7,000. (63 D, Figure 344)

BAKELITE. Torsion. σ_m = 2 ksi. $\eta_s = 4.8 \times 10^{-2}$. (41 Ki*)

CELLULOID. Strains of about 5×10^{-3}. Rotating bending. $\eta_s = 1.4 \times 10^{-2}$. (41 Ki*)

CELLULOSE ACETATE (Butyrate, made from medium hard grades Tenite II, 201 and 203). σ_a = 0.1 to 1.0 ksi. D = 4×10^{-3} to 7×10^{-1}. (49 Saue, Figure 303)

CELLULOSE ACETATE (FM 6). Axial stress. σ_a = 0.2 to 2 ksi. D = 2×10^{-2} to 1. (54 Y, Figure 302-a)

CELLULOSE ACETATE (FM 6, made from compression molded rod, medium soft, 40 parts triacetim plasticizer). σ_a = 0.1 to 1.0 ksi. D = 5×10^{-3} to 7×10^{-1}. (49 Saue, Figure 302-b)

COTTON (11/4/2). T = 25°C. f = 180. G' = 1.49×10^6 and G" = 8.6×10^4. (49 Ly)

EBONITE. T = 25°C. f = 0.0022 to 612. G' $\approx 1.3 \times 10^5$ and G" = 1.2×10^3 to 4.4×10^3. G" = 3×10^3 peak at f = 40. G" = 3.2×10^3 minimum at f = 30. (50 Leth, Figure 368)

EBONITE. In torsion, $\eta_s = 9.2 \times 10^{-3}$. In bending, $\eta_s = 2.7 \times 10^{-2}$. (41 Ki*)

FIBER (Dupont A). T = 21°C. f = 180. E' = 2.4×10^5 and E" = 1.39×10^5. (49 Ly)

FIBER (Dupont V 75/16/2). T = 21°C. f = 180. E' = 1.59×10^6 and E" = 5.15×10^4. (49 Ly)

FOAM (3M Double coated polyurethane tape, 4000 series). T = 25°C. f = 1 to 10^9. G' = 15 to 800 and G" = 4 to 110. (63 Da, Figure 346)

GLASS-RESIN COMPOSITE (1002 Crossply "Scotchply", reinforced plastic with glass filaments linearly aligned in two directions) Rotating bending. f = 0.33. σ_a = 1 to 30 ksi. D = 10^{-2} to 10. D = 2.6×10^{-1} at $\sigma_a = \sigma_g$ = 10 ksi. (58 A, Figure 353)

GLASS-RESIN COMPOSITE (Glass fabric laminate plastic, CTL-91-LD resin, 181-114 fiberglass). Axial stress. T = 70°F. σ_a =

3 to 16 ksi. D = 2×10^{-2} to 1.5×10^{1}. (56 Po, Figure 358)

GLASS-RESIN COMPOSITE (Glass fabric laminate plastic, CTL-91-LD resin, 181-114 fiberglass). σ_a = 1 to 5 ksi. σ_m = 0 to 7 ksi. D = 5×10^{-2} to 2×10^{-1}. No change with σ_m. (56 Pe, Figure 359)

GLASS-RESIN COMPOSITE (Scotchply, Type 100 Unicore Spring). T = 23°C. At f = 1, E' = 1.30×10^{6} and E" = 3.10×10^{4}. At f = 10, E' = 1.32×10^{6} and E" = 1.32×10^{4}. At f = 40, E' = 1.35×10^{6} and E" = 1.35×10^{4}. (58 K)

GLASS-RESIN COMPOSITE (Scotchply, Type 1000 resin). T = 23°C. At f = 1, E' = 3.1×10^{5} and E" = 5,300. At f = 10, E' = 3.2×10^{5} and E" = 6,400. At f = 40, E' = 3.3×10^{5} and E" = 6,300. (58 K)

HYCAR 1014. T = 20°C. f = 100 to 1,850. η = 0.40 to 0.76. At maximum η, G' = 200. (56 Mo, 61 U*)

KAROLITH. T = 25°C. At f = 46,000, E' = 8.95×10^{5} and E" = 47.0×10^{5}. At f = 61,000, E' = 8.96×10^{5} and E" = 55.0×10^{5}. (41 Ri)

KAROLITH. T = 75°C. At f = 44,000, E' = 7.45×10^{5} and E" = 26.0×10^{5}. At f = 59,000, E' = 7.45×10^{5} and E" = 32.0×10^{5}. (41 Ri)

LAMINATED PLASTIC (Bakelite, grade X). Torsion. τ_a = 0 to 4.5 ksi. η = 3.7×10^{-2} to 2×10^{-1}. (43 L, Figure 343)

LAMINATED PLASTIC (Bakelite, grade X). Axial stress. Resonant vibration. σ_a = 1 to 3 ksi. η = 5 x 10^{-2} to 10^{-1}. (43 L, Figure 347)

LAMINATED PLASTIC (Bakelite, closely packed cotton cord reinforcement running parallel to the axis). Torsion. τ_a = 0.3 to 3 ksi. η_s = 3 x 10^{-2} to 7 x 10^{-2}. (39 L, Figure 348)

LAMINATED PLASTIC (Bakelite X199, filled with fabric snippings impregnated with phenol-formaldehyde resin and molded). Torsion. τ_a = 0.3 to 3 ksi. η_s = 3 x 10^{-2} to 5 x 10^{-2}. (39 L, Figure 349)

LAMINATED PHENOLIC (Bakelite, grade X, paper base). Axial stress. σ_a = 0.5 to 3 ksi. D = 10^{-2} to 2. (46 Ro, Figure 350)

LAMINATED PHENOLIC (Various types: bakelite, wood flour, paper, fine and coarse fabric filler). Torsion. τ_a = 0.1 to 0.8 ksi. η_s = 3 x 10^{-2} to 4 x 10^{-2}. Little change with composition. (44 B, Figure 351)

LAMINATED PHENOLIC (Bakelite, commercial molding material with wood-flour filler). Torsion. τ_a = 0.3 to 3 ksi. η_s = 2 x 10^{-2} to 5 x 10^{-2}. (39 L, Figure 352)

LAMINATED PLASTIC (Phenolics: asbestos base and army duck, fast curing phenol-formaldehyde resin). σ_a = 0.5 to 2 ksi. D = 10^{-2} to 2 x 10^{-1}. Little change with composition. (49 Saue, Figure 354)

LAMINATED PLASTIC (Phenolic with canvas). Axial stress. Resonant vibration. σ_a = 2 to 5 ksi. $\eta = 3 \times 10^{-2}$ to 10^{-1}. (43 L, Figure 355)

LAMINATED PLASTIC (Phenolic with canvas). Torsion. τ_a = 1 to 3.5 ksi. $\eta_s = 4 \times 10^{-2}$ to 10^{-1}. (43 L, Figure 356)

LAMINATED PLASTIC (Phenolic with cotton, grade CE). Bending. f = 10 to 200. $\eta_s = 10^{-1}$ to 3×10^{-2}. (57 Mi, Figure 357)

LAMINATED PLASTIC (Phenolic, synthane L, fine weave fabric base). σ_a = 0.2 to 1.0 ksi. D = 10^{-3} to 5×10^{-2}. (49 Saue, Figure 360)

LAMINATED PLASTIC (Phenolic, paper base, grade XX). Axial stress. σ_a = 0.5 to 4.0 ksi. D = 5×10^{-3} to 2×10^{-1}. (54 Y, Figure 361)

LAMINATED PLASTIC (Phenolic, synthane XX, paper base). Rod specimens. σ_a = 0.5 to 2.0. D = 10^{-2} to 3×10^{-1}. (49 Saue, Figure 362)

LAMINATED PLASTIC (Phenolic, Mitcherlich paper and fast curing phenol-formaldehyde). σ_a = 1 to 4 ksi. D = 10^{-2} to 3×10^{-1}. (49 Saue, Figure 363)

LAMINATED PLASTIC (Phenolic, rayon-cotton fabric). σ_a = 0.5 to 3 ksi. D = 7×10^{-3} to 4×10^{-1}. (49 Saue, Figure 364)

LD-400 VISCOELASTIC DAMPING MATERIAL (Developed jointly by Monsanto

Company and Lord, formerly DC-400). f = 75 to 1,000. At $T = 40^{\circ}F$, $E' = 10 \times 10^5$ to 20×10^5 and $\eta = 0.1$ to 0.08. At $T = 60^{\circ}F$, $E' = 8 \times 10^5$ to 14×10^5 and $\eta = 0.4$ to 0.2. At $T = 80^{\circ}F$, $E' = 3 \times 10^5$ to 8×10^5 and $\eta = 0.8$ to 0.7. At $T = 100^{\circ}F$, $E' = 0.8 \times 10^5$ to 2×10^5 and $\eta = 0.6$ to 0.8.

METHYL METHACRYLATE (Made from "Type 1-General Purpose" cast plexiglass). $\sigma_a = 0.1$ to 1.0 ksi. $D = 2 \times 10^{-3}$ to 4×10^{-1}. (49 Saue, Figure 320)

METHYL METHACRYLATE (Lucite). Axial stress. f = 48 and 68. $\sigma_a = 0.5$ to 2.0 ksi. $D = 5 \times 10^{-2}$ to 3. (46 Ro, Figure 316)

METHYL METHACRYLATE (Lucite). Resonant vibration. Stress = 0.5 to 2.0 ksi. Under axial stress, $\eta \approx 1.6 \times 10^{-1}$. Under torsion, $\eta = 10^{-1}$ to 1.4×10^{-1}. (43 L, Figure 318)

METHYL METHACRYLATE (Plexiglass). Axial stress. $\sigma_a = 0.1$ to 1 ksi. $D = 10^{-2}$ to 5×10^{-1}. (54 Y, Figure 319)

NYLON. $T = 30^{\circ}C$. $f = 10^{-3}$ to 10^2. $E' = 3.0 \times 10^5$ to 5.1×10^5 and $E'' = 2.28 \times 10^4$ to 2.45×10^4. (56 Maxw, Figure 307)

NYLON. $T = 23^{\circ}C$. f = 180. $E' = 1.27 \times 10^6$ and $E'' = 3.6 \times 10^4$. (49 Ly)

NYLON. Torsion. $\tau_a = 100$ psi. $\eta = 4.8 \times 10^{-2}$. (64 Bi)

NYLON. $T = 25^{\circ}C$. At f = 10, $G' = 87.5 \times 10^4$ and $G'' = 4.57 \times 10^4$. At f = 40, $G' = 87.5 \times 10^4$ and $G'' = 2.74 \times 10^4$. (51 Du)

NYLON. T = 26°C. At f = 400, E' = 4.7×10^5 and E" = 13.9×10^3. At f = 1,000, E' = 4.7×10^5 and E" = 9.3×10^3. (57 Fit)

NYLON. T = 0°C. f = 10^5. E' = 57,000 and E" = 199. (57 Ya)

PERSPEX. T = 25°C. f = 0.0033 to 800. G' = 1.61×10^5 to 2.78×10^5 and G" = 6.06×10^3 to 14.0×10^3. G" = 14.0×10^3 peak at f = 10. (50 Leth, Figure 309)

PHENOL-FORMALDEHYDE RESIN (White, transparent, and unfilled). Torsion. τ_a = 0.3 to 3 ksi. $\eta_s = 9 \times 10^{-3}$ to 1.5×10^{-2}. (39 L, Figure 349)

PHENOLIC (BM 6260). T = -40 to 40°C. At f = 40, E' = 118×10^4 and E" = 2.27×10^4. At f = 100, E' = 118×10^4 and E" = 1.79×10^4. At f = 400, E' = 118×10^4 and E" = 1.18×10^4. (56 Stre)

PHENOLIC RESINS. T = 0°C. f = 10^5. E' = 10,200 and E" = 204. (57 Ya)

PLASTIC (LKF-1, Russian manufacture). Bending. σ_a = 0.2 to 1.5 ksi. At T = -60°C, $\eta_s = 2 \times 10^{-2}$ to 3×10^{-2}. At T = 60°C, $\eta_s = 5 \times 10^{-2}$ to 7×10^{-2}. (62 Pisa, Figure 338)

PLASTICIZED CELLULOSE NITRATE. T = 65°C. f = 100 to 5,250. G' = 87 to 555 and G" = 57 to 545. (51 Ho, Figure 304)

PLASTICIZED CELLULOSE NITRATE. T = 20°C. At f = 400, G' = 1,045 and G" = 657. At f = 1,000, G' = 1,595 and G" = 881. At f =

4,000, G' = 3,100 and G" = 1,820. (51 Ho)

PLASTICIZED POLYVINYL ACETATE. At T = 5°C: G' = 61 and G" = 67 at f = 1, G' = 450 and G" = 900 at f = 10, G' = 2,030 and G" = 5,280 at f = 100, G' = 1.45×10^4 and G" = 2.32×10^4 at f = 1,000. At T = 35°C: G' = 12 and G" = 4.8 at f = 10, G' = 26 and G" = 18.2 at f = 100, G' = 130 and G" = 195 at f = 1,000, G' = 1,020 and G" = 2,450 at f = 10,000. (64 Sno*)

PLASTICIZED POLYVINYL ACETATE. For all f and T. Maximum η = 2.6 and G' = 2,180 at f = 50, T = 5°C. (61 U*)

PLASTICIZED POLYVINYL BUTYRAL RESIN. T = 23°C. f = 0.1 to 1,000. G' = 290 to 13,050 and G" = 320 to 5,220. (64 Sno*)

PLASTICIZED POLYVINYL CHLORIDE (Koroseal). For all f and T. Maximum η = 1.4 and G' = 3,470 at f = 660, T = 50°C. (61 U*)

PLASTICIZED POLYVINYL CHLORIDE (33.3% Diphthalate). T = 20°C. f = 40 to 350. E' = 4.3×10^4 and E" = 1.93×10^4. (54 Dil)

PLASTICIZED POLYVINYL CHLORIDE. T = 25°C. f = 10 to 1,000. G' = 720 to 7,250 and G" = 550 to 6,380. (51 Ro, Figure 332)

PLASTICIZED POLYVINYL CHLORIDE (33.3% Diphthalate). T = 50°C. f = 40 to 350. E' = 2,150 and E" = 3,400. (54 Dil)

PLASTICIZED POLYVINYL CHLORIDE (VU-1913). T = 25°C. f = 0.001 to 10. E' = 900 to 7,000 and E" = 720 to 3,500. (54 Ph, Figure 334)

PLASTICIZED POLYVINYL CHLORIDE (VU-1920). $T = 25^{\circ}C$. $f = 0.001$ to 10. $E' = 2{,}000$ to $20{,}000$ and $E'' = 1{,}000$ to $12{,}000$. $E' = 6{,}000$ peak at $f = 0.1$. $E'' = 4{,}000$ peak at $f = 0.1$ (54 Ph, Figure 335)

PLYWOOD (Birch, Sp.Gr. = 0.87). Axial stress. $\sigma_a = 0.5$ to 6 ksi. $D = 4 \times 10^{-3}$ to 1. (54 Y, Figure 387)

PLYWOOD (Birch, cross-laminated). Axial stress. Resonant vibration. $\sigma_a = 0.5$ to 3 ksi. $D = 10^{-2}$ to 1. (44 Yor, Figure 326)

PLYWOOD (Birch, Sp.Gr. = 1.05, resin-bonded). Axial stress. $\sigma_a = 0.5$ to 4 ksi. $D = 2 \times 10^{-3}$ to 1. (46 Ro, Figure 314)

POLY B-CHLOROETHYL METHACRYLATE. $T = 20^{\circ}C$. Bending. $f = 200$. $E' = 61.2 \times 10^4$ and $E'' = 1.84 \times 10^4$. (55 Ho)

POLYCAPRONE AND FIBER (Reinforced plastic). Bending. At $T = 20^{\circ}C$, $\eta_s = 1.2 \times 10^{-1}$. At $T = -70^{\circ}C$, $\eta_s = 4 \times 10^{-2}$ to 6×10^{-2}. (62 Pisa, Figure 365)

POLYCYCLOHEXL CHLOROACRYLATE. $T = 20^{\circ}C$. Bending. $f = 200$. $E' = 43.8 \times 10^4$ and $E'' = 0.65 \times 10^4$. (55 Ho)

POLYCYCLOHEXYL METHACRYLATE. $T = 20^{\circ}C$. Bending. $f = 200$. $E' = 321.0 \times 10^3$ and $E'' = 6.4 \times 10^3$. (55 Ho)

POLYESTER. $T = 43^{\circ}C$. At $f = 10$, $E' = 51.0 \times 10^4$ and $E'' = 1.46 \times 10^4$. At $f = 100$, $E' = 58.5 \times 10^4$ and $E'' = 1.17 \times 10^4$. At

f = 1,000, E' = 58.5 x 10^4 and E" = 1.32 x 10^4. At f = 10,000, E' = 58.5 x 10^4 and E" = 1.52 x 10^4. (55 Be)

POLYESTER. f = 10 to 10,000. At T = 4°C, E' = 6.27 x 10^5 and E" = 5.4 x 10^3 to 11.3 x 10^3. At T = 72°C, E' = 4.1 x 10^5 to 5.8 x 10^5 and E" = 4.4 x 10^4 to 7.0 x 10^4. At T = 108°C, E' = 6.7 x 10^3 to 1.12 x 10^5 and E" = 2.6 x 10^3 to 68.6 x 10^3. (55 Be, Figures 340, 341, and 342)

POLYESTER. For all f and T. Maximum η = 1.1 and G' = 10,100 at f = 200, T = 108°C. (61 U*)

POLYESTER (G-651). T = 25°C. At f = 0.1, G' = 0.0016 and G" = 0.036. At f = 1, G' = 0.0088 and G" = 0.29. At f = 10, G' = 0.0073 and G" = 10.2. (54 Ph)

POLYETHYL CHLOROACRYLATE. T = 20°C. Bending. f = 200. E' = 58.3 x 10^4 and E" = 1.16 x 10^4. (55 Ho)

POLYETHYLENE. f = 12. T = 30 to 80°C. G' = 2,900 at $\eta_{maximum}$ = 0.23. (61 U*)

POLYETHYL METHACRYLATE. T = 150°C. f = 40 to 1,000. G' = 35 to 284 and G" = 90 to 228. (57 Fe, Figure 315)

POLYETHYL METHACRYLATE. T = 20°C. Bending. f = 200. E' = 32.1 x 10^4 and E" = 2.25 x 10^4. (55 Ho)

POLYETHYLENE TEREPHTHALAL. T = -15 to 200°C. At f = 1,000, E' = 18.1 x 10^5 and E" = 5.22 x 10^5. At f = 4,000, E' = 19.85 x

10^5 and E'' = 1.20×10^5. At f = 10,000, E' = 2.22×10^5 and E'' = 1.38×10^5. (49 B)

POLYGLYCOL METHACRYLATE. T = 20°C. Bending. f = 200. E' = 43.8×10^4 and E'' = 1.32×10^4. (55 Ho)

POLYHEXANE. T = 6°C. f = 40 to 1,000. E' = 63 to 265 and E'' = 51 to 189. (57 Kur, Figure 308)

POLYISOBUTYLENE. For all f and T. Maximum $\eta > 2.0$ and G' = 290 at f = 6,000, T = 25°C. (61 U*)

POLY-ISO-PROPYL CHLOROACRYLATE. T = 20°C. Bending. f = 200. E' = 73.0×10^4 and E'' = 0.73×10^4. (55 Ho)

POLY-ISO-PROPYL METHACRYLATE. T = 20°C. Bending. f = 200. E' = 45.5×10^4 and E'' = 1.80×10^4. (55 Ho)

POLYMERIZED TUNG OIL (X-6). T = 20°C. At f = 400, G' = 812 and G'' = 840. At f = 1,000, G' = 1,600 and G'' = 1,185. At f = 4,000, G' = 2,610 and G'' = 2,560. (51 Ho)

POLYMERIZED TUNG OIL (X-6). T = 65°C. f = 100 to 5,250. G' = 184 to 1,180 and G'' = 158 to 1,040. (51 Ho, Figure 305)

POLYMERIZED TUNG OIL (X-7). T = 20°C. At f = 1,000, G' = 2,470 and G'' = 1,365. At f = 4,000, G' = 5,370 and G'' = 2,970. (51 Ho)

POLYMERIZED TUNG OIL (X-7). T = 65°C. f = 100 to 5,250. G' = 154 to 2,380 and G'' = 214 to 1,870. (51 Ho, Figure 306)

POLYMETHL CHLOROACRYLATE. T = 20°C. Bending. f = 200. E' = 90.6×10^4 and E" = 1.81×10^4. (55 Ho)

POLYMETHYL CHLORIDE ACETATE. T = 20°C. At f = 100, G' = 297 and G" = 212. At f = 400, G' = 463 and G" = 328. At f = 1,000, G' = 985 and G" = 805. (51 Ho)

POLYMETHYL CHLORIDE ACETATE. T = 65°C. At f = 100, G' = 99 and G" = 22. At f = 400, G' = 93 and G" = 22. At f = 1,240, G' = 121 and G" = 37. At f = 5,250, G' = 155 and G" = 91. (51 Ho)

POLYMETHYL METHACRYLATE. For all f and T. Maximum η = 1.5 and G' = 1.45×10^4 at f = 1,200, T = 142°C. (61 U*)

POLYMETHYL METHACRYLATE. T = 50°C. f = 0.083 to 83. E' $\approx 6 \times 10^5$ and E" $\approx 6 \times 10^4$. (57 K)

POLYMETHYL METHACRYLATE. T = 25°C. f = 0.083 to 83. E' = 7.5×10^5 to 8.0×10^5 and E" = 3.7×10^4 to 5.6×10^4. (57 K, Figure 311)

POLYMETHYL METHACRYLATE. T = 25°C. f = 0.001 to 400. E' = 4.35×10^5 to 7.39×10^5 and E" = 9.3×10^3 to 14.5×10^3. E" = 14.5×10^3 peak at f = 50. (54 Fine, Figure 312)

POLYMETHYL METHACRYLATE. T = 70°C. f = 0.083 to 83. E' = 4.8×10^5 to 4.0×10^5 and E" = 9.6×10^4 to 8.0×10^4. (57 K, Figure 313)

POLYMETHYL METHACRYLATE. T = 30°C. f = 0.001 to 1. E' = 4.4×10^5 and E" = 9.8×10^3 to 26.5×10^3. (56 Maxw, Figure 317)

POLYMETHYL METHACRYLATE. T = 20°C. f = 200. E' = 38.0×10^4 and E" = 2.28×10^4. (55 Ho)

POLYMETHYL METHACRYLATE. T = 50°C. At f = 40, G' = 98.2 and G" = 137. At f = 100, G' = 146 and G" = 292. (55 Wil)

POLYMETHYL METHACRYLATE. T = 25°C. At f = 100, G' = 6.70×10^4 and G" = 1.85×10^4. At f = 400, G' = 7.91×10^4 and G" = 1.85×10^4. (55 Wil)

POLYMETHYL METHACRYLATE. T = 30°C. At f = 10, E' = 55.0×10^4 and E" = 3.24×10^4. At f = 100, E' = 61.0×10^4 and E" = 2.80×10^4. (56 Maxw)

POLYMETHYL METHACRYLATE. T = 92°C. At f = 0.083, E' = 5.5×10^4 and E" = 3.0×10^4. At f = 0.83, E' = 10.0×10^4 and E" = 4.0×10^4. At f = 8.3, E' = 15.0×10^4 and E" = 3.5×10^4. (57 K)

POLYMETHYL METHACRYLATE. T = 0°C. f = 10^5. E' = 550 and E" = 190. (57 Ya)

POLY-N-BUTYL CHLOROACRYLATE. Bending. T = 20°C. f = 200. E' = 29.2×10^4 and E" = 0.44×10^4. (55 Ho)

POLY-N-BUTYL METHACRYLATE. Bending. T = 20°C. f = 200. E' = 16.0×10^4 and E" = 2.08×10^4. (55 Ho)

POLY-N-BUTYL METHACRYLATE. T = 40°C. At f = 400, G' = 42,200 and G" = 47,700. At f = 1,000, G' = 47,700 and G" = 1,460. (57 Ch)

POLY-N-HEXYL METHACRYLATE. T = 19°C. f = 40 to 1,000. G' = 5.9 x 10^3 to 24.3 x 10^3 and G" = 4.9 x 10^3 to 10.6 x 10^3. (57 Chi, Figure 337)

POLY-N-PROPLY CHLOROACRYLATE. Bending. T = 20°C. f = 200. E' = 46.7 x 10^4 and E" = 0.93 x 10^4. (55 Ho)

POLY-N-PROPYL METHACRYLATE. Bending. T = 20°C. f = 200. E' = 29.2 x 10^4 and E" = 2.92 x 10^4. (55 Ho)

POLYNEOPENTYL METHACRYLATE. Bending. T = 20°C. f = 200. E' = 321.0 x 10^3 and E" = 8.0 x 10^3. (55 Ho)

POLYPHENYL METHACRYLATE. Bending. T = 20°C. f = 200. E' = 55.5 x 10^4 and E" = 1.67 x 10^4. (55 Ho)

POLYPINACOLYL METHACRYLATE. Bending. T = 20°C. f = 200. E' = 321.0 x 10^3 and E" = 4.5 x 10^3. (55 Ho)

POLYPROPYLENE. T = -20°C. At f = 10, E' = 58.5 x 10^4 and E" = 1.17 x 10^4. At f = 100, E' = 58.5 x 10^4 and E" = 1.40 x 10^4. At f = 1,000, E' = 58.5 x 10^4 and E" = 1.40 x 10^4. (59 Boh)

POLYPROPYLENE. T = 0°C. At f = 10, E' = 41.0 x 10^4 and E" = 2.40 x 10^4. At f = 100, E' = 44.0 x 10^4 and E" = 3.08. At f = 1,000, E' = 48.0 x 10^4 and E" = 3.84 x 10^4. (59 Boh)

POLYPROPYLENE. T = 20°C. At f = 10, E' = 19.0 x 10^4 and E" = 1.80 x 10^4. At f = 100, E' = 21.9 x 10^4 and E" = 2.85 x 10^4. At f = 1,000, E' = 24.8 x 10^4 and E" = 4.1 x 10^4. (59 Boh)

POLYPROPYLENE SEBACATE. T = 20°C. At f = 400, G' = 189 and G" = 62. At f = 1,000, G' = 203 and G" = 61. At f = 4,000, G' = 261 and G" = 109. (51 Ho)

POLYPROPYLENE SEBACATE. T = 65°C. At f = 100, G' = 65.7 and G" = 23. At f = 400, G' = 81.7 and G" = 66. At f = 1,240, G' = 132 and G" = 47. At f = 5,250, G' = 115 and G" = 106. (51 Ho)

POLY-SEC-BUTYL CHLOROACRYLATE. Bending. T = 20°C. f = 200. E' = 40.8 x 10^4 and E" = 0.82 x 10^4. (55 Ho)

POLY-SEC-BUTYL METHACRYLATE. Bending. T = 20°C. f = 200. E' = 32.1 x 10^4 and E" = 1.28 x 10^4. (55 Ho)

POLYSTEARYL METHACRYLATE. Bending. T = 20°C. f = 200. E' = 36.7 x 10^4 and E" = 1.83 x 10^4. (55 Ho)

POLYSTRYRENE · For all f and T. Maximum $\eta > 2.0$ and G' = 1.45 x 10^4 at f = 2,000, T ≈ 140°C. (61 U*)

POLYSTYRENE. T = 25°C. At f = 0.01, E' = 80.0 x 10^4 and E" = 1.6 x 10^4. At f = 0.1, E' = 86.0 x 10^4 and E" = 1.7 x 10^4. At f = 1, E' = 90.0 x 10^4 and E" = 1.8 x 10^4. At f = 10, E' = 95.0 x 10^4 and E" = 1.86 x 10^4. At f = 100, E' = 95.0 x 10^4 and E" = 1.9 x 10^4. (57 K)

POLYSTYRENE. T = -70 to 90°C. At f = 5×10^4, E' = 3.19×10^5 and E" = 7,000. At f = 10^5, E' = 2.61×10^5 and E" = 5,740. (57 Ya)

POLYSTYRENE. T = 30°C. f = 0.001 to 100. E' = 4.8×10^5 to 5.2×10^5 and E" = 4.8×10^3 to 10.2×10^3. E" = 10.2×10^3 peak at f = 1. (56 Maxw, Figure 323)

POLYSTYRENE. T = 25°C. f = 0.0024 to 703. G' = 1.69×10^5 to 1.90×10^5 and G" = 1.14×10^3 to 2.30×10^3. G" = 2.3×10^3 peak at f = 1. (50 Leth, Figure 324)

POLYSTYRENE. σ_a = 0.1 to 2.0 ksi. D = 5×10^{-3} to 5×10^{-1}. (49 Saue, Figure 325)

POLYSTYRENE (Lustrex). Axial stress. σ_a = 0.1 to 2.0 ksi. D = 10^{-2} to 4×10^{-1}. (54 Y, Figure 321)

POLYSTYRENE (Styrone). σ_a = 0.1 to 1.0 ksi. D = 2×10^{-3} to 2×10^{-1}. (49 Saue, Figure 322)

POLY-TERT-BUTYL METHACRYLATE. Bending. T = 20°C. f = 200. E' = 43.8×10^4 and E" = 1.75×10^4. (55 Ho)

POLYTETRAFLUOROETHYLENE. 1.4% Static deflection. T = 23°C. At f = 100, G' = 10,800 and G" = 800. At f = 1,000, G' = 13,600 and G" = 1,790. (57 Fit)

POLYTETRAFLUOROETHYLENE. T = 21°C. At f = 100, E' = 18.5×10^4 and E" = 1.31×10^4. At f = 400, E' = 11.5×10^4 and E" =

0.77×10^4. At f = 1,000, E' = 10.7×10^4 and E" = 0.79. (57 Fit)

POLYTETRAFLUORETHYLENE (Teflon-TFE). For all f and T. Maximum η = 1.0 and G' = 5,800 at f = 400, T = 23°C. (61 U*)

POLYTHENE. T = 20°C. f = 3,000. E' = 1.69×10^5 and E" = 324. (49 Hi)

POLYTHENE. T = 30°C. At f = 1,000, G' = 22,300 and G" = 4,800. At f = 10,000, G' = 17,350 and G" = 10,850. (49 Hi)

POLYTHENE. T = 25°C. At f = 0.0018 to 19.1, G' = 9,300 to 22,000. At f = 0.0018 to 1.0, G" $\approx$ 1,800; and at f = 1.0 to 19.1, G" = 1,800 to 130. (50 Leth, Figure 327)

POLYTRIFLUERO-ISOPROPYL METHACRYLATE. Bending. T = 20°C. f = 200. E' = 32.0×10^4 and E" = 1.24×10^4. (55 Ho)

POLYTRIFLUOROCHLOROETHYLENE. T = -50°C. At f = 10, E' = 58.5×10^4 and E" = 1.75×10^4. At f = 100, E' = 62.8×10^4 and E" = 2.50×10^4. At f = 1,000, E' = 65.7×10^4 and E" = 4.27×10^4. (59 Boh)

POLYTRIFLUOROCHLOROETHYLENE. T = 0°C. At f = 10, E' = 36.5×10^4 and E" = 4.4×10^4. At f = 100, E' = 42.4×10^4 and E" = 4.6×10^4. At f = 1,000, E' = 48.0×10^4 and E" = 4.7×10^4. (59 Boh)

POLYTRIFLUOROCHLOROETHYLENE. T = 50°C. At f = 10, E' = 3.0×10^4

and $E'' = 0.18 \times 10^4$. At f = 100, $E' = 7.3 \times 10^4$ and $E'' = 0.60 \times 10^4$. At f = 1,000, $E' = 14.6 \times 10^4$ and $E'' = 2.50 \times 10^4$. (59 Boh)

POLYTRIFLUOROCHLOROETHYLENE. T = 20°C. At f = 10, $E' = 26.3 \times 10^4$ and $E'' = 2.20 \times 10^4$. At f = 100, $E' = 32.1 \times 10^4$ and $E'' = 3.85 \times 10^4$. At f = 1,000, $E' = 41.0 \times 10^4$ and $E'' = 6.87 \times 10^4$. (59 Boh)

POLYTRIFLUOROCHLOROETHYLENE (Fluorothene). f = 3.3. T = 90 to 120°C. G' = 11,600 at η maximum = 0.42. (61 U*)

POLYVINYL ACETATE (23.8% concentration). T = 10°C. At f = 500, G' = 1.77 and G'' = 0.86. At f = 1,000, G' = 1.95 and G'' = 1.27. (50 Fe)

POLYVINYL ACETATE (35.1% concentration). T = 10°C. At f = 500, G' = 5.2 and G'' = 3.16. At f = 1,000, G' = 6.28 and G'' = 2.72. (50 Fe)

POLYVINYL ACETATE (Plasticized by tri-m-cresyl). T = 25°C. f = 40 to 1,000. G' = 1,300 to 7,800 and G'' = 1,300 to 13,800. (55 Wi, Figure 328)

POLYVINYL BUTYRATE. T = 25°C. f = 10 to 1,000. G' = 435 to 7,530 and G'' = 456 to 4,550. (55 R, Figure 329)

POLYVINYL BUTYRAL. T = -40 to 100°C. f = 10 to 1,000. η = 0.14 to 2.0. At maximum η, f = 2 and G' = 29,000. (61 U*)

POLYVINYLCARBAZOL. f = 10. T = 200 to 220°C. G' = 1,200 at η maximum > 1.6. (61 U*)

POLYVINYL CHLORIDE. For all f and T. Maximum η = 1.8 and G' = 3,330 at f = 20, T = 92°C. (61 U*)

POLYVINYL CHLORIDE. T = 20°C. f = 10 to 400. G' = 35 to 100 and G'' = 40 to 300. G' = 100 peak at f = 100. (55 Wi, Figure 331)

POLYVINYL CHLORIDE. T = 30°C. f = 0.01 to 10. E' $\approx 4.0 \times 10^5$ and E'' = 1.2×10^3 to 12.9×10^3. (56 Maxw, Figure 336)

POLYVINYL CHLORIDE (With Di-phthalate 25% DOP). T = 80°C. f = 40 to 350. E' = 2,150 and E'' = 1,775. (54 Dil)

POLYVINYL CHLORIDE (With Di-phthalate 25% DOP). T = 20°C. f = 40 to 350. E' = 77,500 and E'' = 7,300. (54 Dil)

POLYVINYL CHLORIDE (With Di-phthalate 25% DOP). T = 50°C. f = 40 to 350. E' = 1.76×10^4 and E'' = 1.53×10^4. (54 Dil)

POLYVINYL CHLORIDE. T = 50°C. At f = 400, G' = 9.1×10^4 and G'' = 4.27×10^4. At f = 1,000, G' = 11.0×10^4 and G'' = 3.48×10^4. (54 Wi)

POLYVINYL CHLORIDE (17% concentration). T = 25°C. At f = 400, G' = 1.01 and G'' = 0.38. At f = 1,000, G' = 1.21 and G'' = 0.55. (50 Fe)

POLYVINYL CHLORIDE (24.1% concentration). T = 25°C. f = 400. G' = 1.05 and G'' = 0.96. (50 Fe)

POLYVINYL CHLORIDE DIMETHYL-THIEN-THRENE. $T = 25^{\circ}C$. f = 40 to 1,000. G' = 2.8 to 8.7 and G" = 1.4 to 13.1. (53 Fit, Figure 333)

POLYVINYL CHLORIDE (Plasticized by tri-m-cresyl). $T = -1^{\circ}C$. f = 40 to 1,000. G' = 1,000 to 8,500 and G" = 900 to 9,100. (55 Wi, Figure 330)

POLYVINYL CHLORIDE. Shear. At $T = 35^{\circ}F$: G' = 3,000 at f = 20, $G' = 10^5$ to 2×10^5 at f = 1,000, $G' = 10^5$ at f = 5,000, $G' = 10^5$ at $f = 10^5$. At $T = 65^{\circ}F$: G' = 3,000 and G" = 1,000 at f = 20, $G' = 6 \times 10^4$ and $G'' = 6 \times 10^3$ at f = 100, $G' = 10^5$ and $G'' = 10^4$ at f = 1,000. At $T = 130^{\circ}F$: G' = 2,000 and G" = 700 at f = 20, G' = 4,000 and G" = 2,000 at f = 100, $G' = 10^4$ and $G'' = 6 \times 10^3$ at f = 1,000. (65 Bl)

POLYVINYLFLUORIDE. f = 1.7. $T = 20$ to $60^{\circ}C$. G' = 5,800 at η maximum = 0.36. (61 U*)

POLYVINYL-N-BUTYL ETHER. f = 0.8. $T = -40$ to $-20^{\circ}C$. G' = 1,500 at η maximum > 1.6. (61 U*)

POLYVINYL-ISOBUTYL ETHER. f = 1.2. $T = -15$ to $10^{\circ}C$. G' = 1,500 at η maximum > 1.6. (61 U*)

POLYVINYL-TERT-BUTYL ETHER. f = 1.7. $T = 70$ to $90^{\circ}C$. G' = 1,500 at η maximum > 1.6. (61 U*)

RAMIE (3-ply cord). $T = 21^{\circ}C$. f = 180. $E' = 4.66 \times 10^6$ and $E'' = 1.27 \times 10^5$. (49 Ly)

RAYON (Viscous yarn). T = 25°C. At f = 10, E' = 1.46×10^6 and E'' = 5.50×10^4. At f = 40, E' = 1.46×10^6 and E'' = 3.66×10^4. (51 Du)

RAYON (Viscous yarn). T = 21°C. f = 180. E' = 2.22×10^6 and E' = 6.6×10^4. (49 Ly)

RUBBER (Buna N, B-1, vulcanized). For all f and T. Maximum η = 1.5 and G' = 1,450 at f = 4,000, T = 20°C. (61 U*)

RUBBER (Buna N, B-5, carbon filled, vulcanized). T = 20°C. f = 10 to 10,000. η = 0.4 to 1.6. At maximum η, G' = 1,500 to 4,400. (50 No, 61 U*)

RUBBER (Buna N, B-5, carbon filled, vulcanized). f = 50. T = 0 to 10°C. G' = 2.9×10^4 at η maximum = 0.15. (50 No, 61 U*)

RUBBER (Butyl, unvulcanized). f = 1. T = -20 to +20°C. G' = 1.5×10^4 at η maximum = 1.2. (61 U*)

RUBBER (Butyl). At T = 1°C: E' = 2,480 and E'' = 4,950 at f = 1,000, E' = 6,570 and E'' = 12,500 at f = 3,000. At T = 22°C: E' = 1,020 and E'' = 917 at f = 1,000, E' = 1,390 and E'' = 2,570 at f = 3,000. At T = 41°C: E' = 583 and E'' = 320 at f = 1,000, E' = 875 and E'' = 1,100 at f = 3,000. (49 Wit)

RUBBER (Butyl, Enjay 9-262-1). T = 21°C. f = 100 to 10,000. η = 0.55 to 2.56. At maximum η, f = 3,000 and G' = 2,900. (61 U*)

RUBBER (Butyl, Enjay 9-262-4). T = 21°C. f = 100 to 10,000. η = 0.4 to 4.0. At maximum η, f = 3,100 and G' = 1,500. (61 U*)

RUBBER (Butyl, Enjay 9-262-3). T = 24°C. f = 100 to 10,000. η = 0.45 to 2.2. At maximum η, f = 3,000 and G' = 2,900. (61 U*)

RUBBER (Butyl). T = 20°C. At f = 1, E' = 109 and E" = 163. At f = 10, E' = 319 and E" = 575. (50 No)

RUBBER (Butyl). T = 25°C. At f = 40, G' = 50 and G" = 27. At f = 100, G' = 58 and G" = 42. At f = 400, G' = 59 and G" = 98. (50 M)

RUBBER (Butyl). T = 20°C. At f = 400, G' = 128 and G" = 128. At f = 1,000, G' = 218 and G" = 201. At f = 4,000, G' = 432 and G" = 475. (51 Ho)

RUBBER (Butyl). T = 40°C. At f = 1,000, G' = 73 and G" = 36. At f = 4,000, G' = 113 and G" = 84. (52 Fer)

RUBBER (Butyl). T = 20°C. f = 10 to 10,000. E' = 580 to 1,595 and E" = 88 to 797. (49 I, Figure 374)

RUBBER (Butyl, M.W. = 1.2×10^6). T = 25°C. At f = 105, G' = 3,620 and G" = 1,820. At f = 106, G' = 14,500 and G" = 8,910. At f = 107, G' = 50,700 and G" = 46,500. (52 Mc)

RUBBER (Butyl, M.W. = 1.2×10^6). T = 70°C. At f = 1,000, G' =

57 and G" = 11. At f = 4,000, G' = 40.8 and G" = 22.9. (52 Fer)

RUBBER (Butyl, M.W. = 1.2×10^6). T = 20°C. At f = 10, G' = 3.1 and G" = 0.8. At f = 100, G' = 16.8 and G" = 6.6. (53 Fe)

RUBBER (Butyl, M.W. = 1.2×10^6). T = 0°C. At f = 100, G' = 19.0 and G" = 27. At f = 400, G' = 55.5 and G" = 73. At f = 1,000, G' = 94.8 and G" = 128. (53 Fi)

RUBBER (Butyl, M.W. = 1.2×10^6). T = 50°C. At f = 100, G' = 55 and G" = 12. At f = 400, G' = 58 and G" = 36. At f = 1,000, G' = 80 and G" = 73. (53 Fi)

RUBBER (Butyl, M.W. = 1.2×10^6). T = 25°C. At f = 160, G' = 219 and G" = 321. At f = 1.6×10^4, G' = 7,300 and G" = 8,750. At f = 1.6×10^6, G' = 87,500 and G" = 73,000. (53 Le)

RUBBER (Butyl, M.W. = 1.2×10^6). T = 30°C. At f = 65, E' = 20 and E" = 39. At f = 79, E' = 29 and E" = 22. At f = 135, E' = 85 and E" = 118. (55 Th)

RUBBER (Butyl, M.W. = 1.2×10^6). T = -30°C. At f = 1, G' = 623 and G" = 995. At f = 10, G' = 2,465 and G" = 3,280. (57 Fl)

RUBBER (Butyl, M.W. = 1.2×10^6). T = 25°C. f = 2×10^{-5} to 16. G' = 7.3 to 75.8 and G" = 7.3 to 48.2. Both G' and G" constant at maximum value for $f > 0.1$. (53 Le, Figure 369)

RUBBER (Butyl, M.W. = 1.2×10^6). T = -30 to 75°C. f = 0.001 to

100. G' = 19 to 95 and G'' = 6.1 to 32.2. G'' < 6.5 for f < 10. (53 Ph, Figure 370)

RUBBER (Butyl, M.W. = 1.2×10^6). T = 25°C. f = 10 to 400. G' = 72.5 to 174 and G'' = 32 to 455. (53 Fi, Figure 373)

RUBBER (Filled Butyl). T = 65°C. f = 100 to 5,250. G' = 555 to 1,210 and G'' = 104 to 642. G' = 400 minimum at f = 500. (51 Ho, Figure 372)

RUBBER (Filled Butyl). T = 26°C. f = 100 to 5,250. G' = 760 to 2,150 and G'' = 310 to 1,440. (51 Ho, Figure 376)

RUBBER (Filled Butyl, 40 parts by weight of MPC carbon black). f = 1 to 10,000. At T = 5°C, G' = 145 to 5,800 and G'' = 32 to 9,860. At T = 35°C, G' = 145 to 1,090 and G'' = 580 to 1,410. (64 Sno*)

RUBBER (Butyl, M-169A-Butyl Gum). T = 65°C. f = 100 to 5,250. G' = 55 to 120 and G'' = 12 to 106. (51 Ho, Figure 371)

RUBBER (GR-S). T = 50°C. At f = 100, G' = 522 and G'' = 796. At f = 400, G' = 522 and G'' = 811. (44 D)

RUBBER (GR-S). T = 5°C. At f = 1,000, E' = 985 and E'' = 532. At f = 4,000, E' = 1,630 and E'' = 1,310. (49 Wit)

RUBBER (GR-S). T = 54°C. At f = 1,000, E' = 627 and E'' = 643. At f = 4,000, E' = 700 and E'' = 1,095. (49 Wit)

RUBBER (GR-S, type S-50, carbon filled, vulcanized). T = 20°C. At f = 4,000, E' = 1,390 and E'' = 278. At f = 10,000, E' =

1,610 and E" = 1,370. (50 No, 61 U*)

RUBBER (GR-S). T = 30 to 75°C. At f = 0.001, G' = 212 and G" = 35. At f = 0.01, G' = 262 and G" = 42. At f = 0.1, G' = 283 and G" = 49. At f = 1.0, G' = 427 and G" = 71. (53 Ph)

RUBBER (GR-S). T = 30 to 75°C. At f = 10, G' = 637 and G" = 113. At f = 40, G' = 708 and G" = 142. At f = 100, G' = 850 and G" = 170. At f = 400, G' = 990 and G" = 212. (53 Ph)

RUBBER (GR-S). T = 3°C. At f = 0.1, G' = 12 and G" = 19. At f = 1.0, G' = 133 and G" = 58. At f = 10.0, G' = 217 and G" = 79. (57 Fl)

RUBBER (GR-S). T = 20°C. f = 10 to 10,000. E' = 218 to 854 and E" = 54 to 1,130. E' $\sim$ 800 for f $>$ 600. (49 I, 61 U*, Figure 375)

RUBBER (GR-S). f < 10. T = -60 to -40°C. G' = 7,200 at η maximum $\approx$ 0.5. (61 U*)

RUBBER (GR-S, Krylene). T = 20°C. f = 1 to 10,000. η = 0.11 to 0.30. At maximum η, G' = 100. (61 U*)

RUBBER (GR-S, 3% Styrene). T = 51°C. f = 365 to 1,368. E' = 351 to 453 and E" = 98 to 178. (56 Mo, 61 U*, Figure 377)

RUBBER (GR-S, 13% Styrene). T = 51°C. f = 473 to 1,735. E' = 597 to 816 and E" = 143 to 269. (56 Mo, Figure 378)

RUBBER (GR-S, 23% Styrene). T = 50°C. f = 472 to 1,736. E' = 583 to 717 and E" = 175 to 337. (56 Mo, Figure 379)

RUBBER (GR-S, 23.5% Styrene). T = 5°C. f = 422 to 1,530. E' = 481 to 598 and E" = 140 to 311. (56 Mo, 61 U*, Figure 380)

RUBBER (Hevea, filled). T = 20°C. f = 1 to 10,000. η = 0.11 to 0.25. At maximum η, G' = 870. (61 U*)

RUBBER (Hevea, vulcanized). T = 20°C. f = 1 to 10,000. η = 0.03 to 0.20. At maximum η, G' = 870. (61 U*)

RUBBER (Natural, gum stock, Type N-1). T = 20°C. f = 1 to 1,000. η = 0.04 to 0.30. At maximum η, G' = 150. (61 U*)

RUBBER (Natural, gum stock). T = 50°C. At f = 100, G' = 47 and G" = 2.1. At f = 400, G' = 50 to G" = 2.5. (44 D)

RUBBER (Natural, gum stock). T = 20°C. At f = 0.01, E' = 24 and E" = 1.9. At f = 0.1, E' = 29 and E" = 4.3. At f = 1.0, E' = 43 and E" = 18.7. (50 No)

RUBBER (Natural, gum stock). T = 79°C. At f = 100, G' = 91 and G" = 14.6. At f = 400, G' = 100 and G" = 19.8. At f = 1,000, G' = 100 and G" = 19.8. (57 Fit)

RUBBER (Natural, gum stock). T = 60°C. At f = 100, G' = 98 and G" = 13.3. At f = 400, G' = 107 and G" = 15.2. At f = 1,000, G' = 109 and G" = 21.3. (57 Fit)

RUBBER (Natural, gum stock). T = 25°C. At f = 100, G' = 100 and G" = 13.3. At f = 400, G' = 106 and G" = 16.1. At f = 1,000, G' = 114 and G" = 30.1. (57 Fit)

RUBBER (Natural, gum stock). $T = 65^{\circ}C$. $f = 100$ to 5,280. $G' = 51$ to 74 and $G'' = 6.8$ to 11.5. $G'' \approx 6.8$ for $f < 1{,}000$. (51 Ho, Figure 366)

RUBBER (Natural, gum stock). $T = 26^{\circ}C$. $f = 100$ to 5,280. $G' = 43$ to 80 and $G'' = 3.2$ to 20.7. $G' \approx 50$ for $f < 100$. (51 Ho, Figure 367)

RUBBER (Natural, high M.W.). $f < 10$. $T = -70$ to $-50^{\circ}C$. $G' = 1{,}500$ at η maximum ≈ 0.5. (61 U*)

RUBBER (Natural, tire tread stock). $T = 25 \pm 50^{\circ}C$. $f = 1$ to 500. $\eta = 0.16$ to 0.20. At maximum η, $G' = 150$. (61 U*)

RUBBER (Natural). $f = 1$ to 10,000. At $T = 5^{\circ}C$, $G' = 67$ to 116 and $G'' = 1.5$ to 52.2. At $T = 35^{\circ}C$, $G' = 67$ to 72 and $G'' = 1.5$ to 5.8. (64 Sno*)

RUBBER (Filled natural, 50 parts by weight of HAF carbon black). $f = 1$ to 10,000. At $T = 5^{\circ}C$, $G' = 1{,}020$ to 1,520 and $G'' = 112$ to 608. At $T = 35^{\circ}C$, $G' = 870$ to 1,380 and $G'' = 96$ to 248. (64 Sno*)

RUBBER (Filled). For all f and T. Maximum $\eta = 0.5$ and $G' = 3.33 \times 10^4$ at $f = 140$, $T = -23^{\circ}C$. (61 U*)

RUBBER (Hard). For all f and T. Maximum $\eta = 1.0$ and $G' = 1.01 \times 10^4$ at $f = 40$, $T = 60^{\circ}C$. (61 U*)

RUBBER (Neoprene). $T = 20^{\circ}C$. $f = 3{,}000$. $E' = 97{,}000$ and $E'' = 450$. (49 Hi)

RUBBER (Neoprene, GN-50, vulcanized). T = 20°C. f = 1,000 to 10,000. η = 0.7 to 1.1. At maximum η, G' = 290. (50 No, 61 U*)

RUBBER (Neoprene). T = 28°C. At f = 40, G' = 0.0022 and G'' = 0.28. At f = 100, G' = 0.0023 and G'' = 0.21. (42 St)

RUBBER (Neoprene). T = 20°C. 10% static deflection. At f = 4,000, E' = 12,400 and E'' = 34,800. At f = 10,000, E' = 15,900 and E'' = 71,500. (50 No)

RUBBER (Neoprene). T = 20°C. 35% static deflection. At f = 4,000, E' = 10,700 and E'' = 38,500. At f = 10,000, E' = 11,700 and E'' = 70,000. (50 No)

RUBBER (Neoprene). T = 20°C. 5% static deflection. At f = 4,000, E' = 700 and E'' = 196. At f = 10,000, E' = 990 and E'' = 845. (50 No)

RUBBER (Neoprene). T = 30°C. f = 461 to 1,775. E' = 612 to 671 and E'' = 409 to 790. (56 Mo, 61 U*, Figure 382)

RUBBER (Neoprene). T = 25°C. f = 1 to 10,000. G' = 116 to 160 and G'' = 12.8 to 48.0. (64 Sno*)

RUBBER (Neoprene). Shear properties measured by one to four methods. At T = 35°F: G' = 10^3 to 10^4 and G'' = 2 x 10^3 at f = 50, G' = 10^4 to 10^5 and G'' = 10^4 at f = 1,000. At T = 60°F: G' = 100 to 600 and G'' = 20 to 400 at f = 3, G' = 400 and G'' = 300 to 10^3 at f = 100, G' = 10^3 to 2 x 10^4 and G'' = 10^3 to

10^4 at f = 1,000. At T = 130°F: G' = 60 to 200 and G" = 10 to 40 at f = 30, G' = 200 to 700 and G" = 40 to 70 at f = 100, G' = 300 to 2,000 and G" = 70 to 700 at f = 1,000. (65 B1)

RUBBER (Nitrile). For all f and T. Maximum η = 0.8 and G' = 1.59 x 10^4 at f = 1,800, T = 20°C. (61 U*)

RUBBER (Nitrile). T = 10°C. At f = 2 x 10^6, G' = 5.38 x 10^5 and G" = 1.88 x 10^5. At f = 5 x 10^6, G' = 5.38 x 10^5 and G" = 1.56 x 10^5. At f = 10^7, G' = 5.38 x 10^5 and G" = 1.35 x 10^5. (52 No)

RUBBER (Nitrile). T = 0°C. At f = 2 x 10^6, G' = 5.9 x 10^5 and G" = 1.12 x 10^5. At f = 5 x 10^6, G' = 5.9 x 10^5 and G" = 1.12 x 10^5. At f = 10^7, G' = 5.9 x 10^5 and G" = 0.94 x 10^5. (52 No)

RUBBER (Nitrile). T = -10°C. At f = 2 x 10^6, G' = 6.18 x 10^5 and G" = 7.4 x 10^4. At f = 5 x 10^6, G' = 6.18 x 10^5 and G" = 8.0 x 10^4. At f = 10^7, G' = 6.18 x 10^5 and G" = 6.8 x 10^4. (52 No)

RUBBER (Nitrile). T = 0°C. At f = 1, E' = 870 and E" = 392. At f = 10, E' = 1,335 and E" = 1,600. (54 Hu)

RUBBER (Nitrile). T = 20°C. f = 0.01 to 10. E' = 133 to 1,320 and E" = 5.5 to 224. (50 No, Figure 381)

RUBBER (SBR). f = 1 to 10,000. At T = 5°C, G' = 87 to 157 and

G" = 10.4 to 126. At T = 35°C, G' = 78 to 130 and G" = 7.8 to 24.7. (64 Sno*)

RUBBER (Silicone). T = 20°C. At f = 100, G' = 7.3 and G" = 2.7. At f = 400, G' = 11.6 and G" = 3.9. At f = 1,000, E' = 11.9 and G" = 5.6. (51 Ho)

RUBBER (Silicone). T = 65°C. At f = 100, G' = 10.2 and G" = 2.5. At f = 400, G' = 13.1 and G" = 2.9. (51 Ho)

RUBBER (Silicone, P.S. C-269). T = 25°C. At f = 2, G' = 14.3 and G" = 36. At f = 10, G' = 22.3 and G" = 51. At f = 20, G' = 28.7 and G" = 48. (57 D)

RUBBER (Silicone filled). T = 25°C. f = 100 to 5,250. G' = 292 to 394 and G" = 37 to 86. (51 Ho, Figure 383)

RUBBER (Silicone filled). T = 65°C. f = 100 to 5,250. G' = 165 to 292 and G" = 28 to 48. (51 Ho, Figure 384)

RUBBER (Thiokol). T = 19°C. At f = 0.1, G' = 87 and G" = 20. At f = 1.0, G' = 130 and G" = 52. (52 Fl)

RUBBER (Thiokol). T = 35°C. At f = 1, G' = 82 and G" = 14. At f = 10, G' = 104 and G" = 49. (57 Fl)

RUBBER (Thiokol). T = -30 to 75°C. f = 0.001 to 100. G' = 64 to 121 and G" = 7.8 to 156. (53 Ph, 61 U*, Figure 385)

RUBBER (Thiokol). T = 30°C. f = 359 to 1,312. E' = 423 to 555 and E" = 191 to 294. (56 Mo)

RUBBER (Thiokol RD). For all f and T. Maximum η = 1.9 and G' = 10^4 at f = 7, T = 5°C. (61 U*)

RUBBER (Thiokol RD). At T = 5°C: G' = 390 and G'' = 585 at f = 1, G' = 1,230 and G'' = 2,214 at f = 10. At T = 35°C: G' = 72 and G'' = 9.36 at f = 1, G' = 1.16 and G'' = 51.0 at f = 100, G' = 4.35 and G'' = 740 at f = 10,000. (64 Sno*)

RUBBER (Thiokol H-5). T = 25 $\pm$ 50°C. f = 1 to 1,000. η = 0.17 to 5.0. At maximum η, G' = 1,500. (61 U*)

RUBBER (Thiokol ST). T = 20°C. f = 100 to 1,300. η = 0.40 to 0.53. At maximum η, G' = 160. (61 U*)

RUBBER (Urethane, 82% Pb powder filler). T = 25°C. f = 100 to 3,000. η = 0.4 to 1.4. At maximum η, G' = 2,500. (61 U*)

RUBBER (Urethane, Disogrin IDSA-7560). T = 25°C. f = 100 to 4,250. η = 0.1 to 0.5. At maximum η, G' = 1,500. (61 U*)

RUBBER (Urethane, Disogrin IDSA-9250). T = 25°C. f = 100 to 10,000. η = 0.1 to 2.6. At maximum η, f = 3,000 and G' = 2,900. (61 U*)

RUBBER (Urethane, Shore 80-A). For all f and T. Maximum η = 0.8 and G' = 2,320 at f = 30, T = -8°C. (61 U*)

RUBBER (Urethane, Shore 94-A). For all f and T. Maximum η = 0.4 and G' = 4.35 x 10^4 at f = 140, T = -23°C. (61 U*)

SILK (Raw). T = 25°C. f = 10. G' = 1.31 x 10^6 and G'' = 1.38 x 10^4. (51 Du)

SILK (Degummed). $T = 25^{\circ}C$. At $f = 10$, $G' = 2.34 \times 10^{6}$ and $G'' = 4.57 \times 10^{4}$. At $f = 40$, $G' = 2.34 \times 10^{6}$ and $G'' = 9.20 \times 10^{4}$. (51 Du)

SLP-83311 (Cured). $T = 25^{\circ}C$. $f = 2$ to 10. $G' = 420$ and $G'' = 306$. (57 D)

SLP-83311 (Uncured). $T = 25^{\circ}C$. At $f = 1$, $G' = 62$ and $G'' = 92.5$. At $f = 10$, $G' = 108$ and $G'' = 230$. (57 D)

VELON (0.012 monofoil). $T = 21^{\circ}C$. $f = 180$. $E' = 9.35 \times 10^{5}$ and $E'' = 1.56 \times 10^{5}$. (49 Ly)

VINYON N (300 den yarn). $T = 21^{\circ}C$. $f = 180$. $E' = 1.55 \times 10^{6}$ and $E'' = 6.25 \times 10^{4}$. (49 Ly)

VINYPLASTA (A Russian plastic). Bending. At $T = 20^{\circ}C$, $\eta_s = 1.5 \times 10^{-2}$. At $T = -70^{\circ}C$, $\eta_s = 4 \times 10^{-2}$. (62 Pisa, Figure 339)

WOOD (Birch, Sp.Gr. = 0.74, along grain). Axial stress. $\sigma_a = 0.5$ to 6 ksi. $D = 3 \times 10^{-3}$ to 1. (54 Y, Figure 386)

WOOD (Beech). Torsion. $\eta_s = 1.6 \times 10^{-2}$. (41 Ki*)

WOOD (Maple). Strains of about 5×10^{-3}. Rotating bending. $\eta_s = 6.7 \times 10^{-3}$. (41 Ki*)

WOOD. Bending. $f = 1$ to 10. $\eta_s = 8.6 \times 10^{-3}$. (41 Ki*)

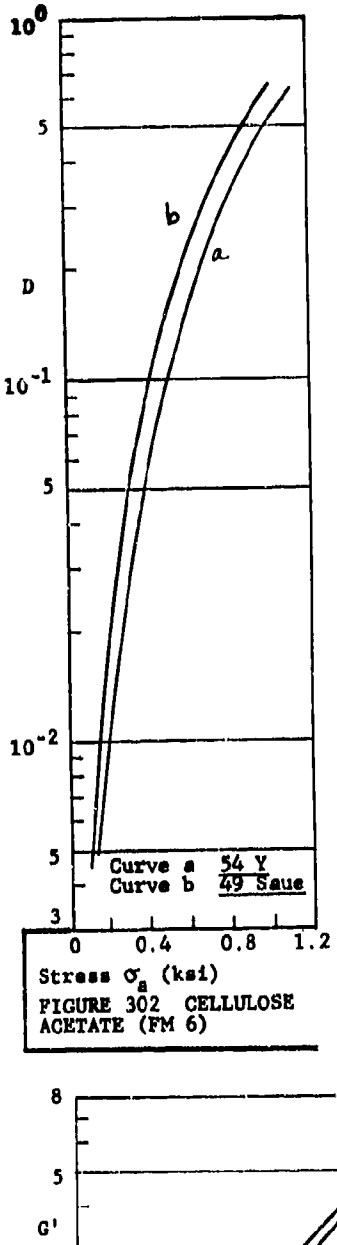

FIGURE 302 CELLULOSE ACETATE (FM 6)

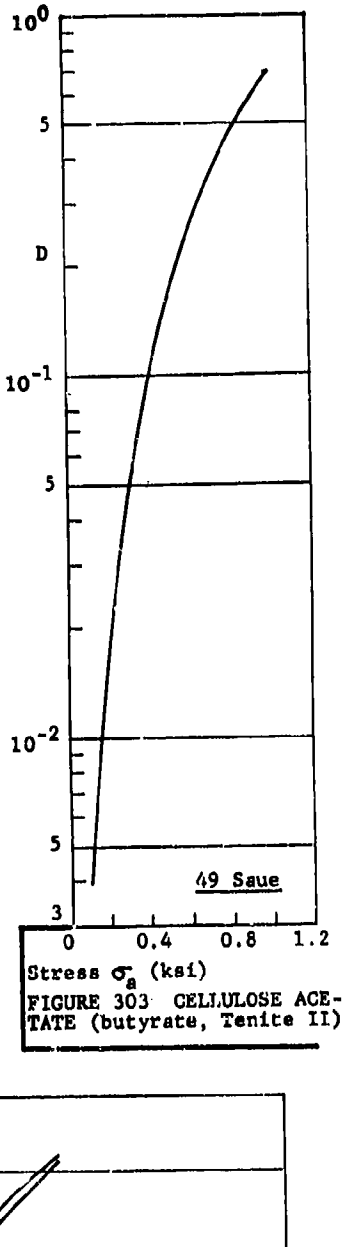

FIGURE 303 CELLULOSE ACETATE (butyrate, Tenite II)

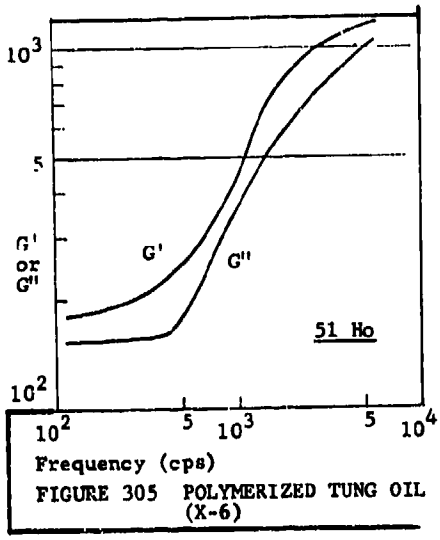

FIGURE 305 POLYMERIZED TUNG OIL (X-6)

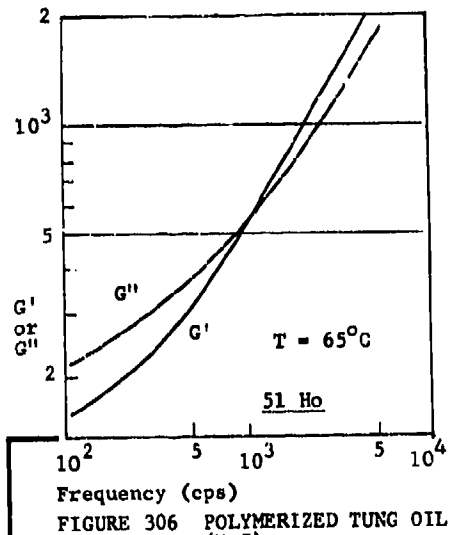

FIGURE 306 POLYMERIZED TUNG OIL (X-7)

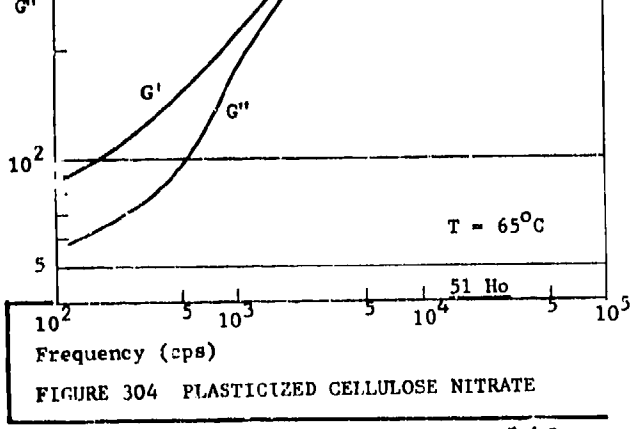

FIGURE 304 PLASTICIZED CELLULOSE NITRATE

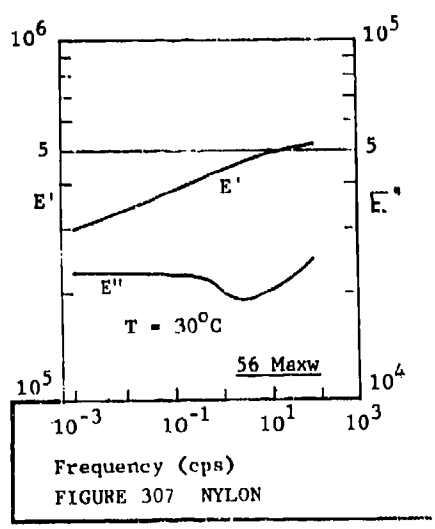

FIGURE 307 NYLON

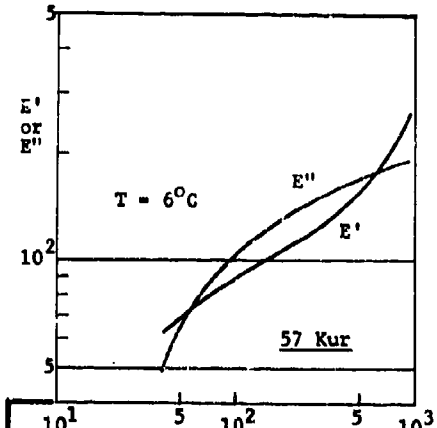

FIGURE 308 POLYHEXANE

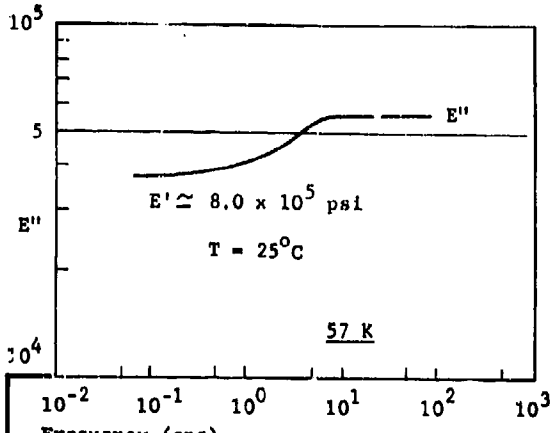

FIGURE 311 POLYMETHYL METHACRYLATE

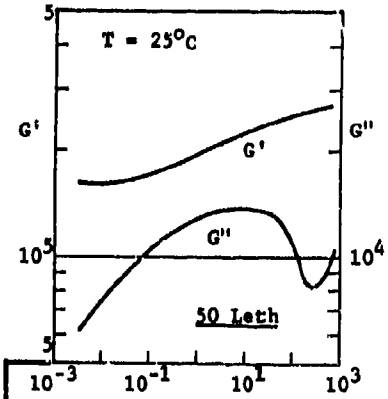

FIGURE 309 PERSPEX

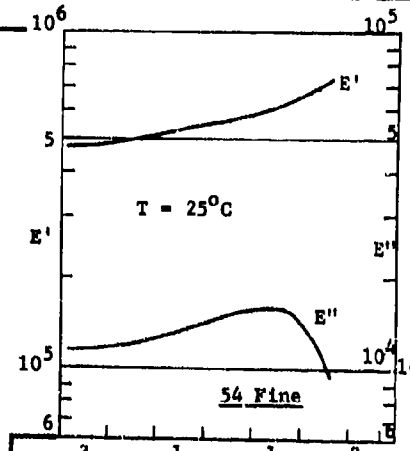

FIGURE 312 POLYMETHYL METHACRYLATE

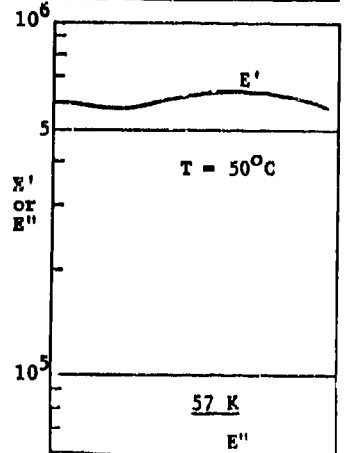

FIGURE 310 POLYMETHYL METHACRYLATE

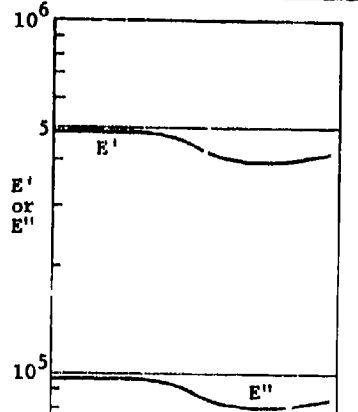

FIGURE 313 POLYMETHYL METHACRYLATE

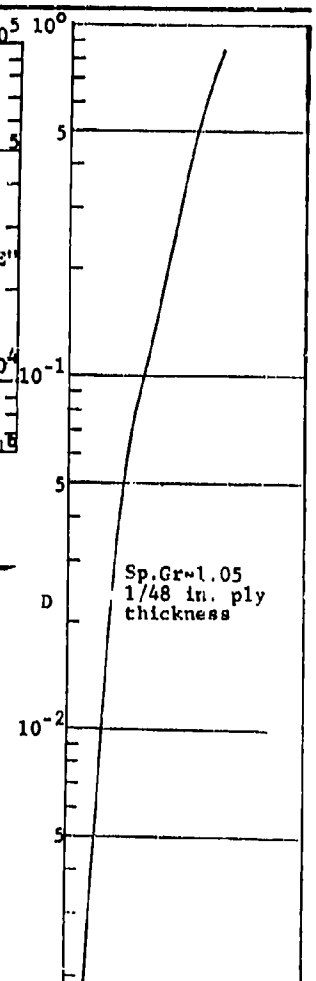

FIGURE 314 PLYWOOD (birch)

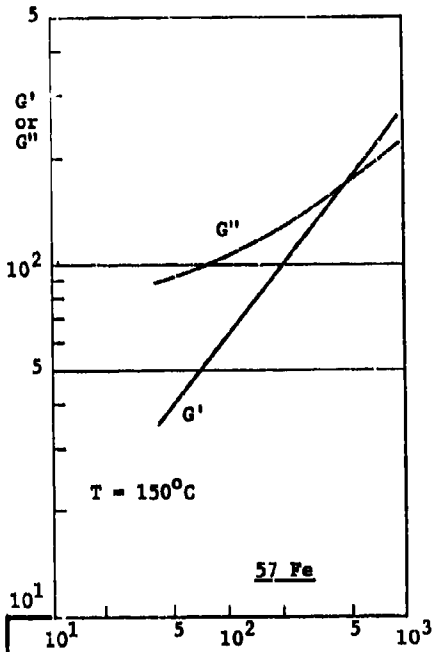

FIGURE 315 POLYETHYL METHACRYLATE

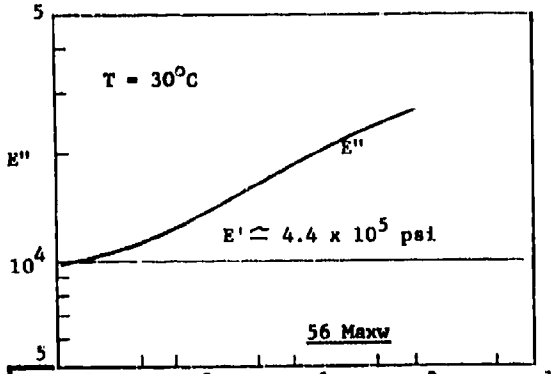

FIGURE 317 POLYMETHYL METHACRYLATE

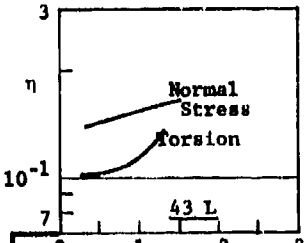

FIGURE 318 METHYL METHACRYLATE (lucite)

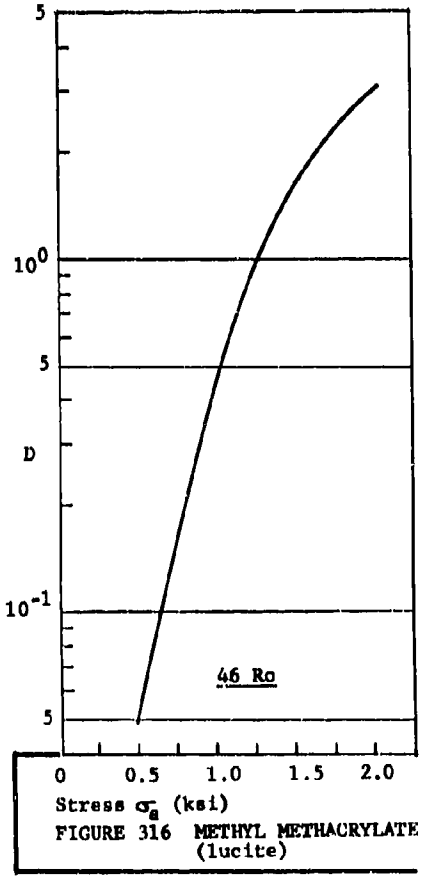

FIGURE 316 METHYL METHACRYLATE (lucite)

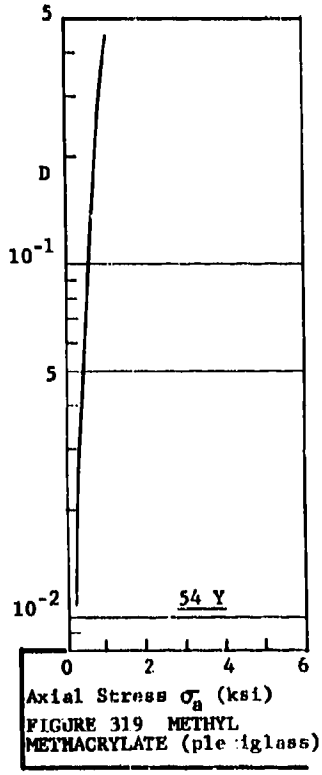

FIGURE 319 METHYL METHACRYLATE (plexiglass)

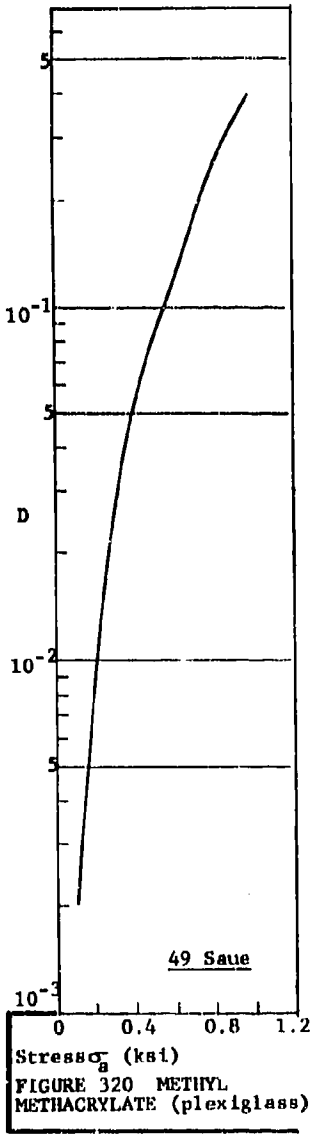

FIGURE 320 METHYL METHACRYLATE (plexiglass)

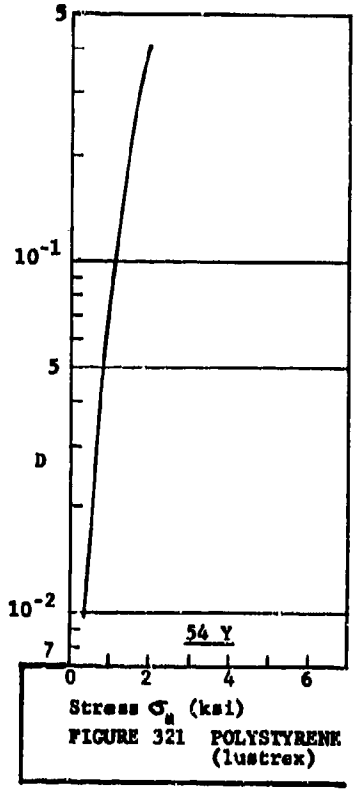

FIGURE 321 POLYSTYRENE (lustrex)

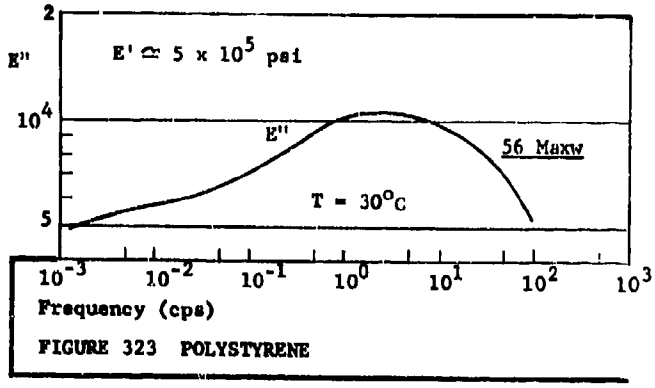

FIGURE 323 POLYSTYRENE

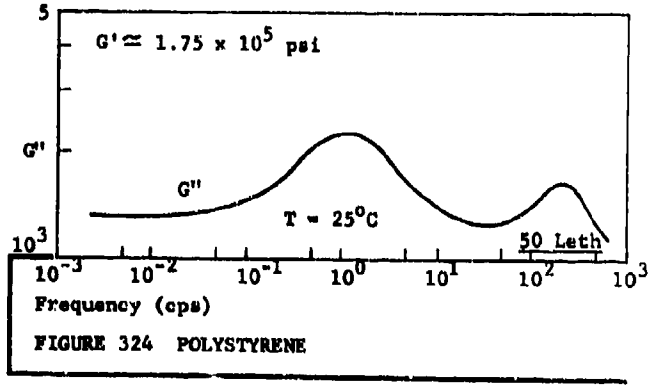

FIGURE 324 POLYSTYRENE

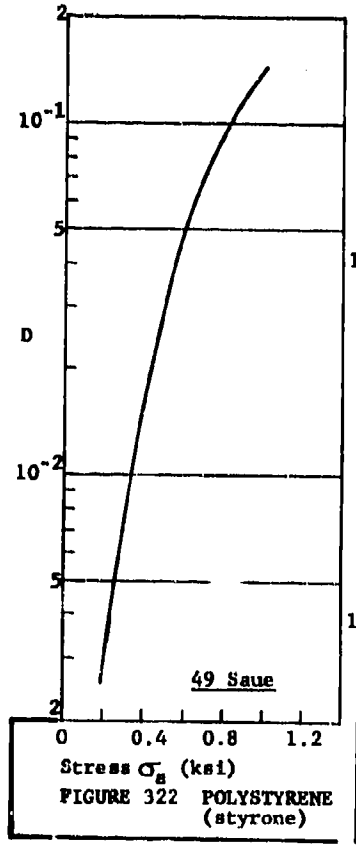

FIGURE 322 POLYSTYRENE (styrone)

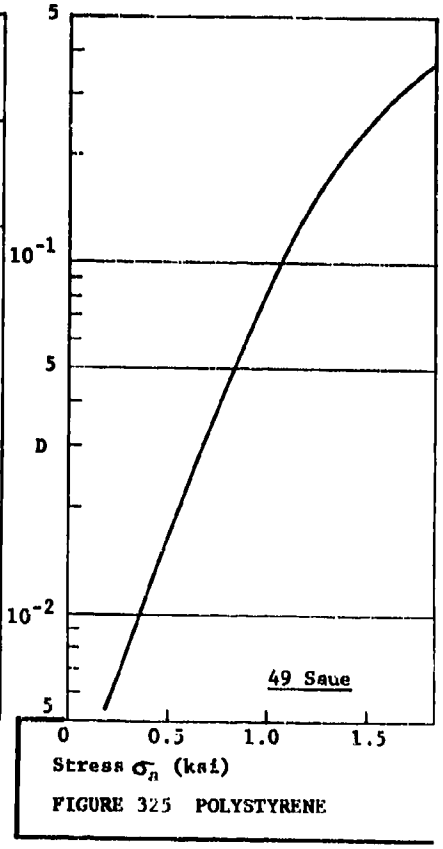

FIGURE 325 POLYSTYRENE

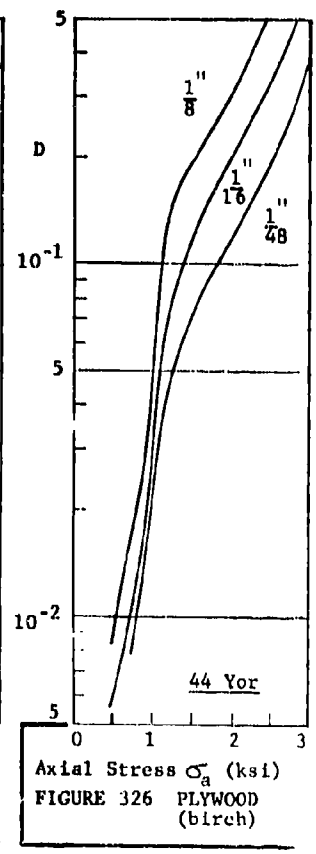

FIGURE 326 PLYWOOD (birch)

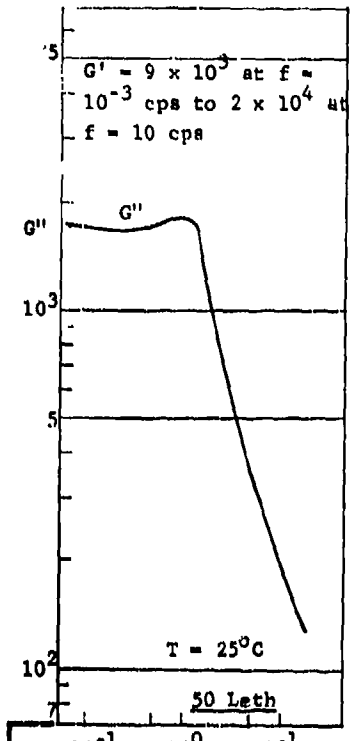

FIGURE 327 POLYTHENE

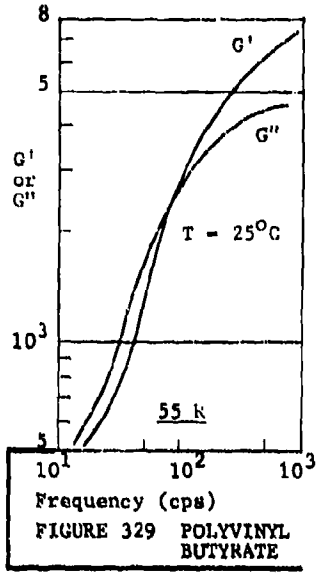

FIGURE 329 POLYVINYL BUTYRATE

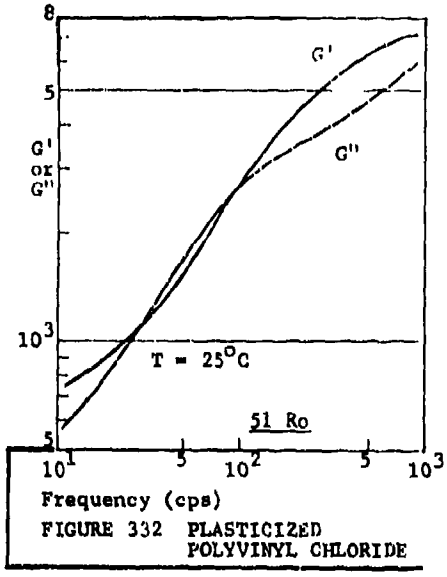

FIGURE 332 PLASTICIZED POLYVINYL CHLORIDE

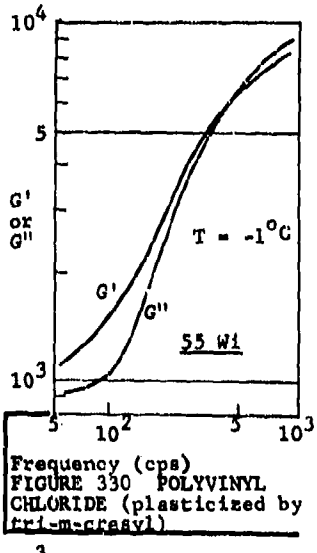

FIGURE 330 POLYVINYL CHLORIDE (plasticized by tri-m-cresyl)

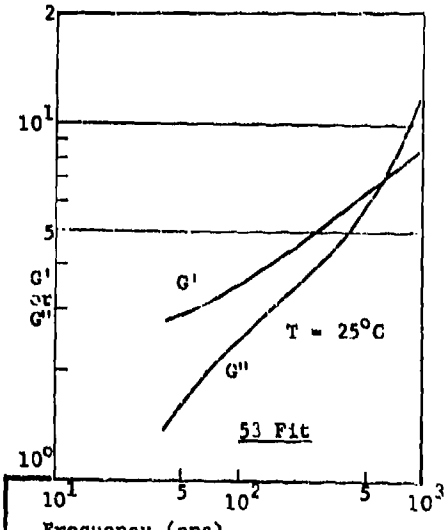

FIGURE 333 POLYVINYL CHLORIDE DIMETHYL-THIEN-THRENE

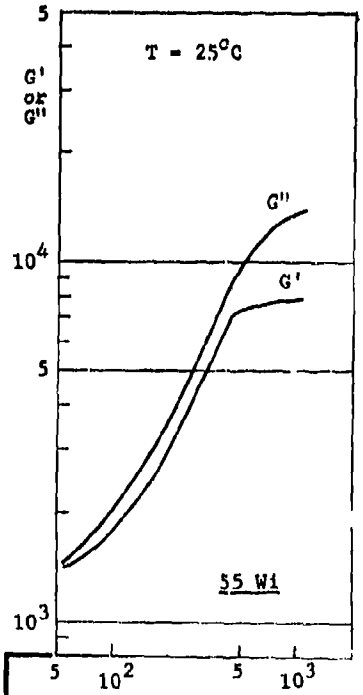

FIGURE 328 POLYVINYL ACETATE (plasticized by tri-m-cresyl)

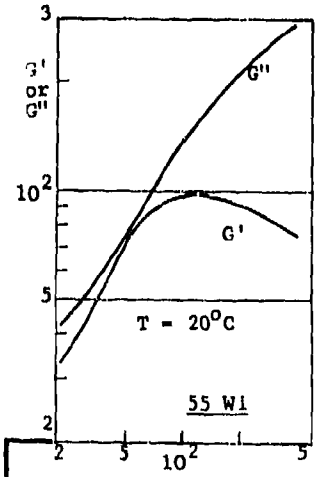

FIGURE 331 POLYVINYL CHLORIDE

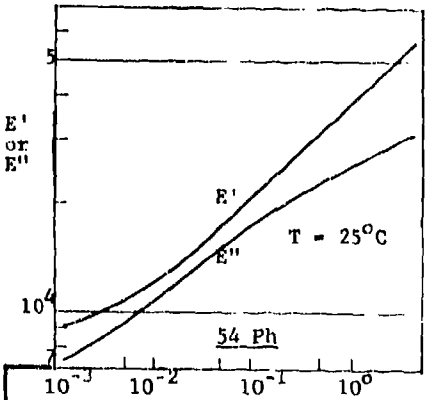

FIGURE 334 PLASTICIZED POLYVINYL CHLORIDE (VU-1913)

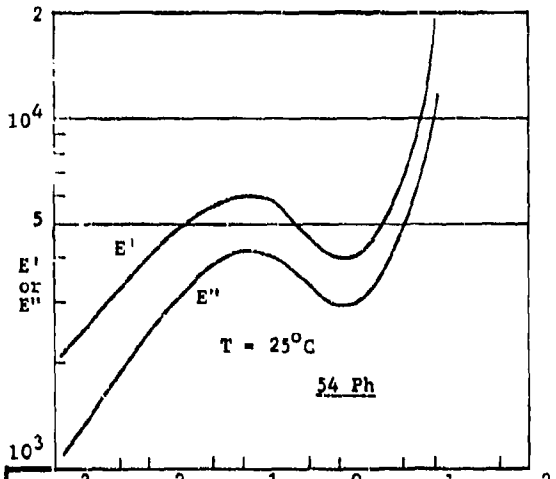

FIGURE 335 PLASTICIZED POLYVINYL CHLORIDE (VU-1920)

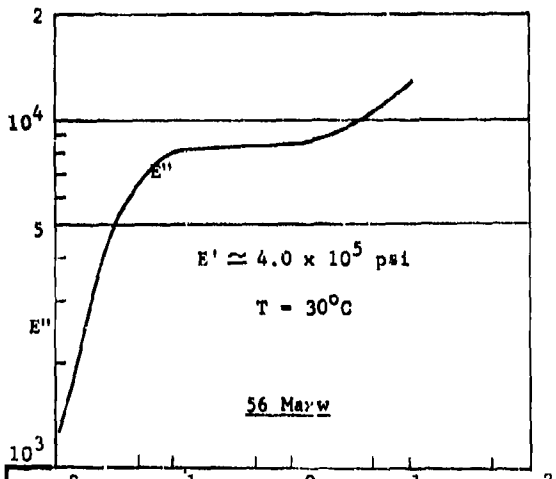

FIGURE 336 POLYVINYL CHLORIDE

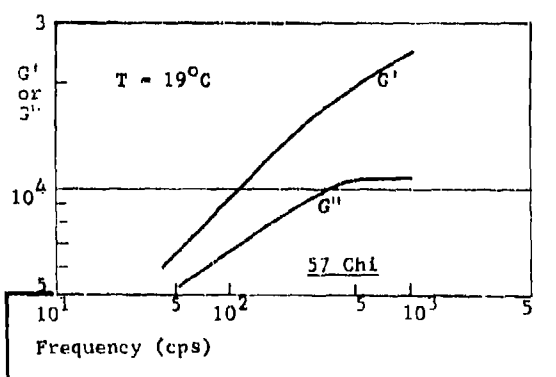

FIGURE 337 POLY N HEXYL METHACRYLATE

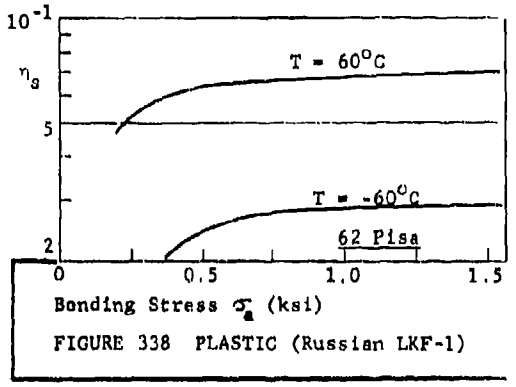

FIGURE 338 PLASTIC (Russian LKF-1)

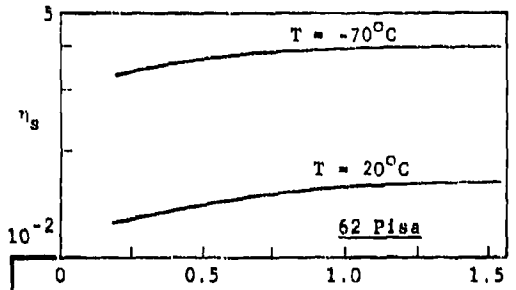

FIGURE 339 VINYPLASTA (Russian plastic)

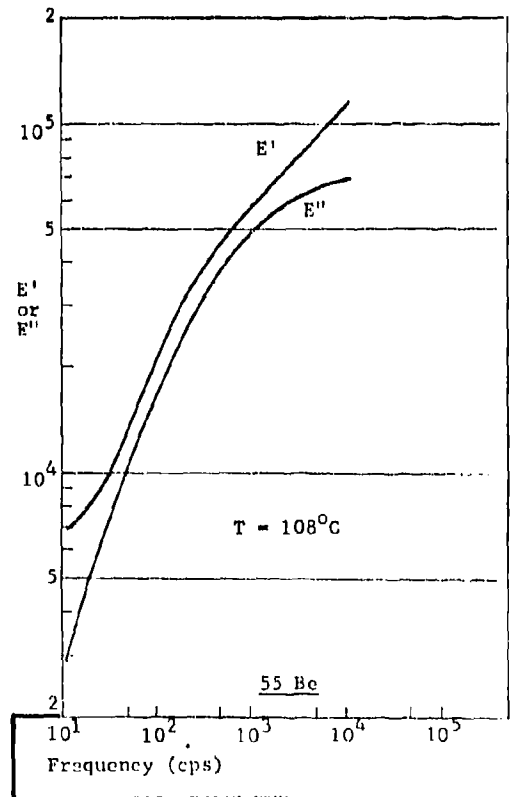

FIGURE 340 POLYESTER

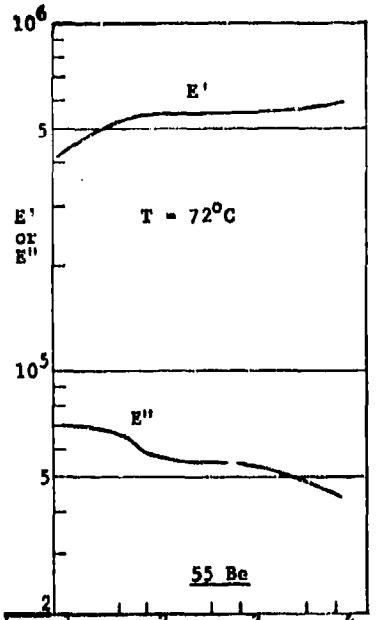

FIGURE 341 POLYESTER

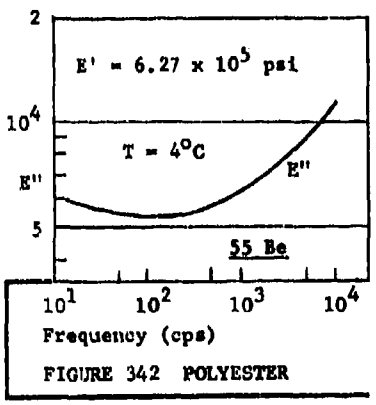

FIGURE 342 POLYESTER

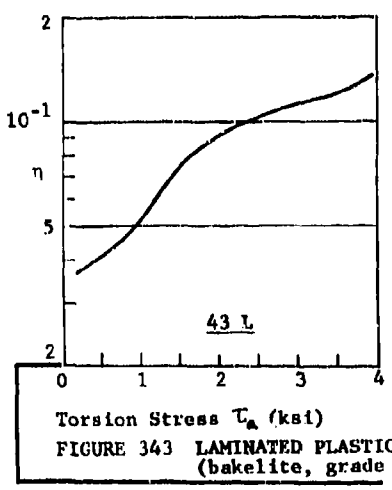

FIGURE 343 LAMINATED PLASTIC (bakelite, grade X)

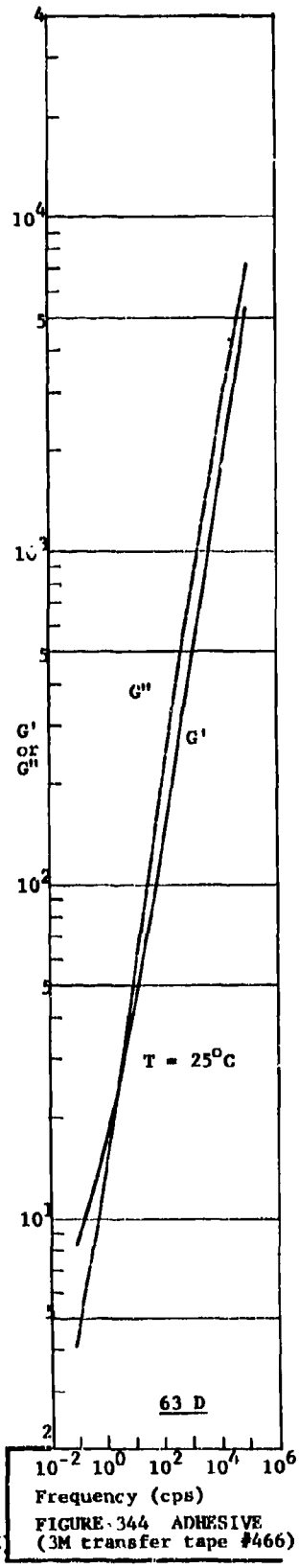

FIGURE 344 ADHESIVE (3M transfer tape #466)

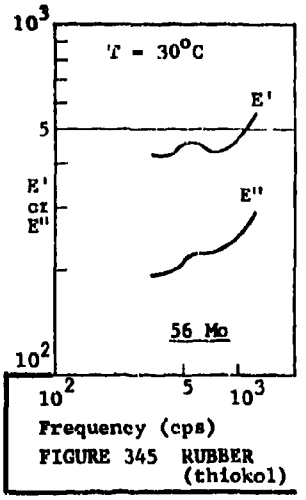

FIGURE 345 RUBBER (thiokol)

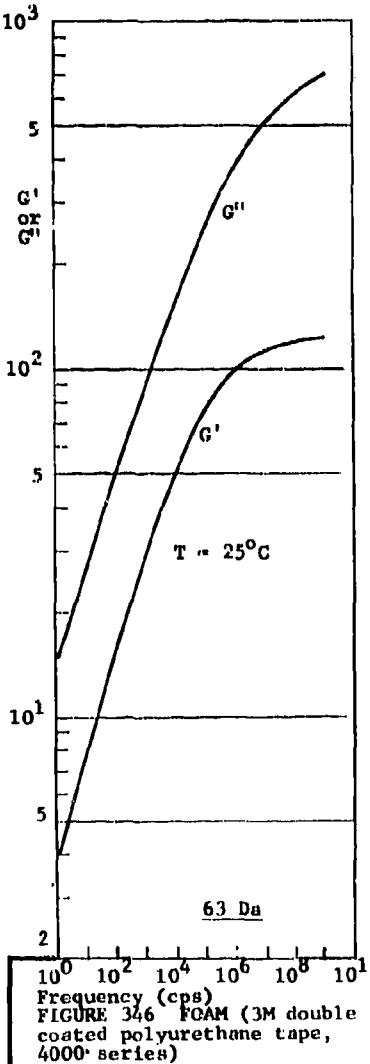

FIGURE 346 FOAM (3M double coated polyurethane tape, 4000 series)

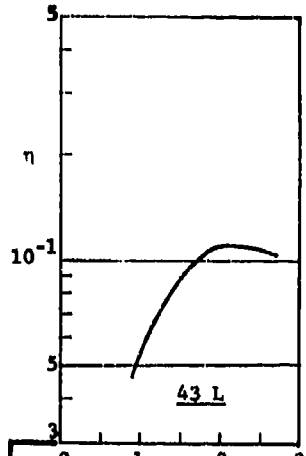

Stress σ_a (ksi)

FIGURE 347 LAMINATED PLASTIC (bakelite, grade X)

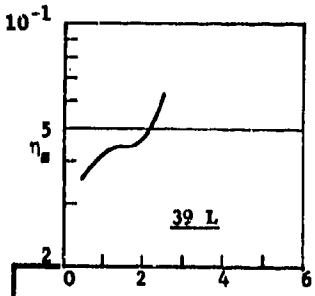

Torsion Stress τ_a (ksi)

FIGURE 348 LAMINATED PLASTIC (bakelite, reinforced)

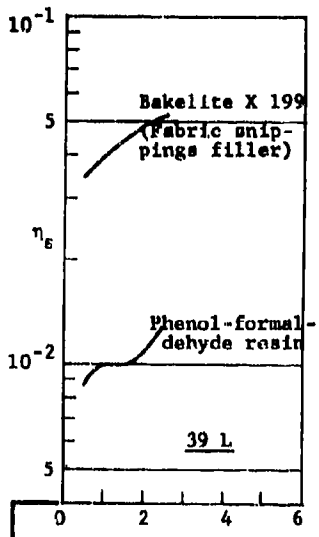

Torsion Stress τ_a (ksi)

FIGURE 349 LAMINATED PLASTIC (bakelite X199, fabric filler)

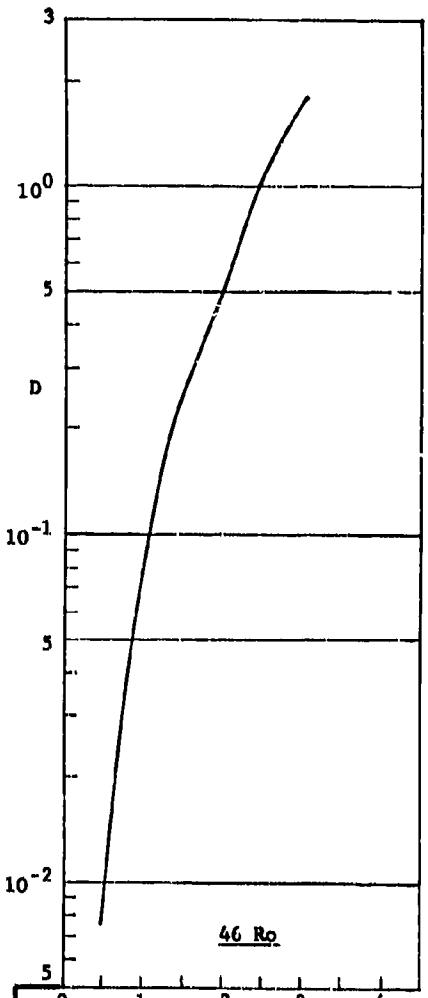

Stress σ_a (ksi)

FIGURE 350 LAMINATED PLASTIC (bakelite, grade X, paper base)

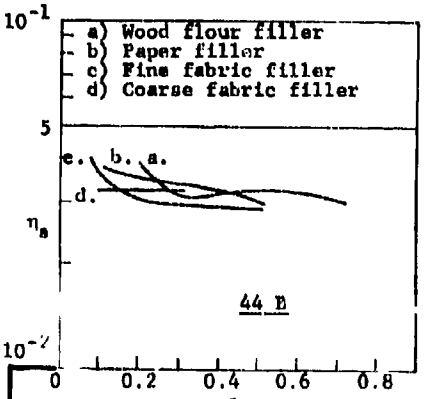

Torsion Stress τ_a (ksi)

FIGURE 351 LAMINATED PHENOLIC (bakelite)

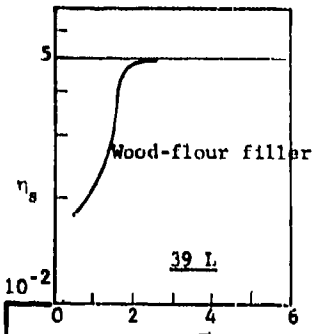

Torsion Stress τ_a (ksi)

FIGURE 352 LAMINATED PHENOLIC (bakelite, wood-flour filler)

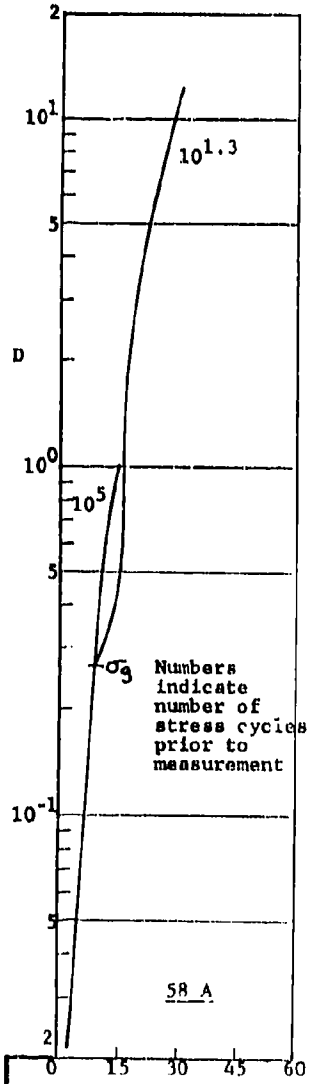

Stress σ_a (ksi)

FIGURE 353 GLASS-RESIN COMPOSITE (1002 crossply "Scotchply")

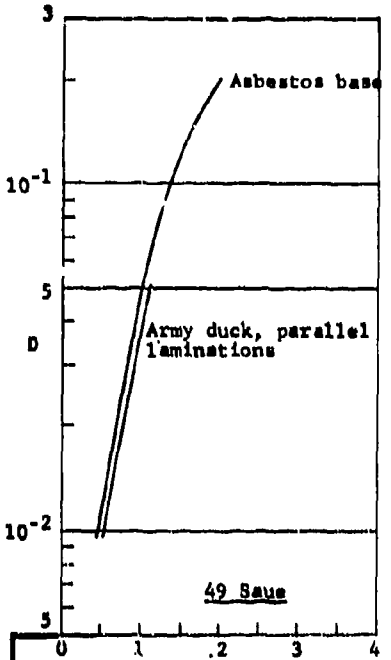

FIGURE 354 LAMINATED PLASTIC (phenolics)

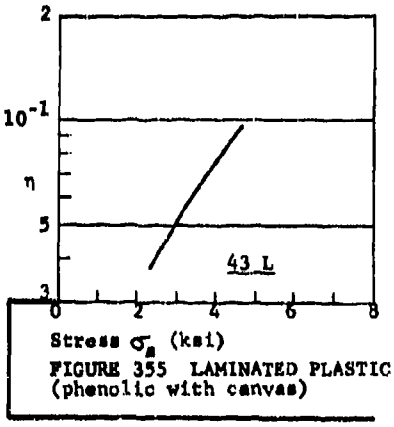

FIGURE 355 LAMINATED PLASTIC (phenolic with canvas)

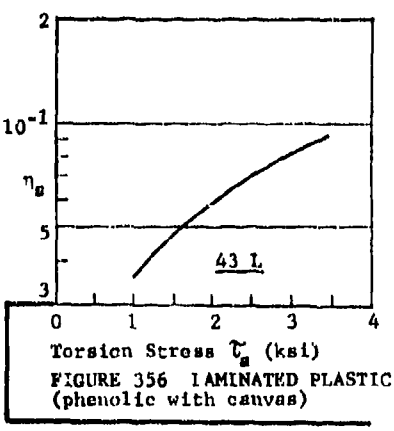

FIGURE 356 LAMINATED PLASTIC (phenolic with canvas)

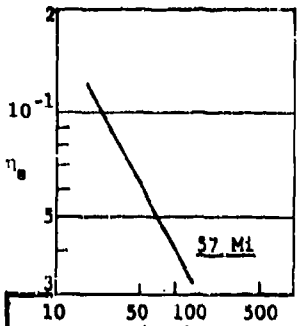

FIGURE 357 LAMINATED PLASTIC (phenolic with cotton)

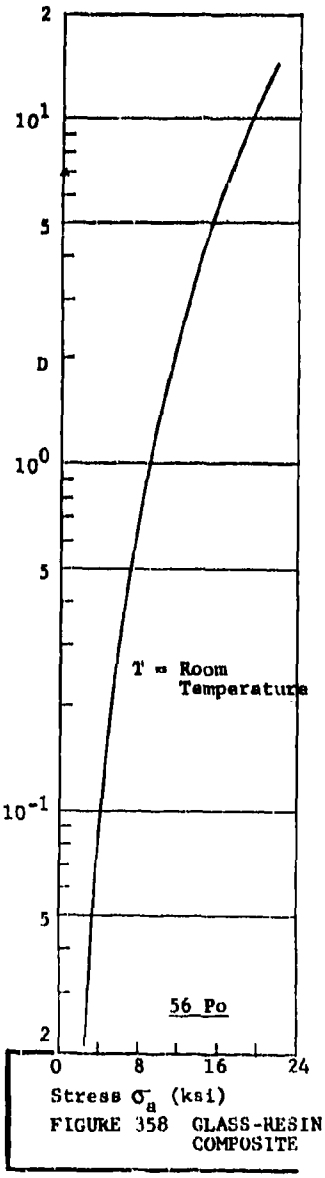

FIGURE 358 GLASS-RESIN COMPOSITE

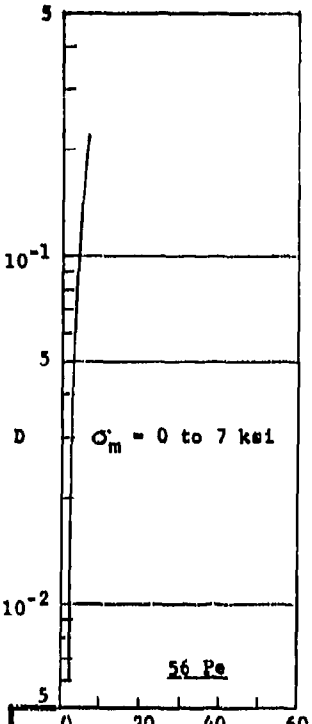

FIGURE 359 GLASS-RESIN COMPOSITE

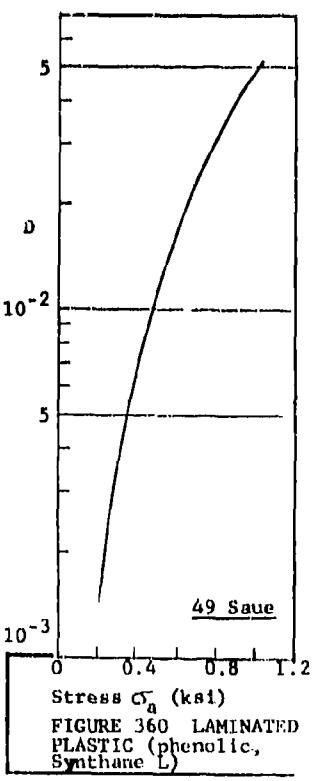

FIGURE 360 LAMINATED PLASTIC (phenolic, Synthane L)

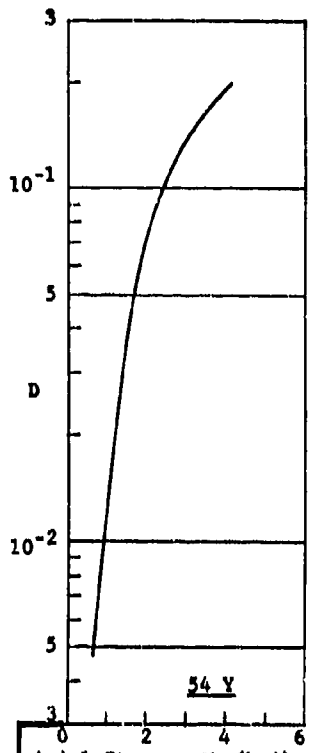

FIGURE 361 LAMINATED PLASTIC (phenolic, paper base)

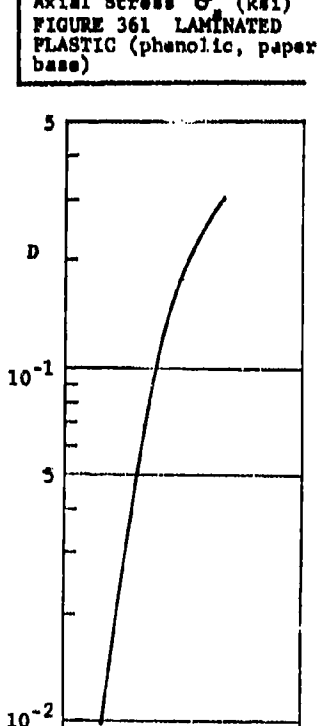

FIGURE 362 LAMINATED PLASTIC (phenolic, synthane XX)

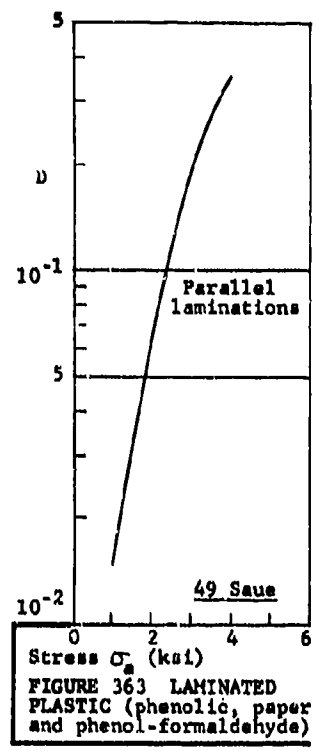

FIGURE 363 LAMINATED PLASTIC (phenolic, paper and phenol-formaldehyde)

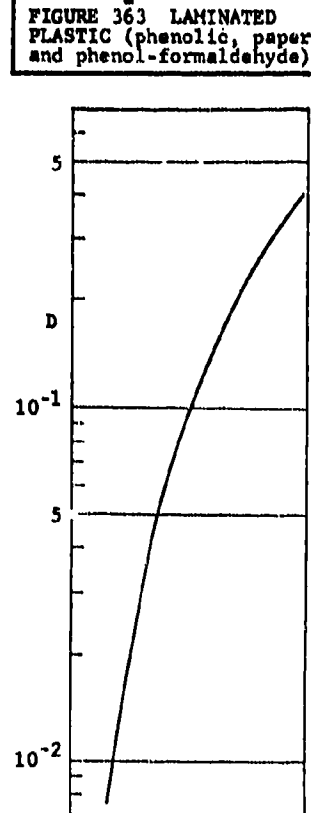

FIGURE 364 LAMINATED PLASTIC (phenolic, Rayon-cotton fabric)

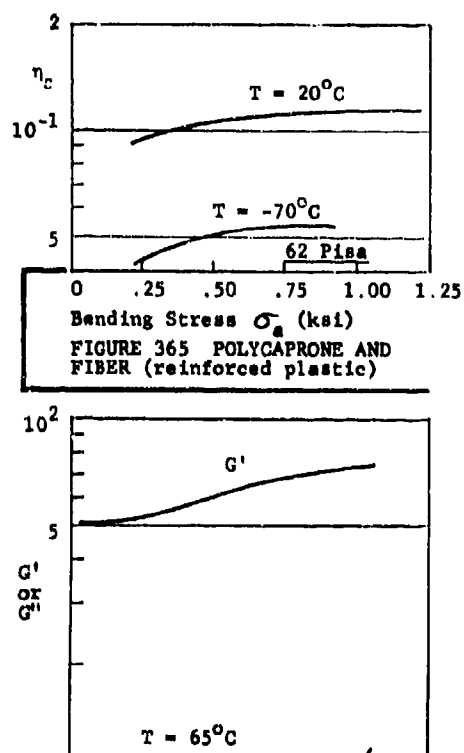

FIGURE 365 POLYCAPRONE AND FIBER (reinforced plastic)

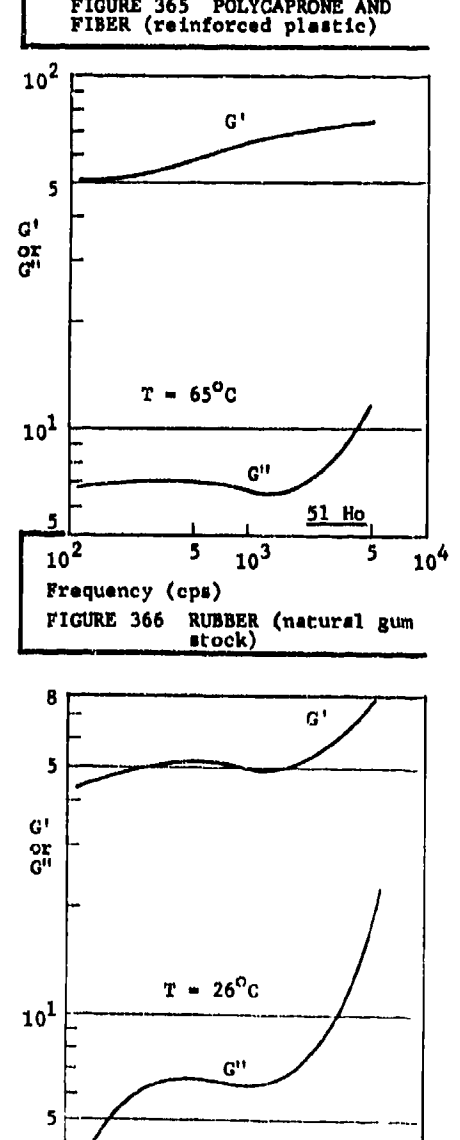

FIGURE 366 RUBBER (natural gum stock)

FIGURE 367 RUBBER (natural, gum stock)

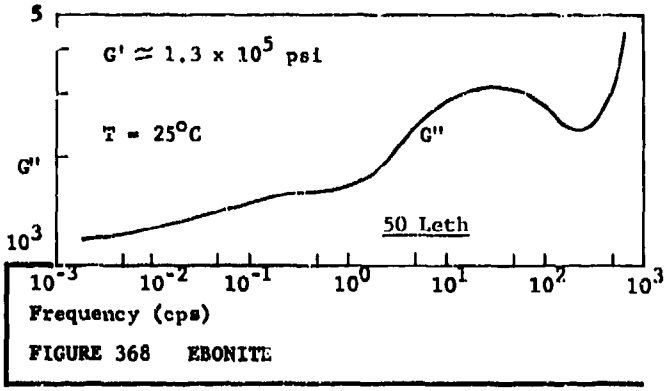

FIGURE 368 EBONITE

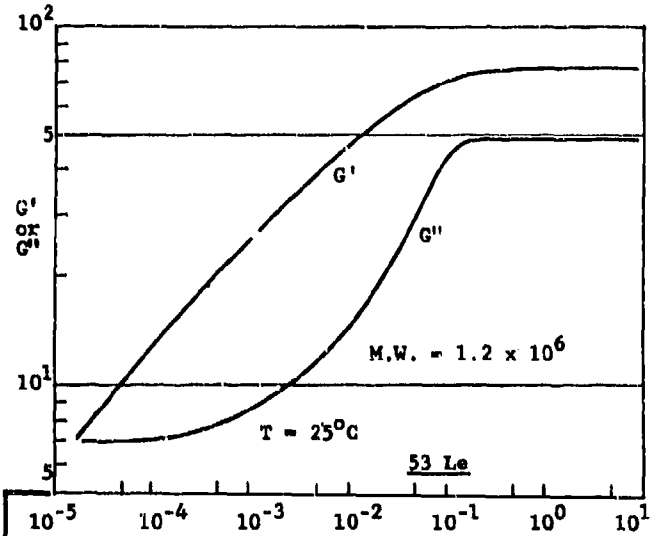

FIGURE 369 RUBBER (butyl)

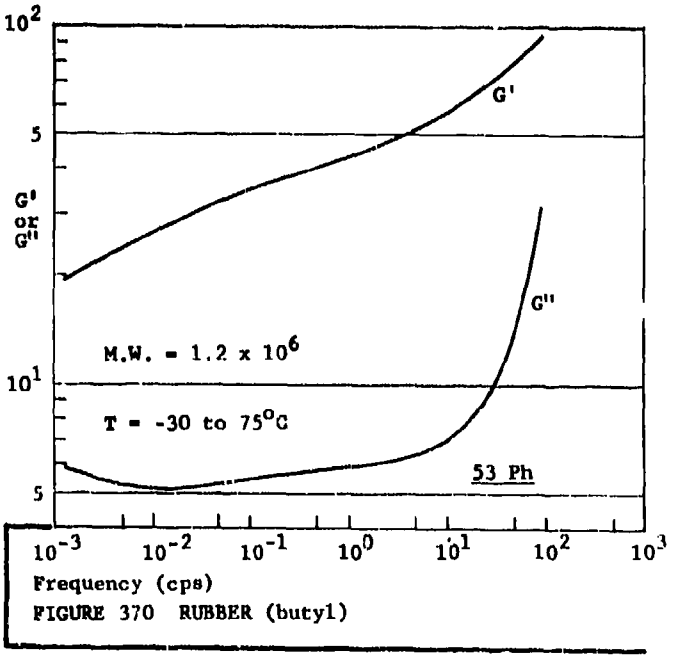

FIGURE 370 RUBBER (butyl)

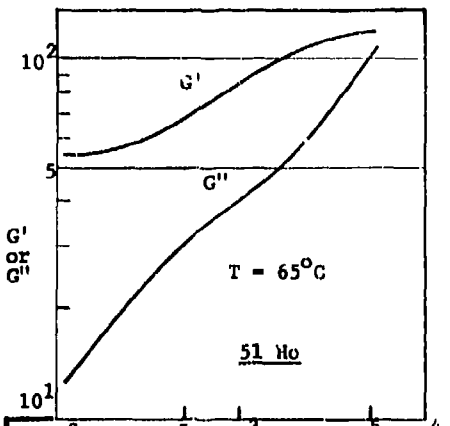

FIGURE 371 RUBBER (butyl)

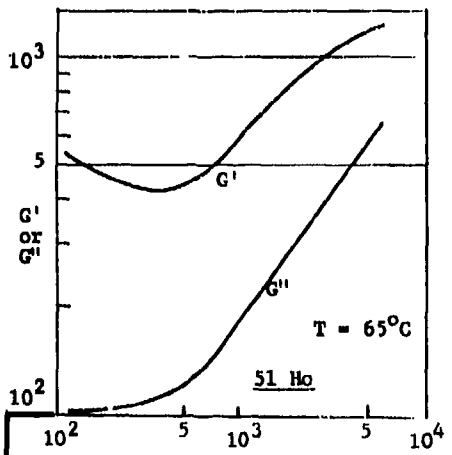

FIGURE 372 RUBBER (filled butyl)

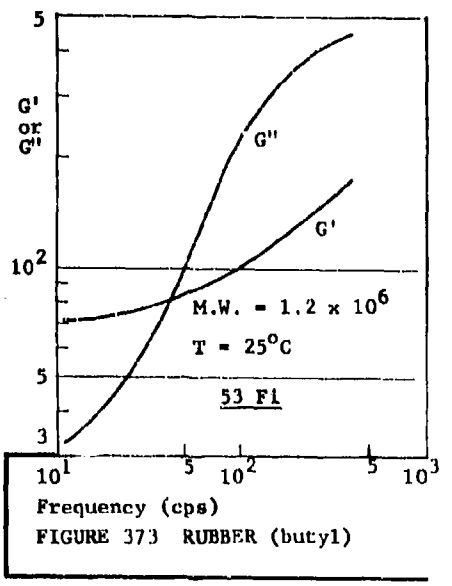

FIGURE 373 RUBBER (butyl)

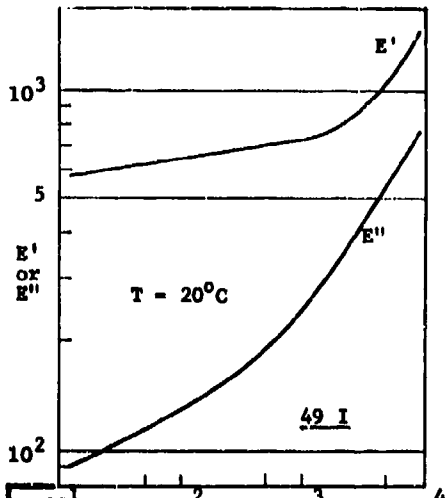

FIGURE 374 RUBBER (butyl)

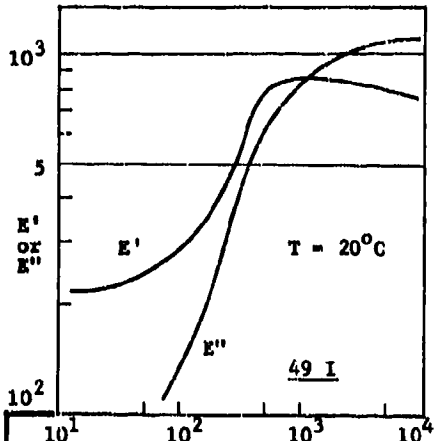

FIGURE 375 RUBBER (GRS)

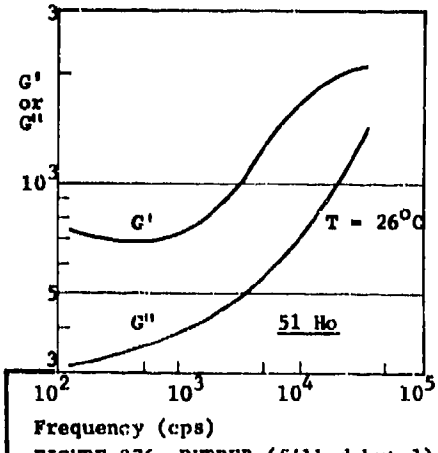

FIGURE 376 RUBBER (filled butyl)

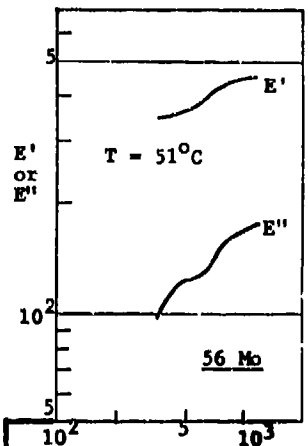

FIGURE 377 RUBBER (GRS + 3% Styrene)

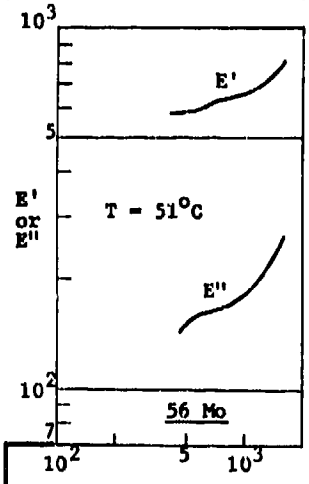

FIGURE 378 RUBBER (GRS + 13% Styrene)

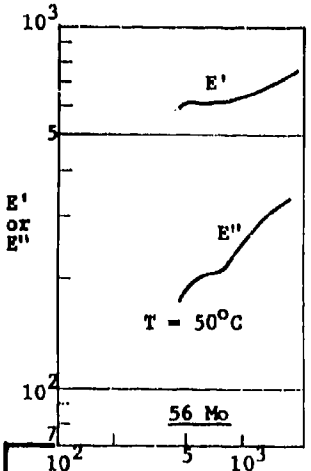

FIGURE 379 RUBBER (GRS + 23% Styrene)

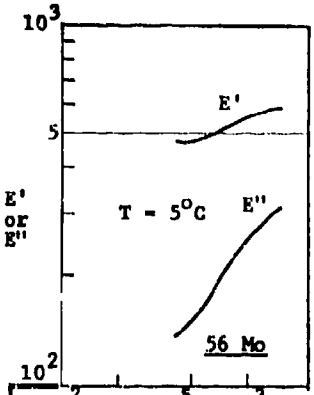

FIGURE 380 RUBBER (GRS + 23.5% Styrene)

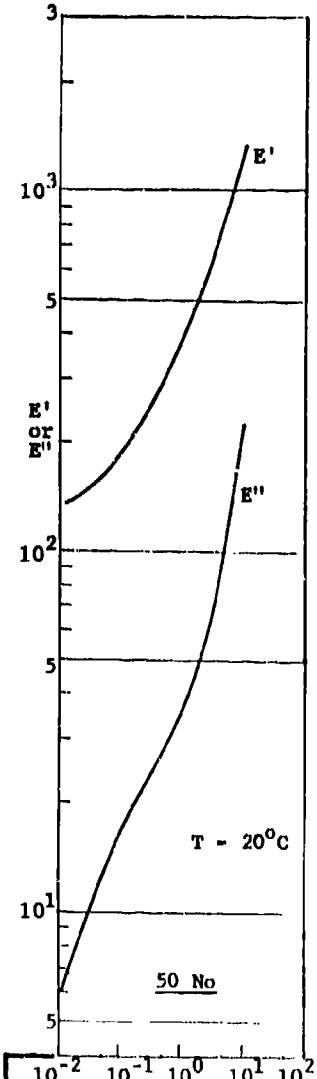

FIGURE 381 RUBBER (nitrile)

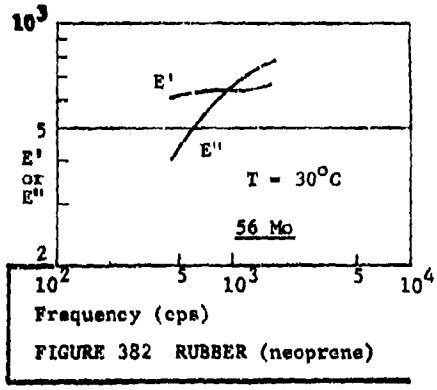

FIGURE 382 RUBBER (neoprene)

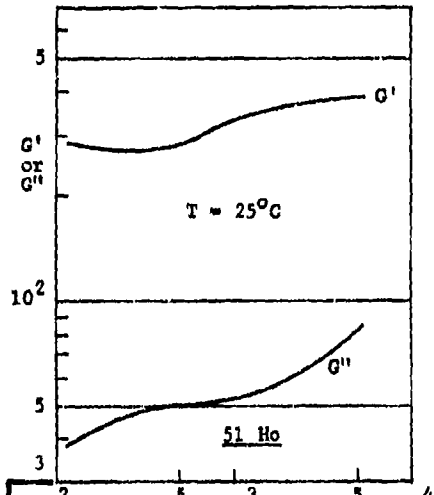

FIGURE 383 RUBBER (silicone filled)

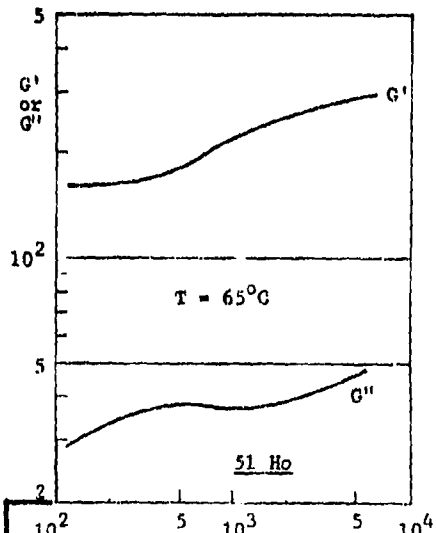

FIGURE 384 RUBBER (silicone filled)

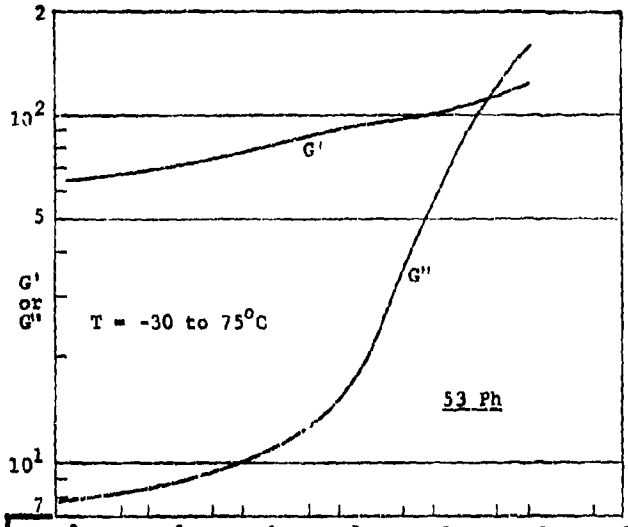

FIGURE 385 RUBBER (thiokol)

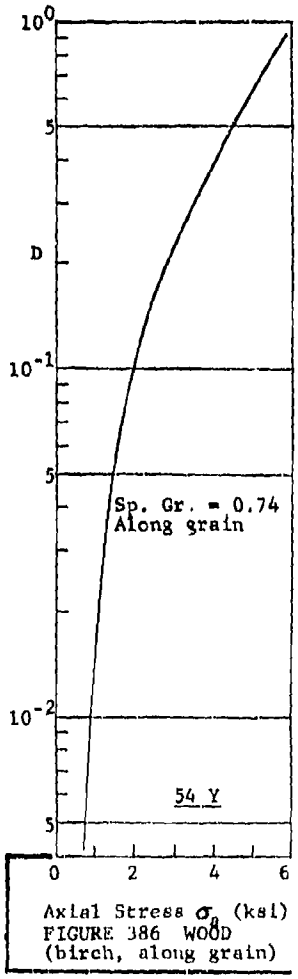

FIGURE 386 WOOD (birch, along grain)

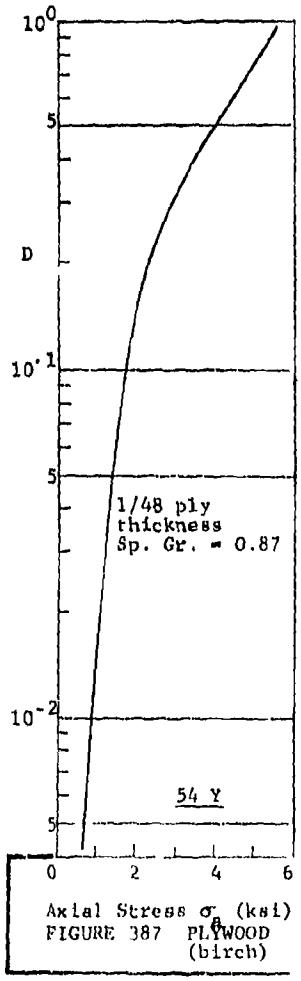

FIGURE 387 PLYWOOD (birch)

IV. REFRACTORIES, GLASS, MASONRY, MINERALS, STONE, NATURAL CRYSTALS, AND OXIDES

4.1 Data Tabulation

ALUMINA. $\eta = 1 - 3 \times 10^{-5}$. (64 Ast)

ALUMINA (Lucalax). $\eta < 10^{-5}$. (64 Ast)

ALUMINUM OXIDE (Single crystals, undeformed and deformed 20% at 1,300°C). Axial stress. T = 0 to 1,200°C. $\eta_s = 10^{-5}$ to 10^{-3}. (61 Hube, Figures 395 and 396)

Al_2O_3 (Polycrystalline, refractory material). At T = 200 to 1,000°C, $\eta = 3 \times 10^{-3}$. At T = 1,100°C, $\eta = 4 \times 10^{-2}$, peak value. η decreases above T = 1,100°C. (61 Cha)

Al_2O_3 (Polycrystalline containing 0.25% by weight of La_2O_3, refractory material). At T = 0 to 800°C, $\eta = 0.3 \times 10^{-2}$. At T = 900°C, $\eta = 2.4 \times 10^{-2}$. At T = 1,000°C, $\eta = 1.4 \times 10^{-2}$. At T = 1,200°C, $\eta = 3.0 \times 10^{-2}$. At T = 1,250°C, $\eta = 6.0 \times 10^{-2}$. (61 Cha)

$Ba_{0.92}\ Ca_{0.08}\ TiO_3$ AND ALSO $BaTiO_3$. Thin ring tested in estensional mode. f = 40,000 and 50,000. σ_a = 0 to 2 ksi. $\eta = 3 \times 10^{-3}$ to 10^{-2}. (60 Ger, Figures 397 and 398)

BeO (Polycrystalline, refractory material). At T = 200 to 1,100°C, $\eta = 10^{-3}$. At T = 1,300°C, $\eta = 2 \times 10^{-2}$. At T = 1,450°C, $\eta = 6.8 \times 10^{-2}$, peak value. η decreases above T = 1,450°C.

Temperature required to produce peak value of η reduced from 1,450°C to 1,380°C as frequency of cyclic stress reduced from f = 30 to f = 5. (61 Cha)

Be O (Polycrystalline, containing 1% by weight of MgO, refractory material). At f = 42, η = 0.004, 0.014, 0.025, 0.045, 0.067 at T = 930, 1,100, 1,300, and 1,400°C respectively, with small peaks at 1,140 and 1,230°C. At f = 31, η = 0.01, 0.024, 0.04, 0.053, 0.067 at T = 930, 1,100, 1,200, 1,300 and 1,350°C with small peaks at 1,100 and 1.200°C. (61 Cha)

BARIUM TITANITE (84% $BaTiO_3$, 8% $PbTiO_3$, 8% $CaTiO_3$ and 80% $RaTiO_3$, 12% $PbTiO_3$, 8% $CaTiO_3$; aged). $\eta_s = 2 \times 10^{-3}$ to 5×10^{-4}. (58 Mas, Figure 400)

CABBRO (French Creek). Under axial stress, $\eta_s = 5.9 \times 10^{-3}$. Under torsion: at 200 atm, $\eta_s = 2.5 \times 10^{-3}$ and at 4,000 atm, $\eta_s = 0.7 \times 10^{-3}$. (42 Bi*)

CHINA (Bone). $\eta = 0.25 \times 10^{-3}$. (64 Ast)

CHROMIC SESQUIOXIDE (Cr_2O_3). Axial stress. f = 85,000. T = 0 to 60°C. $\eta_s = 6 \times 10^{-4}$ to 2×10^{-4}. (61 Ye)

CLAY-LIKE MATERIALS. Cyclic torsion. Strains of 1 to 3%. Earthenware, η_s = 0.38. Ball clay, η_s = 0.61 to 0.65. China Clay, η_s = 0.53 to 0.60. Etruria Marl, η_s = 0.42 to 0.48. Bentomite, η_s = 0.27 to 0.46. Brick Clay, η_s = 0.48. Plastincine, η_s = 0.40. (64 Ast)

CONCRETE. Low stress. Vibration of a 5 ft. fork of concrete. $\eta_s = 2.4 \times 10^{-2}$. (41 Ki*)

DIABASE (Vinal haven). Under axial stress, $\eta_s = 1.7 \times 10^{-3}$. Under torsion: at 200 atm, $\eta_s = 4.2 \times 10^{-3}$ and at 4,000 atm, $\eta_s = 2.8 \times 10^{-3}$. (42 Bi*)

DOLERITE (Clee Hill). At f = 2 to 40, $\eta = 0.0055 \pm 10\%$. At f = 16,000 to 96,000, $\eta = 0.005 \pm 8\%$. (62 Do)

DOLOMITE (Pennsylvania). Axial stress. $\eta_s = 2.6 \times 10^{-3}$. (42 Bi*)

DUNITE (Balsam gap, N.C.). Torsion. At 200 atm, $\eta_s = 2.5 \times 10^{-3}$. At 4,000 atm, $\eta_s = 2.0 \times 10^{-3}$. (42 Bi*)

EARTHENWARE (Porous). $\eta = 10^{-3}$ to 2.5×10^{-3}. (64 Ast)

EARTHENWARE (Vitreous). $\eta = 0.8 \times 10^{-3}$ to 1.5×10^{-3}. (64 Ast)

FIRECLAY. T = 950 to 1,300°C. f = 25,000 to 1,250,000. $\eta = 0.6$ to 4×10^{-3}. (64 Ast)

GLASS. Bending. f = 10 to 100. $\eta_s = 2 \times 10^{-3}$ to 6×10^{-3}. 2x peak at f = 20. (49 K, Figure 409)

GLASS. Strains of about 5×10^{-3}. Rotating bending. $\eta_s = 2.0 \times 10^{-3}$. (41 Ki*)

GLASS. Low strain. Torsion. f = 0.25. $\eta_s = 2 \times 10^{-6}$. (41 Ki*)

GLASS. In torsion, $\eta_s = 4.5 \times 10^{-3}$. In bending, $\eta_s = 2.9 \times 10^{-3}$. (41 Ki*)

GLASS. Small strain. Axial stress. f = 45,000. η_s = 6.4 x 10^{-4}. (41 Ki*)

GLASS (Diabase). T = 0 to 500°C. f = 50,000 to 90,000. η_s = 29 to 155. (42 Bi*)

GLASS (Organical). Bending. σ_a = 0.2 to 1.7 ksi. At T = -55°C, η_s = 1.5 x 10^{-2} to 2.5 x 10^{-2}. At T = 20°C, η_s = 5.5 x 10^{-2} to 7.5 x 10^{-2}. (62 Pisa, Figure 404)

GLASS (Pyrex, 80.6% SiO_2, 11.9% Be_2O_3, 2.0% Al_2O_3, 4.4% Na_2O, and 1.1% other; annealed at 500°C for 3 hrs.). Axial stress. T = -200 to 800°C. f = 37,000. η_s = 5 x 10^{-4} to 3 x 10^{-3}. η_s = 5 x 10^{-4} minimum at T = 0°C. (58 Mas, Figure 388)

GLASS (Pyrex). f = 8,000 to 10,000. η_s = 4.6 x 10^{-4} to 5.5 x 10^{-4}. (42 Bi*)

GLASS (Silica). f = 1 to 10. η_s = 80 to 10^{-5}. (42 Bi*)

GLASS (Soft). At f = 5, η_s = 50 x 10^{-4}. At f = 10,000, η_s = 8 x 10^{-4}. At f = 40,000, η_s = 8 x 10^{-4}. (42 Bi*)

GLASS (Soft, 69% SiO_2, 14% Na_2O, 5% K_2O, 8% CaO, 3% Be_2O_3, 3% Al_2O_3, annealed at 500°C for 3 hrs.). Axial stress. T = -50 to 600°C. f = 37,000. η_s = 6 x 10^{-4} to 3 x 10^{-3}. (55 Mas, Figure 403)

GLASS FIBER (BQT-C). Bending. σ_a = 0.2 to 0.7 ksi. η_s = 2.5 x 10^{-2} to 3.5 x 10^{-2}. (62 Pisa, Figure 404)

GLASS FIBERS (Silica, 0.06 mm diameter). T = 500 to 1,000°C. f = 0.1. $\eta_s = 10^{-4}$ to 160×10^{-4}. (42 Bi*)

GLASS FIBERS (Silica, 1.3 mm diameter). T = 600 to 1,100°C. f = 14. $\eta_s = 10^{-4}$ to 57×10^{-4}. (42 Bi*)

GNEISS (Pelham, Mass.). Under axial stress, $\eta_s = 1.8 \times 10^{-2}$. Under torsion: at 200 atm, $\eta_s = 10^{-2}$ and at 4,000 atm, $\eta_s = 1.9 \times 10^{-3}$. (42 Bi*)

GRAPHITE (Commercial ECA). f = 3. At T = 0°C, $\eta = 9.7 \times 10^{-3}$. At T = 200°C, $\eta = 1.05 \times 10^{-2}$. At T = 500°C, $\eta = 8 \times 10^{-3}$. (61 Cha)

GRANITE (Rockport). Under axial stress, $\eta_s = 7.7 \times 10^{-3}$. Under torsion: at 200 atm, $\eta_s = 5.5 \times 10^{-3}$ and at 4,000 atm, $\eta_s = 0.6 \times 10^{-3}$. (42 Bi*)

GRANITE (Quincy). f = 140 to 1,600. $\eta_s = 5 \times 10^{-3}$ to 10^{-2}. (42 Bi*)

GRANITE (Quincy). Under axial stress, $\eta_s = 10^{-2}$. Under torsion: at 200 atm, $\eta_s = 5.5 \times 10^{-3}$ and at 4,000 atm, $\eta_s = 0.8 \times 10^{-3}$. (42 Bi*)

HARD CHALK (Flamborough Head Pebble). At f = 2 to 40, $\eta = 0.009 \pm 10\%$. At f = 11,000 to 66,000, $\eta = 0.14 \pm 11\%$. (62 Do)

IRON OXIDE (Fe_3O_4). Thin rod specimens. T = 70 to 300°K. f = 50,000 to 130,000. $\eta_s = 10^{-4}$ to 3×10^{-2}. $\eta_s \approx 1.5 \times 10^{-2}$

peak at T = 110°K. $\eta_s \approx 2 \times 10^{-4}$ minimum at T = 140°K. (55 Mas, Figure 389)

LIMESTONE (Portland). At f = 2 to 40. $\eta = 0.0055 \pm 10\%$. At f = 10,000 to 80,000, $\eta = 0.0032 \pm 5\%$. (62 Do)

LIMESTONE (Pennsylvania). Under axial stress, $\eta_s = 6.7 \times 10^{-3}$. Under torsion: at 200 atm, $\eta_s = 3.7 \times 10^{-3}$ and at 4,000 atm, $\eta_s = 1.6 \times 10^{-3}$. (42 Bi*)

LITHIUM FLUORIDE (Single crystal, slightly deformed). Axial stress. T = 0 to 240°K. f = 40,000. $\eta_s = 3 \times 10^{-6}$ to 2×10^{-5}. $\eta_s = 2 \times 10^{-5}$ peak at T = 60°K. (61 T, Figure 399)

MAGNESITE REFRACTORIES. $\eta = 1.2 \times 10^{-3}$ to 3.3×10^{-3}. (64 Ast)

MgO (Polycrystalline, refractory material). At T = 200 to 900°C, $\eta = 3 \times 10^{-3}$. At T = 1,050°C, $\eta = 6 \times 10^{-3}$, peak value. η decreases for T > 1,050°C. (61 Cha)

MANGANOSITE (MnO, polycrystalline). Low axial stress. T = -200 to 0°C. f = 85,000. $\eta_s = 5 \times 10^{-3}$ to 2×10^{-4}. $\eta_s = 5 \times 10^{-3}$ peak at T = -160°C. $\eta_s = 2 \times 10^{-4}$ minimum at T = -150 to -70°C. (61 Ye, Figure 390)

MARBLE (Vermont). Under axial stress, $\eta_s = 50 \times 10^{-3}$. Under torsion: at 200 atm, $\eta_s = 7.1 \times 10^{-3}$ and at 4,000 atm, $\eta_s = 10^{-3}$. (42 Bi*)

NORITE (Sudbury). Under axial stress, $\eta_s = 3.4 \times 10^{-3}$. Under

torsion: at 200 atm, $\eta_s = 4.2 \times 10^{-3}$ and at 4,000 atm, $\eta_s = 3.0 \times 10^{-3}$. (42 Bi*)

$PbZr_{0.52}\ Ti_{0.48}\ O_3$ PLUS 1% Nb_2O_5. Thin ring test specimen in extensional mode. σ_a = 0 to 2 ksi. $\eta = 10^{-2}$ to 5×10^{-2}. (60 Ger, Figure 401)

$Pb_{0.94}\ Sr_{0.06}\ Zr_{0.53}\ Ti_{0.47}\ O_3$. Thin ring test specimen in extensional mode. σ_a = 0 to 2 ksi. $\eta = 2 \times 10^{-3}$ to 6×10^{-3}. (60 Ger, Figure 402)

PORCELAIN (Electric). $\eta = 3 \times 10^{-4}$ to 1×10^{-3}. (64 Ast)

POTTERY GLAZES. $\eta = 2.5 \times 10^{-4}$ to 2×10^{-3}. (64 Ast)

QUARTZ (Single crystal). For plain quartz at f = 40,000, $\eta = 10^{-6}$. For etched and polished quartz at f = 70,000, $\eta = 1.7 \times 10^{-6}$. For ground quartz at f = 70,000, $\eta = 2.2 \times 10^{-5}$. For ground quartz at f = 650,000, $\eta = 1.7 \times 10^{-5}$ to 4.5×10^{-5}. For ground quartz at f = 830,000, $\eta = 1.3 \times 10^{-4}$ to 2.3×10^{-4}. (52 Bi*)

QUARTZ (Single crystal). Shear. $f = 10^5$ to 10^8. $\eta_s = 10^{-7}$ to 7×10^{-6}. (58 Mas, Figure 391)

QUARTZ (Natural clear virgin monocrystal). Flat plate specimens 1 mm thick and with a surface area of 1 to 2 sq. cm. T = 20 to 120°K. $\eta_s = 4 \times 10^{-5}$ to 6×10^{-5}. 1.5x peak at T = 60°K. (55 Vol, Figure 392)

QUARTZ (Single crystal). T = 10 to 120°K. η_s = 2 x 10^{-7} to 1.6 x 10^{-6}. η_s = 1.6 x 10^{-6} peak at T = 55°K. (55 Mas, Figure 393)

QUARTZ (Fused). Low strain. Torsion. f = 0.25. η_s = 4 x 10^{-7}. (41 Ki*)

QUARTZ (Ground and etched). Small strain. Piezoelectric vibration. f = 65,000. For ground quartz, η_s = 10^{-5}. For etched quartz, η_s = 2.0 x 10^{-6}. (41 Ki*)

QUARTZ CRYSTALS. $\eta < 10^{-6}$. (64 Ast)

QUARTZITIC SANDSTONE. Axial stress. η_s = 7.7 x 10^{-3}. (42 Bi*)

SAPPHIRE CRYSTAL. At T = 400 to 1,300°C, η = 1.3 x 10^{-3}. At T = 1,600°C, η = 3 x 10^{-3}. At T = 1,720°C, η = 5 x 10^{-3}. (61 Cha)

SLATE (Pennsylvania). Axial stress. η_s = 3.8 x 10^{-3}. (42 Bi*)

SODIUM CHLORIDE (Single crystal, annealed at 650°C, furnace cooled). Axial stress. T = 20 to 240°K. f = 40,000. For original crystal, η_s = 4 x 10^{-6} to 9 x 10^{-6}. After slight deformation, η_s = 5 x 10^{-6} to 2.2 x 10^{-5}. (61 T, Figure 394)

SILICA (Fused). Shear waves. T = 10 to 170°K. f = 6.6 x 10^4, 2.01 x 10^5, and 10^6. η_s = 2 x 10^{-4} to 2 x 10^{-3}. Peak values occur at T ≈ 60°K. (58 Mas, Figure 405)

SILICA (Fused, 99.9% SiO_2, annealed at 1,000°C for 2 hrs. in air).

T = -200 to 800°C. $\eta_s = 10^{-6}$ to 10^{-4}. $\eta_s = 10^{-6}$ minimum at T = 0°C. (58 Mas, Figure 406)

SILICA (Fused, 99.9% SiO_2). ϵ_a = 5 to 40 x 10^{-5}. At T = 940°C, $\eta_s = 8 \times 10^{-5}$. At T = 28°C, $\eta_s = 1.8 \times 10^{6}$. (58 Mas)

SILICA (Fused, 99.9% SiO_2, annealed at 1,000°C for 2 hrs. in air). Axial stress. T = 4 to 35°K. f = 37,000. $\eta_s = 4 \times 10^{-4}$ to 2×10^{-3}. 2x increase with T. 2.5x increase with f. (58 Mas, Figure 407)

SILICA (Fused). $\eta < 0.05$. (64 Ast)

SILICA (Fused, clear, strain free). T = 46°K. f = 5 x 10^4 to 5 x 10^9. $\eta_s = 2 \times 10^{-5}$ to 8×10^{-4}. Peak at f ≈ 10^6 and 5 x 10^8. (55 An, Figure 408)

SILICA REFRACTORIES. η = 2.5 to 10 x 10^{-3}. (64 Ast)

SILICEOUS REFRACTORIES. η = 6 to 12 x 10^{-3}. (64 Ast)

SILICON NITRIDE. $\eta \simeq 0.025 \times 10^{-3}$. (64 Ast)

SYENITE (Ontario). Torsion at 4,000 atm. $\eta_s = 5 \times 10^{-4}$. (42 Bi*)

ZrH_2 (Refractory material). f = 413. At T = 20°C, $\eta = 5 \times 10^{-3}$. At T = 60°C, $\eta = 10^{-2}$. At T = 90°C, $\eta = 1.8 \times 10^{-2}$ peak value. At T = 140°C, $\eta = 9 \times 10^{-3}$. And at T = 180°C, η = 6×10^{-3}. Peak value shifted from 90°C to 110°C as frequency increased from 413 to 1,106. (61 Cha)

ZrO_2 (Refractory material). f = 4. At T = 0°C, $\eta = 2 \times 10^{-3}$. At T = 230°C, $\eta = 1.05 \times 10^{-2}$, peak value. At T = 400 to 730°C, $\eta = 8 \times 10^{-3}$. Peak value shifted from 230°C to 300°C and increased to $\eta = 1.4 \times 10^{-2}$ as frequency increased from 4 to 11.6. (61 Cha)

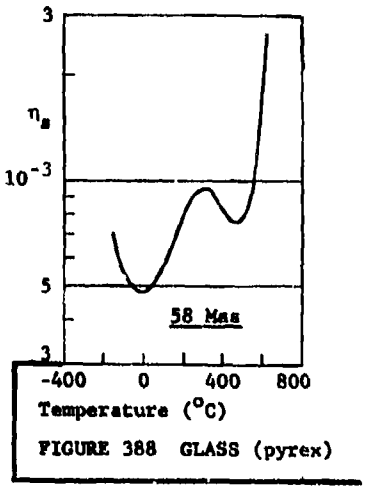

FIGURE 388 GLASS (pyrex)

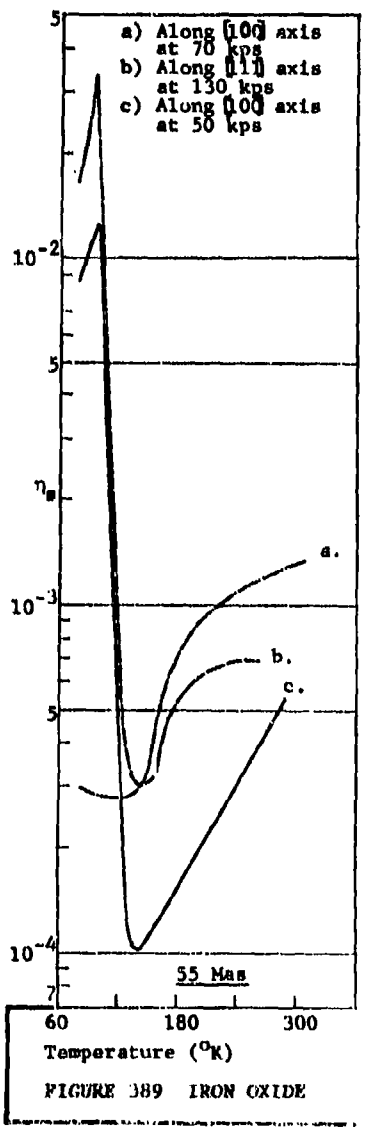

FIGURE 389 IRON OXIDE

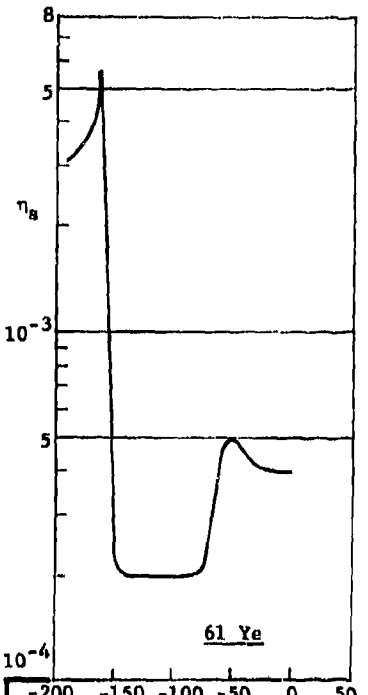

FIGURE 390 MANGANOSITE (polycrystalline)

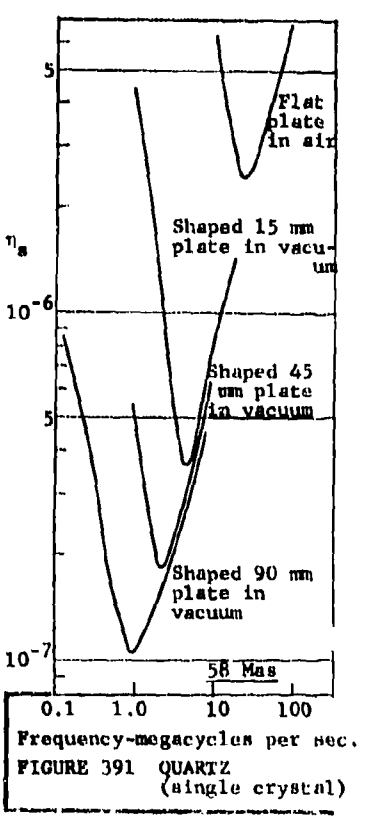

FIGURE 391 QUARTZ (single crystal)

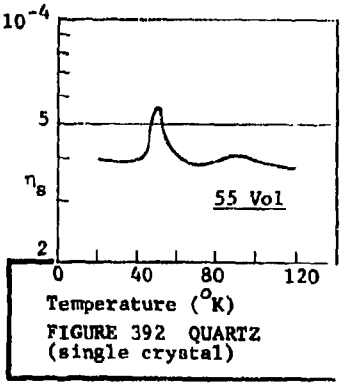

FIGURE 392 QUARTZ (single crystal)

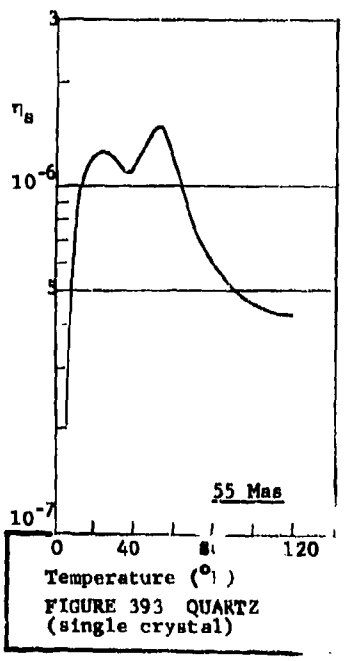

FIGURE 393 QUARTZ (single crystal)

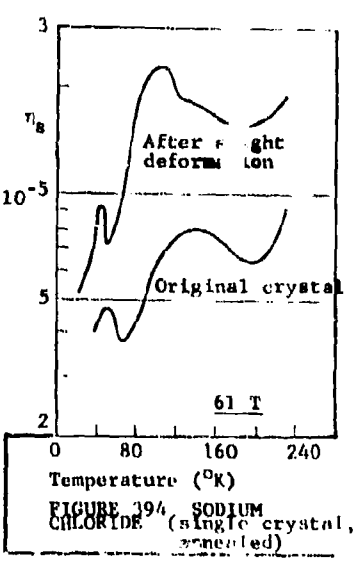

FIGURE 394 SODIUM CHLORIDE (single crystal, annealed)

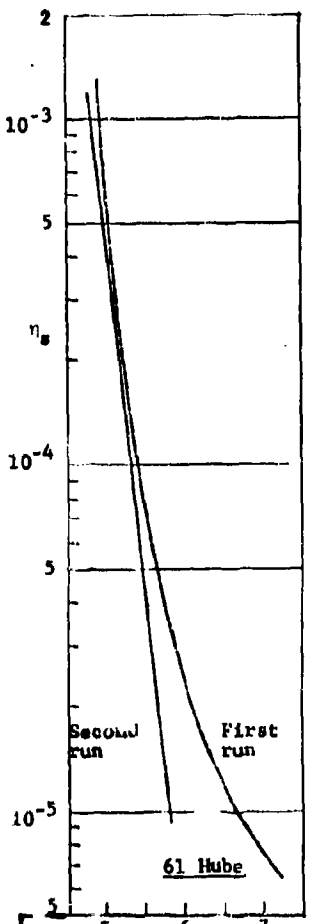

FIGURE 395 ALUMINUM OXIDE (single crystals)

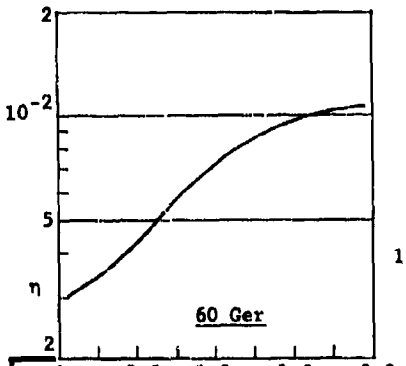

FIGURE 397 $Ba_{0.92}$ $Ca_{0.08}$ TiO_3

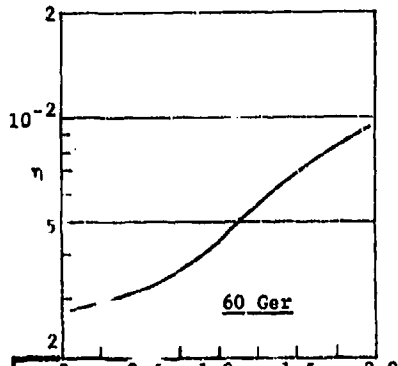

FIGURE 398 $BaTiO_3$

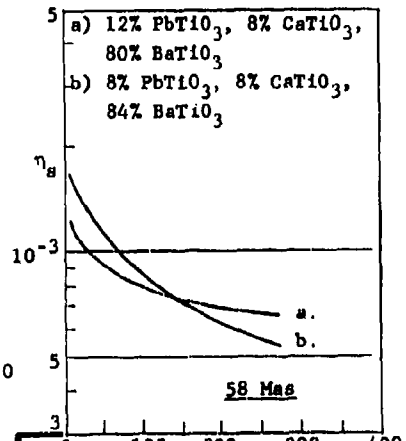

FIGURE 400 BARUIM TITANITE

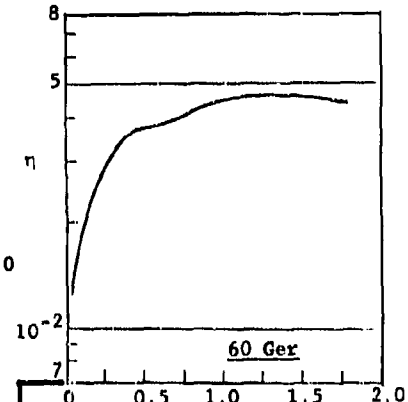

FIGURE 401 $PbZr_{0.52}$ $Ti_{0.48}$ O_3 PLUS 1% Nb_2O_5

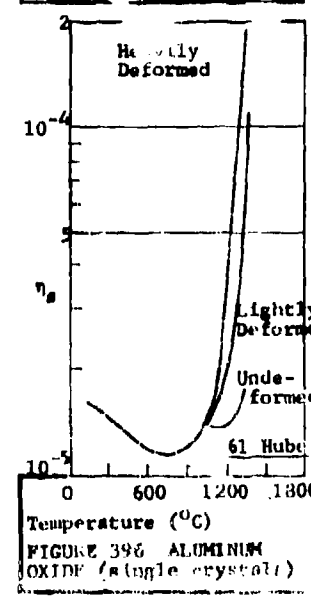

FIGURE 396 ALUMINUM OXIDE (single crystal)

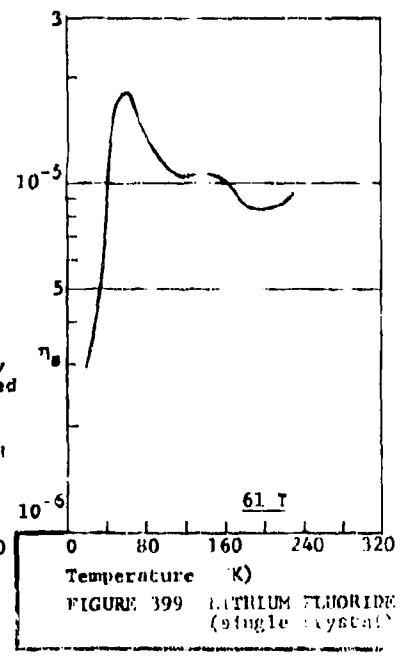

FIGURE 399 LITHIUM FLUORIDE (single crystal)

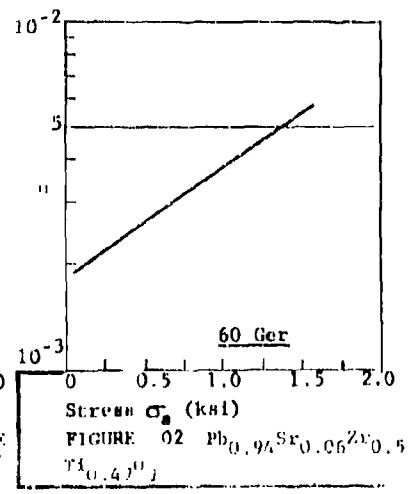

FIGURE 02 $Pb_{0.94}Sr_{0.06}Zr_{0.53}$ $Ti_{0.47}O_3$

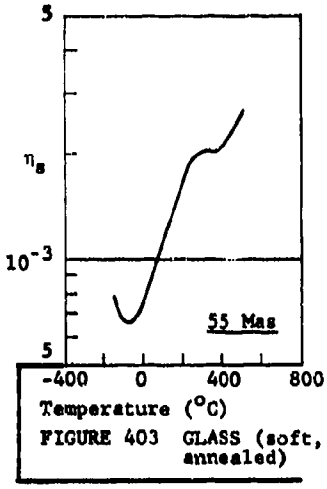

FIGURE 403 GLASS (soft, annealed)

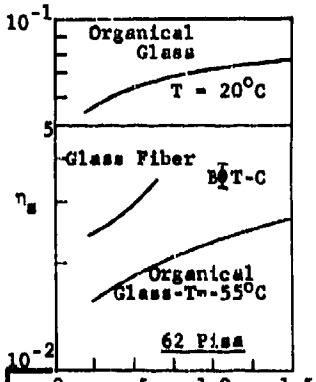

FIGURE 404 GLASS

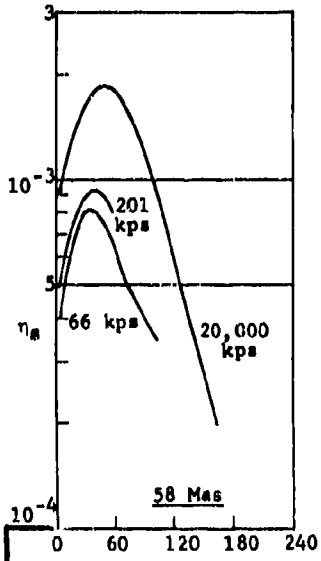

FIGURE 405 SILICA (fused)

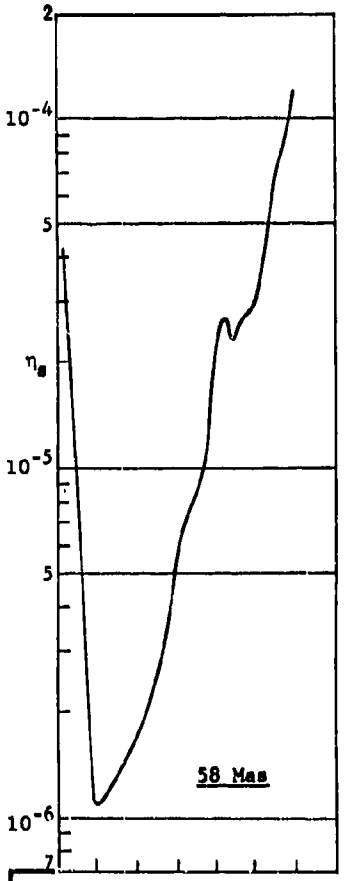

FIGURE 406 SILICA (fused, annealed)

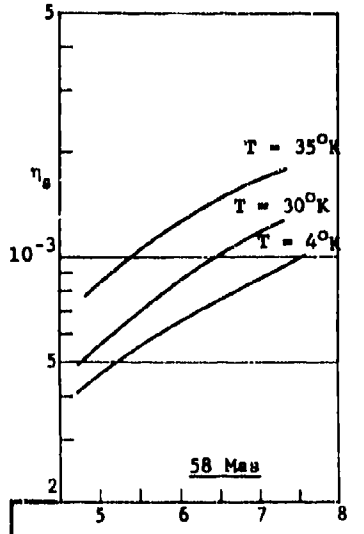

FIGURE 407 SILICA (fused, annealed)

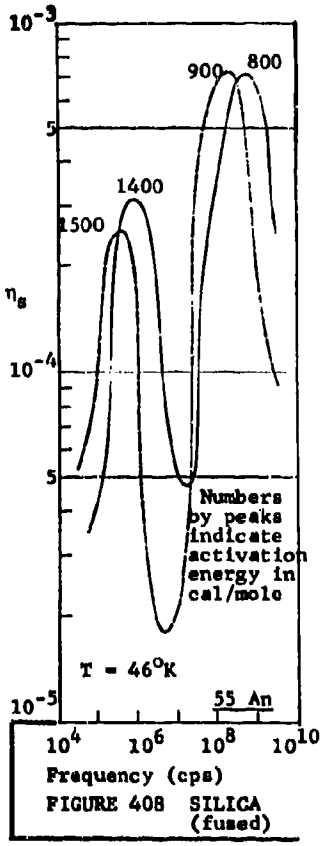

FIGURE 408 SILICA (fused)

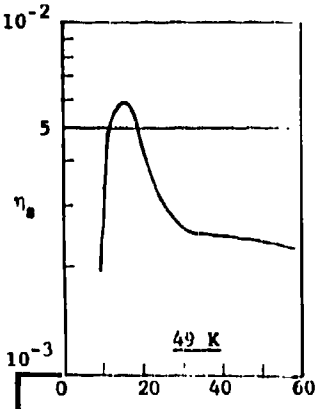

FIGURE 409 GLASS

V. PARTICLE-TYPE MATERIALS, AGGREGATES, SOILS, SAND, AND EARTH'S CRUST

Particle-like materials can dissipate energy either as loose materials or as a confined medium under stress. In the former case large relative motion between particles (such as observed in loose sand applied to surface of vibrating plate) provides mechanisms for energy dissipation. In this case the damping is associated with the cyclic displacement, velocity, or acceleration of the contact surfaces. As a confined medium (soil under triaxial stress, for example), the energy dissipation is associated with the state and magnitude of stress applied.

EARTH'S CRUST. Surface wave measurements. η = 0.0022 to 0.0074. (42 Bi*)

EARTH (As a planet). In shear, η_s = 0.0028. In compression, η_s = 0.001. (61 Mac)

GRANULAR MEDIA in the form of beam in which the grains are laminated together with synthetic sheets. Loss coefficient decreases with increasing thickness of the layer of the granular media. Increasing humidity causes higher E and lower η.

BRICK PARTICLES. Grain size 0 to 10 mm. η = 0.12 to 0.21.

COAL CINDERS. Grain size 0 to 15 mm. η = 0.17 to 0.25.

DRY SAND. Grain size 0.3 to 1 mm. η = 0.06 to 0.12.

GLASS PARTICLES. Grain size 1 mm. η = 0.09 to 0.15.

IRON PARTICLES. Grain size 3 to 15 mm. η = 0.09 to 0.14.

WET SAND. Grain size 0.3 to 1 mm. η = 0.05 to 0.17. (64 Ku)

SAND. (As loose material on aluminum beam under flexural vibra-

tions). For beam alone, η = 0.002 for f = 1,000 to 4,000. For beam with 50% weight layer of sand, η = 0.08 to 0.2. For beam with 100% weight of layer of sand η = 0.2 to 0.9. (64 Ku)

SOIL (Granular, 30% gravel, 40% sand, 30% silt). Soil samples enclosed in a membrane under a static triaxial pressure P_o with a uniaxial cyclic stress applied. At P_o = 2.78 psi, σ_a = 0.5 to 2 psi, D = 1.5 x 10^{-5} to 3.5 x 10^{-4}. At P_o = 6.94 psi, σ_a = 0.5 to 10 psi, D = 1.2 x 10^{-5} to 2.7 x 10^{-3}. At P_o = 12.5 psi., σ_a = 2.5 to 10 psi, D = 8 x 10^{-5} to 1.4 x 10^{-3}. (60 We)

SOIL (Miscellaneous). f = 6 to 30. η = 0.1. (42 Bi*)

31 C. -- Chevenard, P.

Mechanical Properties of Metals at Elevated Temperatures
Proc. ASTM, Vol. 31, pp. 245-268, 1931

38 C. -- Case, S. L.

Damping Capacity and Aging of Steel
Metal Progress, Vol. 33, pp. 54-59, 1938

38 Fl. -- Flinn, R. A. Jr. and Norton, J. T.

Measurements of Internal Friction in Age-Hardening Alloys with a Modified Torsion Pendulum Apparatus
Metals Technology, Vol. 5, Tech. Publ. No. 914, 10 pp., 1938

38 Fors. -- Förster, F. and Köster, W.

Elasticity and Damping in Relation to the State of Material
Engineer, Vol. 166, pp. 626-628, 1938

39 L. -- Leaderman, H.

Creep, Elastic Hysteresis, and Damping in Bakelite Under Torsion
Trans. ASME, Vol. 61, pp. A-79-85, 1939

39 N. -- Norton, J. T.

Torsion Pendulum Instrument for Measuring Internal Friction (of metals)
Rev. Sci. Inst., Vol. 10, pp. 77-78, March 1939

40 Lor. -- Lorig, C. H. and Schnee, V. H.

The Damping Capacity, Endurance, Electric, and Thermal Conductivities of Some Gray Irons
Trans., American Foundrymen's Association, Vol. 48, pp. 425-446, 1940

40 P. -- Parker, E. R.

The Influence of Magnetic Fields on Damping Capacity
Trans. Am. Soc. Metals, Vol. 28, pp. 661-667, 1940

41 D. -- Dean, R. S., Anderson, C. T., and Potter, E. V.

The Alloys of Manganese and Copper: Vibration Damping Capacity
Trans. Am. Soc. Metals, Vol. 29, pp. 402-414, 1941

41 Ki. -- Kimball, A. L.

Vibration Problems. Part V. Friction and Damping in Vibrations
Trans. ASME, Vol. 63, pp. A-135-A-140, 1941

41 R. -- Read, T. A.

Internal Friction of Single Crystals of Copper and Zinc
Trans. Am. Inst. Min. Eng., Vol. 143, pp. 30-44, 1941
also Phys. Rev., Vol. 58, p. 371, 1940

41 Ri. -- Rinehart, J. S.

Temperature Dependence of Young's Modulus and Internal Friction of Lucite and Karolith
J. Appl. Phys., Vol. 12, pp. 811-816, November 1941

42 Bi. -- Birch, F.

Internal Friction in Vibrating Solids. Section 6 of Handbook of Physical Constants
Geological Soc. of Amer., Special Paper, No. 36, Jan. 1942, reprinted 1954

42 St. -- Stambaugh, R. B.

Vibration Properties of Rubber-Like Materials. Dependence on Temperature
Ind. Eng. Chem., Vol. 34, No. 11, pp. 1358-1365, November 1942

42 Ze. -- Zener, C., Winkle, D. van, and Nielsen, H.

High-Temperature Internal Friction of Alpha Brass
Trans. Am. Inst. Min. and Met. Eng., Vol. 147, pp. 98-102, 1942

43 Ku. -- Kutsay, A. U. and Yorgiadis, A. J.

On the Torsional Damping Capacity of Solid Magn)y Rods as Affected by Cold Working
J. Aero. Sci., Vol. 10, No. 8, pp. 303-310, 1943

43 L. -- Lazan, B. J.

Some Mechanical Properties of Plastics and Metal Under Sustained Vibrations (Including Damping Capacity of Duralumin)
Trans. ASME, Vol. 65, pp. 87-104, 1943

44 B. -- Burpo, Jr., R. S.

The Damping Capacity of Engineering Materials
Engineering File Facts, No. 50, Metals and Alloys, pp. 1435-1437, June 1944

44 D. -- Dillon, J. H., Prettyman, I. B. and Hall, G. I.

Hysterectic and Elastic Properties of Rubber-like Materials Under Dynamic Shear Stresses
J. Appl. Phys., Vol. 15, p. 309, 1944

44 Sc. -- Schabtach, C. and Fehr, R. O.

Measurement of the Damping of Engineering Materials During Flexural Vibrations at Elevated Temperatures
J. Appl. Mech., Vol. 11, No. 2, pp. A86-A92, 1944

44 Yor. -- Yorgiadis, A. J. and Robertson, J. M.

Plywood Characteristics Disclosed by Vibration Tests
Aero. Digest, Vol. 45, No. 1, pp. 76-77, 80-81, 196, 198, 201-202, 204, April 1944

46 H. -- Hanstock, R. F.

Damping Capacity and the Fatigue of Metals
Engineering, Vol. 161, pp. 358-360, April 12, 1946

46 K. -- Ke, T'ing-Sui

High Temperature Anelastic Effects in Polycrystalline Aluminum
A paper presented at the meeting of the American Physical Society, Chicago, June 20-22, 1946

46 Ro. -- Robertson, J. M. and Yorgiadis, A. J.

Internal Friction in Engineering Materials
Trans. ASME, Vol. 68, p. A-173, 1946

47 H. -- Hanstock, R. F.

Damping Capacity, Strain Hardening and Fatigue
Proc., Phys. Soc., Vol. 59, pp. 275-287, 1947

49 B. -- Ballou, J. and Smith, J.

Dynamic Measurements of Polymer Physical Properties
J. Appl. Phys., Vol. 20, p. 493, 1949

49 I. -- Ivey, D., Mrowca, B. and Guth, E.

Propagation of Ultrasonic Bulk Waves in High Polymers
J. Appl. Phys., Vol. 20, p. 486, 1949

49 K. -- Kamel, R.

Measurement of the Internal Friction of Solids
Phys. Rev., Ser. 2, Vol. 75, p. 1606, May 15, 1949

49 Ly. -- Lyons, W.

Dynamic Properties of Filaments, Yarns and Cords at Sonic Frequency
Textile Res. J., Vol. 19, p. 123, 1949

49 Saue. -- Sauer, J. A. and Oliphant, W. J.

Damping and Load Carrying Capacities of Polystyrene and Other High Polymers
Proc., ASTM, Vol. 49, pp. 119-132, 1949

49 Wit. -- Witte, R., Mrowca, B. and Guth, E.

Propagation of Audiofrequency Sound in High Polymers
J. Appl. Phys., Vol. 20, p. 481, 1949

50 Fe. -- Ferry, J. D., Sawyer, W. M., Browning, G. and Groth, A. Jr.

Mechanical Properties of Substances of High Molecular Weight. III. Dispersion of Dynamic Rigidity and Viscosity in Concentrated Polyvinyl Acetate Solutions
J. Appl. Phys., Vol. 21, p. 513, 1950

50 Ke. -- Kê, T. S.

Internal Friction of Cold-Worked Metals at Various Temperatures
Trans. AIME, Vol. 188, pp. 575-580, 1950

50 Koe. -- Koehler, J. S.

The Influence of Dislocations and Impurities on the Damping and the Elastic Constants of Metal Single Crystals
Final Rept., Carnegie Inst. of Tech. (N6oni-47, Task Order 1) September 1950

50 Leth. -- Lethersich, W.

The Rheological Properties of Dielectric Polymers
British J. Appl. Phys., Vol. 1, p. 294, 1950

50 M. -- Marvin, R. S., Fitzgerald, E. R. and Ferry, J. D.

Measurement of Mechanical Properties of Polyisobutylene at Audio-frequencies by a Twin Transducer
J. Appl. Phys., Vol. 21, p. 197, 1950

50 No. -- Nolle, A. W.

Dynamic Mechanical Properties of Rubber-like Materials
J. Polymer Science, Vol. 5, pp. 1-54, 1950

51 Bozo. -- Bozorth, R. M., Mason, W. P. and McSkimin, H. J.

Frequency Dependence of Elastic Constants and Losses in Nickel
Bell System Tech. J., Vol. 30, Pt. 1, pp. 970-989, October 1951

51 Du. -- Dunell, B. A. and Dillon, J. H.

The Measurement of Dynamic Modulus and Energy Losses in Single Textile Filaments Subjected to Forced Longitudinal Vibrations
Text. Res. J., Vol. 21, No. 6, pp. 393-403, June 1951

51 F. -- Fast, J. D. and Dijkstra, L. J.

Internal Friction in Iron and Steel
Philips Tech. Rev., Vol. 13, No. 6, pp. 172-179, December 1951

51 Fer. -- Ferro, A. and Montalenti, G.

Internal Friction of Ferromagnetic Materials
J. Appl. Phys., Vol. 22, pp. 565-568, May 1951

51 Ho. -- Hopkins, I. L.

Dynamic Shear Properties of Rubber-like Polymers
ASME Trans., Vol. 73-1, pp. 195-204, 1951

51 Ro. -- Rorden, H. C. and Grieco, A.

Measurement of Dynamic Internal Dissipation and Elasticity of Soft Plastics
J. Appl. Phys., Vol. 22, No. 6, pp. 842-845, June 1951

51 Rot. -- Rotherham, L., Smith, A. D. N. and Greenough, G. B.

Internal Friction and Grain-Boundary Viscosity of Tin
J. Inst. Metals, Vol. 79, pp. 439-454, August 1951

52 Bi. -- Bishop, R. E. D. and Weldbourn, D. B.

The Problem of the Dynamic Vibration Absorber
Eng., Vol. 174, p. 746, December 19, 1952

52 Fer. -- Ferry, J., Fitzgerald, E., Grandine, L. and Williams, M.

Temperature Dependence of Dynamic Properties of Elastomers: Relaxation Distribution
Ind. Eng. Chem., Vol. 44, p. 703, 1952

52 Fl. -- Fletcher, W. and Gent, A.

Apparatus for the Measurements of Dynamic Shear Modulus and Hysteresis of Rubber at Low Frequencies
J. Sci. Instr., Vol. 29, p. 186, 1952

52 M. -- Majors, H. Jr.

Dynamic Properties of Nodular Cast Iron. Part I.
Trans. ASME, Vol. 74, pp. 365-375; disc. 375-380, April 1952

52 Mc. -- McSkimin, H.

Measurement of Dynamic Shear Viscosity and Stiffness of Viscous Liquids by Means of Traveling Torsional Waves
J. Acous. Soc. Am., Vol. 24, p. 355, 1952

52 No. -- Nolle, A. and Sieck, P.

Longitudinal and Transverse Ultrasonic Waves in Synthetic Rubbers
J. Appl. Phys., Vol. 23, p. 888, 1952

53 B. -- Barber, W. J.

Determination of Damping Capacity of Typical Metals by Free Vibration Method
Kentucky Univ., Eng. Exp. Sta. Bul. No. 27, 32 pp., March 1953

53 Ch. -- Chang, L. C. and Gensamer, M.

Internal Friction of Iron and Molybdenum at Low Temperatures
Acta Metallurgica, Vol. 1, No. 5, pp. 483-486, September 1953

53 Co. -- Cochardt, A. W.

The Origin of Damping in High-Strength Ferromagnetic Alloys
J. Appl. Mech., Trans. ASME, Vol. 75, pp. 196-200, June 1953

53 Coc. -- Cochardt, A. W.

A Method for Determining the Internal Damping of Machine Members
Westinghourse Res. Lab., East Pittsburgh, Pa., Scientific Paper No. 1721, also ASME annual meeting paper No. 53-a-44, January 29, 1953

53 Fe. -- Ferry, J., Grandine, L. Jr. and Fitzgerald, E.

The Relaxation Distribution Function of Polyisobutylene in the Transition from Rubber-like to Glass-like Behavior
J. Appl. Phys., Vol. 24, p. 911, 1953

53 Fi. -- Fitzgerald, E., Grandine, L. and Ferry, J.

Dynamic Mechanical Properties of Polyisobutylene
J. Appl. Phys., Vol. 24, pp. 650-655, 1953

53 Fit. -- Fitzgerald, E. and Ferry, J.

Method for Determining the Dynamic Mechanical Behavior of Gels and Solids at Audio Frequencies; Comparison of Mechanical and Electrical Properties
J. Colloid Sci., Vol. 8, pp. 1-34, 1953

53 Jo. -- Jones, E. R. W. and Munro, W.

The "Elastic Hysteresis" of Uranium
J. Mech. and Phys. of Solids, Vol. 1, pp. 182-188, 1953

53 Le. -- Leaderman, H. and Marvin, R. S.

Dynamic Compliance, Dynamic Modulus, and Equivalent Voigt and Maxwell Models for Polyisobutylene
J. Appl. Phys., Vol. 24, No. 6, pp. 812-813, June 1953

53 Mas. -- Mash, D. R. and Hall, L. D.

Anelastic Behavior of Pure Gold Wire
Trans. AIME, Vol. 197, pp. 937-942, 1953

53 Pe. -- Pearson, S.

Internal Friction and Grain Boundary Viscosity of Silver and of Binary Silver Solid Solutions
Roy. Aircraft Establishment (Gr. Brit.), Rept. No. MET 71, 16 pp., January 1953

53 Ph. -- Philippoff, W.

Mechanical Investigations of Elastomers in a Wide Range of Frequencies
J. Appl. Phys., Vol. 24, p. 685, 1953

53 Ro. -- Rozin, K. M. and Finkelshtein, B. N.

Phase Transformation by Method of Internal Friction. (In Russian)
Dokl. Akad. Nauk SSSR, Vol. 91, No. 4, pp. 811-812, August 1, 1953

54 Dil. -- Dilke, M. and Millane, J.

The Dynamic Properties of Plasticized Polyvinyl Chloride
J. Appl. Chem., Vol. 4, pp. 507-513, 1954

54 E. -- Entwistle, K. M.

Changes of Damping Capacity in Quench-Ageing Aluminum-Rich Alloys
J. Inst. of Metals, Vol. 82, pp. 249-263, February 1954

54 Fine. -- Fine, M. E., Van Duyne, H. and Kenney, N. T.

Low-Temperature Internal Friction and Elasticity Effects in Vitreous Silica
J. Appl. Phys., Vol. 25, No. 3, pp. 402-405, March 1954

54 Hu. -- Hutton, A. and Nolle, A.

Experimental Study of Low Frequency Effects on the Dynamic Modulus of a Buna-N Rubber
J. Appl. Phys., Vol. 25, p. 350, 1954

54 M. -- Marsh, K. J.

Some Observations on the Anelastic Properties of Copper and Tin Bronzes
Acta Metallurgica, Vol. 2, No. 3, pp. 530-545, May 1954

54 Ph. -- Philippoff, W.

Further Dynamic Investigation on Polymers
J. Appl. Phys., Vol. 25, pp. 1102-1107, 1954

54 Pr. -- Pratt, J. N., Bratine, W. J. and Chalmers, B.

Internal Friction in Titanium and Titanium-Oxygen Alloys
Acta Metallurgica, Vol. 2, No. 2, pp. 203-208, March 1954

54 Wi. -- Williams, M. and Ferry, J.

Dynamic Mechanical Properties of Polyvinyl Acetate
J. Colloid Sci., Vol. 9, pp. 479-492, 1954

54 Y. -- Yorgiadis, A.

Damping Capacity of Materials
Product Engineering, Vol. 25, pp. 164-170, November 1954

55 An. -- Anderson, O. L. and Bömmel, H. E.

Ultrasonic Absorption in Fused Silica at Low Temperatures and High Frequencies
J. Ceramic Soc., Vol. 38, pp. 125-131, April 1955

55 Be. -- Becker, G.

Mechanical Relaxation in Unplasticized High Polymers. (In German)
Kolloid Z., Vol. 140, p. 1, 1955

55 Co. -- Cochardt, A. W.

Effect of Static Stress on the Damping Some Engineering Alloys
Trans., Am. Soc. for Metals, Vol. 47, pp. 440-450, 1955

55 Ho. -- Hoff, D., Robinson, D. and Willbourn, A.

Relation Between the Structure of Polymers and Their Dynamic Mechanical Properties and Electrical Properties. II. Acrylic Polymer
J. Polymer Sci., Vol. 18, p. 161, 1955

55 Mas. -- Mason, W. P.

Letters to the Editor: Ultrasonic Attenuation Due to Lattice-Electron Interaction in Normal Conduction Metals
Phys. Rev., Vol. 97, No. 2, pp. 557-559, January 15, 1955

55 R. -- Robinson, D. W.

An Apparatus for the Measurement of Dynamic Mechanical Properties of Polymers Over a Wide Temperature Range
J. Sci. Instr., Vol. 32, p. 2, 1955

55 Ro. -- Rowland, J. A., Armantrout, C. E. and Walsh, D. F.

Casting and Fabriction of High Damping Manganese-Copper Alloys
U.S. Bureau of Mines Rept. of Investigations, Rept. 5127, April 1955

55 Th. -- Thomas, D. and Robinson, D.

Some Dynamic Mechanical Properties of Polyisobutylene Over a Wide Range of Temperature
Brit. J. Appl. Phys., Vol. 6, p. 41, 1955

55 Vol. -- Volger, J., Stevels, J. M. and Van Amerongen, C.

Dielectric Losses of Various Monocrystals of Quartz at Very Low Temperatures
Philips Res. Rept., Vol. 10, No. 4, pp. 260-280, 1955

55 Wi. -- Williams, M. and Ferry, J.

Dynamic Mechanical Properties of Plasticized Polyvinyl Acetate
J. Colloid Sci., Vol. 10, p. 1, 1955

56 Co. -- Cochardt, A. W.

High Damping Ferromagnetic Alloys
Trans. J. of Metals, Vol. 8, No. 10, Sec 2, pp. 1295-1298, 1956.
Also Trans. Am. Inst. Min. and Met. Eng., Vol. 226, p. 1295, 1956

56 D. -- Demer, L. J.

Bibliography of the Material Damping Field
WADC TR 56-180, Air Force Tech. Rept., June 1956

56 Hun. -- Hunter, H. F.

The Structural Damping Titanium at Elevated Temperatures
Aero. Eng. Rev., Vol. 15, pp. 18-21, 1956

56 M. -- Maringer, R. E., Marsh, L. L. and Manning, G. K.

Investigation of Plastic Behavior of Binary Aluminum Alloys by Internal-Friction Methods
NACA TN 3681, 44 pp., 1956

56 Mas. -- Mason, W. P.

Physical Acoustics and the Properties of Solids
J. Acous. Soc. Am., Vol. 28, No. 6, pp. 1197-1206, 1956

56 Maxw. -- Maxwell, B.

An Investigation of the Dynamic Mechanical Properties of Polymethyl Methacrylate
J. Polymer Sci., Vol. 26, pp. 551-566, 1956

56 Mi. -- Miki, H.

On the Internal Friction of Metals. Part II. Experimental Results and Inspections
Doshisha Eng. Rev., Vol. 6, No. 4, pp. 173-184, January 1956

56 Mo. -- Morris, R. E., James, R. R. and Guyton, C. W.

A New Method for Determining the Dynamic Mechanical Properties of Rubber
Rubber Age, Vol. 78, pp. 725-730, February 1956

56 Pe. -- Person, N. L. and Lazan, B. J.

The Effect of Static Mean Stress on the Damping Properties of Materials
Proc., ASTM, Philadelphia, Pa., Vol. 56, pp. 1399-1409, 1956

56 Po. -- Podnieks, E. R. and Lazan, B. J.

Damping, Elasticity, and Fatigue Properties of Titanium Alloys, High Temperature Alloys, Stainless Steels, and Glass Laminate at Room and Elevated Temperatures
WADC TR 56-37, March 1956

56 Stre. -- Strella, S.

Vibrating Reed Tests for Plastics
ASTM Bull, No. 214, p. 47, 1956

57 A. -- Anderson, V. W. and Lazan, B. J.

Damping and Fatigue Properties of Magnesium and Manganese-Copper Alloys Proposed as New High Damping Materials
Internal Rept., Aero Lib., University of Minnesota, 1957

57 Ch. -- Child, W., Jr. and Ferry, J. D.

Dynamic Mechanical Properties of Poly-n-Butyl Methacrylate
J. Colloid Sci., Vol. 12, pp. 327-341, 1957

57 Chi. -- Child, W., Jr. and Ferry, J. D.

Dynamic Mechanical Properties of Poly-n-hexyl Methacrylate
J. Colloid Sci., Vol. 12, pp. 389-400, 1957

57 D. -- Dahlquist, C. and McCutchan, A.

Vibration Damping Studies
Internal Rept., Minn. Mining and Manufacturing Co. Rept., 1957

57 En. -- Entwistle, K. M.

Damping Behavior of Quenched Aluminium-Copper-Magnesium-Silicon Alloys
J. Inst. Metals, Vol. 85, pp. 425-450, 1957

57 Fe. -- Ferry, J. D., Williams, M., Child, W. Jr., Zand, R., Stern, D. and Landel, R.

Dynamic Mechanical Properties of Polyethyl Methacrylate
J. Colloid Sci., Vol. 12, p. 53, 1957

57 Fit. -- Fitzgerald, E. R., Fitzgerald, Jr. and Woodward, A.

Dynamic Mechanical Properties of Plastic Materials
Final Report of Navy Contract No. Nobs-72106, Index No. NS-034-045, Subtask No. 59, June 1957

57 Fl. -- Fletcher, W. P. and Gent, A. N.

Dynamic Shear Properties of Rubber-like Materials
Brit. J. Appl. Phys., Vol. 8, p. 194, 1957

57 H. -- Hagel, W. C. and Clark, J. W.

The Specific Damping Energy of Fixed-Fixed Beam Specimens
J. Appl. Mech., Vol. 24, No. 3, pp. 426-430, September 1957. Also Trans. ASME, Vol. 79, p. A-426, September 1957

57 K. -- Kaelble, D.

Dynamic Mechanical Properties of Rigid Plastics
Internal Rept., Minn. Mining and Manufacturing Co. Rept., 1957

57 Kea. -- Ke, T. S., Yung, P. T. and Chang, C. Y.

Internal Friction in the Process of Plastic Deformation of Metals
Sci. Record (Peking), Vol. 1, No. 4, pp. 231-236, 1957

57 Kur. -- Kurath, S., Passaglia, E. and Pariser, R.

Dynamic Mechanical Properties of Polyhexane
J. Appl. Phys., Vol. 28, pp. 499-502, 1957

57 Mi. -- Milligan, H. L.

The Effect of Frequency and Physical Structure Upon the Solid Damping Property of Materials
An unpubl. rept., Bellevue, Wash., 1957

57 Tr. -- Trapp, W. J. and Anderson, V.

Damping Properties of Some Magnesium Base, Aluminum Base, and Ferrous Alloys
Internal Rept., Univ. of Minn., 1957

57 Y. -- Yamada, Y.

On the Vibrational Damping of Structural Steel Beams
Kyoto Univ., Fac. of Eng. Memoirs, Vol. 19, No. 1, pp. 1-13, 1957

57 Ya. -- Yamamoto, K. and Wage, Y.

An Investigation of Dynamic Mechanical Properties of Glassy Polymers by the Composite Oscillator Method
J. Phys. Soc. Japan, Vol. 12, p. 374, 1957

58 A. -- Anderson, V. W.

Damping and Fatigue Properties of Plastic Materials
Internal Rept., Aero Lib., Univ. of Minn., 1958

58 Co. -- Cochardt, A.

Magnetomechanical Damping
Scientific Paper 8-0161-P7, Westinghouse Res. Lab., Pittsburgh, Pa., November 6, 1958

58 K. -- Kaelble, D. H.

Dynamic Mechanical Properties of Scotchply Type 1000
Minn. Mining and Manufacturing Co. Rept., 1958

58 Mas. -- Mason, W. P.

Internal Friction, Plastic Strain, and Fatigue in Metals and Semiconductors
ASTM, STP No. 237, p. 36, 1958

58 Su. -- Sumner, G. and Entwistle, K. M.

The Measurement of the Strain-Dependent Damping of Metals Vibrating Torsionally
Brit. J. Appl. Phys., Vol. 9, No. 11, pp. 434-438, November, 1958

58 Wei. -- Weissmann, G. F. and Babington, W.

A High Damping Magnesium Alloy for Missile Applications
Proc., ASTM, Vol. 58, pp. 869-892, 1958

59 Boh. -- Bohn, L. and Oberst, H.

Information from the Vibration Measurements on the Behavior of Plastics in Short-time (Shock) Loading
Akustische Beihefte, No. 1, pp. 191-199, 1959

59 Co. -- Cochardt, A.

Magnetomechanical Damping
In book: Magnetic Properties of Metals and Alloys, Chapter 11, Proc., of a Seminar held October 1958; Am. Soc. for Metals, 1959

59 Laza. -- Lazan, B. J.

Energy Dissipation Mechanisms in Structures, with Particular Reference to Material Damping
Structural Damping, J. E. Ruzicka, Ed., ASME, Sect. 1, pp. 1-34, 1959

59 Sc. -- Schnitzel, R. H.

High Temperature Damping of Tantalum, Rhenium, and Tungsten
J. Appl. Phys., Vol. 30, No. 12, pp. 2011-2012, December, 1959

59 Tor. -- Torvik, P. J.

Damping, Elasticity, and Fatigue Properties of Brush QMV Beryllium
Internal Rept., Univ. of Minn., 1959

59 Wil. -- Wilks, J.

The Dependence of Internal Friction on Frequency
Phil. Mag., Vol. 4, Ser. 8, pp. 1379-1381, 1959

60 Cl. -- Clark, J. W. and Hagel, W. C.

Influence of Static Stress and Temperature on Internal Damping
Trans., Am. Soc. for Metals, Vol. 52, pp. 95-115, 1960

60 Ger. -- Gerson, R.

Dependence of Mechanical Q and Young's Modulus of Ferroelectric Geramics on Stress Amplitude
J. Acoust. Soc. Am., Vol. 32, No. 10, pp. 1297-1301, October 1960

60 Pigu. -- Piguzov, Y. V. and Blanter, M. S.

The Effect of Quenching Temperature on the Nitrogen Peak of Internal Friction in Iron
Fiz. Metallov i Metallovedenie, USSR, Vol. 19, No. 6, pp. 931-933, 1960

60 We. -- Weissmann, G. F. and Hart, R. R.

The Damping Capacity of Some Granular Soils
Bell Telephone Laboratories, Inc., Murray Hill, N. J., 26 pp., 1960

61 Bo. -- Bodner, S. R. and Fraser, A. F.

Vibrations and Wave Propagation in Aluminum Alloys at Elevated Temperatures
Brown Univ. Tech. Rept. No. 24, Office of Naval Research Contract Nonr-562(20), August 1961

61 Cha. -- Chang, R.

The Elastic and Anelastic Properties of Refractory Materials for High Temperature Applications
Proc. of Conference at North Carolina State College, March 1960. Published in "Mechanical Property of Engineering Ceramics," Interscience Publishers, 1961, edited by W. Kriegel and H. Palmour III

61 Dash. -- Dashkovskii, A. I. and Savitskii, E. M.

The Damping Capacity of Strontium
Phys. Met. Metall., Vol. 11, No. 5, pp. 153-154, 1961

61 Fa. -- Fast, J. D. and Verrijp, M. B.

Internal Friction in Lightly Deformed Pure Iron Wires. (In French)
Metaux-Corrosion Ind., Vol. 36, pp. 91-99, 1961. Also Philips Res. Rept. Netherlands, Vol. 16, No. 1, pp. 51-65, 1961

61 Ga. -- Garber, R. I. and Soloshenko, I. I.

Influence of Annealing on the Decrement of Decay of Varying Elastic-Plastic Flexure
Phys. Met. Metall., Vol. 12, No. 1, pp. 136-137, March 1961

61 Hube. -- Huber, R. J., Baker, G. S and Gibbs, P.

High-Temperature Kilocycle Internal Friction in Al_2O_3 Single Crystals
J. Appl. Phys., Vol. 32, No. 12, pp. 2573-2579, 1961

61 Lea. -- Leak, G. M. and Miles, G. W.

Grain Boundary Damping. II. Iron Interstitial Alloys
Proc. Phys. Soc., Vol. 78, pp. 1529-1542, December 1961

61 Mac. -- MacDonald, G. J. F.

The Earth's Free Oscillation
Science, Vol. 134, p. 1663, 1961

61 Mort. -- Morton, M. E. de

Magnetomechanical Damping in Chromium
Phil. Mag., Vol. 6, No. 67, pp. 825-831, July 1961

61 Ni. -- Niblett, D. H.

Low-Frequency Measurements on the Bordoni Internal Friction Peak in Copper
J. Appl. Phys., Vol. 32, No. 5, pp. 895-899, May 1961

61 R. -- Rawlings, R. and Robinson, P. M.

Internal Friction Effects in Iron-Silicon-Nitrogen Alloys
J. Iron St. Inst., Vol. 197, Pt. 3, pp. 211-215, March 1961

61 Shu. -- Shushaniya, V. R. and Golovin, S. A.

Influence of Quenching Temperature on the Damping Capacity of Carbon Steel
Phys. Met. Metall., Vol. 11, No. 5, pp. 150-151, 1961

61 T. -- Taylor, A.

Low-Temperature Internal Friction Peaks in Single Crystals of NaCl and LiF
J. Appl. Phys., Vol. 32, No. 9, pp. 1799-1800, September 1961

61 U. -- Ungar, E. E. and Hatch, D. K.

High-Damping Materials
Prod. Eng., Vol. 32, No. 16, pp. 44-56, April 17, 1961

61 W. -- Whittier, J. S.

Phenomenological Theories of Hysteretic Material Damping With Application to the Vibrations of Circular Plates
ASD TR 61-264, November 1961

61 Ye. -- Yevtushchenko, L. A. and Levitin, R. Z.

Anomalies in the Modulus of Elasticity in Shear of the Antiferromagnetic Materials MnO, CoO, and Cr_2O_3
Phys. Met. Metall., Vol. 12, No. 1, pp. 139-140, 1961

62 Chi. -- Chi, S. H.

Bibliography and Tabulation of Damping Properties of Non-Metallic Materials
WADD TR 60-540, 147 pp., September 1962

62 Do. -- Donato, R. J., etc.

Absorption and Dispersion of Elastic Energy in Rocks
Nature, Vol. 193, pp. 764-765, February 24, 1962

62 K. -- Kaufman, J. G.

Damping of Light Metals
Materials in Design Engineering, Vol. 56, No. 2, pp. 104-105, August 1962

62 Pisa. -- Pisarenko, G. S.

Dissipation of Energy in Mechanical Vibrations. (In Russian)
Kiev, Izd-vo Akad. Nauk USSR, 435 pp., 1962

62 Pl. -- Plénard, E.

The Role of Graphite in Grey Irons Subjected to Constraints of Traction. (In French)
Fonderie, Vol. 191, pp. 1-14, January 1962

62 Sm. -- Edited by Smithells, C. J.

Metals Reference Book
Third Edition, Vol. II, N. Y. Intersc. Pub., 1962

63 Ai. -- AiResearch Manufacturing Company

Evaluation of Internal Damping Properties for Several Materials
Report SA-6371-MR, June 11, 1963

63 D. -- Dahlquist, C. A.

Letter to Richard R. Rowand
Tape Research Dept., 3M Company, St. Paul, Minn., 1963

63 Da. -- Dahlquist, C. A.

Letter to B. J. Lazan
Tape Research Dept., 3M Company, St. Paul, Minn., November 26, 1963

64 As. -- Astbury, N. F. and Moore, F.

Torsional Hysteresis in Plastic Clay and Its Interpretation
ASTM, International Conference on Materials, Reprints of Papers, pp. 405-419, February 1964

64 Ast. -- Astbury, N. F. and Davis, W. R.

Internal Friction in Ceramics
Trans. Brit. Ceramic Soc., Vol. [illegible], No. 1, pp. 1-18, January 1964

64 Bi. -- Birchon, D.

High Damping Alloys for the Reduction of Noise and Vibration
English Materials and Design, September and October 1964 (London)

64 Ku. -- Kurtze, G.

Physic und Technik der Larmbekampfung
Book. Verlag G. Braun, Karlsruke, 1964

64 Sno. -- Snowden, J. C.

Rubberlike Materials, Their Internal Damping and Role in Vibration Isolation
Ordnance Research Lab., Penna. State Univ., University Park, Pa., June 1964

64 Wo. -- Wood, J. and Lee, L.

Bibliography and Abstracts of Publications for Period 1956-1964 Dealing with Damping Properties of Materials
TR 65-22, Air Force Tech. Rept., August 1965

65 Bl. -- Blasingame, W.

Comparison of Dynamic Shear Modulus Measurements on Two Damping Materials
U.S. Navy Marine Engineering Lab. Rept. 244/65, July 1965

65 Gr. -- Granick, N. and Stern, J. E.

Material Damping of Aluminum by a Resonant-Dwell Technique
NASA TN D-2893, August 1965

65 L. -- Lazan, B. J.

Damping of Materials and Members in Structural Mechanics
Pergamon Press, Inc., New York, manuscript submitted August 10, 1964, to be published in 1966

UNCLASSIFIED
Security Classification

DOCUMENT CONTROL DATA - R&D

(Security classification of title, body of abstract and indexing annotation must be entered when the overall report is classified)

1. ORIGINATING ACTIVITY (Corporate author)	2a. REPORT SECURITY CLASSIFICATION
Dept. of Aeronautics & Engineering Mechanics University of Minnesota Minneapolis, Minnesota 55455	Unclassified 2b. GROUP

3. REPORT TITLE

A Graphical Compilation of Damping Properties of Both Metallic and Non-Metallic Materials

4. DESCRIPTIVE NOTES (Type of report and inclusive dates)

Compilation Report - June 1963 to February 1966

5. AUTHOR(S) (Last name, first name, initial)

Lee, Larry T.

6. REPORT DATE	7a. TOTAL NO. OF PAGES	7b. NO. OF REFS
May 1966	210	159

8a. CONTRACT OR GRANT NO.	9a. ORIGINATOR'S REPORT NUMBER(S)
AF 33(615)-1055 b. PROJECT NO. 7351 cTask No. 735106 d.	AFML-TR-66-169 9b. OTHER REPORT NO(S) (Any other numbers that may be assigned this report)

10. AVAILABILITY/LIMITATION NOTICES This document is subject to special export controls and each transmittal to foreign governments or foreign nationals may be made only with prior approval of the Metals and Ceramics Division (MAM), Air Force Materials Laboratory, Wright-Patterson AFB, Ohio 45433.

11. SUPPLEMENTARY NOTES	12. SPONSORING MILITARY ACTIVITY
	Metals and Ceramics Division (MAMD) Air Force Materials Laboratory Wright-Patterson AFB, Ohio 45433

13. ABSTRACT

This report is a compilation of data on the damping properties of uniform materials and test specimens that has been collected from a wide range of publications. There are 420 entries on metals and alloys of which 300 are also illustrated with figures. There are 250 entries on polymers, elastomers, wood products, composites and similar synthetic and natural nonmetallic materials of which 85 are illustrated with figures. There are 80 entries on refractories, glass, masonry, minerals, stone, natural crystals, and oxides of which 20 are illustrated with figures. In addition there are 7 entries on particle-type materials, aggregates, soils, and Earth's crust. The earliest data included comes from a 1931 publication while the latest data comes from 1964 publications. If possible the data for metals, alloys, and some nonmetals is given in either unit damping energy D or loss coefficient η, otherwise the data is presented in either total damping energy D_s or loss coefficient η_s of the specimen. The data for the polymers and elastomers is usually given in complex notation (G', G" or E', E"). The primary purpose of this report is to present conveniently and concisely a compilation of published test data in a consistent set of units and to provide a useful reference for engineers and designers.

DD FORM 1 JAN 64 1473

UNCLASSIFIED
Security Classification

14. KEY WORDS	LINK A		LINK B		LINK C	
	ROLE	WT	ROLE	WT	ROLE	WT
damping properties metallic and nonmetallic materials						

INSTRUCTIONS

1. ORIGINATING ACTIVITY: Enter the name and address of the contractor, subcontractor, grantee, Department of Defense activity or other organization *(corporate author)* issuing the report.

2a. REPORT SECURITY CLASSIFICATION: Enter the overall security classification of the report. Indicate whether "Restricted Data" is included. Marking is to be in accordance with appropriate security regulations.

2b. GROUP: Automatic downgrading is specified in DoD Directive 5200.10 and Armed Forces Industrial Manual. Enter the group number. Also, when applicable, show that optional markings have been used for Group 3 and Group 4 as authorized.

3. REPORT TITLE: Enter the complete report title in all capital letters. Titles in all cases should be unclassified. If a meaningful title cannot be selected without classification, show title classification in all capitals in parenthesis immediately following the title.

4. DESCRIPTIVE NOTES: If appropriate, enter the type of report, e.g., interim, progress, summary, annual, or final. Give the inclusive dates when a specific reporting period is covered.

5. AUTHOR(S): Enter the name(s) of author(s) as shown on or in the report. Enter last name, first name, middle initial. If military, show rank and branch of service. The name of the principal author is an absolute minimum requirement.

6. REPORT DATE: Enter the date of the report as day, month, year; or month, year. If more than one date appears on the report, use date of publication.

7a. TOTAL NUMBER OF PAGES: The total page count should follow normal pagination procedures, i.e., enter the number of pages containing information.

7b. NUMBER OF REFERENCES: Enter the total number of references cited in the report.

8a. CONTRACT OR GRANT NUMBER: If appropriate, enter the applicable number of the contract or grant under which the report was written.

8b, 8c, & 8d. PROJECT NUMBER: Enter the appropriate military department identification, such as project number, subproject number, system numbers, task number, etc.

9a. ORIGINATOR'S REPORT NUMBER(S): Enter the official report number by which the document will be identified and controlled by the originating activity. This number must be unique to this report.

9b. OTHER REPORT NUMBER(S): If the report has been assigned any other report numbers *(either by the originator or by the sponsor)*, also enter this number(s).

10. AVAILABILITY/LIMITATION NOTICES: Enter any limitations on further dissemination of the report, other than those imposed by security classification, using standard statements such as:

(1) "Qualified requesters may obtain copies of this report from DDC."

(2) "Foreign announcement and dissemination of this report by DDC is not authorized."

(3) "U. S. Government agencies may obtain copies of this report directly from DDC. Other qualified DDC users shall request through

_____."

(4) "U. S. military agencies may obtain copies of this report directly from DDC. Other qualified users shall request through

_____."

(5) "All distribution of this report is controlled. Qualified DDC users shall request through

_____."

If the report has been furnished to the Office of Technical Services, Department of Commerce, for sale to the public, indicate this fact and enter the price, if known.

11. SUPPLEMENTARY NOTES: Use for additional explanatory notes.

12. SPONSORING MILITARY ACTIVITY: Enter the name of the departmental project office or laboratory sponsoring *(paying for)* the research and development. Include address.

13. ABSTRACT: Enter an abstract giving a brief and factual summary of the document indicative of the report, even though it may also appear elsewhere in the body of the technical report. If additional space is required, a continuation sheet shall be attached.

It is highly desirable that the abstract of classified reports be unclassified. Each paragraph of the abstract shall end with an indication of the military security classification of the information in the paragraph, represented as *(TS)*, *(S)*, *(C)*, or *(U)*.

There is no limitation on the length of the abstract. However, the suggested length is from 150 to 225 words.

14. KEY WORDS: Key words are technically meaningful terms or short phrases that characterize a report and may be used as index entries for cataloging the report. Key words must be selected so that no security classification is required. Identifiers, such as equipment model designation, trade name, military project code name, geographic location, may be used as key words but will be followed by an indication of technical context. The assignment of links, rules, and weights is optional.